Antifouling Compounds Isolated from Two Red Sea Organisms: a *Hyrtios* sp. Sponge and an *Okeania* sp. Cyanobacterium

(紅海由来の海綿 *Hyrtios* sp.およびラン藻 *Okeania* sp.から得られた付着阻害物質)

Julie G. PETITBOIS

Ph.D Dissertation

2018

Graduate School of Environmental Science
Hokkaido University

To my grand-parents, Papy Robert and Mamie Annick.
I learnt a lot from you and will always love you.

Abstract

Biofouling is defined as the accumulation of organisms on submerged structures such as ships' hulls, underwater pipelines, oil rigs, piers, buoys etc. It causes large economic loss and serious ecological problems worldwide. For instance, in naval industry, not removing biofouling leads to corrosion, resistance in the water and increase of the weight of ships, which contribute to an increase of fuel consumption. This increase results in a raise of contaminant gases, harmful particles and so of global warming. To avoid all these troubles and keep our planet livable, antifouling strategies are needed. One of them is to copy Nature by mimic sessile organisms which produce chemical defenses to be free of fouling and avoid predation. Several marine natural compounds have already been isolated from marine organisms, mainly from cnidaria, sponges and algae.

For this study, about eighty extracts of different marine organisms from the Red Sea were tested on barnacle larvae which are hard-to-remove macrofoulers and found worldwide. The Red Sea is a special ecosystem because it is partially isolated from the open ocean and, because of its location between deserts, evaporation occurs, making this sea the warmest and most saline one in the world. So, because of these hard conditions, organisms should produce compounds to adapt, including antifouling ones. About 18 % of the tested extracts were very active (active at 1 µg/mL) and 31 % were moderately active (active at 10 µg/mL). Among the active extracts, two were selected because of their large amount of material: the sponge *Hyrtios* sp. and the cyanobacterium *Okeania* sp. Sponge are prolific producers of antifouling compounds while cyanobacteria are not yet well studied for such compounds although they can be cultured in large scale to afford large amounts of active compounds for the industries.

Three known compounds were isolated from *Hyrtios* sp.: *N*-phenethylacetamide and the two fatty acid methyl esters (FAMEs), methyl-(5*Z*,9*Z*)-hexacosa-5,9-dienoate and methyl-(*Z*)-octadec-11-enoate. The position of the double bonds of these FAMEs was determined by study of GC-MS-MS fragments of their dimethyl disulfide adducts while their configuration was ascertained by NMR (coupling constants, carbon shifts of the allylic methylenes). *N*-Phenethylacetamide was previously isolated from a fungus while methyl-(5*Z*,9*Z*)-hexacosa-5,9-dienoate was isolated from different sponges. Both FAMEs have already been synthesized but, to our knowledge, it is the first time that methyl-(*Z*)-octadec-11-enoate was isolated from a natural source.

Okeania sp. afforded two fatty acid amides, serinolamides C and D, the known

antifoulant dolastatin 16, and several lyngbyabellins: the known 27-deoxylyngbyabellin A, lyngbyabellins F, G, H and the new lyngbyabellins O and P. The absolute configuration of the two serinolamides was established by partial synthesis and Marfey's analysis of the synthetic (*R*)- and (*S*)-*O*-methyl serinol and the hydrolysate of both fatty acid amides. They were named serinolamides in reference to serinolamides A and B, isolated from *Moorea producens*, a cyanobacterium genetically close to *Okeania* sp. The planar structures of the two new lyngbyabellins, O and P, were elucidated by MS and NMR techniques. The absolute configuration at C-14 and C-20 of lyngbyabellin O was determined to be *R* and *S*, respectively, by chiral-phase chromatography of its degradation products: the glyceric acid and the 2,3-dihydroxyisovaleric acid methyl ester residues. Its configuration at C-2 and C-3 was assessed by methanolysis of lyngbyabellin G. Methanolysis of lyngbyabellin G opens its structure at C-16, giving lyngbyabellin O. Both lyngbyabellins have as a result a 2*S* and 3*S* configuration. Lyngbyabellin F was deacetylated to give lyngbyabellin P, which therefore shares the same absolute configuration 2*S*, 3*S*, 14*R*, 20*S*, 26*R* and 27*S*. Methanolysis of lyngbyabellins F, G and P led to a regioselective ester cleavage at C-14 and C-16, respectively, giving lyngbyabellin O. Therefore, we can wonder if acyclic lyngbyabellins and lyngbyabellins without a side chain are artifacts. But, as previously reported with the biosynthetic pathways of lyngbyabellin A and hectoclorin, macrocyclization occurs, meaning that lyngbyabellins with cyclic structure are natural compounds. Clusters for incorporation of side chain were not observed in both pathways so lyngbyabellins without a side chain are probably precursors, and other clusters are used for addition of a side chain. Only acyclic structures are probably artifacts.

Antifouling study was conducted on *Amphibalanus amphitrite* barnacle larvae. *N*-Phenethylacetamide was the least active compounds from *Hyrtios* sp. (EC_{50} 9.8 µg/mL), while both FAMEs were potent (EC_{50} 0.37 and 0.55 µg/mL, respectively). Structure of *N*-phenethylacetamide is close to dopamine, which is a reported antifoulant. Dopamine induces metamorphosis without prior settlement in *A. amphitrite* and inhibits the ciliary activity in mussel larvae. Mussel larvae stop swimming and therefore cannot reach the substratum. As some FAMEs were reported as antioxidants, they could act as antifoulants by inhibiting the oxidative chemistries barnacle larvae use to settle and metamorphose. *Okeania* sp. gave interesting compounds such as the potent serinolamides C and D (EC_{50} 0.88 and 0.04 µg/mL, respectively), the extra acetyl of serinolamide D apparently increasing the activity. However, after 120 hour-exposure, larvae started to settle a little and the recovery test with serinolamide D showed that almost all the exposed larvae could attach after seven days, which means that

the activity of serinolamides is reversible. As fatty acid amides, they could have biosurfactant properties which reduce the surface tension and so avoid settlement from larvae. Some fatty acid amides such as oleamide and erucamide are already used in antifouling paints because of these properties. Lyngbyabellins are known antineoplastic compounds and their structure seems to play an important role in their cytotoxicity toward cancer cells, with the cyclic structure with a side chain being the most potent. Their structural features are apparently also important to prevent larval settlement for barnacle. Indeed, the acyclic structure (lyngbyabellin O, EC_{50} 0.24 µg/mL) seems more active while cyclic structure (lyngbyabellin G, EC_{50} 4.4 µg/mL) and addition of a side chain (lyngbyabellin P, EC_{50} 0.62 µg/mL) decrease the activity. 27-Deoxylyngbyabellin A, which is different from the other lyngbyabellins by additional lactams, exhibits almost total toxicity at 0.1 µg/mL, making it potent but also toxic, which is not the strategy of ecologically friendly antifouling compounds.

This study showed that Red Sea organisms such as *Hyrtios* sp. and *Okeania* sp. produce antifouling compounds. Up to now, only one paper reported such compounds and three papers active extracts. The structure elucidation of compounds from *Hyrtios* sp. and *Okeania* sp. was possible thanks to MS and NMR techniques, together with partial synthesis, study of degradation products, derivatization and chiral chromatography. A relation between structure and activity of the lyngbyabellins was observed, leading to a possible future further research to understand their mode of action on barnacle larvae.

Table of Contents

- INTRODUCTION -

Biofouling is defined as the accumulation of organisms on submerged structures such as ships' hulls, underwater pipelines (external and also internal accumulation can occur), oil rigs, piers, buoys etc. Indeed, on land, air brings too few nutrients to allow this kind of settlement, except in very wet climate, but biofouling is not as dense, and its establishment is not as fast as in the aquatic environment.[1] Moreover, migration (active or passive) to a substrate is easier. As a result, submerge surfaces are more quickly colonized. Life attached to a substrate is mandatory for many organisms (bacteria, algae, barnacles etc.) to have continuous access to nutrients, so there is a very strong competition between sessile organisms. Organisms will develop defenses to prevent other species from colonizing their substrate. Conversely, they can also produce molecules attracting species over others, thus allowing the formation of an organized community that increases the size and/or density of the fouling.

Biofouling formation

This colonization commonly occurs in four main stages (Figure 1). It begins with (1) the formation of microfouling with initially the conditioning of the surface by inert particles (proteins, carbohydrates, humic substances from the decomposition of phytoplankton, etc.). Then, a few seconds to a few minutes later, (2) bacteria are adsorbed on this primary film, first reversibly through weak bonds, then irreversibly with the secretion of exopolymers leading to stronger interactions (hydrogen bonds, dipole-dipole interaction etc.). Several hours or days later, (3) unicellular organisms (diatoms, protozoa, fungi) or macroalgae spores attach themselves to bacterial biofilm. Several weeks or months after this colonization, (4) macrofouling phase starts: multicellular eukaryotes complete this epibiosis (macroalgae, shellfish etc.).[2] The biofouling development kinetics depends on various factors: physical and chemical parameters of the medium (pH, temperature, dissolved oxygen, chlorophyll content, conductivity, salinity, turbidity), chemical nature of the substrate, surface microtopography (rough surfaces will promote adhesion), hydrodynamic conditions depending on surface waves and currents, the presence of some species (species can secrete chemical repellants or attractants).

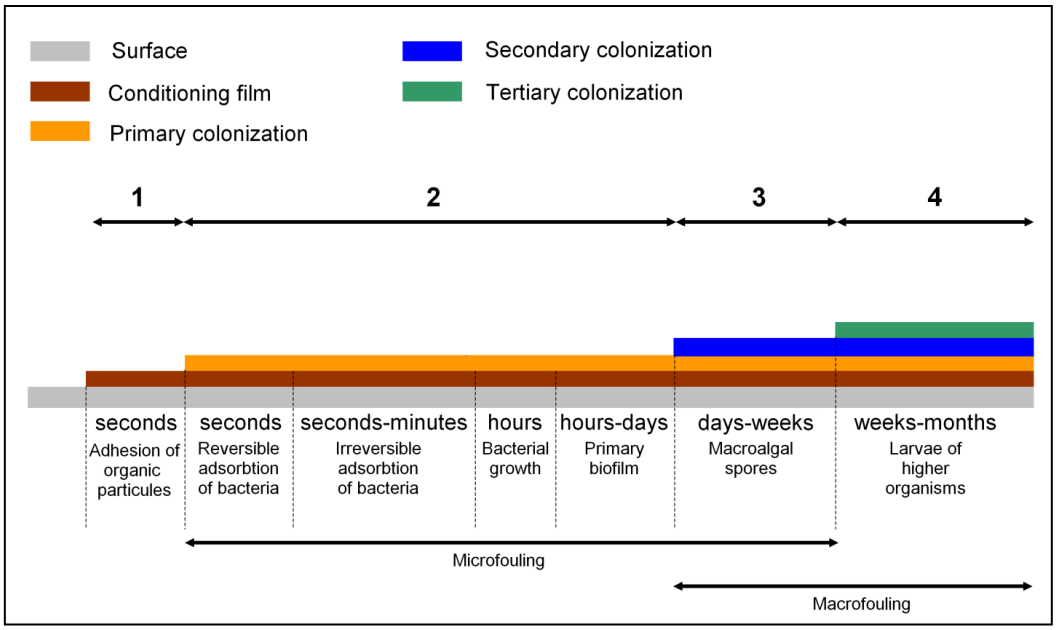

Figure 1: Steps of formation of biofouling

In an organism's point of view, also several steps are observed during colonization of a substrate. The organism first moves toward a surface, by its own movement (active transport) or thanks to currents (passive transport). Settlement consists of five parts: movement towards the surface, contact with it, exploration, evaluation and selection (or rejection) of it. Attachment to the substrate consists of several stages controlled by different mechanisms. After the larvae of invertebrates or spores of macroalgae settled, they develop and grow in multi-stage and complex processes.[3] Each step could be a target to prevent organisms to settle.

Antifouling strategies

Biofouling causes economic loss and serious ecological problems worldwide (Figure 2). When not removed, it can lead to corrosion so to the increase of costs of maintenance. Moreover, because it increases the weight of ships and the resistance in the water, propulsion power is impacted, causing an increase of fuel consumption. This increase of fuel consumption leads to an increase of contaminant gases and harmful particles release which are responsible of global warming. And, because of this, the temperature of ocean increases, promoting biofouling, creating a vicious cycle. Biofouling in maritime transportation also contributes to the introduction of alien and potentially harmful species in ecosystems via water ballast release. Biofouling is also a serious problem in aquaculture where the risks of diseases and mortality

become higher when no antifouling strategy is taken. Heat exchanges and membrane processes can also be impacted by this phenomenon.[4,5]

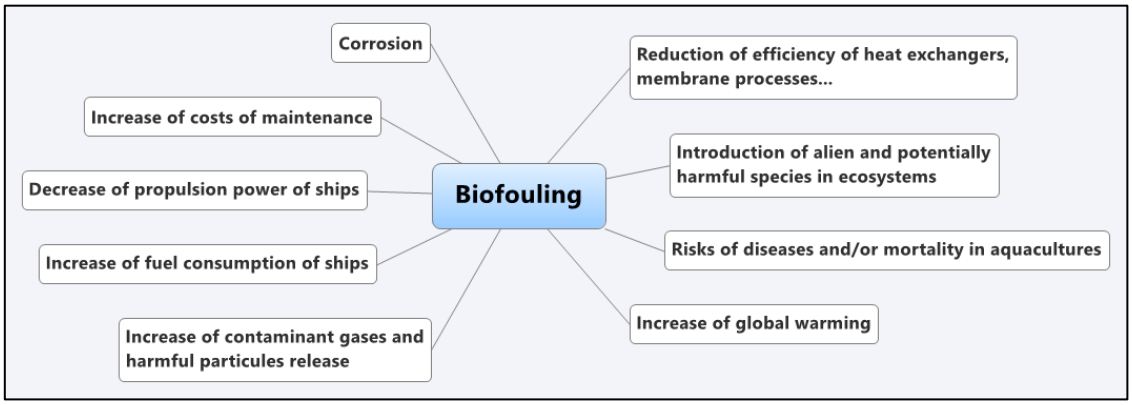

Figure 2: Issues caused by biofouling

Biofouling has been combated for more than 2000 years. Early Phoenicians and Carthaginians used pitch and copper sheathing. Other methods such as wax, tar and asphaltum were also used. Mid 1800s, paints containing toxicants such as copper oxide, arsenic and mercury oxide were developed. After the Second World War, new synthetic petroleum-based resins replaced the organo-mercurials and organo-arsenicals which caused some safety and health concerns. In the mid-1950s, the famous tributyltin (TBT) containing antifouling paints arrived on the market and, because of their high-performance, they were wildly used on the commercial vessels.[6] However, due to side-effects on non-targeted organisms caused by TBT, first observed in the bay of Arcachon (France) on oysters at the end of 1970s, the International Maritime Organization and Marine Environment Protection Committee decided to ban the application of TBT from January 1, 2008.[7] Some countries have already banned TBT, like Japan, which was the first country in 1991 to ban it almost totally.[8] After this ban, copper paints and other antifouling biocides such as Irgarol 1051, diuron, dichloroflumid, zinc pyrithione and pyridine have started to be used as an alternative but some of them are under strict regulations in various regions as they have possible effects on marine ecosystems. Because of these sides effects, “eco-friendly” alternatives are studied. They can be classified into three categories: physical, chemical and biological methods.

Physical methods are based on electricity and surface modification. Electric power can be used as antifouling system in two ways. The first one is by using a weak positive electric current on a conductive surface to attract and kill bacterial cells which are negatively charged. By switching the polarity, dead bacteria are repelled from the surface. Unfortunately, this

technique is expensive and its efficiency has not been established.[9] The second method based on electricity is electrolysis of seawater which produces hypochlorous acid, ozone bubbles, hydrogen peroxide or bromide. These compounds being bactericidal, no biofilm can grow on the surface, which make further colonization by higher organisms more difficult.[10] Surface modifications are based on hydrophobic properties and microtopography. Modifying hydrophobicity of a surface is possible by using silicone which has a low surface energy. This low surface energy will reduce the adhesion strength of organisms and facilitate their removal while vessels are in high speeds.[11] Surface topography also affects biofouling formation. Otherwise, by modifying microtopography by alternating depressions and protuberances, as in the skin of certain organisms such as the dolphin or the shark, there are fewer possible attachment points for the microorganisms and macrofoulers' larvae. However, as biofoulers have all of them their own way to settle, more studies to understand their adhesion mechanisms are needed to develop more efficient surfaces.[12]

Chemical methods contain the biocides cited previously, but also chlorination, self-polishing copolymers and foul release coatings. Chlorination is used in cooling water systems where fouling is mainly formed by mussel and can disrupt normal operation of power plant.[13] The self-polishing copolymer paints contain an acrylic polymer with an ester linkage to an organometallic group or a biocide such as Cu_2O. By hydrolysis of the ester linkage occurring in contact with the seawater, the organometallic group or the biocide is released and can act on biofoulers. The remaining polymer becomes water-soluble and is also released, taking with it the organisms which have succeeded to settle on it. Another alternative is the foul release paint which is composed of a nonstick coating (generally silicone). The mechanism of action is like self-polishing copolymer paints but without any biocide. The coating is hydrolyzed and released in the water, washing off the biofoulers. This technique is only used on fast moving vessels and is quite expensive.[14]

Biological biofouling management include "living paints", enzyme based coatings and natural products. "Living" paints contain encapsulated living bacteria, hence their name. This kind of paints aim at mimic naturally occurring bacterial biofilms which produce inhibitory metabolites.[15,16] These inhibitory metabolites can be enzymes, the same which can be used in enzyme based coatings. These enzymes could have different modes of action: degrading adhesives used by organisms to settle (mainly proteases as organisms largely use proteins and proteoglycans to adhere on a surface), disrupting the biofilm matrix (hydrolases and lyases to degrade the exopolysaccharides used by bacteria to form their biofilm), generating deterrents

and biocides (glucose and hexose oxidases are used to generate hydrogen peroxide which induces oxidative damage in cells) or interfering with the quorum sensing of bacteria (*N*-acyl homoserine lactones (AHL) acylase degrades AHL, which are molecules used by bacteria to communicate to form a biofilm). There are some challenges using enzymes as these molecules have some optimal temperatures or pH to work. They can also be degraded quickly.[10] The last biological antifouling technique is the use of natural compounds, other than enzymes. As it is the main topic of this thesis, this point will be further described.

Natural compounds as antifouling strategy

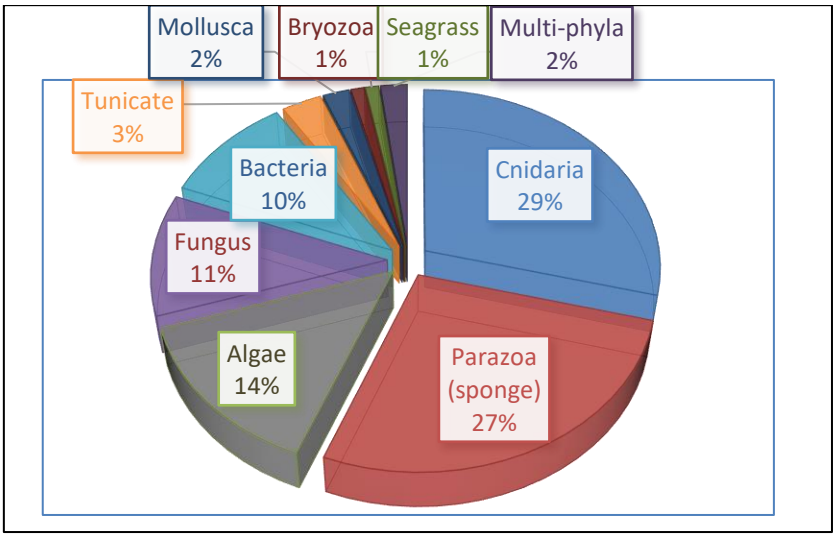

Figure 3: Phyletic distribution of about 300 compounds with antifouling activities (2003-2017)[19-22]

The increase of the restrictions regarding the use of antifouling alternatives (same or higher effectiveness, environmentally friendly) has led to an urgent demand of new compounds for coating industries. Known to have the largest biodiversity, marine organisms are a rich source of bioactive compounds and what is better than inspiration from the Nature to find effective and less harmful antifouling compounds?[17,18] Marine organisms are good sources of this kind of compounds, mainly sessile organisms which need to produce chemical defenses in order to fight against predation or other organisms which could take their place. Over the last several decades, many marine natural products have been isolated from seaweeds and marine invertebrates (Figure 3). Cnidaria afforded for almost 30 % of antifouling compounds, followed by parazoa, or sponges, with 27 %. Several reasons can explain these statistics. Cnidaria and sponges are well studied phyla. Moreover, they seem very prolific and their phyla regroup lots

of species (about 10,000 for cnidaria and 15,000 for parazoa). The third phylum, algae, produced only 14 % of reported antifouling compounds, despite being probably the most obvious producers of antifouling substances are they are visible on beaches and free of biofoulers. Then fungus and bacteria follow with 11 and 10 %, respectively. They will probably bring more interest in a near future as these organisms can be grown in large scale and so supply large amounts of active compounds, not only antifouling but also pharmaceutical ones. Tunicates, bryozoan, seagrass and other phyla bring up the rear, presumably because they are less studied for antifouling compounds than the other mentioned phyla. The compounds accounted in Figure 3 have most of them EC_{50} values < 25.0 µg/mL and a therapeutic ratio (LC_{50}/EC_{50} ratio) > 15, a standard established by the U.S. Navy program to highlight effective and low or even non-toxic antifouling compounds. But, for some researchers, an EC_{50} value of 25 µg/mL is still too high. That is why, in this section, only compounds with an EC_{50} value below 5 µg/mL will be presented.[19-22]

Cnidarian compounds

Cnidaria is a phylum containing over 10,000 species of aquatic animals, such as jellyfish, gorgonians, soft corals, sea anemones, hydra etc. Jellyfish are known to produce toxins to avoid predation. The sessile cnidarians also need to secrete chemical defenses against predation but also foulers. Lots of compounds with antifouling properties are from this phylum.

The study of the Chinese gorgonian *Astrogorgia* sp. afforded 18 compounds, among which 14-deacetoxycalicophirin B (**1**) showed significant antifouling activity against the larval settlement of *Amphibalanus amphitrite*, with an EC_{50} value of 0.59 µg/mL, while the other compounds could not be considered as effective, with EC_{50} values between 5.17 and 17.8 µg/mL.[23]

The gorgonian *Dicholetta gemmacea* produces several potent antifouling compounds which inhibit the larval settlement of *A. amphitrite*, such as: juncins O (**2**) and Z1 (**3**) and juncenolide H (**4**) (EC_{50} < 0.125 µg/mL), but also juncin P (**5**) (EC_{50} 0.77 µg/mL), junceellolide D (**6**) (EC_{50} 0.8 µg/mL) and suberoretisteroid A (**7**) (EC_{50} 0.81 µg/mL).[24] Another study of this gorgonian reported several 16 diterpenoids, some of them with good antifouling activity on barnacle larvae: dichotellides H **(8**) (EC_{50} 4.1 µg/mL), M (**9**) (EC_{50} 4.6 µg/mL), N (**10**) (EC_{50} 1.2 µg/mL), P (**11**) (EC_{50} 0.79 µg/mL) and U (**12**) (EC_{50} 2.0 µg/mL), together with junceellolide C (**13**) (EC_{50} 0.2 µg/mL).[25]

The Sea Pansy supplied three diterpenes: renillafoulins A-C (**14-16**), with EC_{50} values towards barnacle larvae of 0.02 to 0.2 μg/mL.[26]

Two diterpenoids, pukalide (**17**) and epoxypukalide (**18**), are one of the most active antifoulants reported in this review as their EC_{50} values were 19 ng/mL and 55 ng/mL.[27]

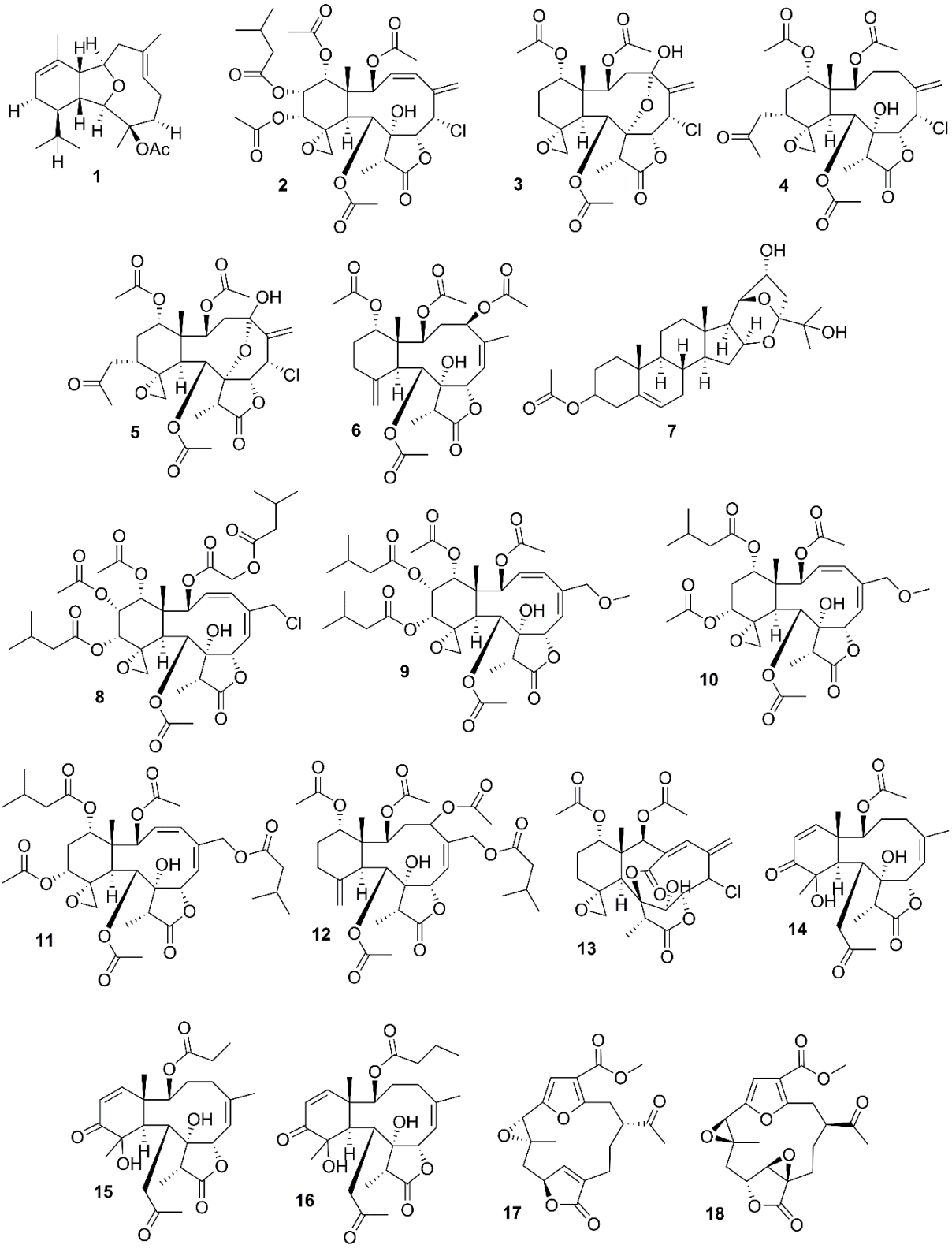

Spongial compounds

Sponges, or parazoans, are animal which don't have tissues or organs. They have a porous body with channels in which water circulates. They often host endosymbionts such as cyaonbacteria. These symbionts can form a third of the total mass of some sponges. Sponges can gain energy from their symbionts and use molecules produced by these microorganisms. Because of this close relation between sponges and endosymbionts, it is sometimes difficult to affirm that a compound is produced by the sponge and not by its symbionts.[28]

Barettin (**19)** and two analogues were isolated from the cold-water sponge *Geodia barretti*: 8,9-dihydrobarettin **(20)** and bromobenzisoxazolone barettin **(21**).[29] While **19** and **20** inhibit settlement of barnacle cyprids with EC_{50} values of 0.9 and 7.9 µM, respectively, **21** was even more potent, with a EC_{50} value of 15 nM, which is about 60 times higher than **19**. This higher potency is probably due to its brominated benzisoxazolone side chain. Moreover, the settlement inhibition was found to be reversible: after exposition at 10 µM, cyprids could metamorphose after transferred to fresh seawater. However, these three compounds are likely produced by a microbial symbiont in the sponge, since sponges cannot produce the tryptophan that makes up the cyclic peptide structure.

Kalihinols (**22** and **23)** and axamide-3 (**24**) isolated from the sponge *Acanthella cavernosa* collected off Hachijo-jima Island (Japan), are also potent antifouling compounds, with an EC_{50} value of about 0.05 µg/mL on larvae of the barnacle *A. amphitrite*. Other related compounds were also isolated but were less active.[30] The same sponge afforded three kalihinenes, X-Z (**25**-**27**) which inhibited half of the larval settlement of barnacle at 0.49, 0.45 and 1.1 µg/mL, respectively.[31]

Hachijo-jima Island was also the motherland of axinyssimide A (**28**), which was the most potent compound among four sesquiterpenes isolated from *Axinyssa* spp. It could inhibit 50 % of the settlement of cypris larvae of barnacle *A. amphitrite* at 1.2 µg/mL.[32]

The sesquiterpene hydroquinone avarol (**29**) was isolated from *Dysidea avatara*, and the corresponding quinone avarone (**30**) is the product of oxidation of **29**. Addition of thiols or *p*-chloroaniline gave five analogues of **30**. The natural compound **29** has a low EC_{50} value of 0.65 µg/mL on *A. amphitrite* but exhibits toxicity toward cyprid (LC_{50} value of 13.28 µg/mL) and more toward nauplii (LC_{50} value of 1.58 µg/mL). Its corresponding quinone, **30**, was less active (EC_{50} value of 3.41 µg/mL) and also less toxic (LC_{50} value of 27.12 and 25.12 µg/mL on cyprid and nauplii, respectively). However, its analogues, especially 3'-(*p*-chlorophenyl)-

avarone (**31**) and 4'-propylthioavarone (**32**) were very potent with EC_{50} value of 0.65 (like **29**) and 0.45 µg/mL, respectively, without being toxic (LC_{50} > 50 µg/mL).[33]

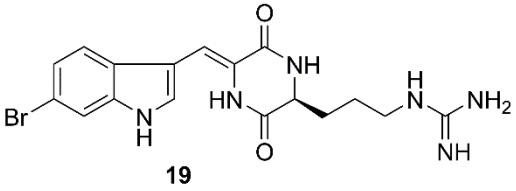

19

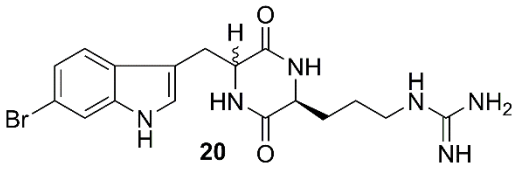

20

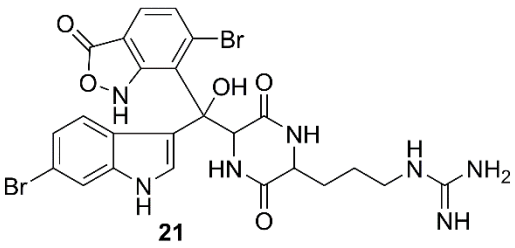

21

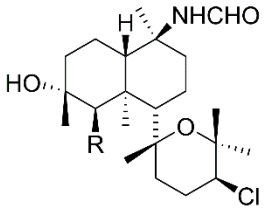

22, R = NC
23, R = NCS

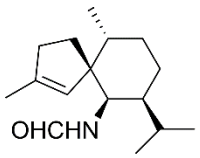

24

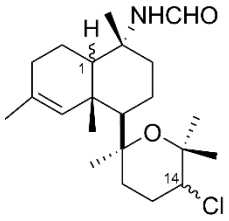

25: 1β-H, 14 α-Cl
26: 1α-H, 14 α-Cl
27: 1α-H, 14 β-Cl

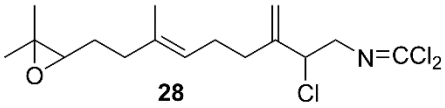

28

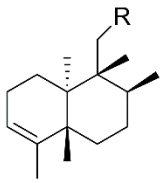

29, R =

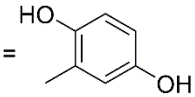

30, R =

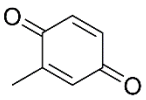

31, R =

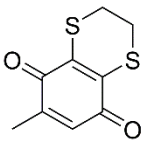

32, R =

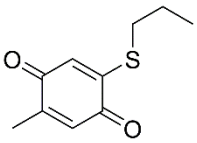

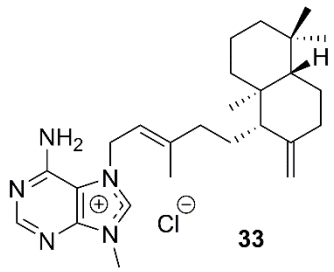

33

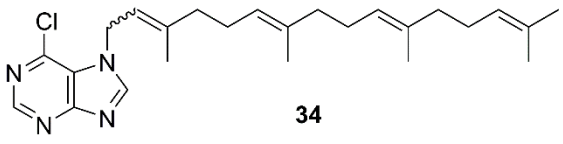

34

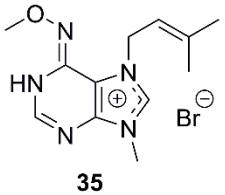

35

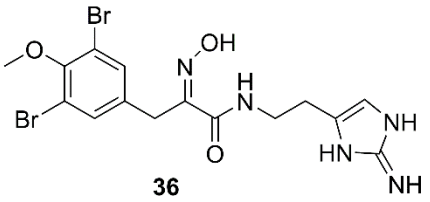

36

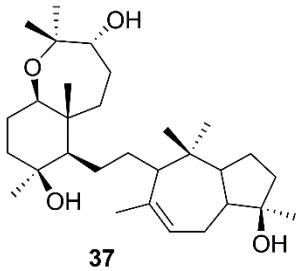

37

A screening study of compounds from marine sponges of the genus *Agelas* afforded the active agelasine D (**33**) with an EC_{50} value of 0.11 µM on *Amphibalanus improvises* cypris larvae, while two synthetic analogues (AV1033A (**34**) and AKB695 (**35**)) had higher, yet potent, EC_{50} values of 0.23 and 0.3 µM, respectively. None of these compounds showed toxicity.[34]

Ianthelline (**36**), a bromotyrosine derivative, was first isolated from the Caribbean sponge *Ianthella ardis*, then in other warm water sponges and more recently in the Arctic sponge *Stryphnus fortis*. It was tested on various organisms such as marine bacteria, microalgae, on the blue mussel *Mytilus edulis* and the barnacle *Amphibalanus improvisus*. Interestingly, it was able to inhibit both marine micro- and macrofoulers, mainly bacterial growth (minimum inhibitory concentration (MIC) values 0.1-10 µg/mL) and barnacle larvae settlement (EC_{50} of 3.0 µg/mL). Its effects on the blue mussel was so moderate (EC_{50} of 45.2 µg/mL) that we can consider it as inactive on this organism.[35]

A team from Saudi Arabia studied forty-two marine macroorganisms from the Red Sea and isolated a potent antifouling compound, sipholenol A (**37**), with an EC_{50} of 0.2 µg/mL on barnacle larvae settlement. Two other compounds, isolated from a red alga by the same team, are described in the following section.[36]

Algal compounds

Together with the spongial compound **37**, a study on Red Sea organisms led to the isolation of the potent antifoulants 2,10-dibromo-3-chloro-7-chamigrene (**38**) (EC_{50} 0.14 µg/mL) and 12-hydroxyisolaurene (**39**) (EC_{50} 1.34 µg/mL on barnacle larvae) from the red alga *Laurencia obtuse*.[36]

Another *Laurencia* sp., collected in Omaezaki (Japan), produces omaezallene (**40**), a tribrominated compound with potent antifouling activity against barnacle larvae (EC_{50} 0.22 µg/mL) but it was also toxic with a LC_{50} of 4.8 µg/mL. But, as its LC_{50}/EC_{50} is higher than 15 (21.8), it can still be considered as a good antifoulants. However, two synthetic omaezallenes (**41**, **42**), while being a little less active (EC_{50} 1.1 and 1.2 µg/mL), were not toxic at 10 µg/mL ($LC_{50}/EC_{50} > 9.1$) and can be good candidates for further studies.[37]

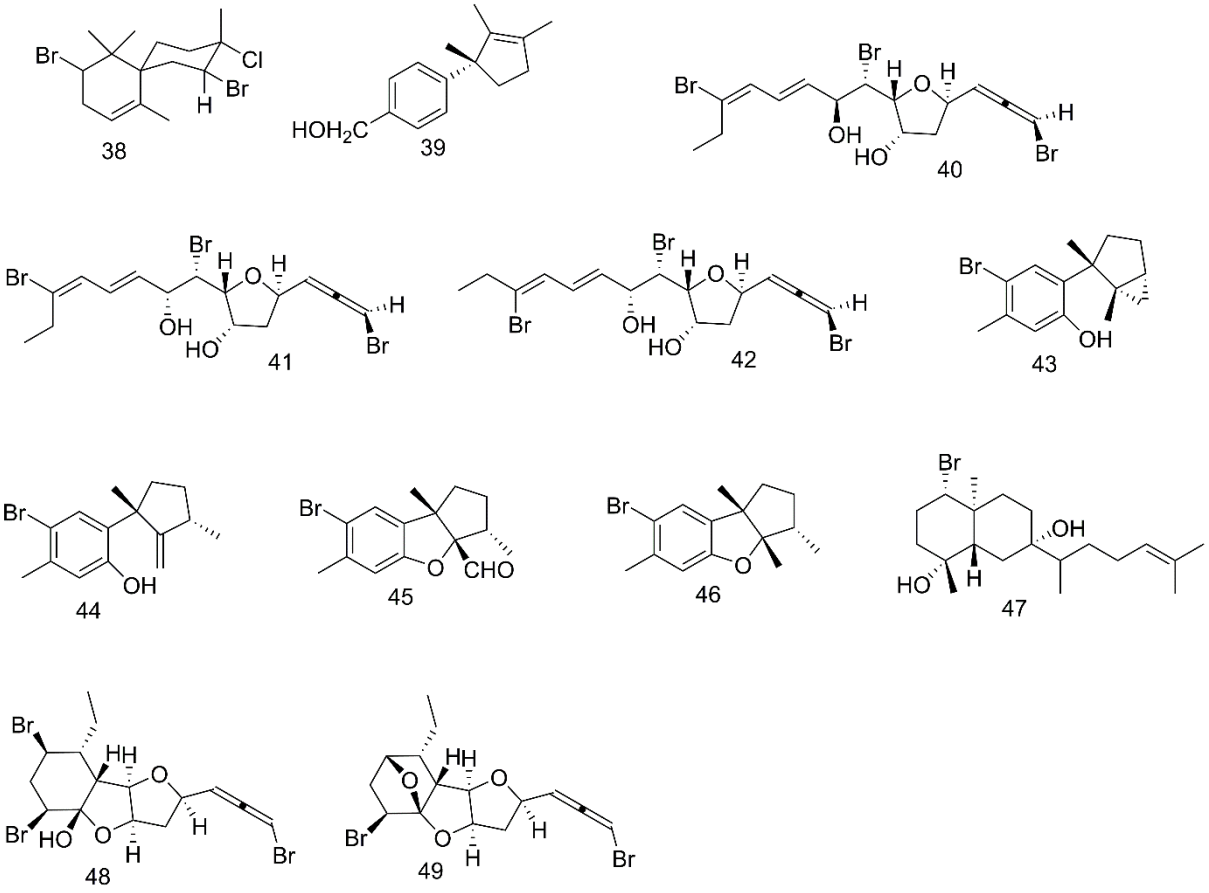

Investigation of antifouling compounds from another *Laurencia*, *L. okamurae*, led to the isolation of laurinterol (**43**), isolaurinterol (**44**), aplysinal (**45**) and aplysin (**46**). All of them inhibit the settlement of barnacle larvae, with EC_{50} values of 0.18, 10, 5 and 5 µg/mL, respectively. However, **44**-**46** could inhibit the settlement because they were toxic towards nauplii. **44** did not show any toxicity and is so a potent antifoulant.[38]

Laurencia is a well-studied genus but seems an endless source of interesting compounds. A recent study reported new compounds from Japanese collections with potent antifouling activity towards barnacle larvae: omaezol (**47**) and hachijojimallenes A (**48**) and B (**49**), with EC_{50} values of 0.59, 0.31 and 0.76 µM, respectively.[39]

Fungal compounds

Fungus are mainly found as symbionts with other organisms and produce a variety of interesting compounds, including the most potent antifoulant reported in this review:

aniduquinolone A (**50**), isolated from the gorgonian coral-derived fungus *Scopulariopsis* sp. It can inhibit the larval settlement of *A. amphitrite* with an incredibly low EC_{50} value of 17.5 pM. Other compounds isolated in the same study were also very potent, such as aflaquinolones A (**51**) (EC_{50} 0.028 µM), D (**52**) (EC_{50} 0.0028 µM) and F (**53**) (EC_{50} 0.86 µM) and 6-deoxyaflaquinolone E (**54**) (EC_{50} 1.04 µM).[40]

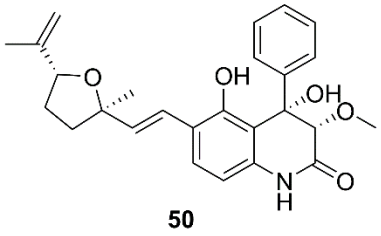

50

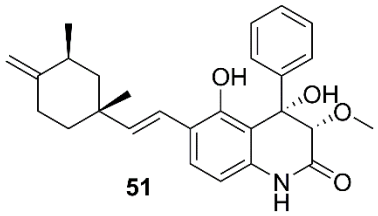

51

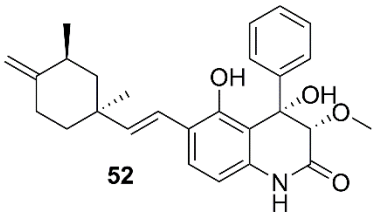

52

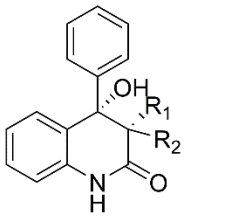

53, $R^1 = OCH_3$, $R^2 = H$
54, $R^1 = OH$, $R^2 = OH$

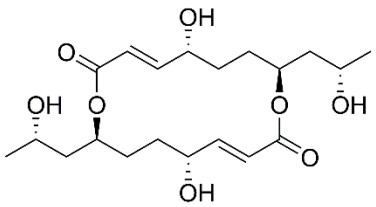

55

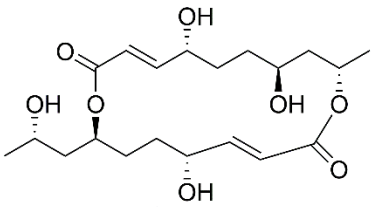

56

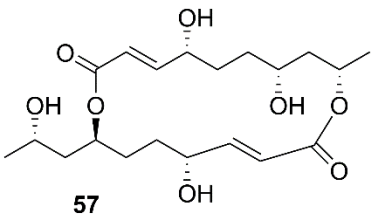

57

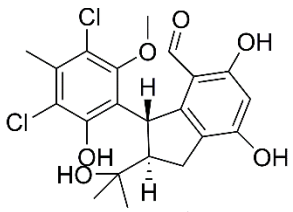

58

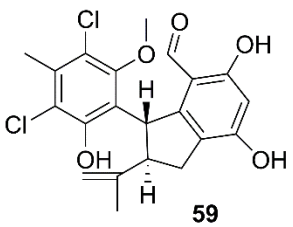

59

A symmetric 16-membered macrodiolide trichobotryside A (**55**) and the two asymmetric 18-membered trichobotrysides B (**56**) and C (**57**), were isolated from the deep-sea-derived fungus *Trichobotrys effuse* DFFSCS021. Only **55** could inhibit strongly the larval settlement of *B. neritina* (bryozoan) and *A. amphitrite* with EC_{50} values of 7.3 and 2.5 µg/mL, respectively, without toxicity. Interestingly, **56** was less active towards *B. neritina* (EC_{50} 9.2 µg/mL) and not active at all on barnacle larvae. **57** was found toxic (41 % lethality at 25 µg/mL). This study shows that very similar compounds could have different effects.[41]

Pestalachlorides E (**58**) and F (**59**), two dechlorinated compounds from the fungus *Pestalotiopsis* ZJ-2009-7-6, both showed potent antifouling activity against the larval

settlement of the barnacle *A. amphitrite*, with EC_{50} values of 1.65 and 0.55 µg/mL, respectively, without toxic effects.[42]

Bacterial compounds

Marine bacteria, including cyanobacteria, are considered as bountiful sources of active metabolites, including those preventing colonization of surface by organisms.[43] Dolastatin 16 (**60**) is probably the most potent and known cyanobacterial compound, inhibiting half of the settlement of barnacle larvae at a concentration of 0.003 µg/mL.[44] Originally isolated from the sea hare *Dolabella auricularia*, it was finally found to be a cyanobacterial compound produce by *Moorea producens* (previously *Lyngbya majuscula*) which is eaten by the sea hare.[45]

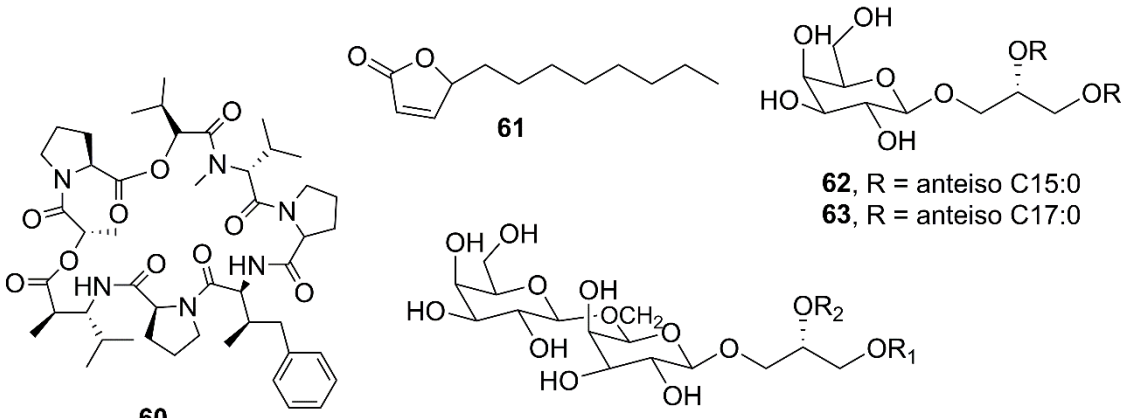

Butenolide (**61**), also known as 5-octylfuran-2(5*H*)-one, was isolated from the marine bacterium *Streptoverticillium luteoverticillatum*. It is considered as a very promising antifoulant, despite its simple structure. It was very effective in a 3-month antifouling field test. A study of its mode of action on the barnacle *A. amphitrite* and the bryozoan *B. neritina* showed that it acts on energy-related proteins. The animals became less active and so their competency to settle decreased.[46]

Four glycoglycerolipids (**62-65**) were isolated from the marine bacterium *Streptomyces coelescens* PK206-15 and showed potent antisettlement activity toward zoospore of the alga *Ulva pertusa* (EC_{50} of 0.008-0.03 µg/mL), the diatom *Navicula annexa* (EC_{50} of 0.005-0.03 µg/mL) and larvae of the mussel *Mytilus edulis* (EC_{50} of 0.009-0.2 µg/mL).[47]

Compounds from other sources

10-Isocyano-4-cadienne (**66**) is a sesquiterpene isolated from nudibranchs of the family *Phyllidiidae*. Test on larvae of the barnacle *A. amphitrite* revealed its potency as antifoulant, with an EC_{50} value of 0.14 µg/mL.[48]

Even if marine sources can be considered as "obvious" sources of antifouling compounds, terrestrial organisms can produce interesting compounds. Polygodial (**67**) was first isolated from the shrub *Tasmannia lanceolata* (Tasmanian native pepper). This sesquiterpene can strongly inhibit the settlement of different organisms, sush as the ascidian *Ciona savignyu*, the polychaeta *Spirobranchus caraniferus*, and the mussel *Mytilus galloprovincialis* at nanomolar scale.[49] Recently, a study showed that polygodial has an EC_{50} value of 0.25 µg/mL on *Amphibalanus improvises* but also that one of its synthetic analogue (**68**) was more potent on this sessile organism with an EC_{50} value of 0.1 µg/mL.[50]

Eugenol (**69**) is another compound from terrestrial plants. It can be extracted from certain essential oils, especially clove (*Syzygium aromaticum*), nutmeg (*Myristica argentea*) and cinnamon (*Cinnamomum verum*). It inhibits 50 % of the settlement of *A. amphitrite* larvae at 0.023 µM.[51]

Insects can also be a source of antifouling compounds, such as juvenoids which are juvenile hormones. The synthetic derivative 3,7-dimethyloctyl-2-methyl-5-pyridyl ether (**70**) displayed an EC_{50} value of 0.006 µg/mL. Moreover, test panels covered by paint containing the compound were kept in seawater for 8 months and no barnacle was found on them, showing the potency of this juvenoid.[52]

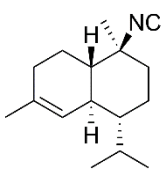

66

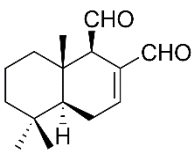

67

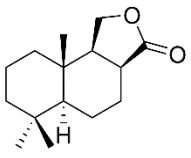

68

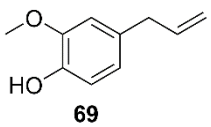

69

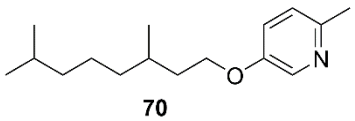

70

Using natural antifouling compounds as model in the paint industry seems promising. However, as generally active compounds are obtained in poor yields, commercial supply can be problematic. Still, some alternatives are available to overcome this issue, such as using easy culturable organisms such as bacteria, synthesize promising compounds or optimize studied of

structure/activity relationships to lead to even more active synthetic analogues based on natural models.[53]

Objective

As pointed out in this introduction, marine organisms are a great source of antifouling (AF) compounds and, even if hundreds have already been discovered, continuing research in this field is important. By discovering new antifoulants, we can have a better understanding of how biofoulers choose their surface, how they settle, how they metamorphosis, how they live. Each step can be controlled to avoid biofouling. So new active compounds should be isolated but also their mechanism of action should be studied to develop effective antifoulants for industrial applications. Moreover, if lots of antifoulants are discovered, it allows more structural diversity which avoids adaptation from biofoulers like we can see for bacteria becoming more resistant to antibiotics. Research of new antifouling compounds has ecological and economical importance but is also useful to understand biofoulers physiology. To continue a project aiming at isolating AF molecules from Red Sea organisms, about eighty extracts were tested on barnacle larvae of *A. amphitrite*.[36]

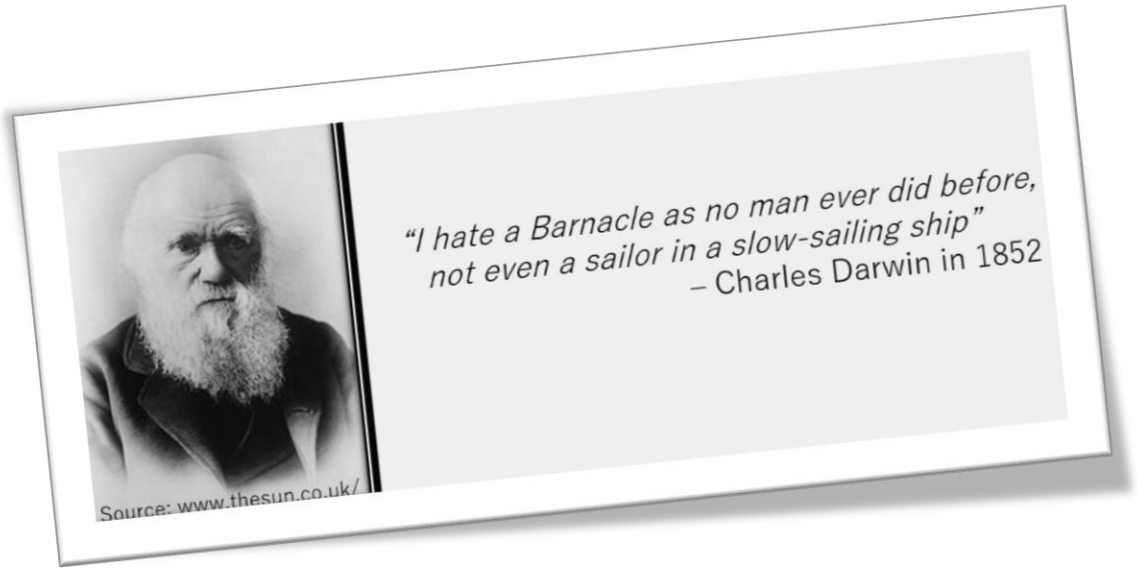

"I hate a Barnacle as no man ever did before, not even a sailor in a slow-sailing ship" said Charles Darwin in 1852, after years and years studying and classifying barnacles but we can keep this citation to illustrate an historical problem which continues nowadays: biofouling

and among this phenomenon, barnacles which are hard to remove.[54] That is why in this study, antifouling assays were conducted on barnacle larvae.

About 51 % of the tested extracts were inactive (not active at 10 µg/mL), 31% were moderately active (active at 10 µg/mL but not at 1 µg/mL) and only 18% were very active (active at 1 µg/mL). However, among these very active extracts, lots were from cyanobacteria and very toxic (Appendix S1-S5). Nonetheless, the cyanobacterium *Okeania* sp. was picked out among the very active non-toxic extracts because cyanobacteria are not well studied for AF compounds. Moreover, as cyanobacteria are more easily culturable at large industrial scale, they could be promising source of bioactive compounds, for antifouling but also pharmaceutical industries. *Hyrtios* sp. extract displayed moderate activity but was also studied because of its large amount of material, and also because sponges are prolific producers of AF compounds. Chapter I deals with the isolation, structure elucidation and activity of three compounds from this parazoa: *N*-phenethylacetamide, methyl-(5*Z*,9*Z*)-hexacosa-5,9-dienoate and methyl-(*Z*)-octadec-11-enoate. Chapter II covers the isolation, structure elucidation and bioactivities of two new fatty acid amides, serinolamides C and D, from this cyanobacterium, while Chapter III concerns the new lyngbyabellins O and P, the known lyngbyabellins F, G and H, 27-deoxylyngyabellin A and dolastatin 16 from this same archaic organism.

- Chapter I -

N-Phenethylacetamide and fatty acid methyl esters from the sponge *Hyrtios* sp.

A *Hyrtios* sp. sponge was collected in the Red Sea. The *n*-BuOH fraction showing great antifouling towards *Amphibalanus amphitrite* was further partitioned by ODS open-column chromatography. HPLC purification afforded *N*-phenethylacetamide (**71**) and two fatty acid methyl esters (FAMEs): methyl-(5*Z*,9*Z*)-hexacosa-5,9-dienoate (**72**) and methyl-(*Z*)-octadec-11-enoate (**73**). This chapter aims at describing their isolation, the structure elucidation and their bioactivities.

I. 1. Isolation of *N*-phenethylacetamide, methyl-(5*Z*,9*Z*)-hexacosa-5,9-dienoate and methyl-(*Z*)-octadec-11-enoate

I. 1. 1. Materials and Methods

I. 1. 1. a. Experimental Procedures

LC-MS data were obtained on an Agilent 1100 Series HPLC system coupled with a Bruker Daltonics micrOTOF-HS mass spectrometer, which was configured for electrospray ionization (ESI). The HPLC system was equipped with a Cadenza CD-C18 column (2 × 150 mm, 3 µm, 0.2 mL/min, 25 °C). The HPLC system was operated under the following conditions: 0–20 min, linear gradient from 50% to 100% MeCN with 0.1% (*v/v*) formic acid in

MilliQ H_2O; 20–35 min, isocratic 100% MeCN with 0.1% (*v/v*) formic acid. Preparative HPLC purifications were conducted over a Cosmosil Cholester column (10 × 250 mm, 5 µm) at a flow rate of 3 mL/min, with UV detection at 210 nm, except when other conditions are mentioned.

I. 1. 1. b. Biological material

The *Hyrtios* sp. sponge was collected twice (in 2013 and in 2015) in the Red Sea, near Jeddah, Saudi Arabia. It was identified by its morphology. Foreign particles were removed by hand and the samples went through homogenization and MeOH extraction. Solvent was evaporated and samples sent as it was from Saudi Arabia to Japan.

I. 1. 1. c. Extraction and Isolation

Figure I. 1 shows the isolation scheme used to obtain *N*-phenethylacetamide (**71**). The first dried MeOH extract (2.7 g) was partitioned between EtOAc and H_2O (1:1, *v/v*). The H_2O fraction was further purified using *n*-BuOH (1:1, *v/v*). The dried *n*-BuOH fraction (0.5 g) was purified by RP-column chromatography over ODS. A stepwise gradient composed of MeOH and H_2O (2:8, 4:6, 6:4, 8:2, 100:0 *v/v*), followed by MeOH and $CHCl_3$ (100:0, 75:25, 0:100 *v/v*) was used. Isolation of compounds from the 6:4 MeOH/H_2O fraction was performed using semi-preparative RP-HPLC (Cosmosil Cholester 10 x 250 mm, gradient 0–50 min, 20%–80% MeCN). The fraction eluted at 14.0 min was further purified by RP-HPLC (Cosmosil Cholester 10 x 250 mm, gradient 0–30 min, 20%–35% MeCN) to yield **71** (t_R 16.3 min, 4.7 mg).

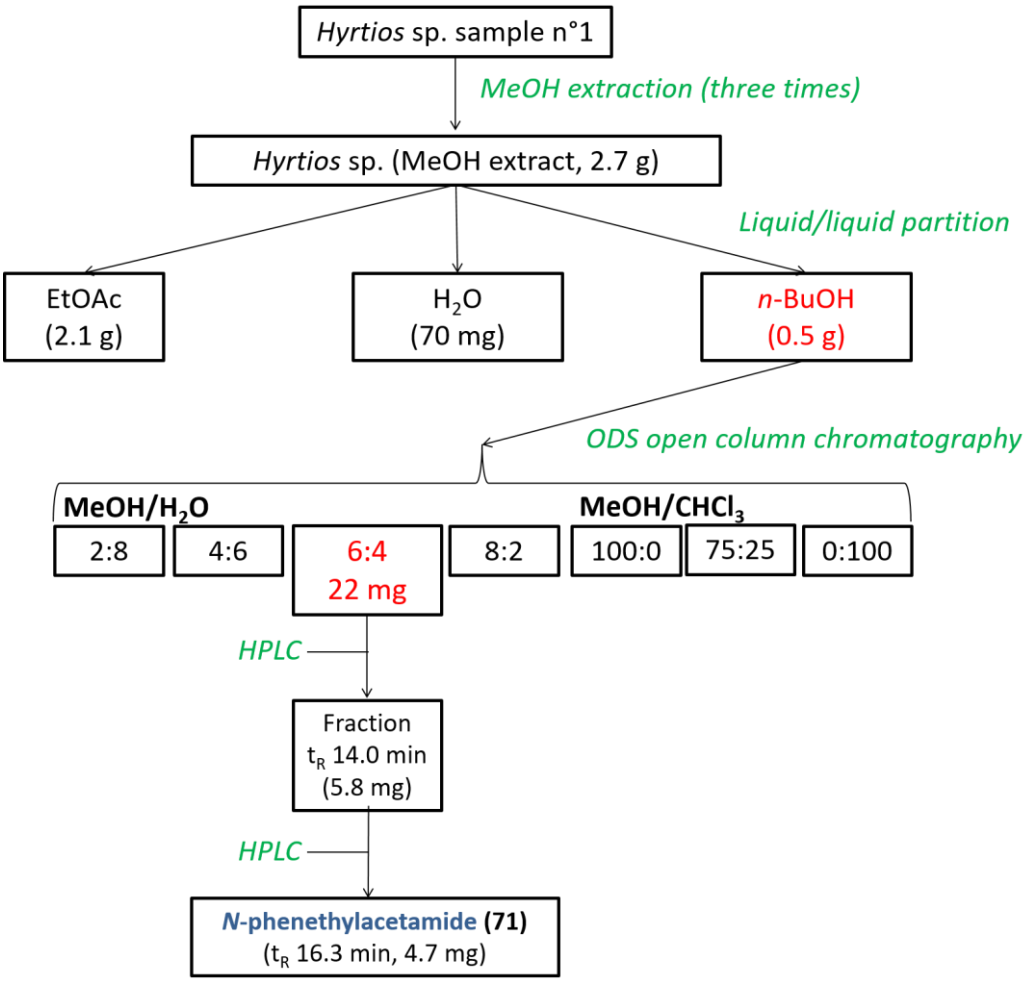

Figure I. 1: Isolation scheme for **71**.

Figure I. 2 shows the isolation scheme used to obtain the two FAMEs: methyl-(5*Z*,9*Z*)-hexacosa-5,9-dienoate (**72**) and methyl-(*Z*)-octadec-11-enoate (**73**). The second dried MeOH extract (10 g) was partitioned as the first one and RP-column chromatography was performed at previously described. Semi-preparative RP-HPLC fractionation was used to partition the biggest fraction, the 100 % MeOH (0.9 g) one (column: Cosmosil 5C18-MS-II 10 x 250 mm; gradient 0–30 min, 75%–100% MeCN, 3 mL/min). The fraction eluted between 39.5 and 41.1 min was further purified by RP-HPLC (gradient 0–30 min, 95-100 % MeCN) to yield **73** (t_R

12.6 min, 2.5 mg). The fraction eluted at 101.5 min was further purified by RP-HPLC (isocratic 100 % MeOH) to give **72** (t_R 32.7 min, 3.6 mg).

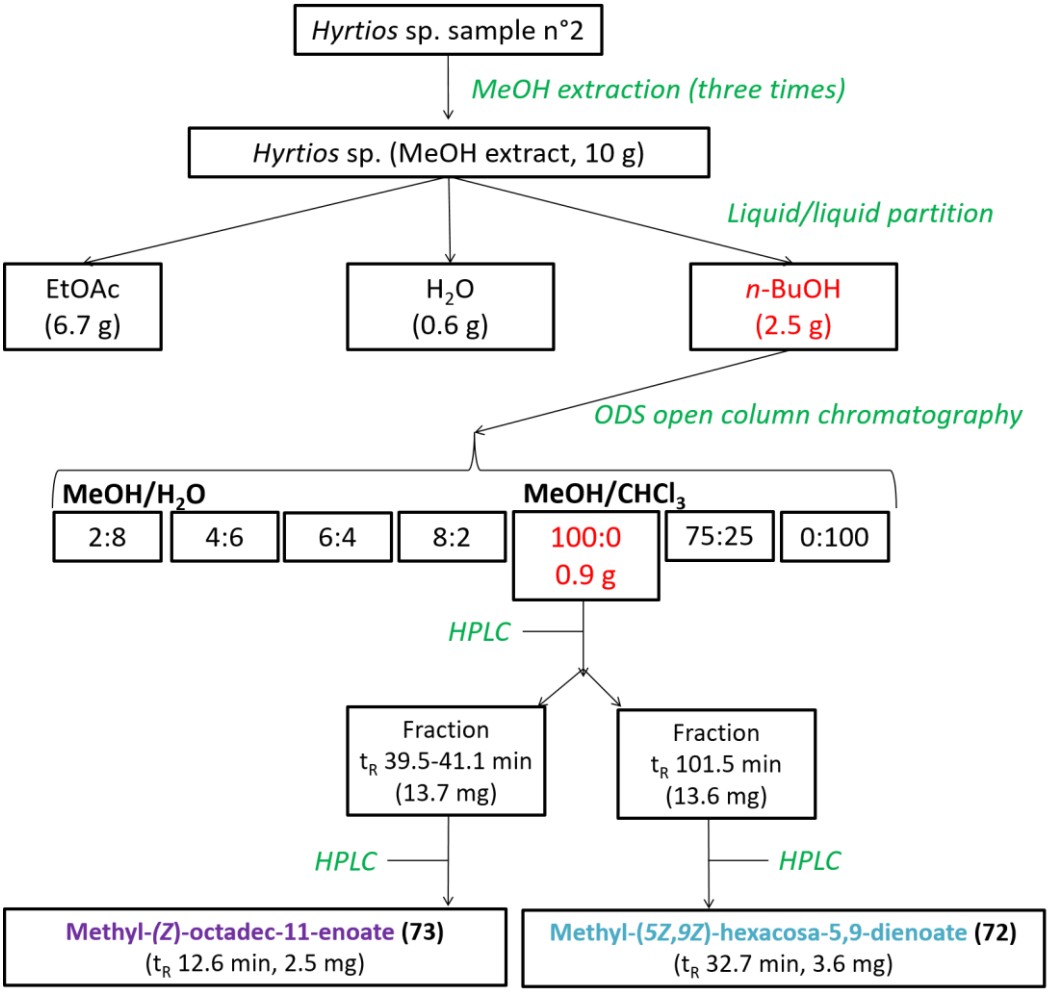

Figure I. 2: Isolation scheme for **72** and **73**.

I. 1. 2. Results

The MeOH extract was partitioned between EtOAc and H_2O, and the aqueous fraction was further partitioned with *n*-BuOH. The *n*-BuOH fraction was separated into seven subfractions by reverse-phase (RP) column chromatography. The 6:4 MeOH/H_2O and the 100% MeOH were purified by HPLC and gave **71** (4.7 mg) and the two FAMEs **72** (3.6 mg) and **73** (2.5 mg), respectively.

I. 2. Characterization of *N*-phenethylacetamide

I. 2. 1. Materials and Methods

The ^{1}H and ^{13}C NMR spectra for *N*-phenethylacetamide (**71**) were recorded on a JEOL 400 MHz spectrometer, whereas their 2D NMR spectra were recorded on a Bruker Advance 300 MHz. All the NMR spectra were recorded in $CDCl_3$ (Cambridge Isotope Laboratories, Inc.) using the residual solvent peak ($CHCl_3$) as an internal reference (δ_H 7.27 and δ_C 77.00 ppm).

I. 2. 2. Results

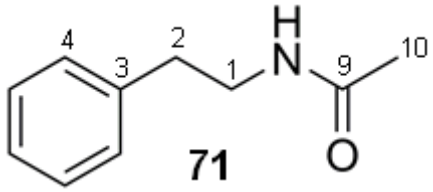

71

The planar structure of **71** was elucidated using NMR and MS analyses. Its molecular formula was determined to be $C_{10}H_{13}NO$ by ESI-TOF-MS, indicating 5 degrees of unsaturation. ^{1}H and ^{13}C NMR analyses (Table I. 1) revealed the characteristic signals of a monosubstituted benzene ring (five protons at δ_H 7.17-7.35, six carbons at δ_C 126.7–128.9 and 139.0 ppm). HMBC spectrum (Figures I. 3 and 8) revealed that a methylene (δ_H 2.82, δ_C 35.7) was attached to this quaternary carbon, but also to an additional methylene (δ_H 3.52, δ_C 40.7). This last methylene also showed HMBC with this quaternary carbon, and COSY correlation (Figures I. 3 and 6) with a proton giving a broad signal at δ_H 5.50 ppm. This proton did not show any correlation on the HSQC spectrum (Figure I. 7). It could be attached to the oxygen or the nitrogen revealed by the determination of the molecular formula of the compound. However, the carbonyl (δ_C 170.3) eliminated the possibility of the presence of a hydroxy group, thus revealing an amino proton. HMBC showed a methyl group (δ_H 1.94, δ_C 20.8) attached to the

carbonyl group (δ_C 170.3), giving an acetyl group. The methylene at δ_C 40.7 was correlated to the carbonyl of this acetyl group. All these observations gave the all structure of **71**.

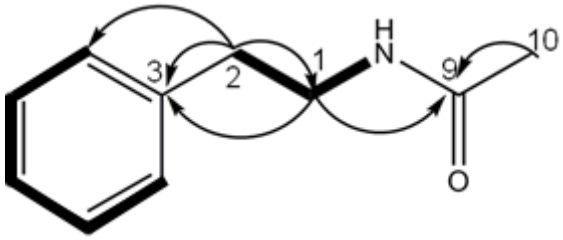

Figure I. 3: COSY and HMBC of **71**.

Table I. 1: NMR Spectroscopic Data (^{1}H 400 MHz, ^{13}C 100 MHz, $CDCl_3$) for *N*-phenethylacetamide (**71**).

position	δ_C, type	δ_H (*J* in Hz)	HMBC[a]	COSY[a]
1	40.7, CH_2	3.52, m	9, 3	2, NH
2	35.7, CH_2	2.82, m	1, 3, 4	1
3	139.0, C			
4	128.9 CH	7.32, m		5
5	128.8, CH	7.20, m		4, 6
6	126.7, CH	7.19, m		5, 7
7	128.8, CH	7.20, m		6, 8
8	128.9, CH	7.32, m		7
9	170.3, C			
10	23.4, CH_3	1.94, s	9	
NH		5.50, br		1

[a]HMBC data optimized for 8 Hz are from proton(s) stated to the indicated carbon.

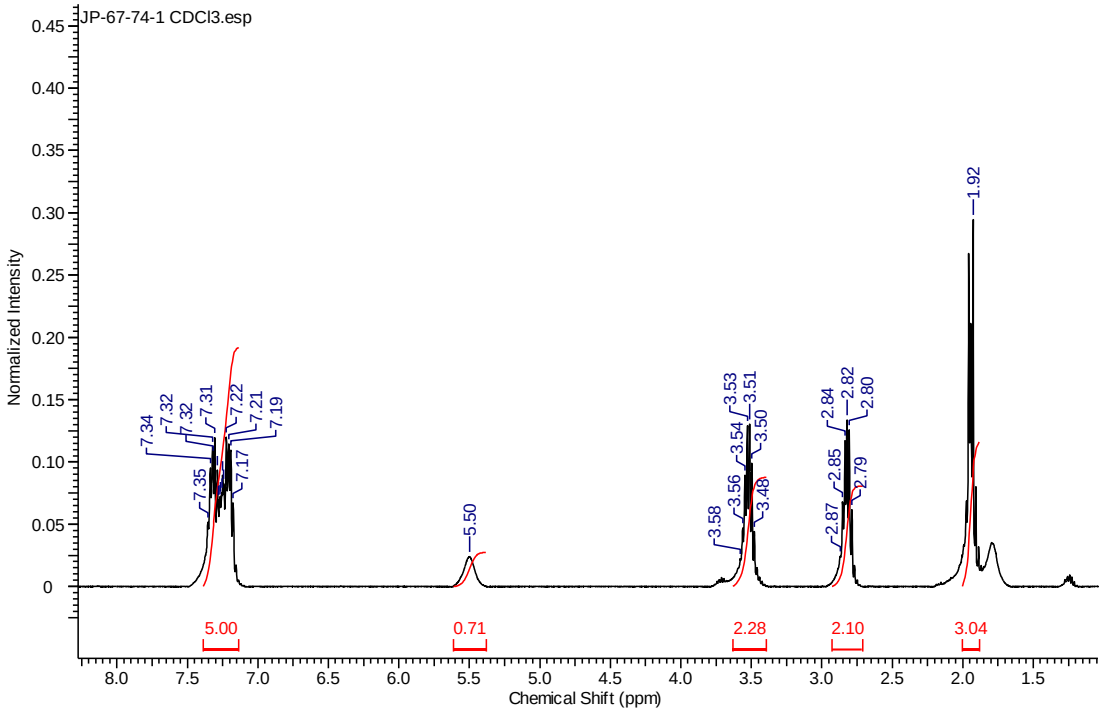

Figure I. 4: ^{1}H NMR spectrum of **71** (400 MHz, $CDCl_3$).

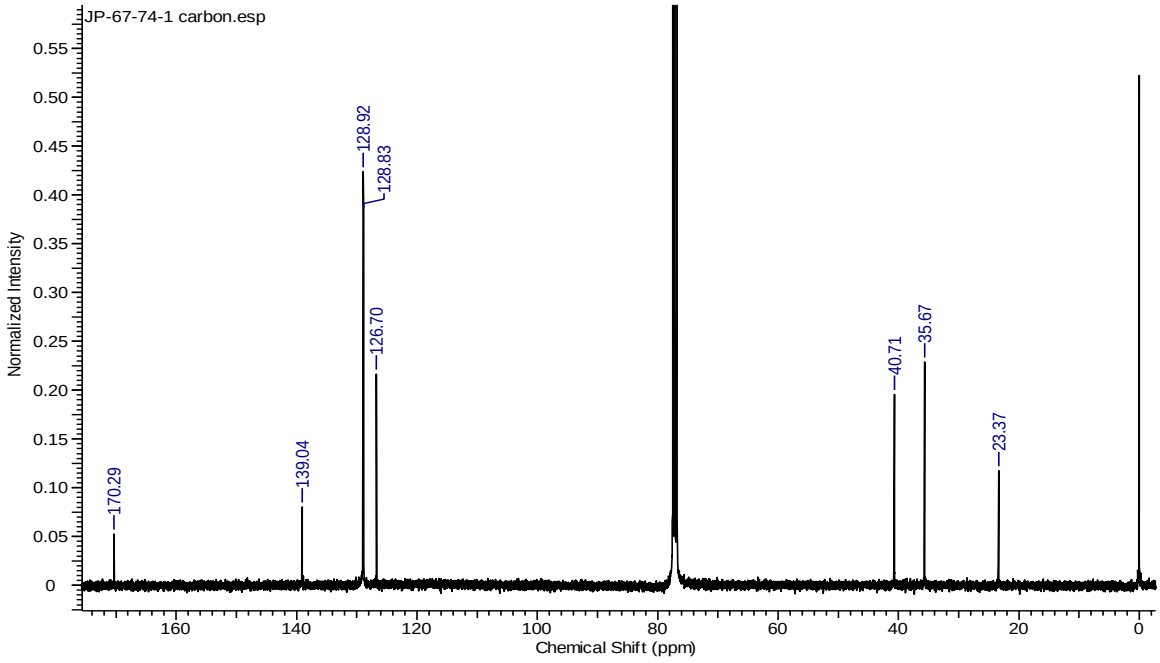

Figure I. 5: ^{13}C NMR spectrum of **71** (100 MHz, $CDCl_3$).

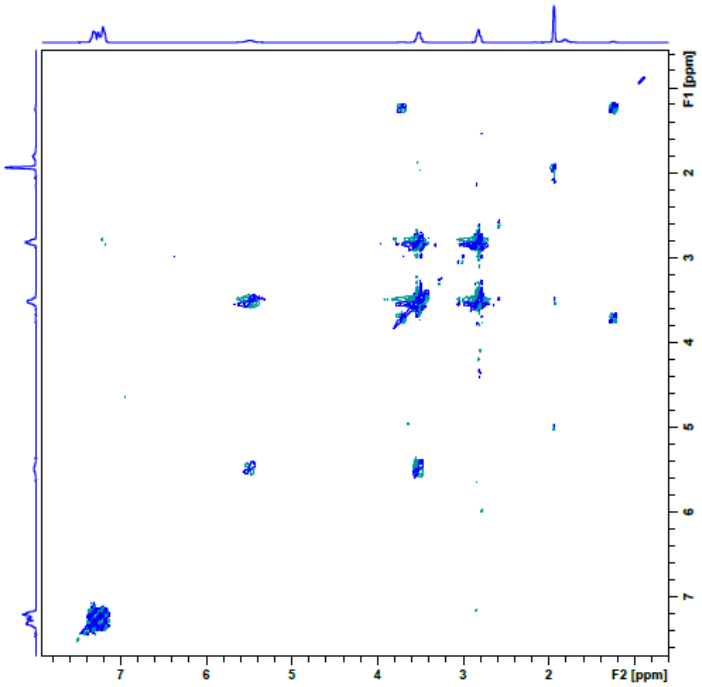

Figure I. 6: COSY spectrum of **71** (300 MHz, $CDCl_3$).

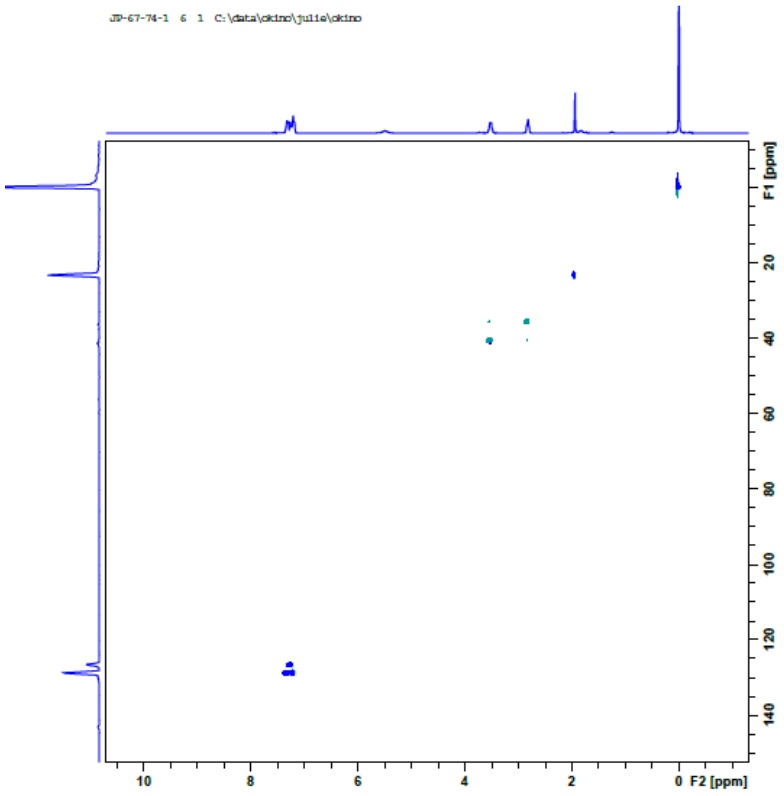

Figure I. 7: HSQC spectrum of **71** (300 MHz, $CDCl_3$).

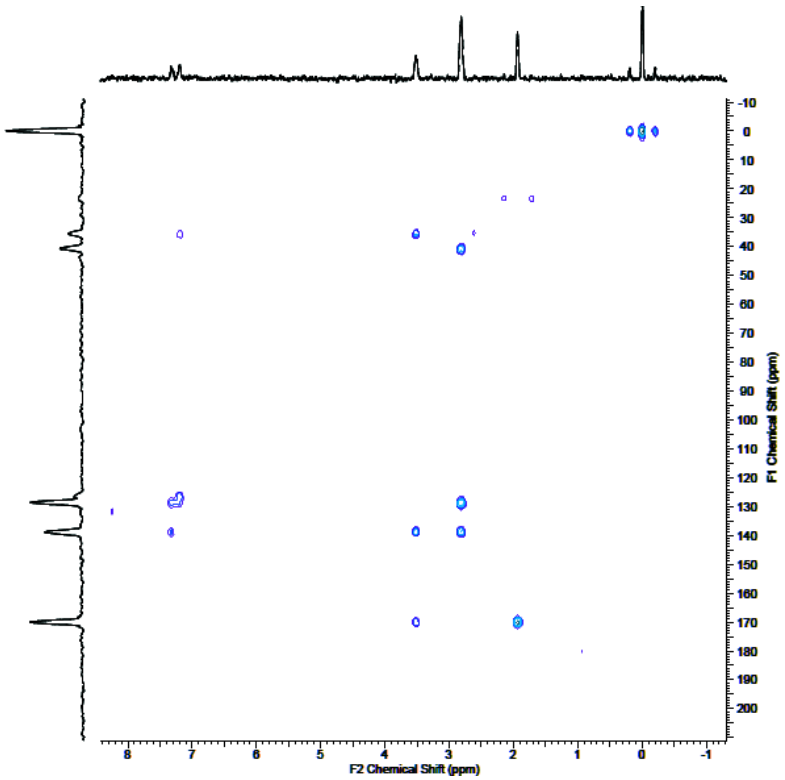

Figure I. 8: HMBC spectrum of **71** (300 MHz, $CDCl_3$).

I. 3. Characterization of methyl-(5*Z*,9*Z*)-hexacosa-5,9-dienoate and methyl-(*Z*)-octadec-11-enoate

I. 3. 1. Materials & Methods

I. 3. 1. a. General Experimental Procedures

Same instruments as for **71** were used for the two FAMEs **72** and **73**.

IR spectra were recorded on a JASCO FT/IR-4100 type A. GC-MS data were obtained on a Varian CP-3800 GC system coupled with a Varian 1200L mass spectrometer which was configured for electron ionization (EI) at 70 eV. The ion temperature of the ion source was 250

°C. The column used was a GL Sciences TC-5 (30 m, 0.25 mm ID, 0.25 µm film), the carrier gas was helium and the injector temperature was 250 °C.

For measurement of the DMDS adducts of **72** and **73**, flow rate was 1.5 and 1.2 mL/min, respectively. The oven temperature program for **72** was as followed: 0-1 min: 80 °C, then 40 °C/min to 240 °C, then 2 °C/min to 250 °C and 1 °C/min to 260 °C. For **73**, the oven temperature program was: 0-1 min: 120 °C, then 40 °C/min to 280 °C, 2 °C/min to 300 °C and then 1 °C/min to 305 °C.

I. 3. 1. b. Derivatization of the FAMEs and GC-MS

Both **72** and **73** were derivatized to elucidate the position of their double bonds. The FAMEs (0.2 mg) were dissolved in dimethyl disulfide (DMDS, 0.2 mL) and a solution of iodine in diethyl ether (0.05 mL of a 60 mg/mL) was added. The reaction was let at room temperature for 24 hours. Hexane (5 mL) was then added and the mixture washed with sodium thiosulfate (5 % solution) to reduce the excess of iodine. The organic layer was collected. The aqueous layer was washed with hexane and the new organic layer also collected. The combined organic layers were dried over a steam of Ar.[55] The samples were then analyzed by GCMS.

I. 3. 1. c. Absolute configuration of the FAMEs

^{13}C Nondecoupled HSQC with ^{1}H homodecoupling technique was used for both FAMEs to determine the absolute configuration of their double bonds. A JEOL 600 MHz spectrometer was used to record the spectra.

I. 3. 2. Results

I. 3. 2. a. Planar structure of the FAMEs

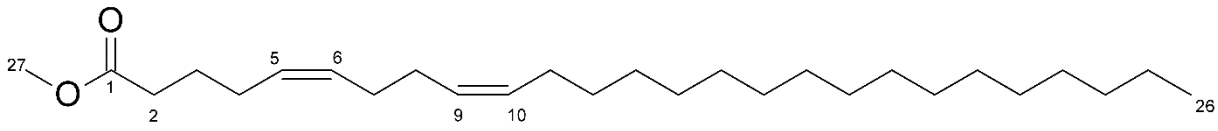

72

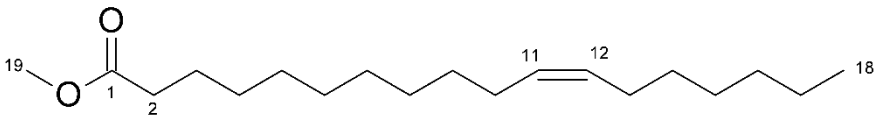

73

The planar structure of **72** was elucidated using NMR and MS analyses. Its molecular formula was determined to be $C_{27}H_{50}O_2$ by GC-MS, indicating 3 degrees of unsaturation (Figure I. 9). The ^{1}H and ^{13}C NMR spectra (Figures I. 11 and 12, Table I. 2) showed four olefinic protons at δ_H 5.38 and four olefinic carbons (δ_C 128.9-130.6, C-5, C-6; C-9 and C-10). They accounted for two degrees of unsaturation in the molecule. The remaining degree of unsaturation was the ester carbonyl at δ_C 174.3 (C-1), which showed a HMBC cross-peak (Figures I. 10 and 15) with a methoxy at δ_C 51.7 (C-27), forming a methyl ester. The 1D NMR spectra revealed characteristic signals of a terminal methyl (C-26) of fatty acid at δ_C 14.0 and δ_H 0.89, and broad signals at δ_H 1.26 for methylene protons. All these observations suggested the fatty acid methyl ester nature of the compound. COSY correlations between H-6 and H-7, H-7 and H-8, and H-8 and H-9 showed the diene nature of **72**. 2D data also revealed the position of the double bonds to be at C-5 and C-9.

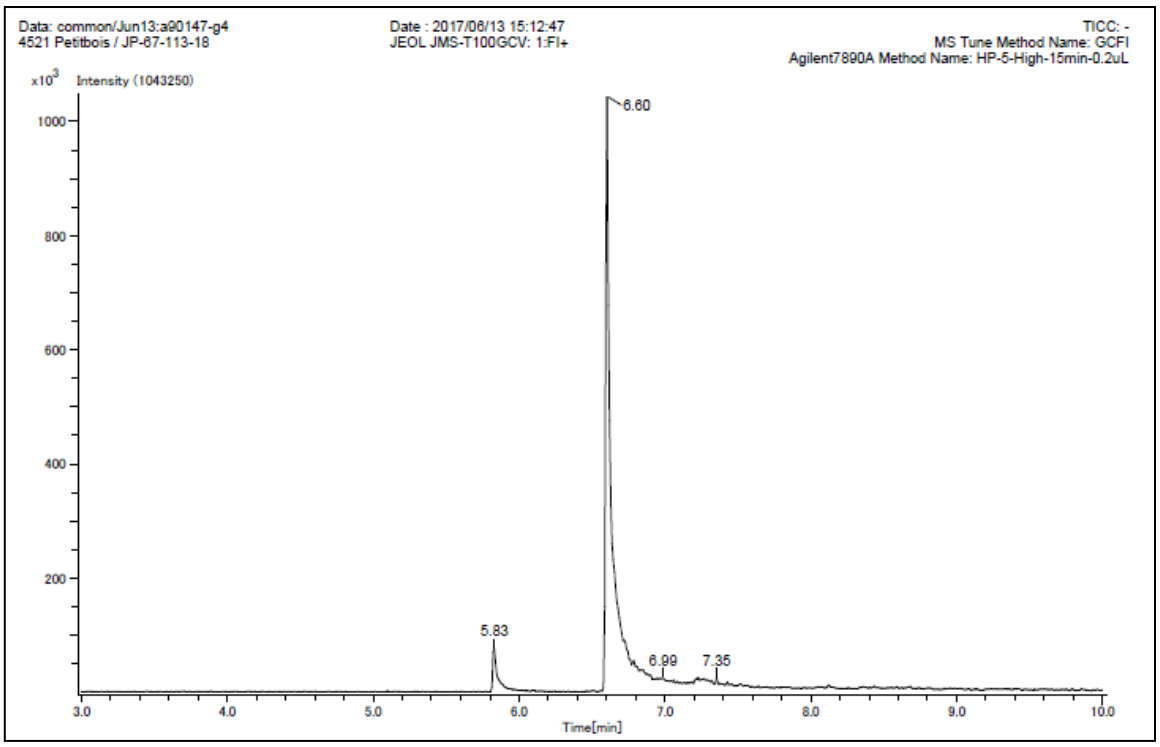

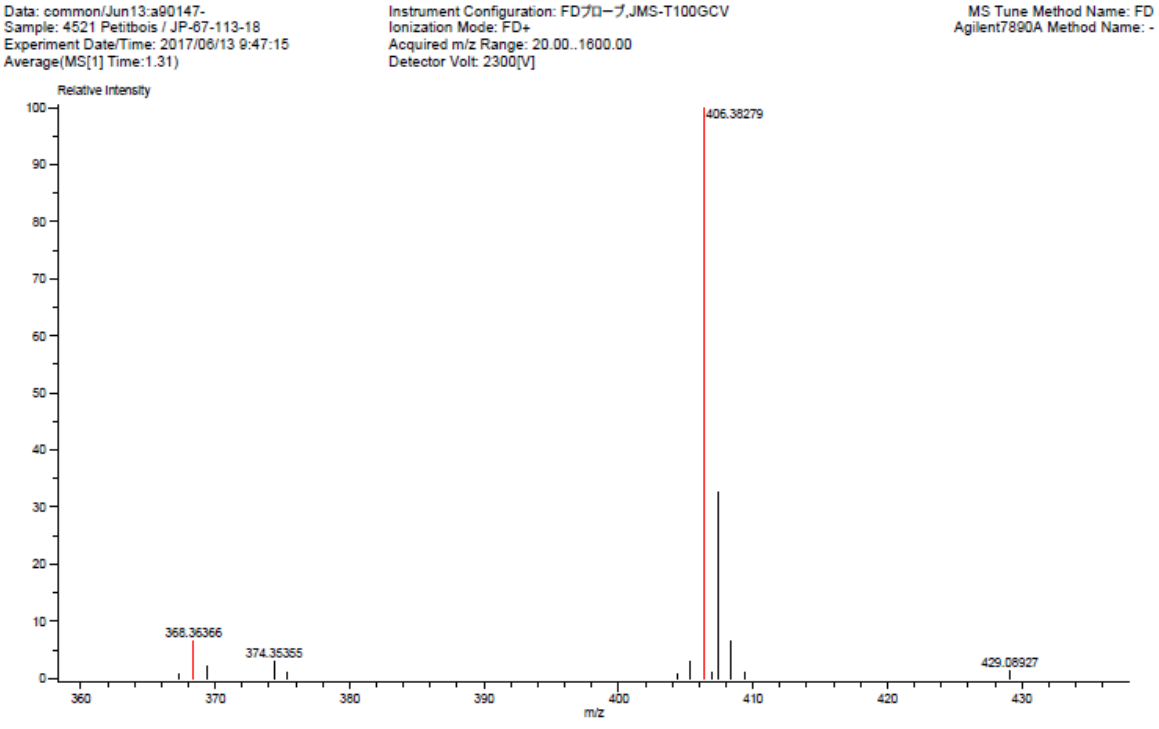

Charge number:1 Tolerance:5.00(mmu)

Element:^{12}C:0 .. 100, ^{1}H:0 .. 200, ^{16}O:0 .. 10

Mass	Calc. Mass	Mass Difference (mmu)	Mass Difference (ppm)	Possible Formula	Unsaturation Number
368.36366	368.36543	-1.77	-4.80	$^{12}C_{24}{}^{1}H_{48}{}^{16}O_2$	1.0
406.38279	406.38108	1.72	4.22	$^{12}C_{27}{}^{1}H_{50}{}^{16}O_2$	3.0

Figure I. 9: GC-MS chromatogram obtained with 7**2.**

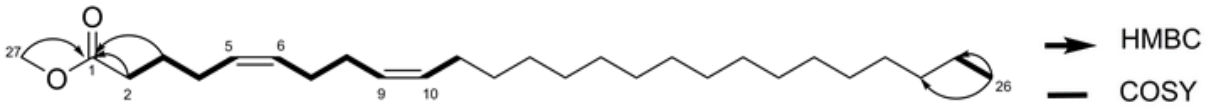

Figure I. 10: COSY and HMBC correlations for **72.**

Table I. 2: NMR spectrometric data (^{1}H 400 MHz, ^{13}C 100 MHz, $CDCl_3$) for methyl-(5*Z*,9*Z*)-hexacosa-5,9-dienoate (**72**).

position	δ_C, type	δ_H (*J* in Hz)	HMBC[a]	COSY[a]
1	174.3, C			
2	33.4, CH_2	2.32, t (7.2)	1	3
3	24.8, CH_2	1.70, dt (8.0, 14.0)	1	2, 4
4	26.5, CH_2	2.02-2.08, m		3, 5
5	130.6, CH	5.38, m		4
6	130.5, CH			7
7	27.3, CH_2	2.02-2.08, m		6, 8
8	27.2, CH_2			7, 9
9	129.0, CH	5.37, m		
10	128.9, CH			11
11	27.3, CH_2	2.02-2.08, m		10, 12
12-23	29.3-29.7, CH_2	1.26, m		
24	31.9, CH_2	1.26, m		
25	22.6, CH_2	1.26, m		26
26	14.0, CH_3	0.89, t (6.8)	24, 25	25
27	51.4, CH_3	3.67, s	1	

[a]HMBC data optimized for 8 Hz are from proton(s) stated to the indicated carbon.

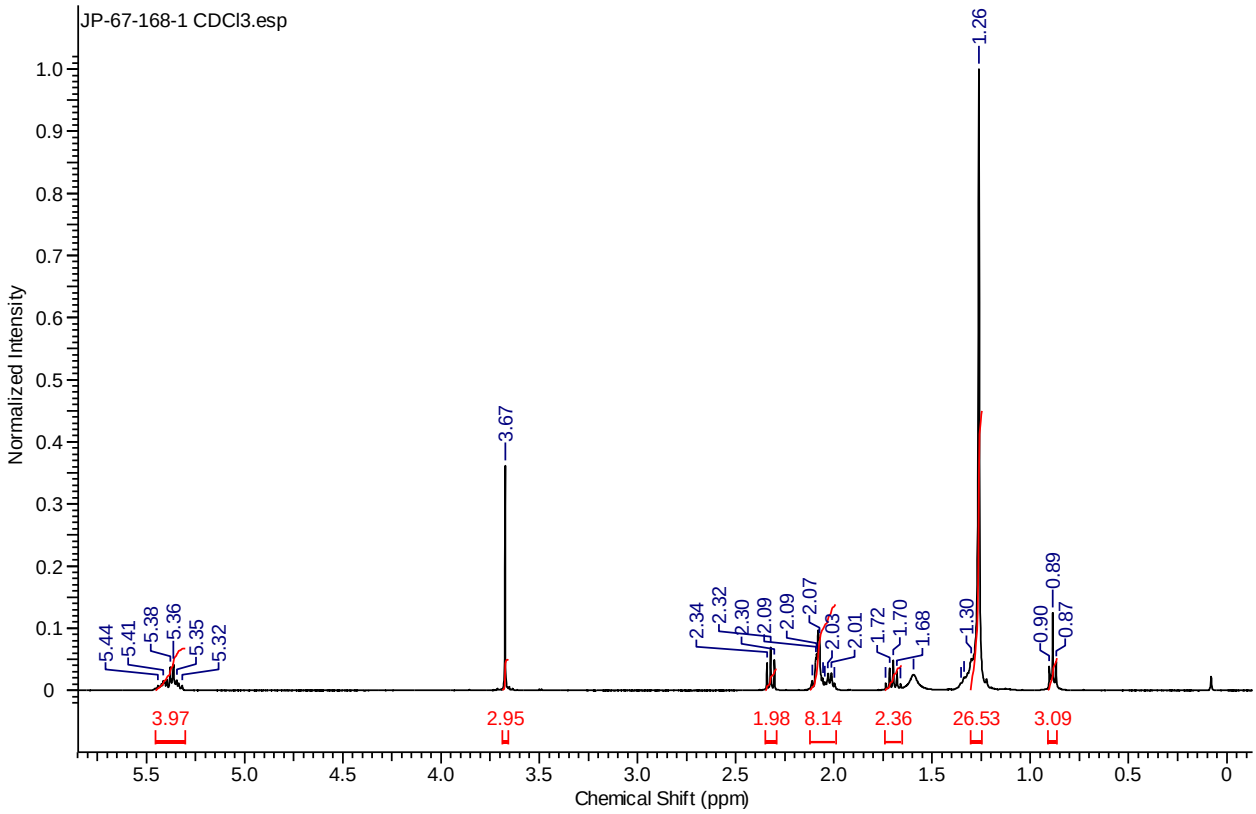

Figure I. 11: ^{1}H NMR spectrum of **72** (400 MHz, $CDCl_3$).

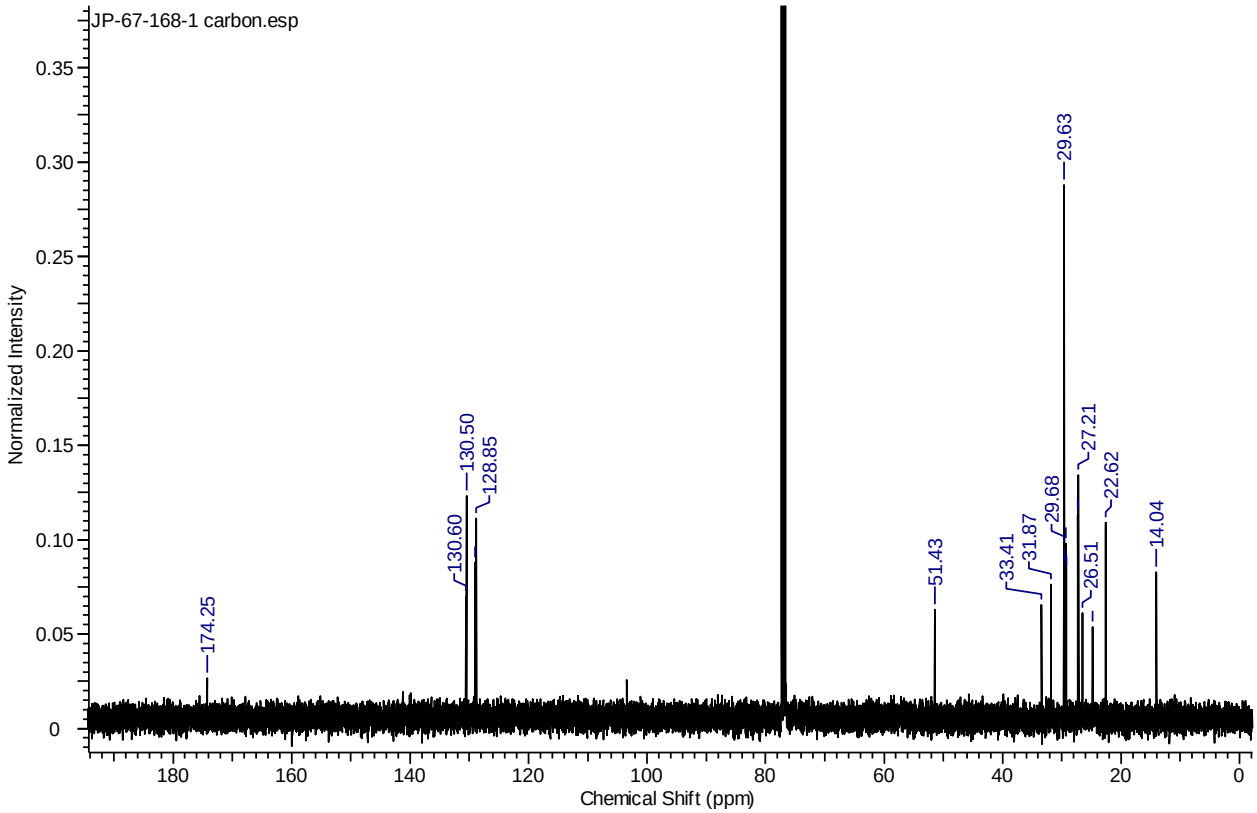

Figure I. 12: ^{13}C NMR spectrum of **72** (100 MHz, $CDCl_3$).

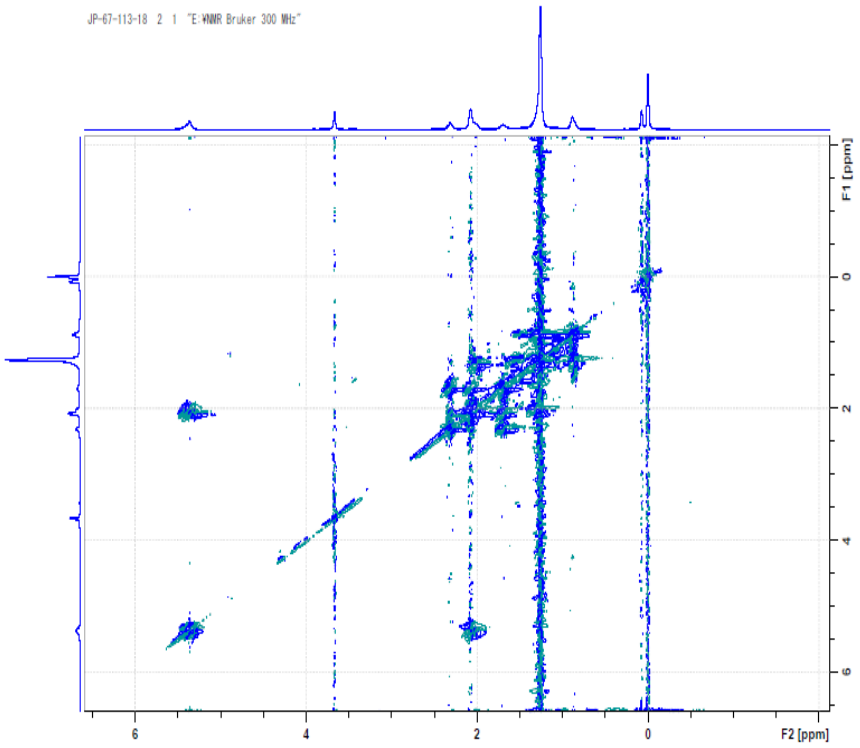

Figure I. 13: COSY spectrum of **72** (300 MHz, $CDCl_3$).

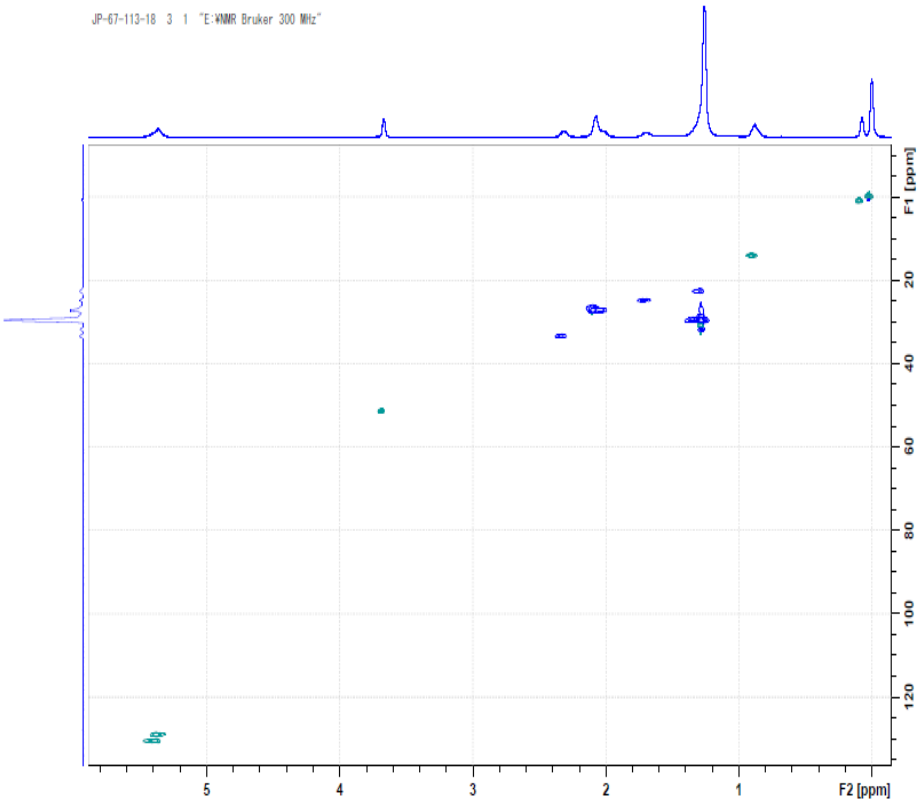

Figure I. 14: HSQC spectrum of **72** (300 MHz, $CDCl_3$).

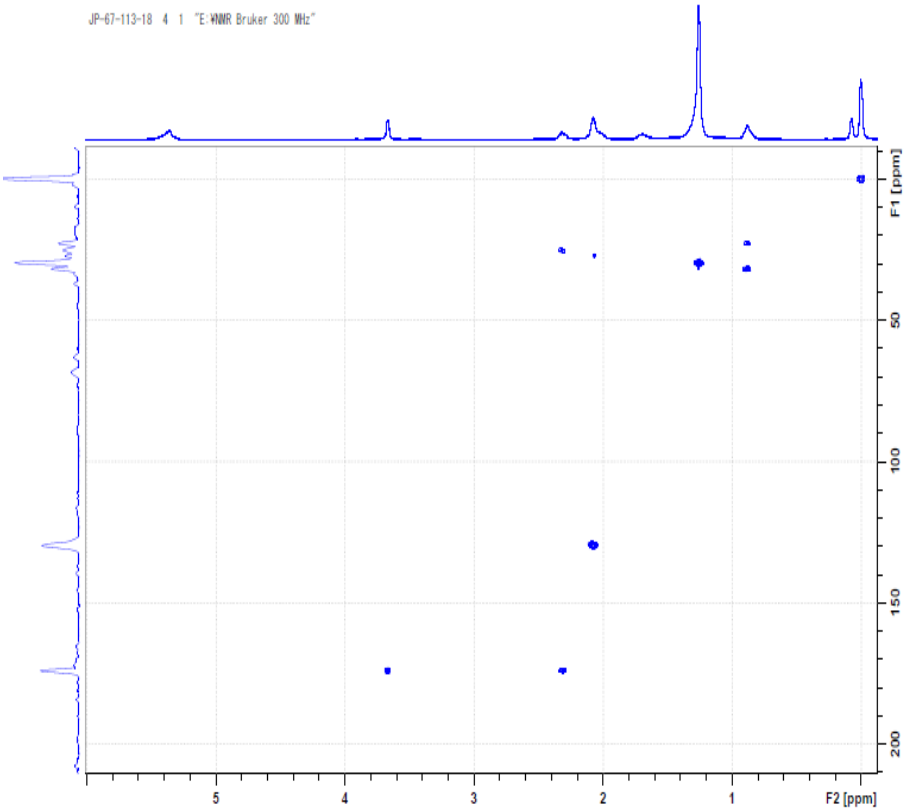

Figure I. 15: HMBC spectrum of **72** (300 MHz, $CDCl_3$).

The position of the double bonds of **72** was confirmed by derivatization with DMDS and study of the fragmentation by GC-MS/MS. The dimethyl disulfide adducts are formed by a one-step reaction by "fixation" of the DMDS to the double bonds. Then, by GC-MS/MS, a cleavage occurs between the olefinic carbons and this leads to two main fragment ions: the one containing the terminal methyl part, and the one with the methyl ester part. Another ion corresponding to the latter fragment with the loss of the elements of methanol could also be observed.

In the case of close double bonds in dienoic fatty acid methyl esters (double bonds separated by one, two or three methylene groups), several products can occur. When mild conditions are used (short time reaction and low temperature), only one double bond reacts, giving an equimolar mixture of monoadducts.[56] However, when vigorous conditions are chosen

(higher temperature up to 60 °C and longer reaction times such as 40 hours), a second mole of DMDS is added and cyclization occurs, given different heterocyclic compounds.[57]

Two adducts were obtained with **72** (Figure I. 16) and observable by GC-MS with an *m/z* of 500 (Figure I. 17). Their fragmentation pattern led to the confirmation of the position of the double bonds. The key fragments were observed at *m/z* 161 for $[C_7H_{13}O_2S]^+$ and *m/z* 339 for $[C_{22}H_{43}S]^+$, showing a cleavage between C-5 and C-6, and at *m/z* 215 for $[C_{11}H_{19}O_2S]^+$ and *m/z* 285 for $[C_{18}H_{37}S]^+$, showing a cleavage between C-9 and C-10 (Figure I. 18).

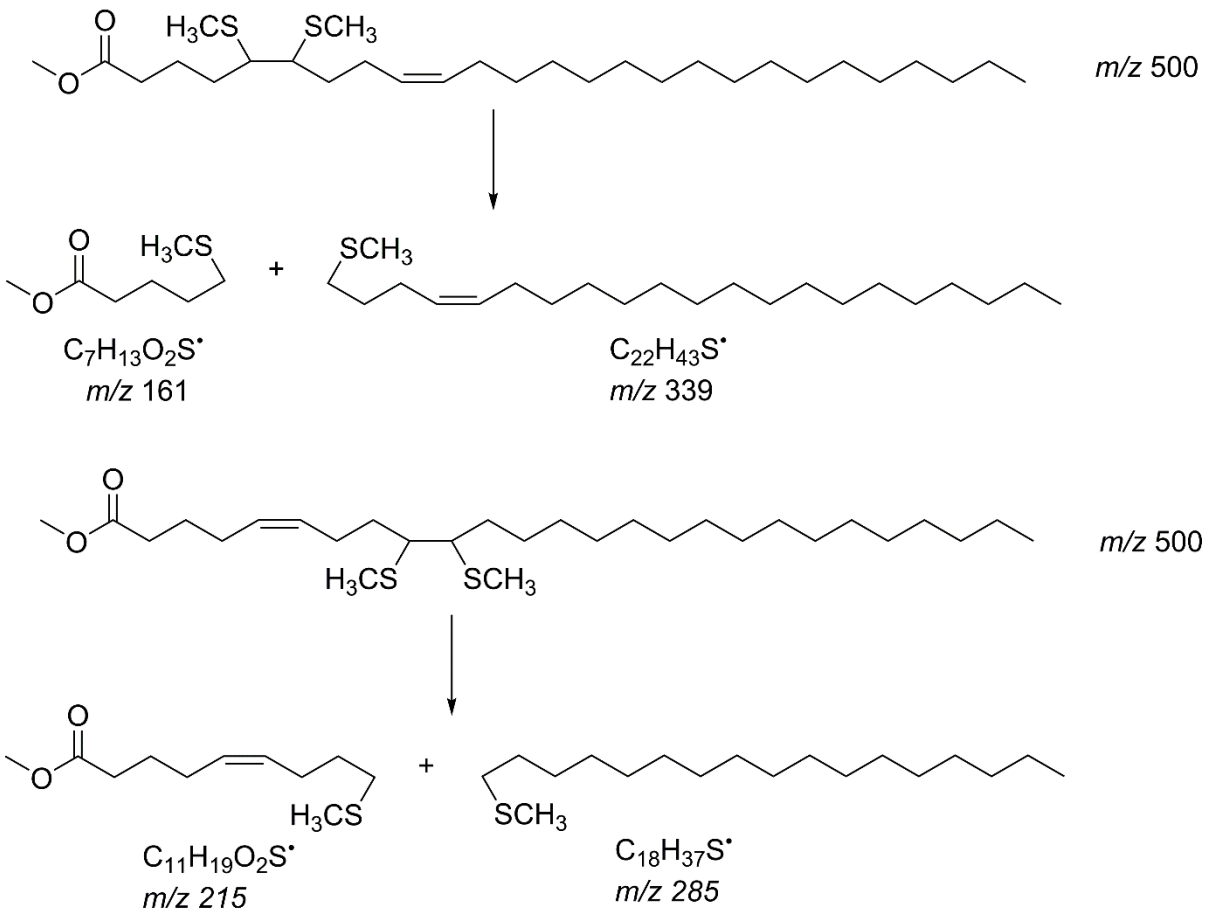

Figure I. 16: DMDS adducts obtained from **72** under mild conditions.

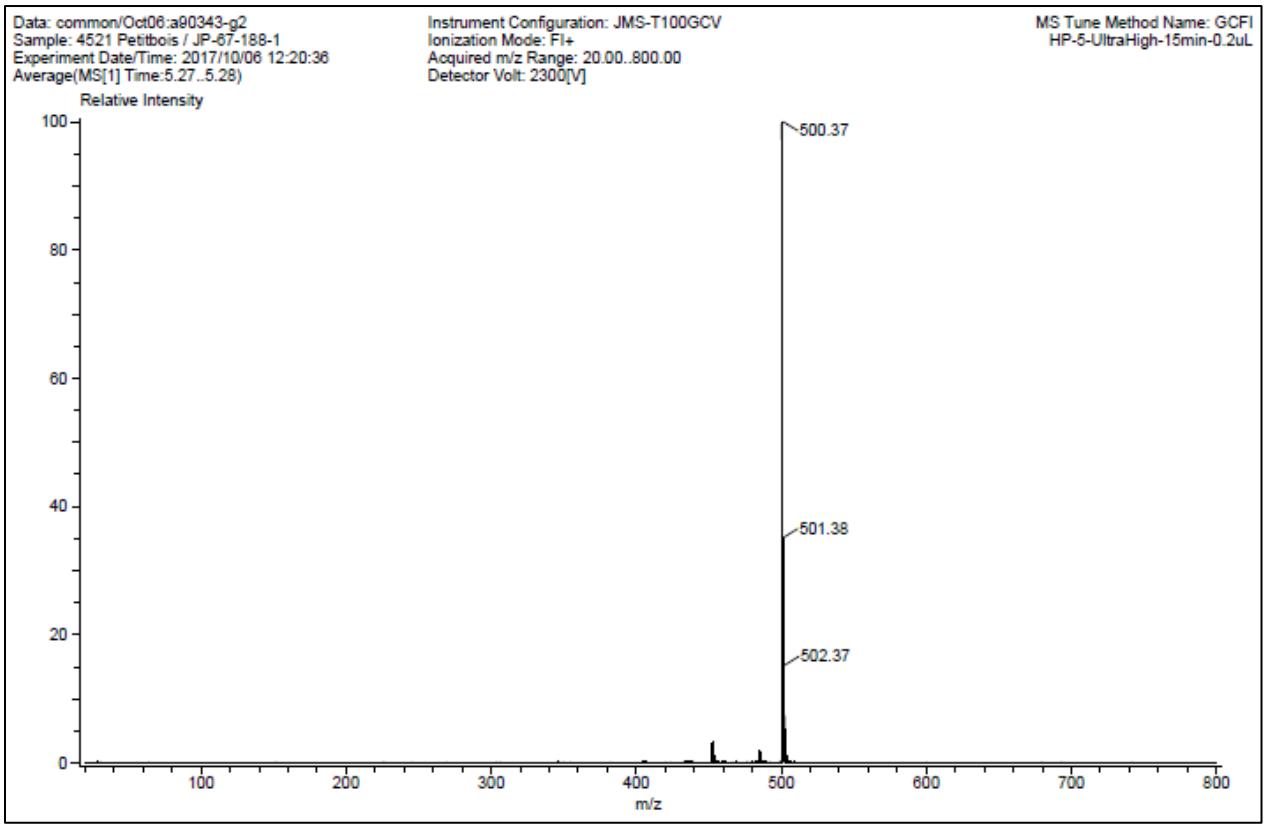

Figure I. 17: MS of the adducts obtained from **72** with mild conditions.

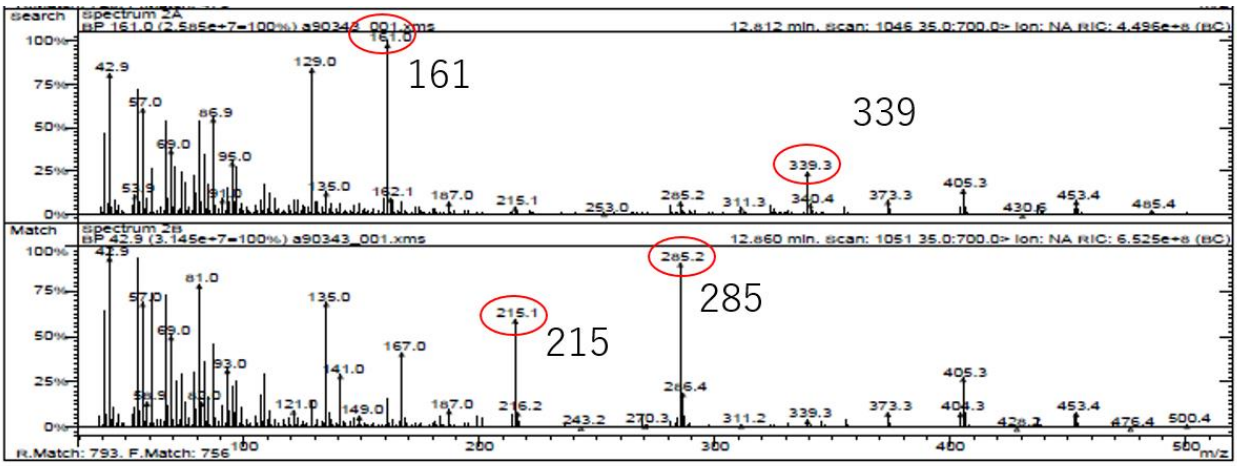

Figure I. 18: MS-MS of the two adducts obtained from **72** with mild conditions.

The planar structure of **73** was elucidated using NMR and MS analyses. Its molecular formula was determined to be $C_{19}H_{38}O_2$ by GC-MS, indicating two degrees of unsaturation (Figure I. 19).

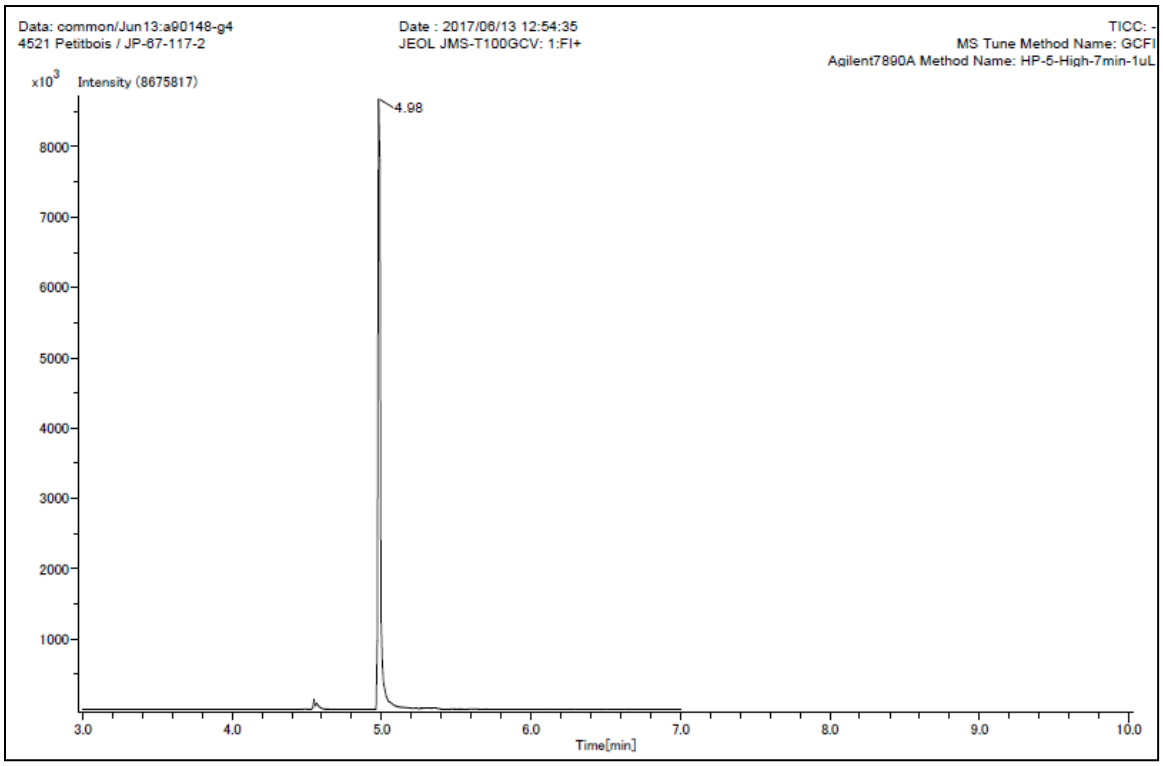

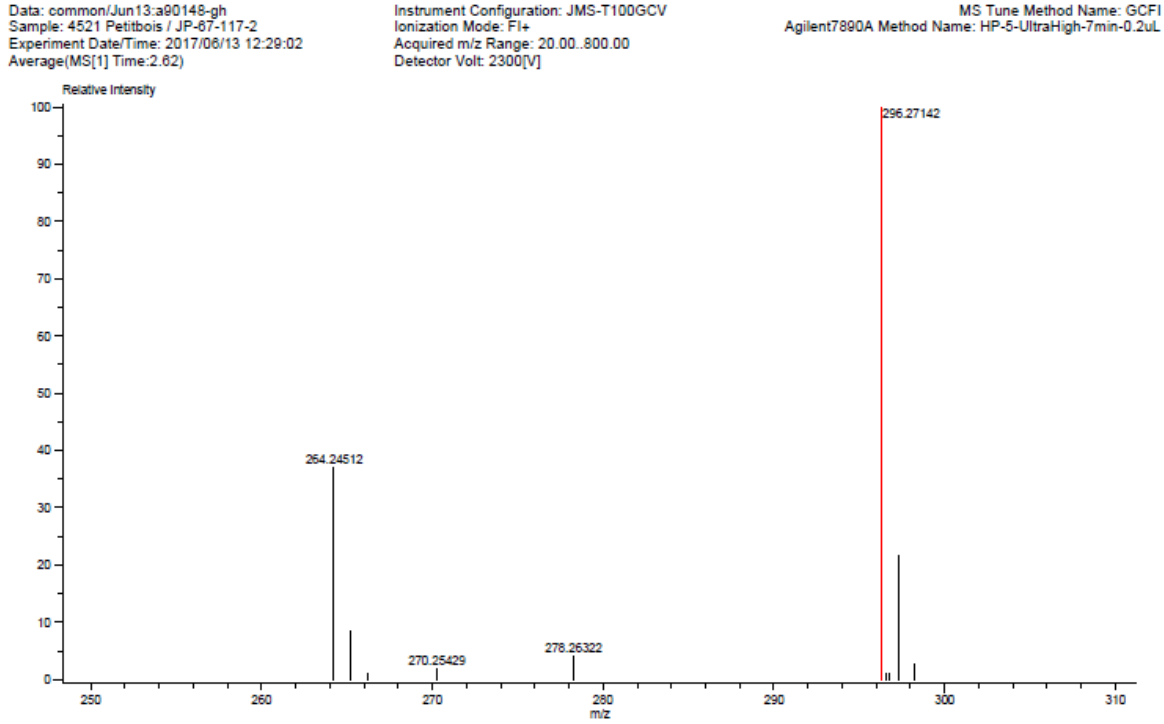

Charge number:1 Tolerance:5.00(mmu)

Element:^{12}C:0 .. 100, ^{1}H:0 .. 200, ^{16}O:0 .. 10

Mass	Calc. Mass	Mass Difference (mmu)	Mass Difference (ppm)	Possible Formula	Unsaturation Number
296.27142	296.27153	-0.11	-0.36	$^{12}C_{19}{}^{1}H_{36}{}^{16}O_2$	2.0

Figure I. 19: GC-MS chromatogram obtained with **73**.

The ^{1}H and ^{13}C NMR spectra (Figures I. 21 and 22, Table I. 3) showed two olefinic protons at δ_H 5.36 and two olefinic carbons at δ_C 129.9 and 130.0 (C-11 and C-12). A methyl ester (δ_C 51.4, δ_H 3.67) and an ester carbonyl (δ_C 174.5) were observed. A terminal methyl (C-18) at δ_C 14.0 and broad signals at δ_H 1.29 were also present. These observations suggested that the compound was a fatty acid methyl ester, too (Figure I.20). However, the position of the double bond could not be determined by NMR. As for **72**, derivatization and DMDS adducts were studied.

Table I. 3: NMR spectrometric data (^{1}H 400 MHz, ^{13}C 100 MHz, $CDCl_3$) for methyl-(*Z*)-octadec-11-enoate (**73**).

position	δ_C, type	δ_H (*J* in Hz)	HMBC[a]	COSY[a]
1	174.5, C			
2	34.1, CH_2	2.31, t (7.2)	1, 3	3
3	24.9, CH_2	1.62, br		2, 4
4-9	28.9-29.7, CH_2	1.29, m		
10	27.2, CH_2	2.02, m	11	9, 11
11	130.0, CH	5.36, m		
12	129.9, CH			
13	27.1, CH_2	2.02, m	12	12, 14
14-15	29.9-29.7, CH_2			
16	31.7, CH_2	1.29, m		
17	22.6, CH_2			
18	14.0, CH_3	0.89, t (8.0)	17	16, 17
19	51.4, CH_3	3.67, s	1	

[a]HMBC data optimized for 8 Hz are from proton(s) stated to the indicated carbon.

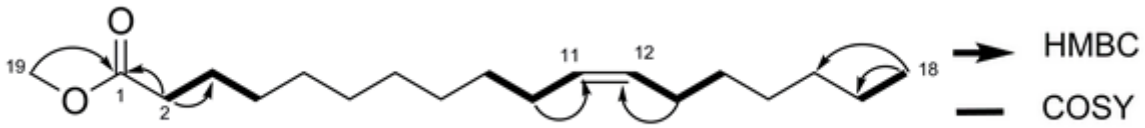

Figure I. 20: COSY and HMBC for **73**.

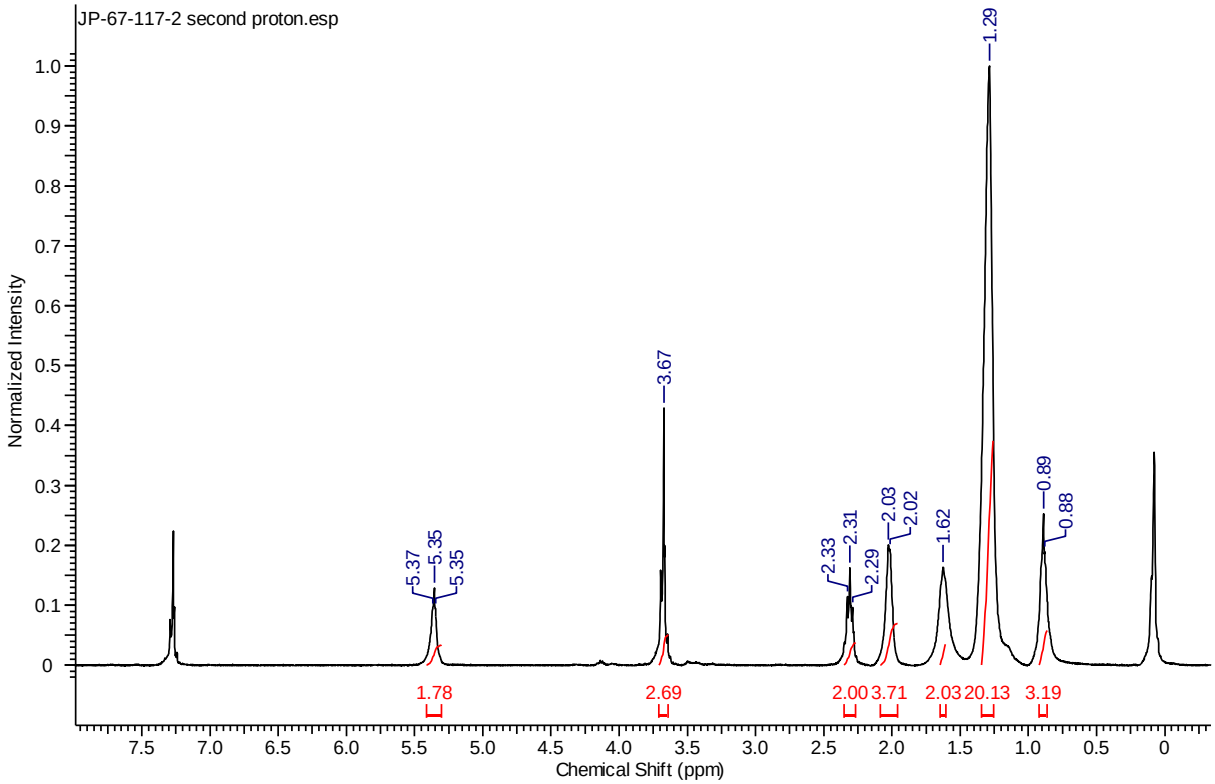

Figure I. 21: ^{1}H NMR spectrum of **73** (400 MHz, $CDCl_3$).

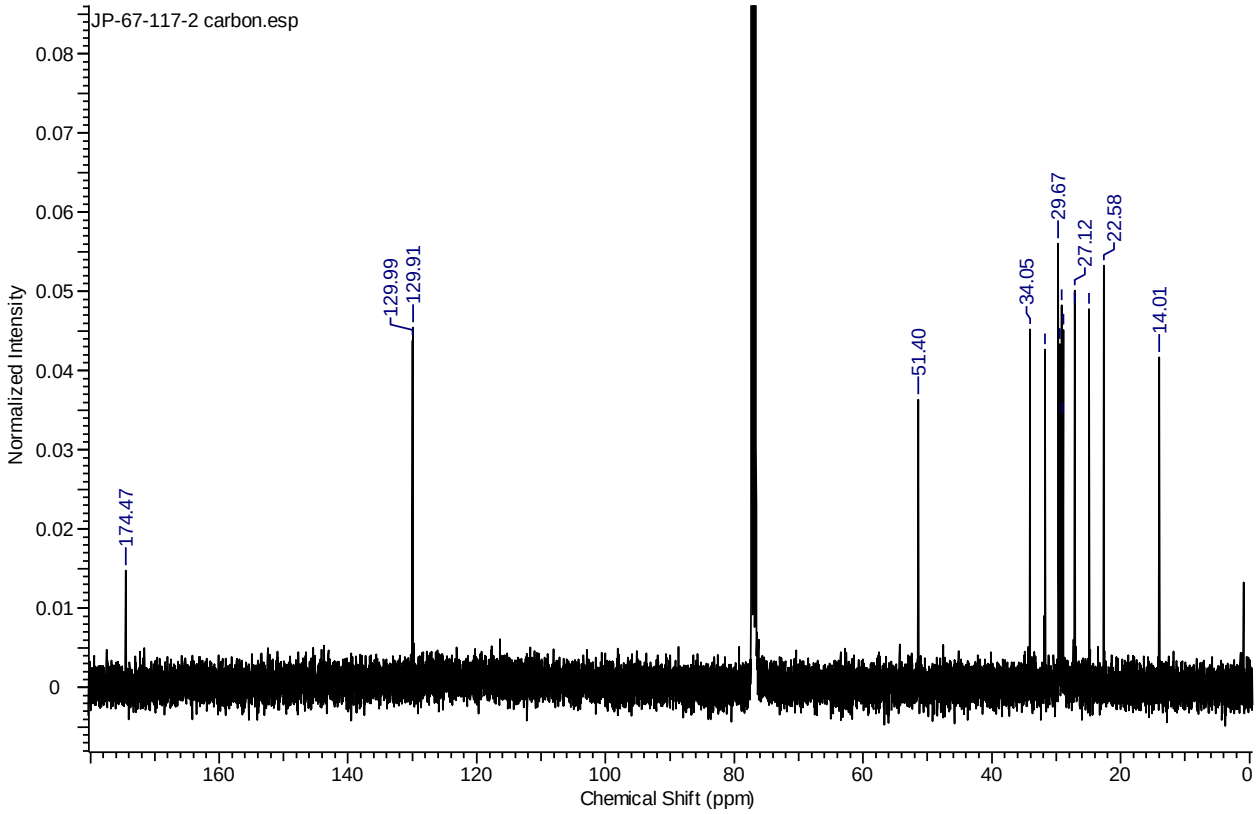

Figure I. 22: ^{13}C NMR spectrum of **73** (100 MHz, $CDCl_3$).

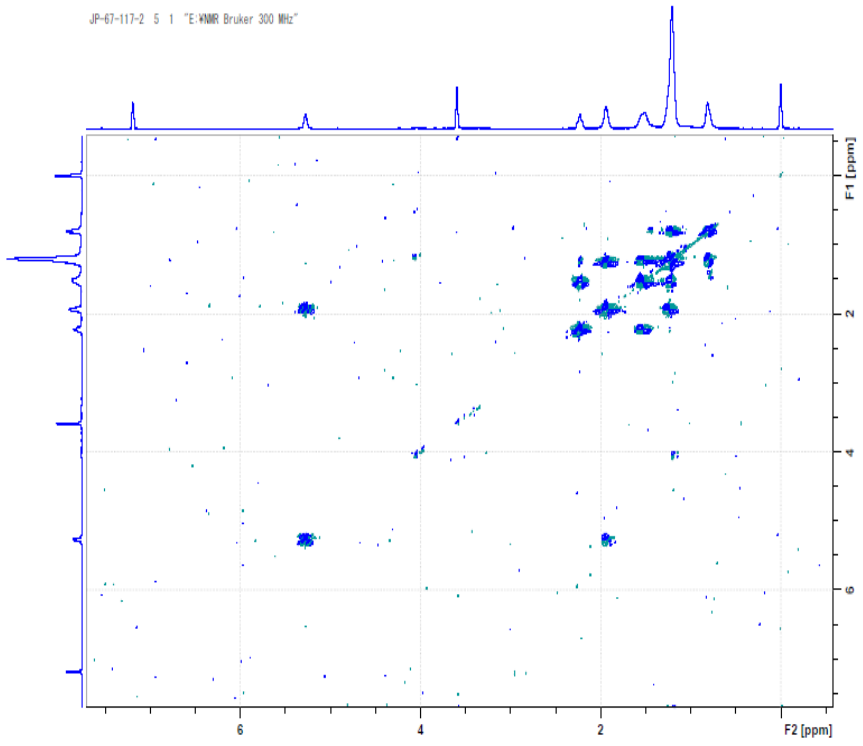

Figure I. 23: COSY spectrum of **73** (300 MHz, $CDCl_3$).

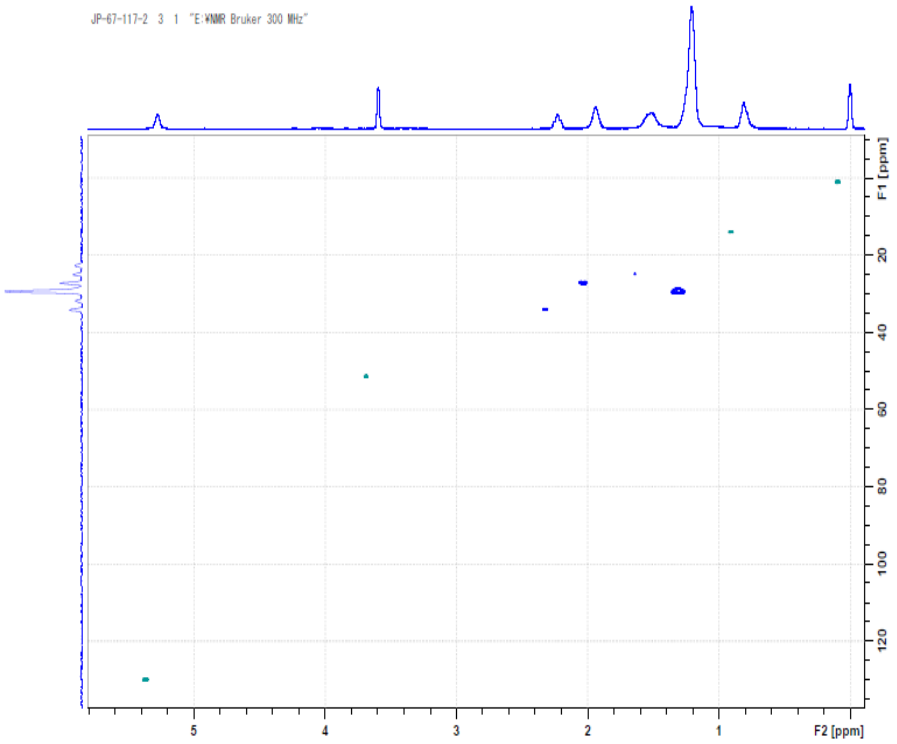

Figure I. 24: HSQC spectrum of **73** (300 MHz, $CDCl_3$).

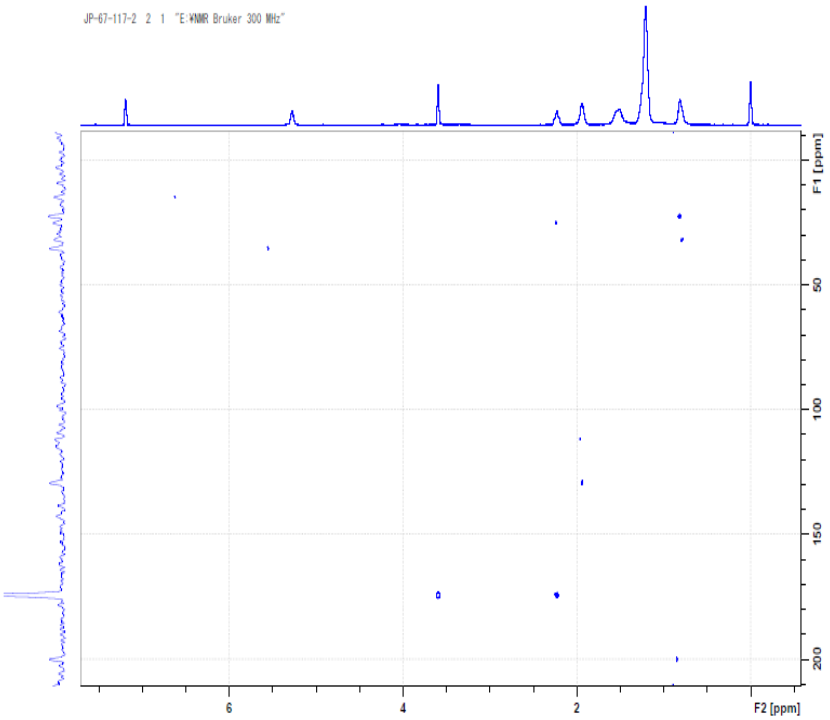

Figure I. 25: HMBC spectrum of **73** (300 MHz, $CDCl_3$).

The fragmentation of the DMDS adduct of **73** gave two major peaks at *m/z* 245 corresponding to the fragment $[C_{13}H_{25}O_2S]^+$ and at *m/z* 145 corresponding to $[C_8H_{17}S]^+$ (Figures I. 26 and 27). This shows that a cleavage occurred between C-11 and C-12 so that the position of the double bond is at C-11. The other major peak at *m/z* 213 corresponds to the loss of the component of methanol.

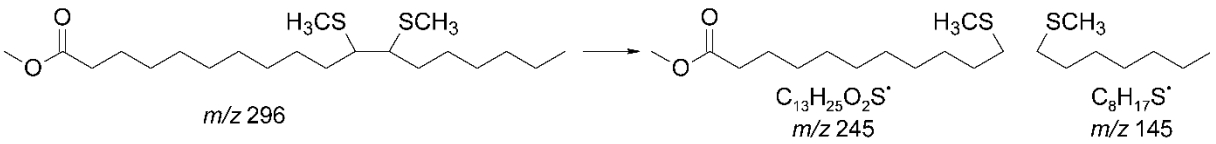

Figure I. 26: DMDS adduct obtained from **73**.

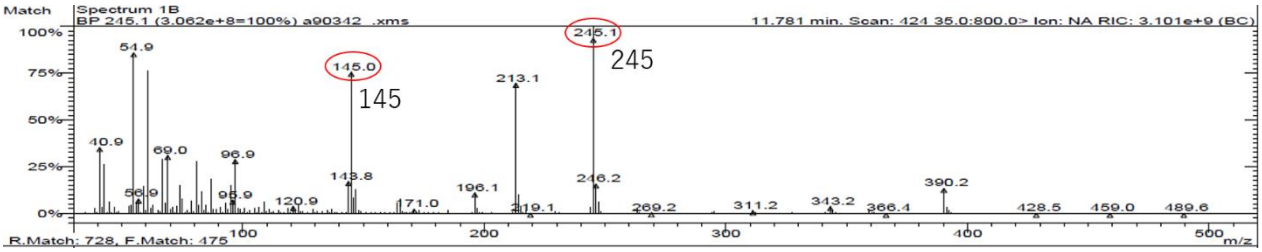

Figure I. 27: MS-MS of the adduct obtained from **73**.

I. 3. 2. b. Configuration of the FAMEs

The configuration of the double bonds of **72** and **73** was determined by ^{13}C nondecoupled HSQC with ^{1}H homodecoupling technique and study of the allylic carbons chemical shifts. Usually, the configuration of a double bond can be determined by studying the coupling constants of olefinic protons on 1D ^{1}H NMR spectrum. However, in the case of **72** and **73**, due to overlapping of the signals of the olefinic protons (δ_H 5.36-5.38 ppm), determination of the couplings was not possible. As a result, ^{13}C nondecoupled HSQC with ^{1}H homodecoupling technique was used. This method can be applied when low resolution occurred,

or when too small chemical shifts differences preclude the determination of coupling constants.[58,59] ^{13}C Nondecoupled HSQC allows to focus on specific carbons, here the olefinic ones. For **72**, only three carbons (C-5, C-6 and C-9) were studied as C-9 (δ_C 129.00) and C-10 (δ_C 128.92) were too close from each other to allow clear results (only 0.08 ppm separates C-9 and C-10, while the limit is 0.09 ppm. The difference between C-5 (δ_C 130.50) and C-6 (δ_C 130.59) is 0.09 ppm). In basic HSQC, in which ^{13}C decoupling is used, only one signal corresponding to the correlation between one carbon and its protons is observed but, for ^{13}C nondecoupling (or ^{13}C coupling), the signal is split depending on the number of attached protons. Here, in the case of methine, the signal is divided in two. The distance separating the two signals corresponds to the coupling constant between the carbon and its corresponding proton ($^1J_{CH}$). This $^1J_{CH}$ can give useful information about the hybridization of the carbon (for **72** and **73**, the $^1J_{CH}$ were between 150 and 152 Hz, corresponding to sp^2 carbons). Other information can be obtained from this spectrum. When transformed into 1D spectrum, couplings between protons can be read, leading to the determination of the configuration of a double bond. Unfortunately, for **72** and **73**, the signals were too broad to have clear values. So it was decided to use the ^{1}H homodecoupling technique. ^{1}H Homodecoupling consists in irradiating a specific resonance (here the allylic protons at about 2.02-2.08 ppm). Irradiation avoids any interaction/coupling between the irradiated protons (here allylic protons) and the studied protons (here the olefinic protons). As a result, a simpler pattern is obtained and the coupling constants can be read. For **72** and **73**, as the couplings with the allylic protons are not observed, only a doublet corresponding to the couplings with the other olefinic proton is observed.

For **72**, as three carbons were studied (Figure I. 28), three 1D spectra corresponding to to H-9, H-6 and H-5, respectively, were obtained (Figure I. 29). A coupling constant of 11.48, 11.70 and 11.28 Hz was observed, respectively. This could indicate a *cis* configuration as

coupling constants for *cis* configuration are theoretically between 4 and 14 Hz, with typically 10 Hz. Coupling constants for *trans* configuration are between 11 and 18 Hz, with typically 16 Hz. But, as explained, *trans* configuration can also give coupling constant of about 11 Hz, so study of the chemical shifts of carbons at allylic position was needed. In the case of *cis* configuration, allylic carbons have chemical shifts from 25 to 28 ppm, and for *trans* configuration, their shifts are between 32 and 36 ppm. As C-4, C-7, C-8 and C-11 have chemical shifts between 26.5 and 27.3 ppm, it means that the configuration of both double bonds is *cis* (or *Z*).[60]

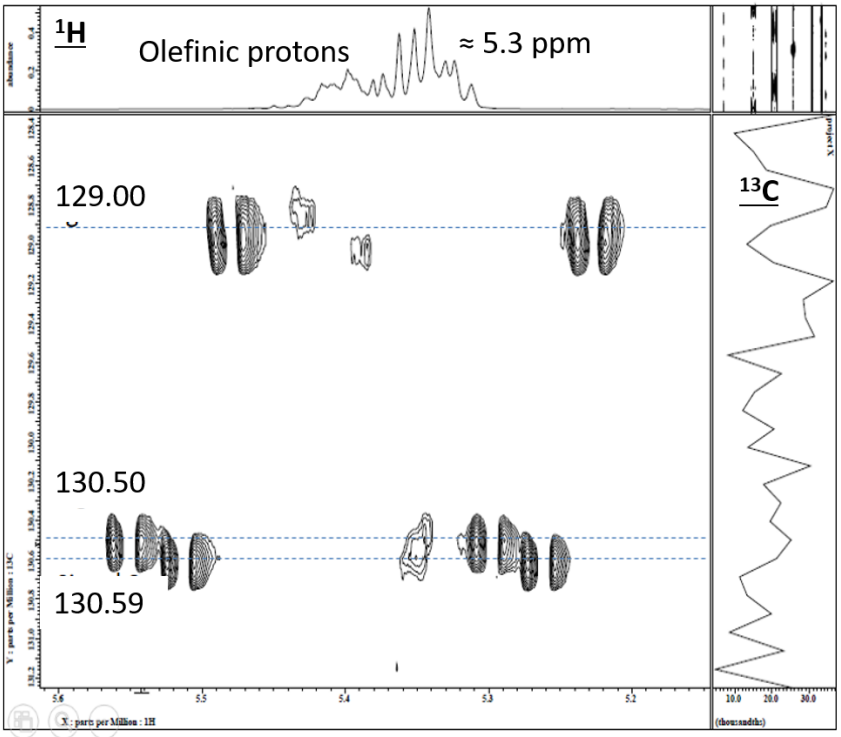

Figure I. 28: ^{13}C nondecoupled HSQC spectrum with ^{1}H homodecoupling for **72** with irradiation of the allylic protons (600 MHz, $CDCl_3$).

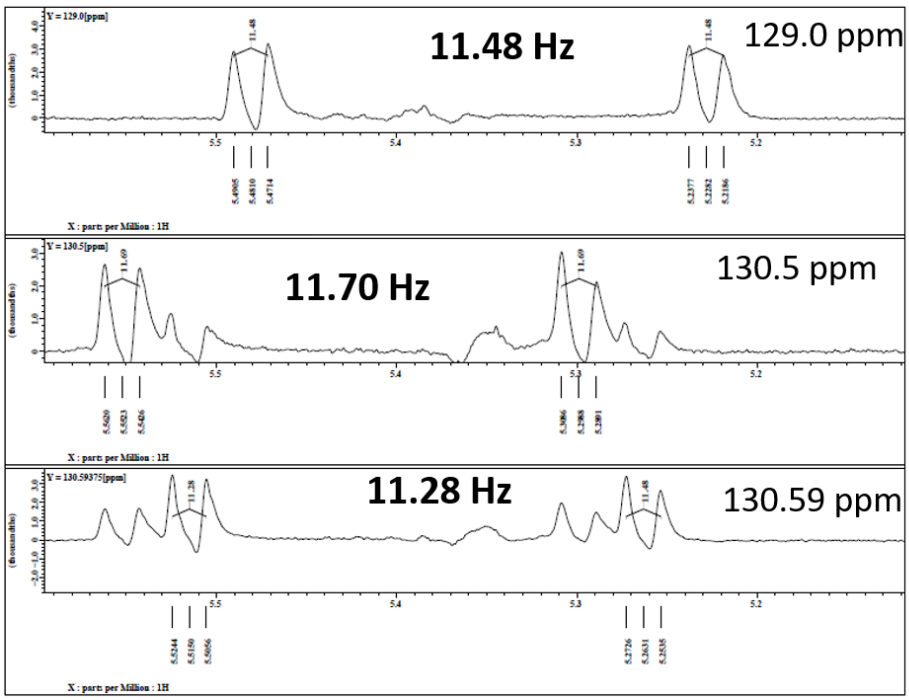

Figure I. 29: 1D HSQC spectra of three of the four olefinic protons of **72**.

The **s**ame observations were obtained with **73**. ^{13}C nondecoupled HSQC with ^{1}H homodecoupling technique with irradiation of the allylic protons gave coupling constants of 11.48 and 12.29 Hz (Figure I. 30). Chemical shifts of the allylic carbons were 27.1 and 27.2 ppm, giving a *cis* configuration of the double bond at C-11.

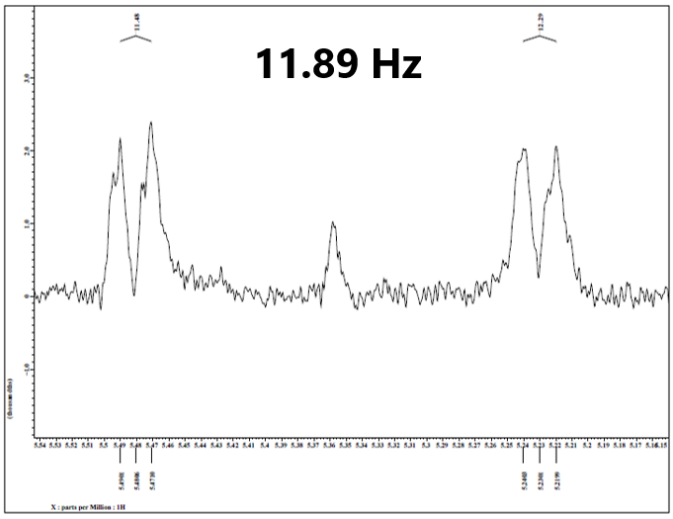

Figure I. 30: 1D HSQC at the olefinic protons of **73**.

I. 3. 2. c. IR spectra of the two FAMEs

Analysis of IR spectra of the two FAMEs also confirmed the configuration of the double bonds. The spectrum of **72** (Figure I. 30) displays a peak at 721 cm^{-1} and the one of **73** (Figure I. 31) a peak at 804 cm^{-1}. The range for *cis* double bond is between 620 and 850 cm^{-1} and for *trans* double bond is between 920 and 1065 cm^{-1}.[61] The signal of the carbonyl was observed at 1743 cm^{-1} for both FAMEs. The *O*-methyl gave a peak at 1260 cm^{-1} for **73**.

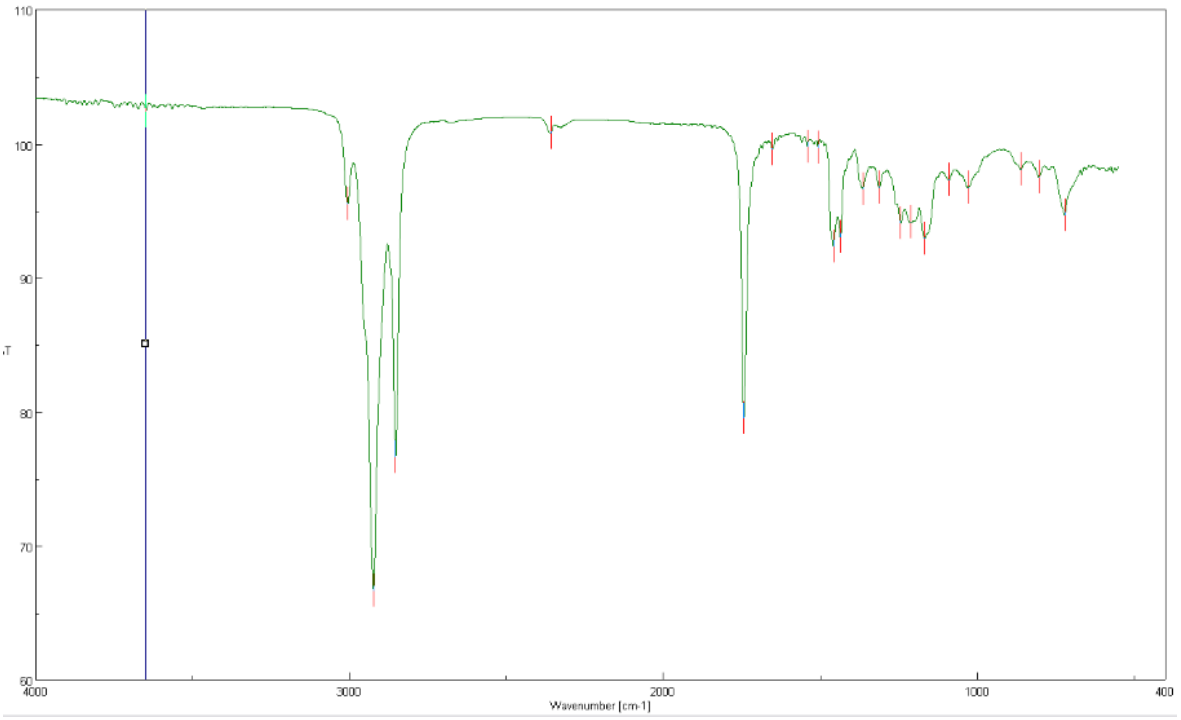

Figure I. 31: IR spectrum of **72**.

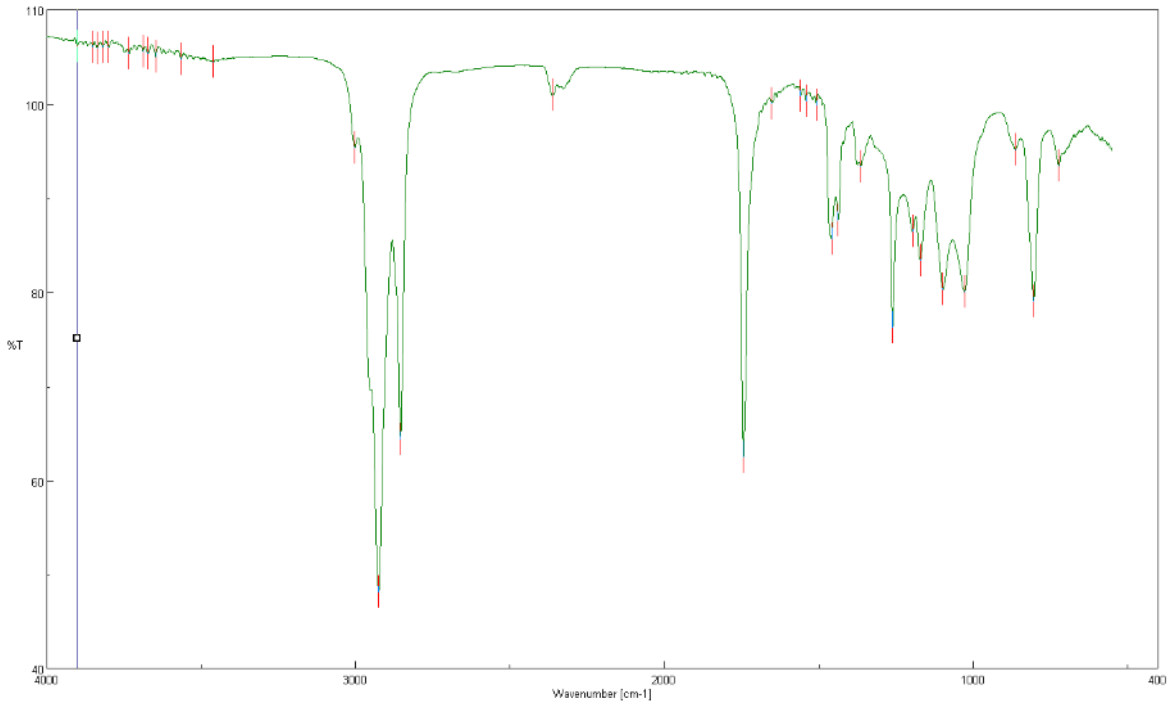

Figure 32: IR spectrum of **73**.

I. 4. Antifouling assay

I. 4. 1. Materials and Methods

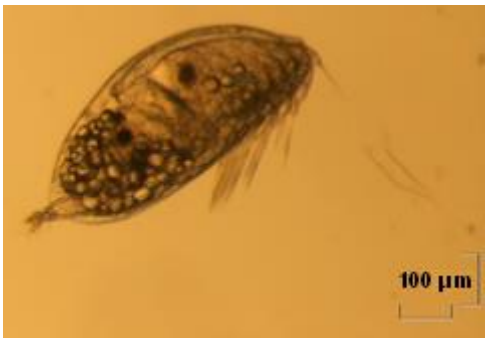

Figure I. 33: Cyprid of *Amphibalanus amphitrite* under microscopy.

An antifouling assay was performed on *Amphibalanus amphitrite* cypris larvae (Figure I. 33) according to the method described by Kitano *et al.* (2002).[62] Adult barnacles were procured from oyster farms in Lake Hamana, Japan, as well as a pier at Shimizu bay, Shizuoka,

Japan. These barnacles were kept in an aquarium at 20 °C, where they were fed brine shrimp *Artemia salina* nauplii. The barnacles were dried at room temperature overnight before being immersed in seawater, which lead to the release of I-II nauplii from the broods. These nauplii were cultured at 25 °C in 80% filtered (0.20 µm of pore filter) natural seawater (diluted with deionized water) containing 30 µg/mL streptomycin and 20 µg/mL penicillin G, where they were fed on the diatom *Chaetoceros gracilis* until they reached the cyprid stage within 5 days. The day that the newly transformed cyprids were collected was designated as day 0. The test samples and compounds were dissolved in ethanol. The antifouling assays were conducted in flat-bottomed 24-well polystyrene culture plates and four wells containing six healthy cyprids were used for each concentration. After an exposure time of 48 h in the dark at 25 °C, the numbers of larvae that had attached, metamorphosed, did not settle or floating, were counted under a microscope. After an exposure time of 120 h, the number of dead cyprids was counted in the same way. Cyprids were considered as dead when no movement was observed, even after a light touch by a metal probe. Pure compounds were tested at six different concentrations in triplicate (n=3), including 0.03, 0.1, 0.3, 1.0, 3.0 and 10 µg/mL. The antifouling activity of each compound was expressed as an EC_{50} value, which represents the concentration of compound required to reduce larval settlement to 50% of the control after 48 hours. Probit analysis was used to calculate the EC_{50} values. Each graph representing antifouling results shows the settlement rate, the floating rate (larvae at the surface of the water) and dead larvae. The rate of larvae swimming in the water column is not shown on the graph for sake of clarity but should be kept in mind when the sum of the settlement rate, floating rate and mortality does not represent 100%, meaning that the remaining larvae are swimming elsewhere than at the surface. For pure compounds, settlement rate, floating rate and mortality are shown after 48 and 120 hours of exposure to see if larvae need more time to settle (so to see if the compound only slows down and does not totally inhibit the settlement) and finally die after 120 hours.

I. 4. 2. Results

N-Phenethylacetamide (**71**), methyl-(5*Z*,9*Z*)-hexacosa-5,9-dienoate (**72**) and methyl-(*Z*)-octadec-11-enoate (**73**) were tested on barnacle larvae. Figure I. 34 shows the results. Compound **71** was the least active among the three compounds, with an EC_{50} value of 9.8 ± 0.97 µg/mL after 48-hour exposure. Almost same number of larvae were floating at 48 and 120 hours. However, after 120 hours of exposure, some swimming larvae could settle.

The activities of the two FAMEs were almost identical and potent. The EC_{50} of **72** and **73** were 0.37 ± 0.10 and 0.55 ± 0.08 µg/mL, respectively. However, after 120 hours, some floating larvae were able to settle. The two FAMEs can slow down the settlement but not inhibiting it completely.

None of the compounds was toxic below 10 µg/mL (LC_{50} > 10 µg/mL).

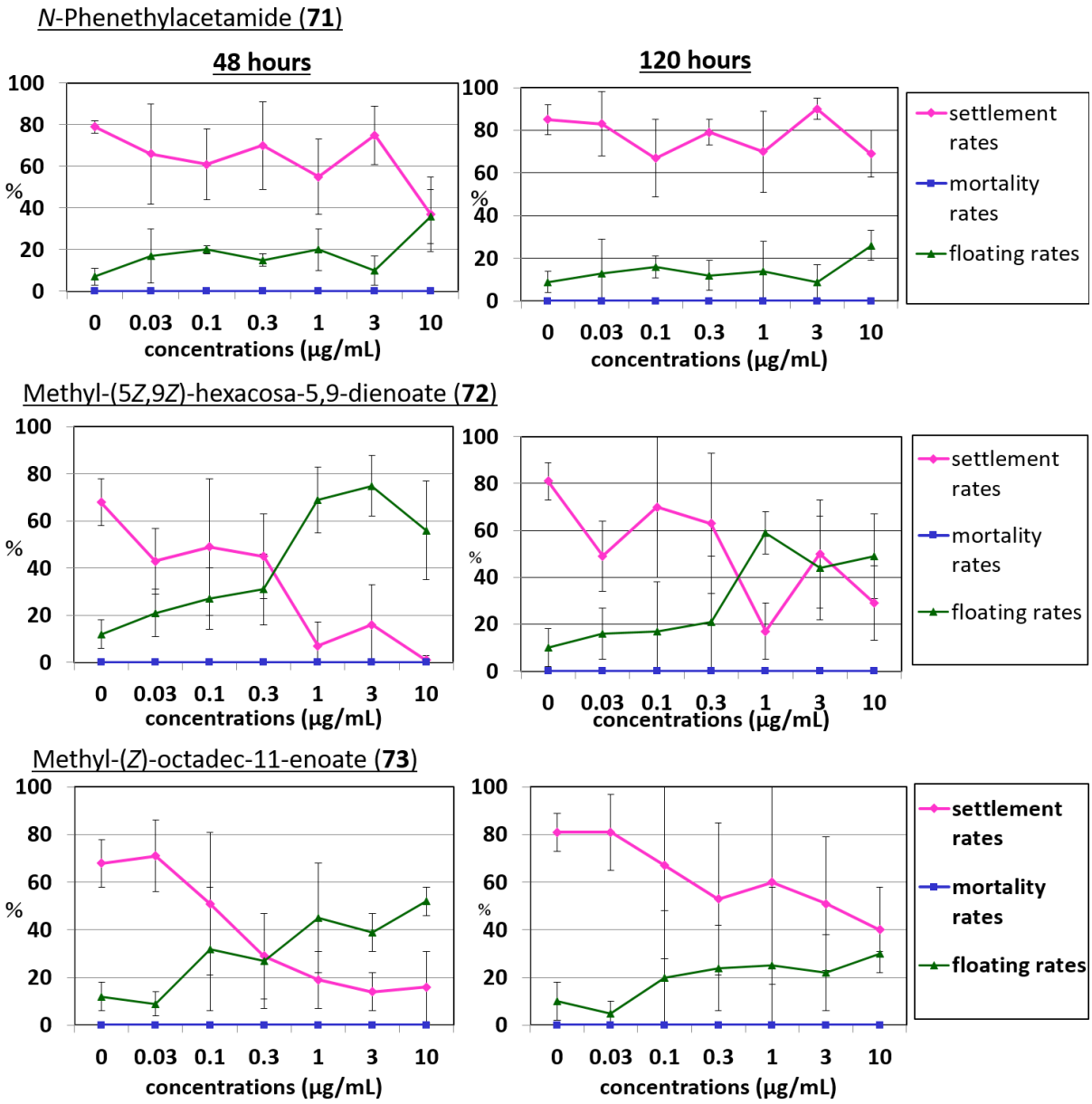

Figure I. 34: Antifouling activity of **71-73** on barnacle larvae after 48 and 120 hours of exposure. Error bars correspond to standard deviation (SD, n = 3).

I. 5. Discussion

Three compounds were isolated from the sponge *Hyrtios* sp. collected in the Red Sea: *N*-phenethylacetamide (**71**) and fatty acid methyl esters methyl-(5*Z*,9*Z*)-hexacosa-5,9-dienoate (**72**) and methyl-(*Z*)-octadec-11-enoate (**73**). The *cis-trans* isomerism of the two FAMEs was determined by NMR and study of the fragments of their DMDS adducts by GC-MS/MS.

Compound **71** has a simple structure and looks like dopamine (**74**), which is a known antifoulant.[63] It was reported that catechlolamines, including **74**, are responsible of the release of cement substance from the cement gland of barnacle cyprids. Cyprids produce this cement for their attachment to the substratum. However, Kon-ya *et al.* reported that treatment with **74** induced metamorphosis without prior attachment in *A. amphitrite* larvae.[64] Therefore, as Yamamoto *et al.* suggested, **74** may induce cement release without complete searching behavior for attachment and this cement release is followed by metamorphosis.[65] Moreover, **74** was also reported as inhibiting the ciliary activity in the larvae of the mussel *Mytilus edulis*. As a result, the mussel larvae stop swimming and cannot reach the substratum.[66] Because of its close structure, **71** can be an agonist of **74** and displays similar activities, which could explain its antifouling activity observed on *A. amphitrite* larvae in this study. Compound **71** is a known compound as it was previously isolated from a marine fungus collected from *Clerodendrum inerme*, a tree from the inter-tidal zone of the South China Sea.[67]

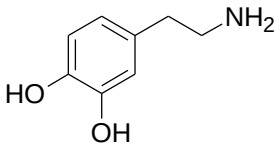

74

Fatty acids are common compounds in sponges. These organisms are even known as leaders in fatty acids diversity among aquatic animals.[68] Among them are a class of fatty acids

with Δ5,9 unsaturation system called for a long period demospongic acids. This designation suggests that they are originally produced by Demospongia sponges but such acids were then observed in other marine and even terrestrial organisms. Demospongic acids are more precisely described as compounds with "bis-methylene-interrupted *cis*-double bonds, ranging in chain-length from C_{16} to C_{34} with a *cis,cis*-dienoic system, either with the double bonds in position 5 and 9, or derived from 5,9-16-2 by chain elongation.[69] Compound **72** isolated in this study from the sponge *Hyrtios* sp. can be considered as a demospongic acid methyl ester. It was apparently isolated from the sponge *Chondrosia* sp., synthesized in order to study phospholipids of marine organisms and is commercially available (CAS 90913-50-1).[70,71] Compound **73**, which can also be named *cis*-vaccenic acid methyl ester, is also commercially available (CAS 1937-63-9) but has not, at our knowledge, been isolated yet from natural source. It is therefore the first time that its natural form is reported.

Several fatty acid methyl esters, isolated from plants, were reported as antibacterial and antifungal.[72,73] Thus, they can have antimicrofouling activities (meaning that they can act on microfoulers such as bacteria and fungus). Fatty acids from marine organisms have also proved to have antifouling activities, such as palmitic acid (**75**) which inhibits barnacle larvae settlement, the growth of the diatom *Cylindrotheca closterium* and the germination of *Ulva lactuca* spore and is antibacterial.[74,75] Myristic acid (**76**), from the fungus *Aureobasidium pullulans*, also inhibits barnacle larvae settlement.[75] The marine bacterium *Shewanella neidensis* SCH0402 produces the two active fatty acids, 2-hydroxymyristic acid (**77**) and *cis*-9-oleic acid (**78**), blocked the germination of *Ulva pertusa* spores and both fatty acids, when incorporated into a paint, could inhibit the attachment of micro- and macrofoulers during a 1.5 year-field test in seawater.[76] A homolog of **78**, 12-methyltetradecanoid acid (**79**) from *Streptomyces* sp., could inhibit the settlement of the polychaete *Hydroides elegans* larvae.[77] A fermentation broth of a fungus *Aureobasidium* sp. led to the isolation of (3*R*,5*S*)-3,5-

dihydroxudecanoic acid (**80**) and aureobasidin (**81**), both demonstrating anti-attachment activity against barnacle larvae.[78]

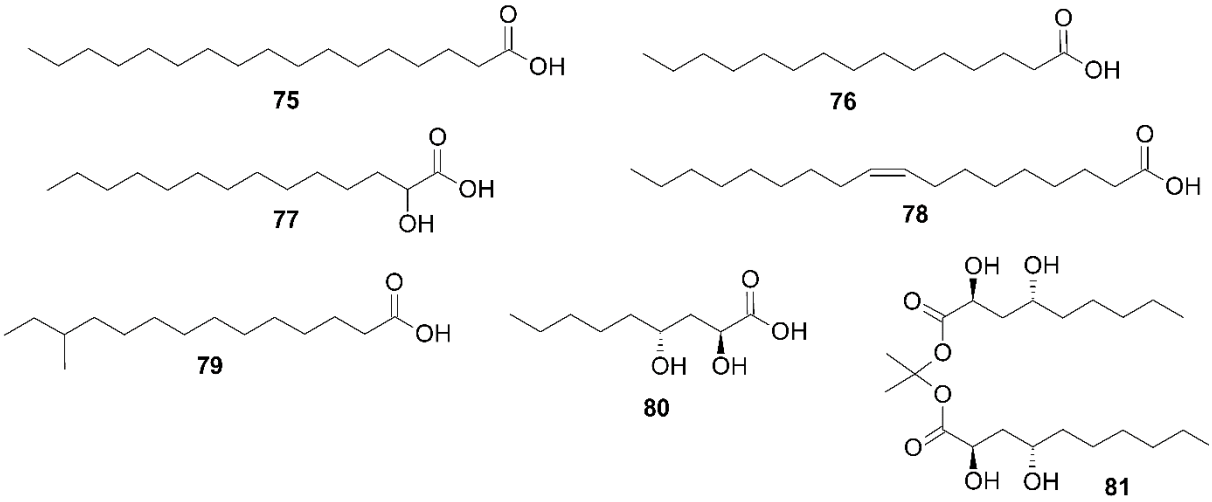

While there is no reason to believe that fatty acid methyl esters should act as antioxidants, based on their structure, some of them were reported as such.[73] Coating containing antioxidant compounds have been found to inhibit the settlement of mussels. Indeed, antioxidants quench oxidative chemistry which takes part in glue formation. Biological adhesion is inhibited without any observed toxicity, making antioxidant fatty acid methyl esters good antifoulants with low environmental impacts.[79] Oxidative chemistries are also observed in barnacle during the development of cuticle and the secretion of one type of cement secretion leading to settlement and metamorphosis.[80] The two FAMEs obtained from *Hyrtios* sp. in this study could inhibit the settlement of barnacle larvae thanks to oxidative activity. However, as they only slow down the settlement, the antifouling activity of the *Hyrtios* sp. extract is probably not totally due to these two FAMEs and other compounds may display more potent activity. Attempt to isolate compounds from the EtOAc fraction led to two phthalates (their structures were not elucidated but their ^{1}H NMR spectra displayed specific signals of phthalates between 7.5 and 7.7 ppm. See Appendix S6 and S7). One of them with a *m/z* of 398 was tested on barnacle larvae and was

active ($1.47 < EC_{50} < 2.06$ µg/mL) but after 120 hours, the larvae were able to settle (see Appendix S8). The origin of these phthalates is unknown. They could be contaminants from laboratory equipment (ex. tips of pipettes) or from the environment as the Red Sea is a big maritime pathway and is probably polluted. Further studies of *Hyrtios* sp. could lead to more potent antifouling compounds.

- Chapter II -

New fatty acid amides from the cyanobacterium *Okeania* sp.: Serinolamides C and D

An *Okeania* sp. cyanobacterium was collected in the Red Sea and partitioned between EtOAc and H_2O. Its EtOAc layer showed great antifouling activity towards *Amphibalanus amphitrite* barnacle larvae. An ESI-LC-MS analysis of this fraction revealed a major $[M + H]^+$ ion peak with an *m/z* value of 356.3165 The compound corresponding to this peak was isolated and identified by using NMR techniques as serinolamide C, together with its acetylated analogue, serinolamide D. This chapter aims at describing their isolation, the structure elucidation and their bioactivities.

II. 1. Isolation of serinolamides C and D

II. 1. 1. Materials and Methods

II. 1. 1. a. Experimental Procedures

LC-MS data were obtained on an Agilent 1100 Series HPLC system coupled with a Bruker Daltonics micrOTOF-HS mass spectrometer, which was configured for electrospray ionization (ESI). The HPLC system was equipped with a Cadenza CD-C18 column (2 × 150 mm, 3 µm, 0.2 mL/min, 25 °C). The HPLC system was operated under the following conditions: 0–20 min, linear gradient from 50% to 100% MeCN with 0.1% (*v/v*) formic acid in MilliQ H_2O; 20–35 min, isocratic 100% MeCN with 0.1% (*v/v*) formic acid. Preparative HPLC purifications were conducted over a Cosmosil Cholester column (10 × 250 mm, 5 µm) at a flow rate of 3 mL/min, with UV detection at 210 nm.

II. 1. 1. b. Biological material

The dark brown cyanobacterial sample S1501 (Figure II. 1) was collected by scuba diving at a depth of 10–15 m on the Algetah Alkabira reef near Jeddah, Saudi Arabia (N 21°41′23.98″; E 39°00′52.94″) in April 2015. Foreign particles were removed by hand and the samples were squeezed by hand to remove any seawater before being stored in MeOH for transportation. A small portion of this material was also preserved in 10 mL of RNA*later* solution for genetic analysis. The sample was identified as *Okeania* sp. by phylogenetic analysis (Figure II. 2) of its 16S rRNA gene sequence (GenBank KY889150). A voucher specimen (S1501) preserved in RNA*later* was deposited at Hokkaido University, Japan.

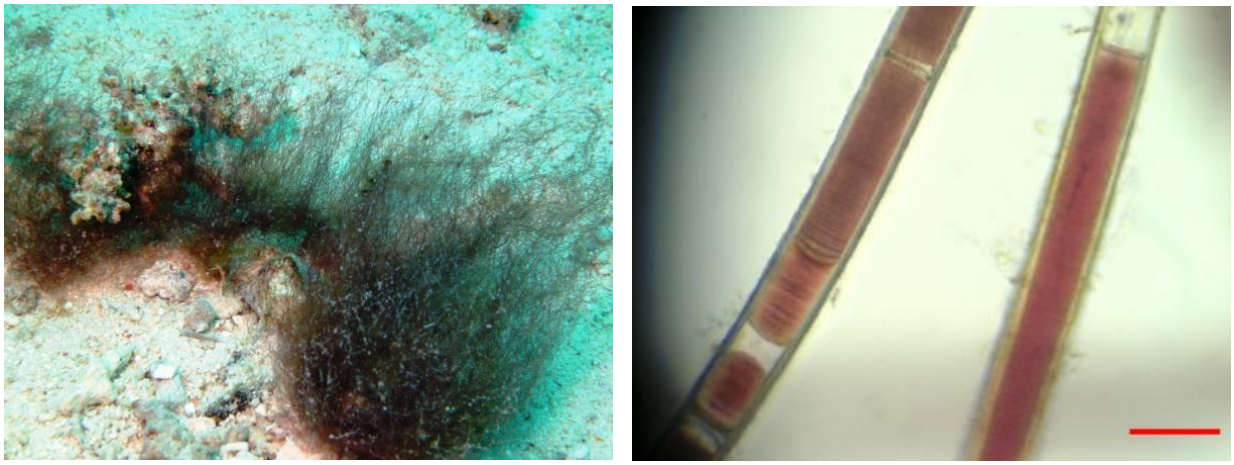

Figure II. 1: Underwater (left) and microscopic (right) images of *Okeania* sp. S1501.

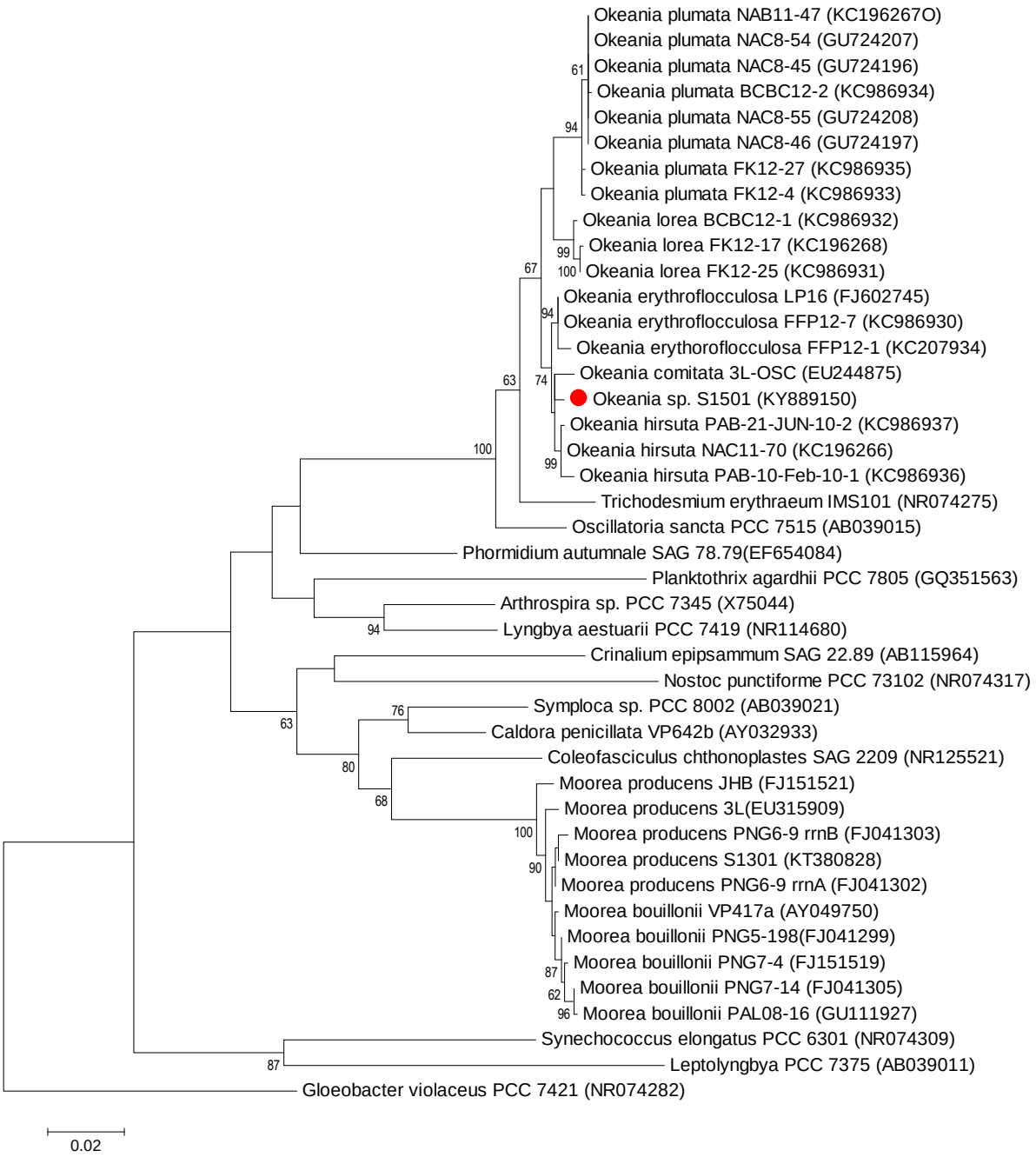

Figure II. 2: Evolutionary tree of *Okeania* sp. S1501. Evolutionary history was inferred using the Maximum Likelihood method (MEGA6) based on the 16S rRNA gene sequences with Gloeobacter violacens PCC 7421 as an outgroup. Bootstrap support data are indicated at the n odes (values < 60% are not shown). This tree has been drawn to scale, with branch lengths indicating the number of substitutions per site. All positions with less than 95% site coverage were eliminated. The final dataset contained a total of 1255 positions (credits to Dr. Julius A. V. Lopez).

II. 1. 1. c. Extraction and Isolation

A sample of the cyanobacterium was homogenized and extracted three times with MeOH. Figure II. 3 shows the isolation scheme used to obtain serinolamides C (**82**) and D (**83**). The fractionation process was monitored by LC-ESI-MS analysis. The dried MeOH extract (3.5 g) was partitioned between EtOAc and H_2O (1:1, *v/v*). The H_2O fraction was further purified using *n*-BuOH (1:1, *v/v*). The dried EtOAc fraction (2.8 g) was purified by NP-column chromatography over silica gel. A stepwise gradient composed of hexane and EtOAc (100:0, 9:1, 8:2, 6:4, 4:6, 2:8 *v/v*), followed by EtOAc and MeOH (100:0, 75:25, 0:100 *v/v*) was used. LC-MS analysis revealed that the 2:8 (*v/v*) hexane/EtOAc fraction (118 mg) contained the main compound of the mother fraction, with an *m/z* value of 356.31. Isolation was performed using semi-preparative RP-HPLC (Cosmosil Cholester 10 x 250 mm, 3 mL/min, UV detection at 210 nm, gradient 0–30 min, 40%–80% MeCN; 30–40 min, 80%–100% MeCN). The fraction eluted at 40 min was further purified by RP-HPLC (Cosmosil Cholester 10 x 250 mm, 3 mL/min, UV detection at 210 nm, gradient 0–40 min, 90%–100% MeCN) to yield **82** (t_R 15.7 min, 12 mg). The fraction eluted with 6:4 (*v/v*) hexane/EtOAc (245 mg) was fractionated by RP-HPLC (Cosmosil Cholester 10 x 250 mm, 3 mL/min, UV detection at 210 nm, gradient 0–50 min, 75%–90% MeCN containing 0.05% (*v/v*) trifluoroacetic acid). The fraction eluted at 24.3 min was further purified by RP-HPLC (Cosmosil Cholester 10 x 250 mm, 3 mL/min, UV detection at 210 nm, isocratic 90% MeCN containing 0.05% (*v/v*) trifluoroacetic acid) to yield **82** (t_R 14.6 min, 10 mg) and another fraction (t_R 18.4 min, 10 mg). This fraction was further purified by RP-HPLC (Cosmosil MS-5C18-II 10 × 250 mm, 5 µm, 3 mL/min, UV detection at 210 nm, isocratic 87% MeCN) to give more of **82** (t_R 21.3 min, 1.7 mg), and **83** (t_R 30.3 min, 1.6 mg).

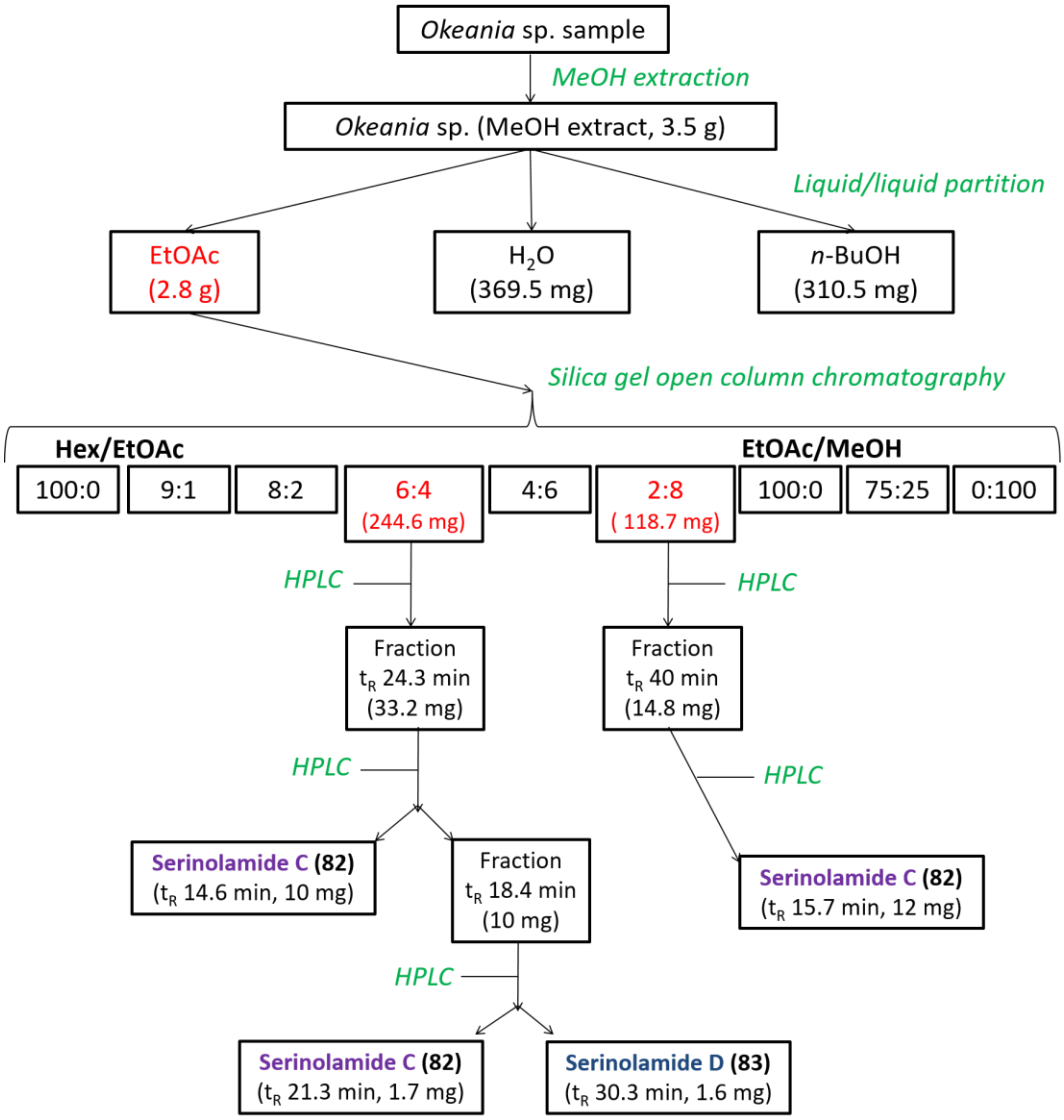

Figure II. 3: Isolation scheme of serinolamides C (**82**) and D (**83**) from *Okeania* sp.

II. 1. 2. Results

The morphological characteristics of this material (hair-like, dark brown color, cell width around 55 µm), as well as the detection of malyngamide C acetate by LC-MS analysis, suggested that S1501 was more closely related to *O. hirsuta* than *O. comitata*.[81] The MeOH extract of this sample was partitioned between EtOAc and H_2O, and he aqueous fraction was further partitioned with *n*-BuOH. The EtOAc fraction was separated into nine subfractions by column chromatography over normal-phase (NP) silica gel. The fractionation process was monitored by

LC-ESIMS analysis. The major compound in the EtOAc extract was determined to the new compound **82**, which was mainly eluted from the column using 2:8 (v/v) mixture of hexane/EtOAc. Purification of the 6:4 hexane/EtOAc led to additional **82** and the related compound **83**.

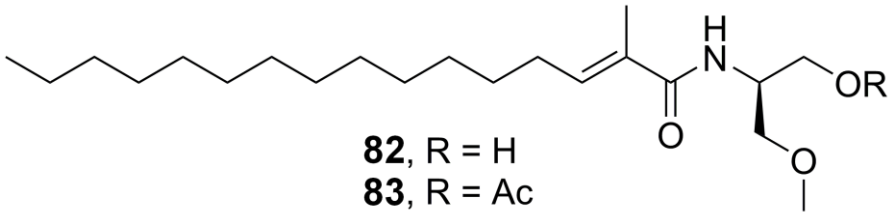

82, R = H
83, R = Ac

II. 2. Characterization of serinolamides C and D

II. 2. 1. Materials and Methods

II. 2. 1. a. Experimental Procedures

IR spectra were recorded on a JASCO FT/IR-4100 type A. The ^{1}H and ^{13}C NMR spectra for **82** and **83** were recorded on a JEOL 400 MHz spectrometer, whereas their 2D NMR spectra were recorded on a Bruker Advance 300 MHz. All the NMR spectra were recorded in $CDCl_3$ (Cambridge Isotope Laboratories, Inc.) using the residual solvent peak ($CHCl_3$) as an internal reference (δ_H 7.27 and δ_C 77.00 ppm). Optical rotation data were acquired on a HORIBA SEPA-300 polarimeter using a 0.1-dm cuvette with chloroform or methanol as the solvent. UV spectra were recorded on JASCO multiwavelength UV detector MD-1510.

II. 2. 1. b. Synthesis of (*R*)- and (*S*)-*O*-methylserinol

The (*R*)- and (*S*)-*O*-methylserinol were synthesized according to the method reported by Gao *et al.* (2013)[82] (Figure II. 4). Each step was checked by ^{1}H NMR (Figures II. 5-8).

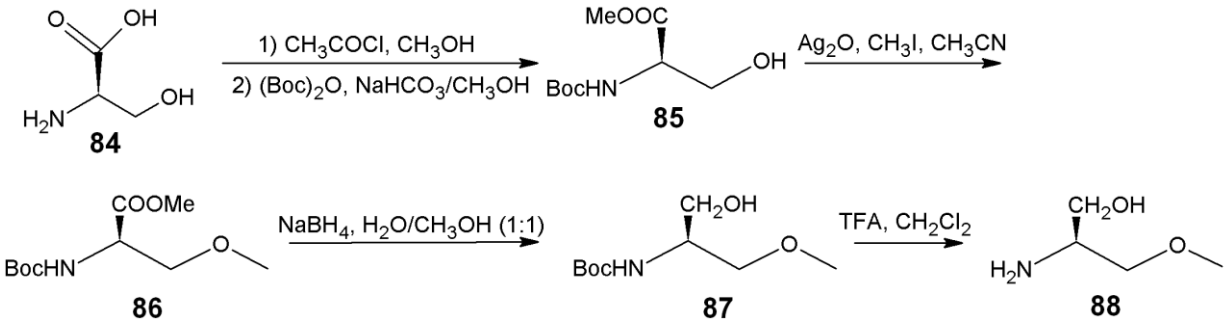

Figure II. 4: Synthesis of the (*S*)-O-methylserinol (**88**).

To a solution of D-serine (**84**) (1 g, 9.52 mmol) in CH_3OH (47.6 mL) was dropwise added acetyl chloride (2 mL, 28.6 mmol). The reaction mixture was then stirred overnight at 80 °C. Solvent was evaporated to quench the reaction and the D-serine methyl ester hydrochloride salt was obtained as a white solid. It was dissolved in a 1:5 *v/v* saturated solution of $NaHCO_3$ in MeOH (60 mL) and a solution of Boc_2O (2.62 mL, 11.42 mmol). The reaction mixture was stirred overnight at room temperature. Dichloromethane (100 mL) was added and washed with HCl (1 N, 3 x 50 mL) and brine (50 mL). The organic layer was dried over anhydrous sodium sulfate. After filtration, the solvent was evaporated to obtain (*R*)-methyl 2-(*tert*-butoxycarbonyl)-3-hydroxypropanoate (**85**) as a white oil (820 mg, 82 %). The residue was used without further purification.

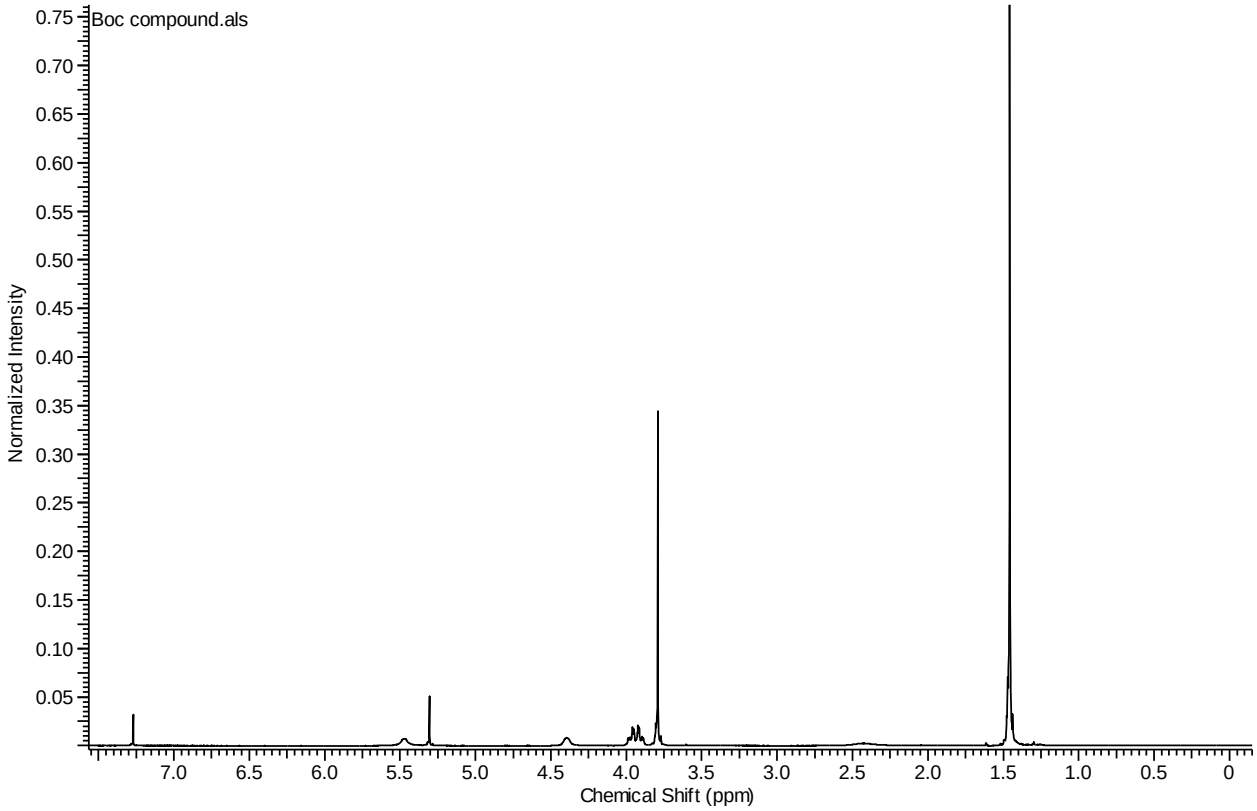

Figure II. 5: ^{1}H NMR spectrum of **85** ($CDCl_3$, 400 MHz).

To a solution of **85** (200 mg, 0.912 mmol) in CH_3CN (7.9 mL) was added Ag_2O (1.08 g, 4.65 mmol) and CH_3I (130 µL, 0.115 mmol). The reaction mixture was protected from the light, stirred and heated overnight. The mixture was then brought to room temperature and filtered through a pad of Celite. After evaporation of the solvent, the residue was purified by flash chromatography on silica gel (5:95 EtOAc/Hex) to afford (*R*)-methyl 2-(*tert*-butoxycarbonyl)-3-methoxypropan (**86**).

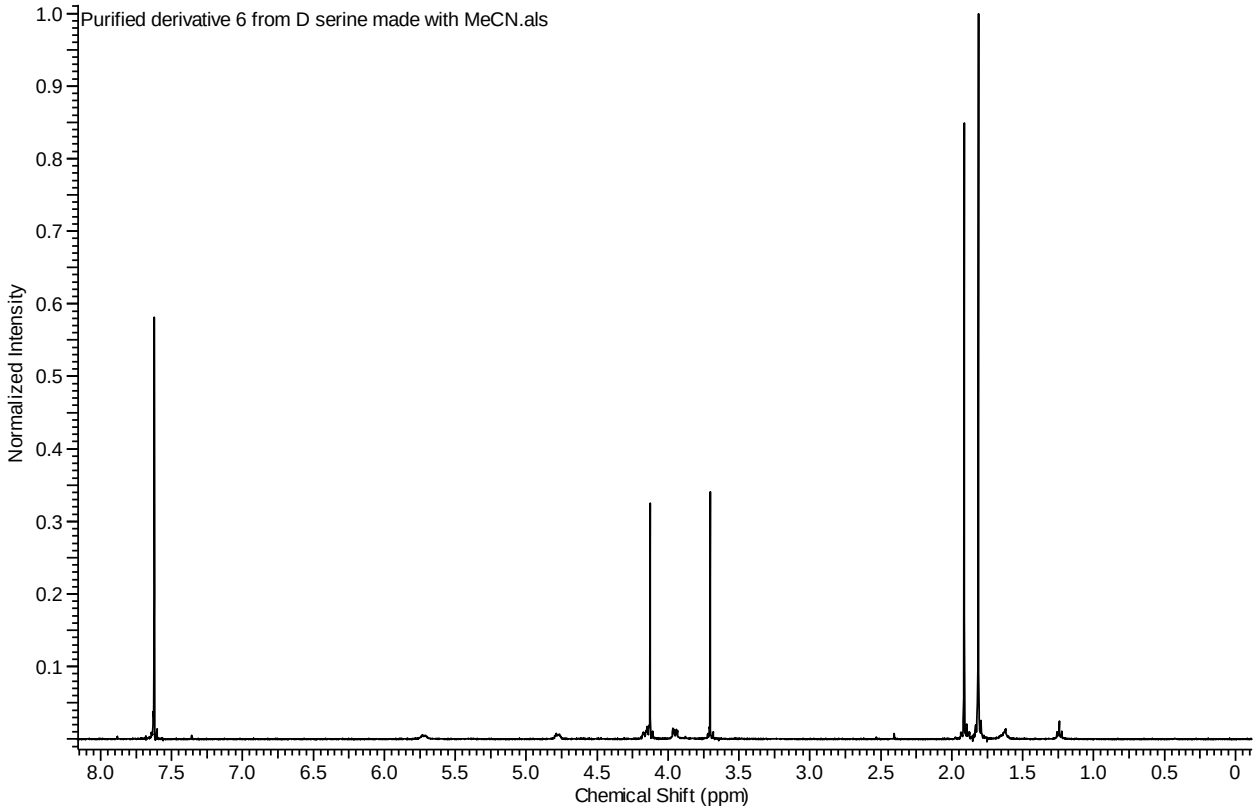

Figure II. 6: ^{1}H NMR spectrum of **86** ($CDCl_3$, 400 MHz).

To **86** (62 mg, 0.226 mmol) in CH_3OH/H_2O (1:1, 532 µL) was added $NaBH_4$ (20.1 mg, 0.532 mmol) in four portions at 0 °C. The mixture was then stirred overnight at room temperature. It was then extracted with EtOAc (3 x 15 mL) and the organic layer was washed with brine (15 mL), dried over anhydrous Na_2SO_4 and concentrated. The residue was purified by flash chromatography on silica gel (1:2 EtOAc/Hex) to afford (*S*)-tert-butyl-1-hydroxy-3-methoxypropan-2-ylcarbamate (**87**).

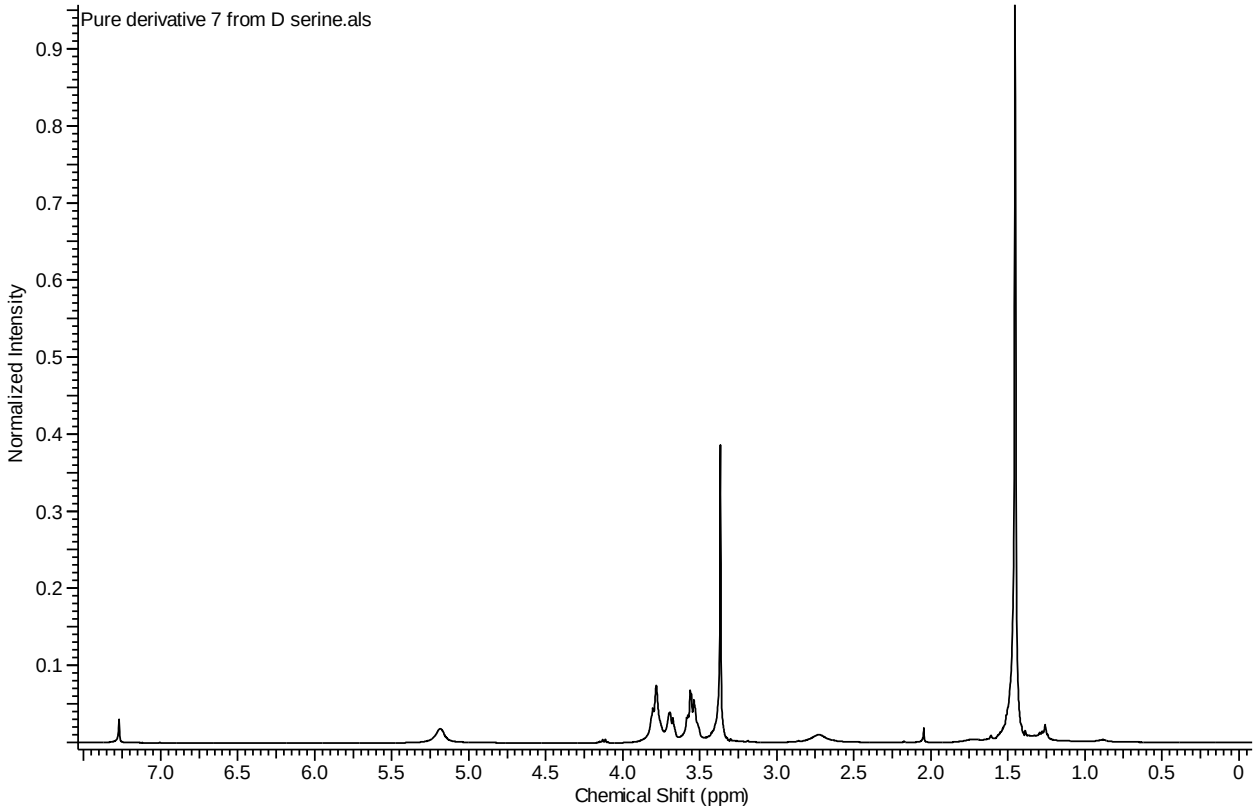

Figure II. 7: ^{1}H NMR spectrum of **87** ($CDCl_3$, 400 MHz).

To a solution of **87** (40.4 mg, 0.2 mmol) in CH_2Cl_2 (3.57 mL) was added TFA (1.43 mL) dropwise and stirred for one hour at room temperature. The reaction was then quenched by evaporation of the solvent and the obtained (*S*)-*O*-methyl serinol (**88**) (or (*S*)-2-amino-3-methoxypropan-1-ol, 40.2 mg). The same synthesis was performed with L-serine to obtain the (*R*)-*O*-methyl serinol (13.2 mg). The two serinol derivatives were used as they were for Marfey's analysis.

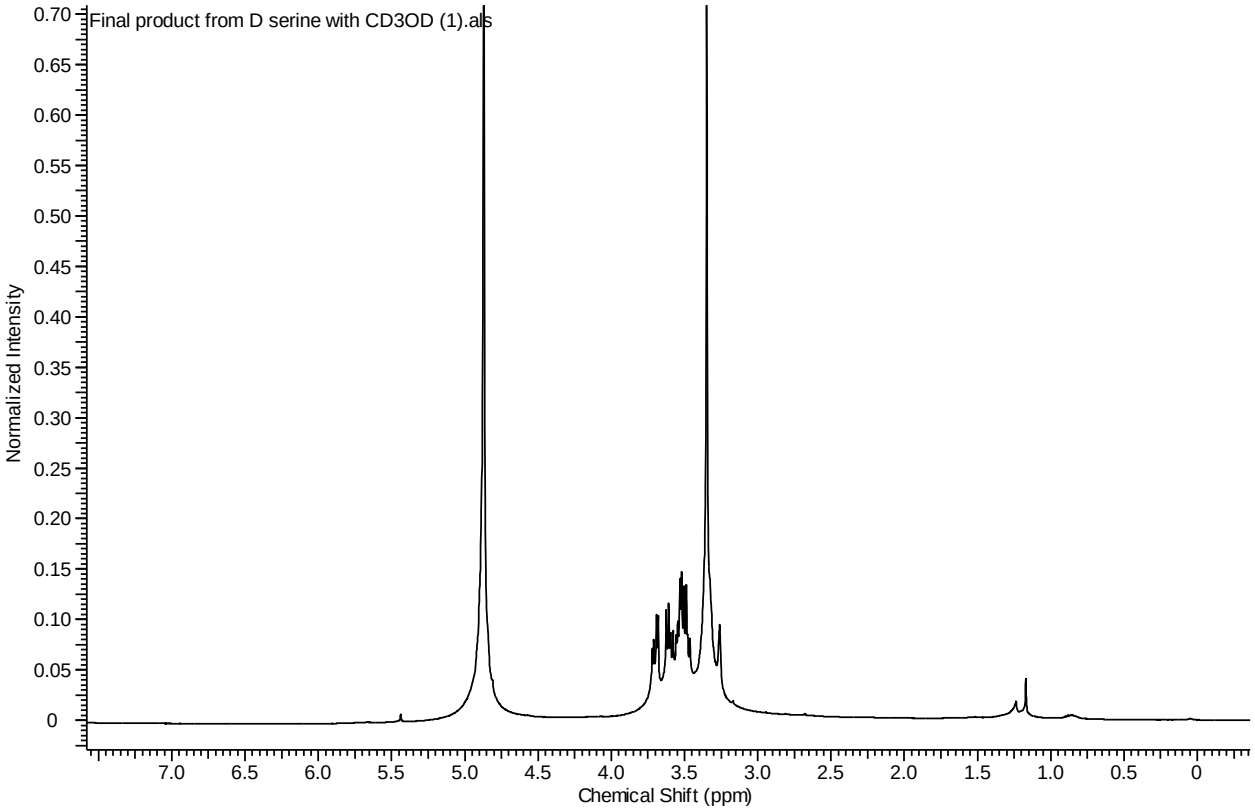

Figure II. 8: ^{1}H NMR spectrum of **88** (CD_3OD, 400 MHz).

II. 2. 1. c. Marfey's analysis of *O*-methylserinol

A small aliquot of **82** (0.1 mg) was hydrolyzed using 6 M HCl at 110 °C for 16 h. **83** was hydrolyzed in a similar manner using 12 M HCl at 120 °C to convert its acetate group to an alcohol. The hydrolysates were dried *in vacuo* and subjected to Marfey's analysis. The hydrolysates and the two synthesized *O*-methylserinol enantiomers were analyzed by RP-HPLC (Cosmosil 5C18-AR-II 4.6 × 250 mm, 5 µm, 1 mL/min, UV detection at 340 nm, gradient 0–45 min, 10%–50% MeCN containing 0.05% (*v/v*) trifluoroacetic acid). A comparison of the retention times (t_R) of the standard (21 and 31 min for (*R*)- and (*S*)-*O*-methylserinol, respectively) and the hydrolysates (31 min for **82** and **83**) led to the assignment of the chiral centers in compounds **82** and **83** as *S* and *R*, respectively.

II. 2. 2. Results

II. 2. 2. a. Planar structures of serinolamides C and D

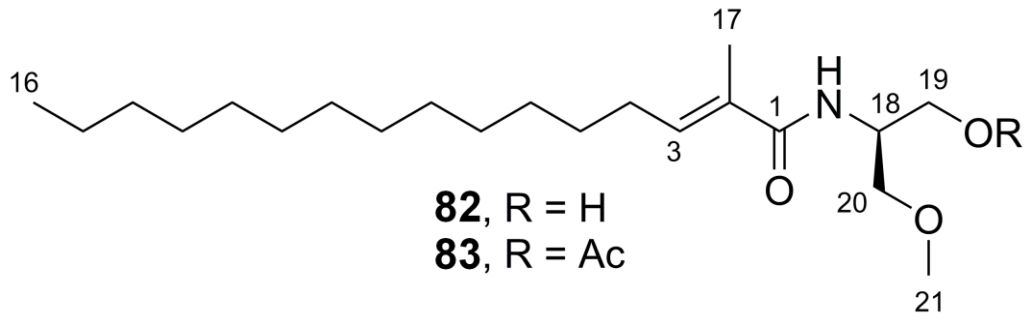

The planar structure of **82** was elucidated using NMR and MS analyses. The molecular formula of **82** was determined to be $C_{21}H_{41}NO_3$ by ESI-TOF-MS, indicating 2 degrees of unsaturation. ^{1}H and ^{13}C NMR analyses (Table II. 1) revealed the characteristic signals of an unsaturated acyl chain composed of eight methylene groups (δ_H 1.26, δ_C 29.3–29.6 ppm) and a terminal methyl group (δ_H 0.88, δ_C 14.0), as well as signals consistent with one *O*-methyl (δ_H 3.38, δ_C 59.3), one carbonyl (δ_C 169.9), one trisubstituted olefinic methyl (δ_H 1.86, δ_C 12.6) and one amide proton (δ_H 6.41), forming a fatty acid amide with an *O*-methylserinol.

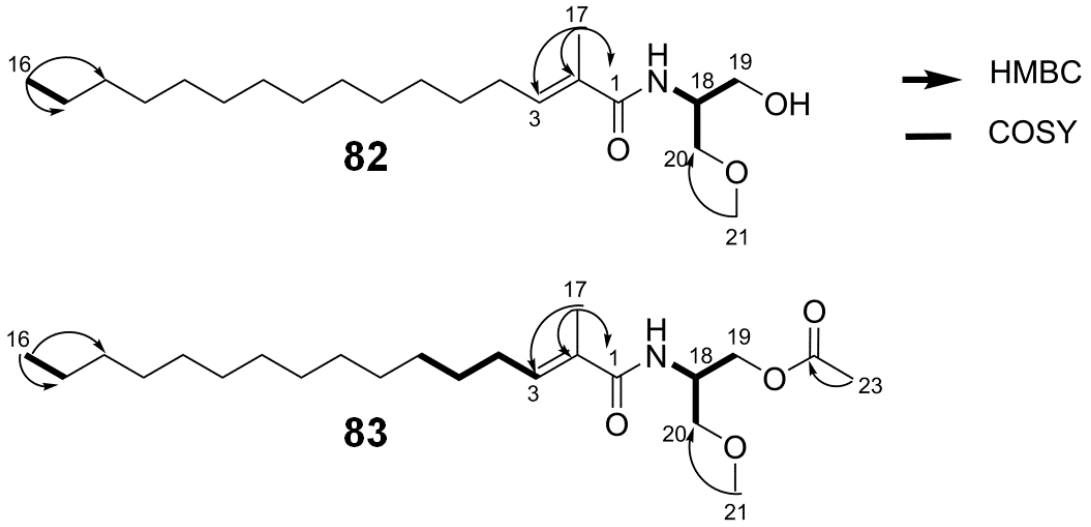

Figure II. 9: HMBC and COSY correlations of **82** and **83**.

Fatty acid amides are common metabolites of the genera *Moorea*[83,84], *Lyngbya*[85] and *Okeania*.[81] Moreover, two fatty acid amides bearing an *O*-methylserinol moiety have previously been isolated from *Moorea producens*[83,84], namely serinolamides A (**89**) and B (**90**). HMBC analysis (Figure II. 9 and 14) of **82** allowed for the assignment of the spin system formed by H-17, C-1, as well as the double bond formed by C-2 and C-3.

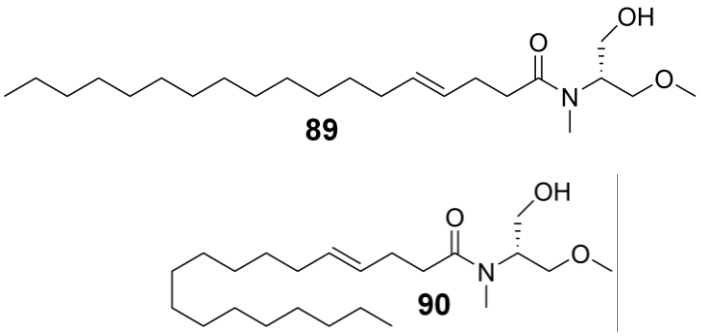

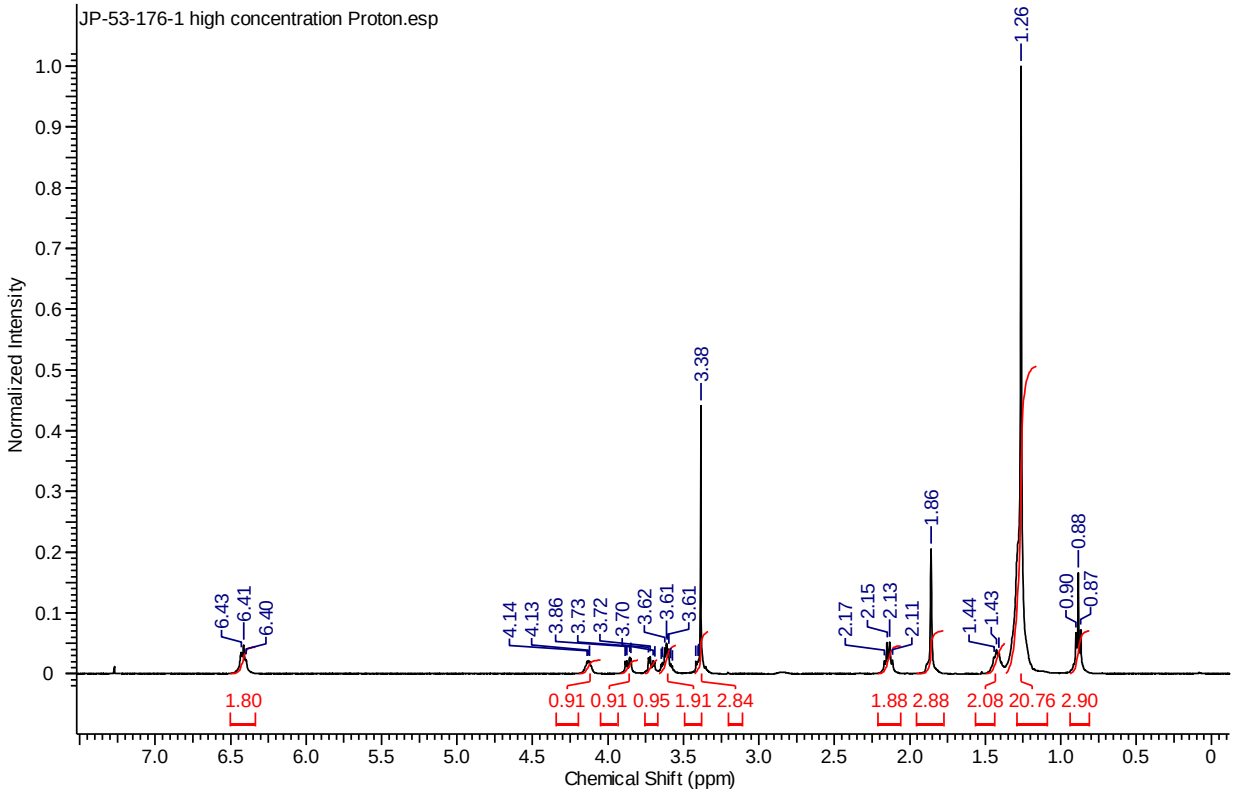

Figure II. 10: ^{1}H NMR spectrum of **82** (400 MHz, $CDCl_3$).

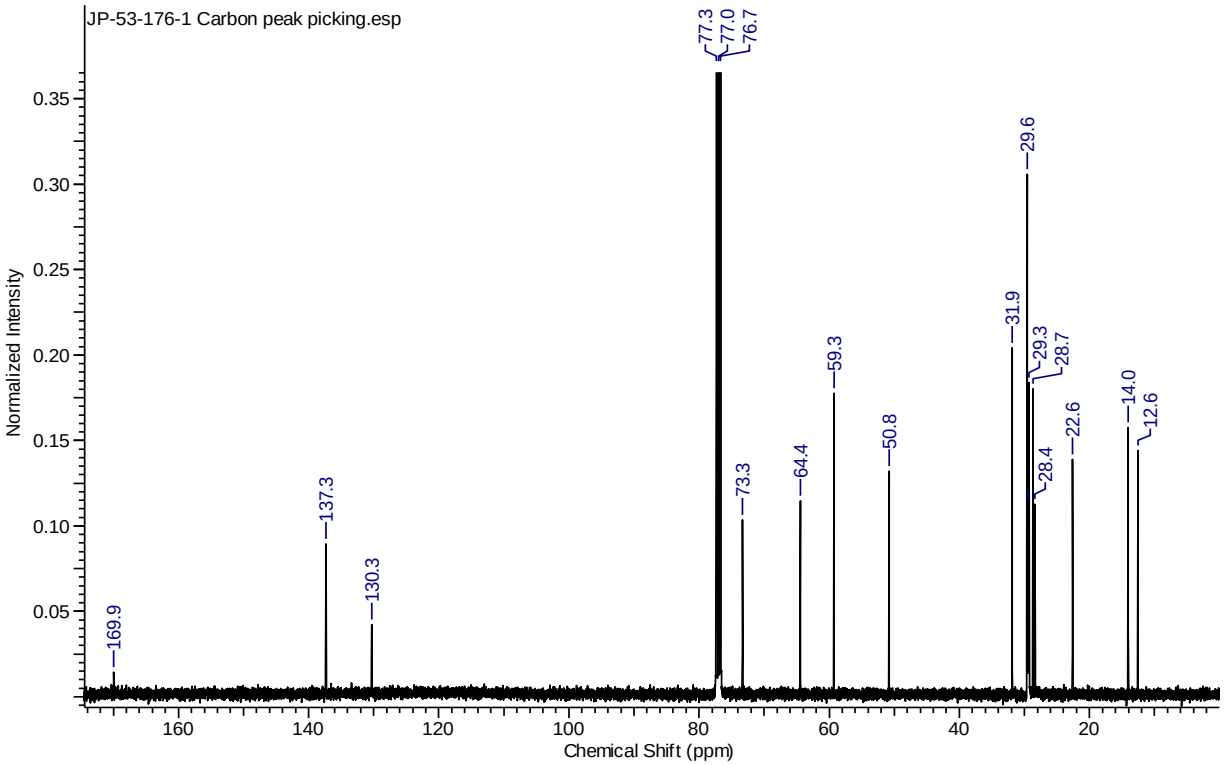

Figure II. 11: ^{13}C NMR spectrum of **82** (100 MHz, $CDCl_3$).

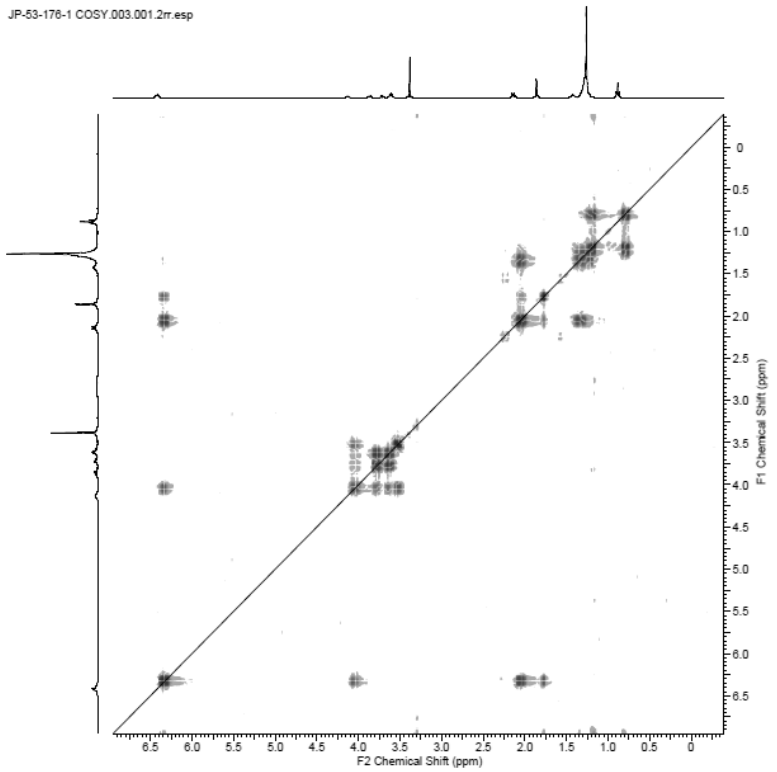

Figure II. 12: COSY spectrum of **82** (300 MHz, $CDCl_3$).

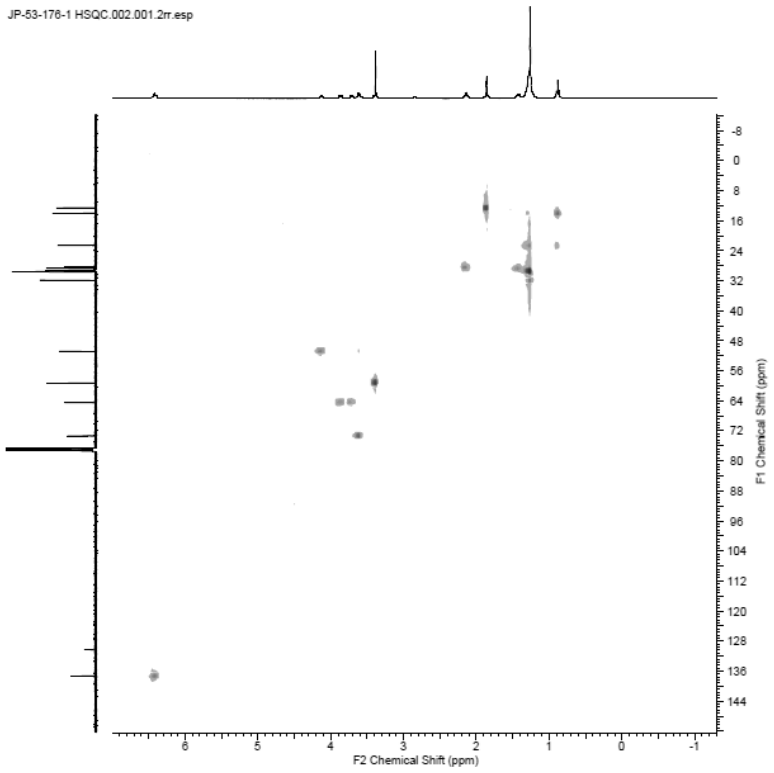

Figure II. 13: HSQC spectrum of **82** (300 MHz, $CDCl_3$).

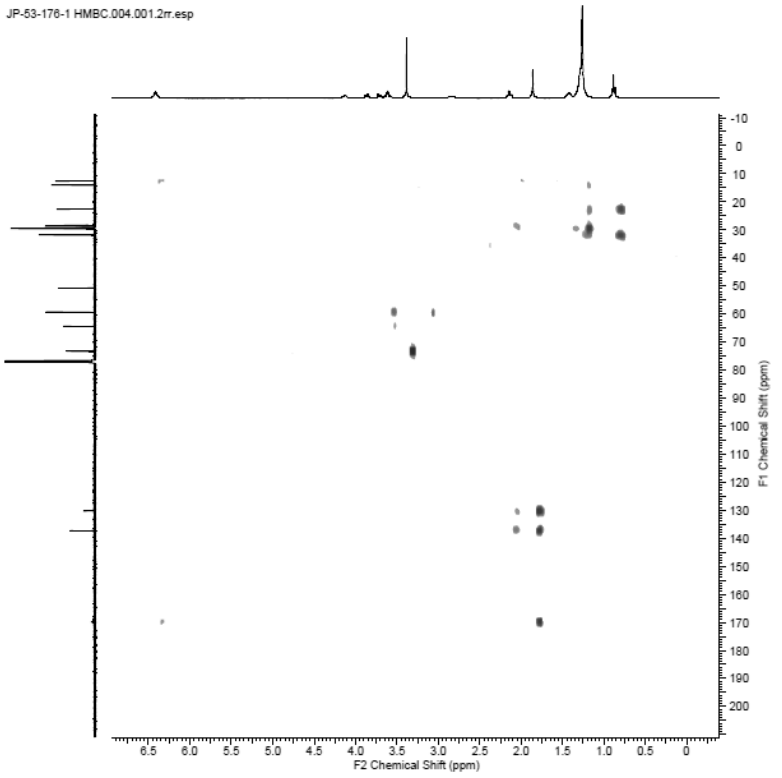

Figure II. 14: HMBC spectrum of **82** (300 MHz, $CDCl_3$).

The molecular formula of **83** was determined to be $C_{23}H_{43}NO_4$ by ESI-TOF-MS analysis, indicating 3 degrees of unsaturation. The ^{1}H NMR data (Figure II. 15) for **83** were quite similar to those obtained for **82** (Table II. 1), except for the presence of an additional methyl singlet (δ_H 2.07), as well as shielded shift in the signal for the amide proton (δ_H 6.11 instead of 6.41 for **82**) and a deshielded shifts for H-19 (δ_H 4.14 and 4.28 instead of 3.71 and 3.86 for **82**) and H-18 (δ_H 4.40 instead of 4.13 for **82**). Moreover, the ^{13}C NMR spectrum (Figure II. 16) of this compound revealed the presence of an extra carbonyl group (δ_C 171.3), as well as an extra methyl group (δ_C 20.8) compared with **82**. HMBC analysis (Figure II. 9 and 19) showed that the serinol was *O*-acetylated.

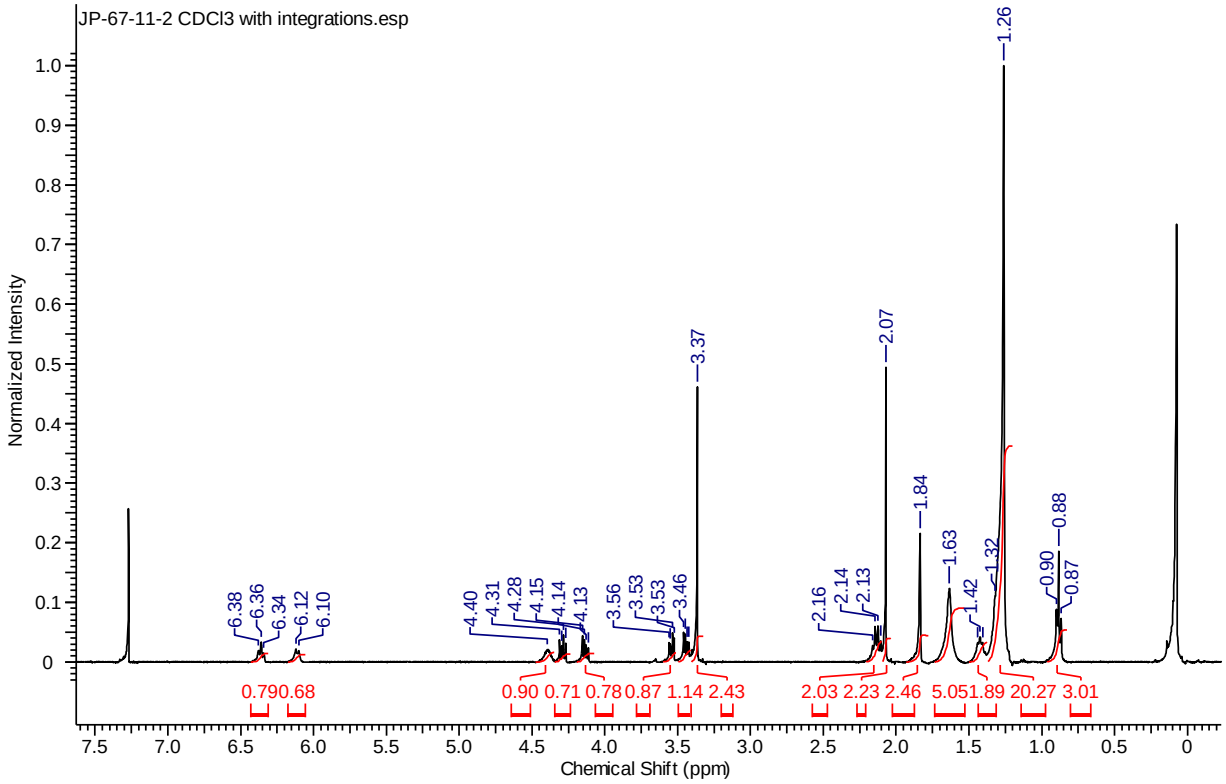

Figure II. 15: ^{1}H NMR spectrum of **83** (400 MHz, $CDCl_3$).

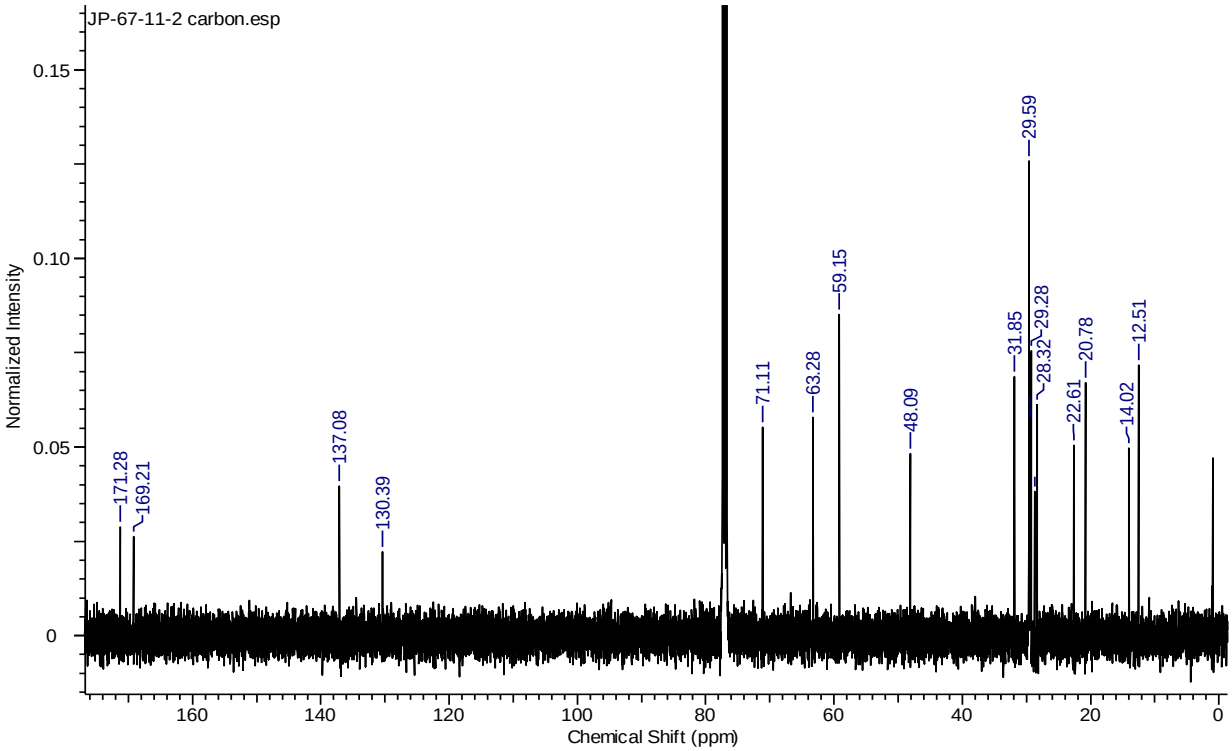

Figure II. 16: ^{13}C NMR spectrum of **83** (100 MHz, $CDCl_3$).

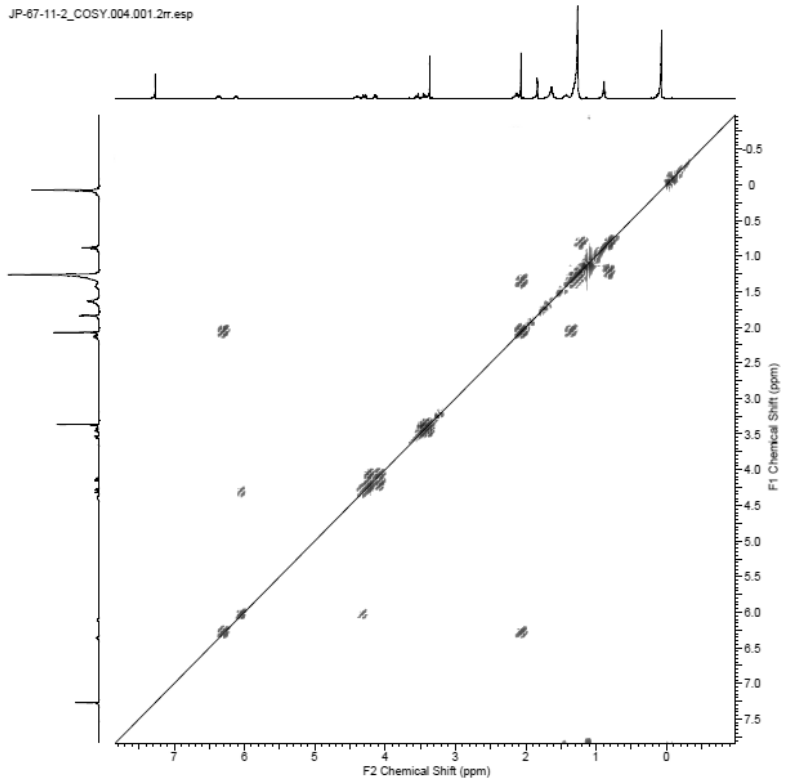

Figure II. 17: COSY spectrum of **83** (300 MHz, $CDCl_3$).

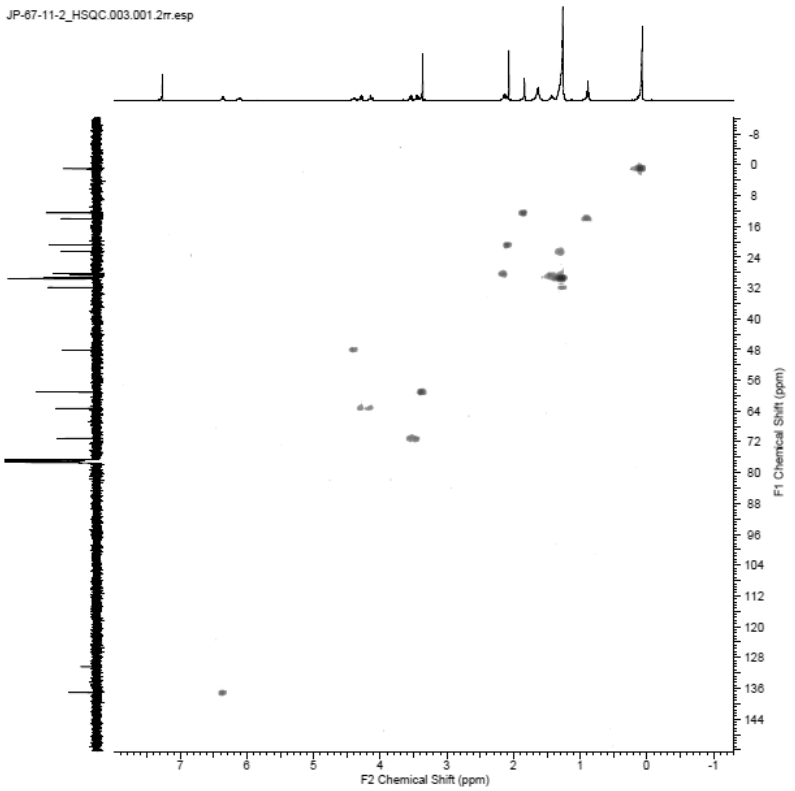

Figure II. 18: HSQC spectrum of **83** (300 MHz, $CDCl_3$).

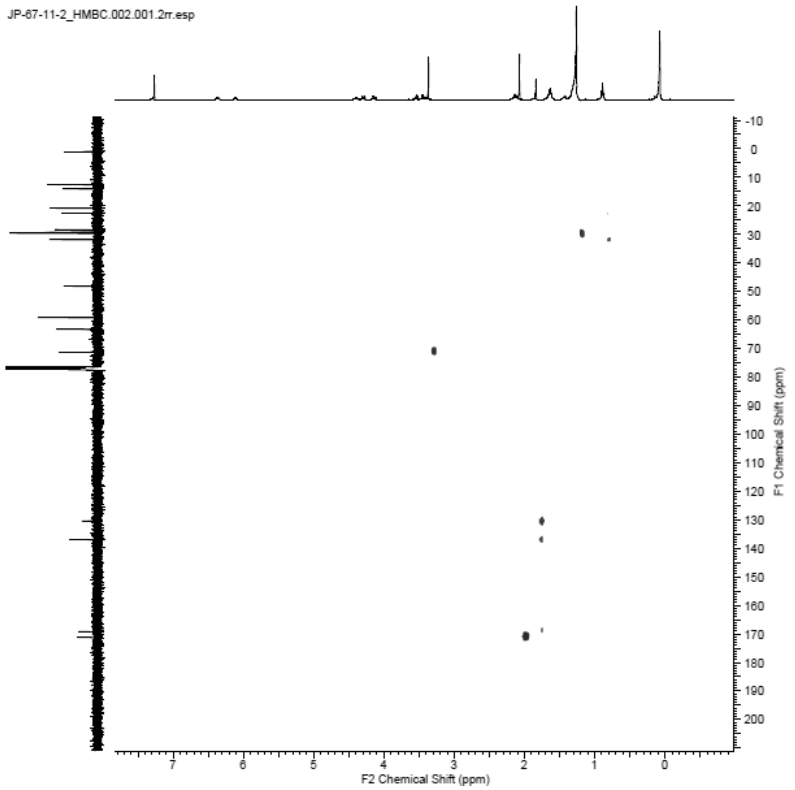

Figure II. 19: HMBC spectrum of **83** (300 MHz, $CDCl_3$).

Table II. 1: NMR spectroscopic data (^{1}H 400 MHz, ^{13}C 100 MHz; $CDCl_3$) for serinolamides C (**82**) and D (**83**).

	serinolamide C (**82**)			serinolamide D (**83**)		
position	δ_C, type	δ_H (J in Hz)	HMBC[a]	δ_C, type	δ_H (J in Hz)	HMBC[a]
1	169.9, C			169.2, C		
2	130.3, C			130.5, C		
3	137.4, CH	6.41, m		137.1, CH	6.36, m	
4	28.4, CH_2	2.14, ddd (7,7,7)		28.3, CH_2	2.14, ddd (7,7,7)	
5	28.7, CH_2	1.43, m		28.7, CH_2	1.42, m	
6-13	29.3 – 29.6, CH_2	1.26, m		29.3—29.6, CH_2	1.26, m	
14	31.9, CH_2	1.26, m		31.9, CH_2	1.26, m	
15	22.6, CH_2	1.26, m		22.6, CH_2	1.26, m	
16	14.0, CH_3	0.88, t (7.0)	14, 15	14.0, CH_3	0.88, t (6.4)	14, 15
17	12.6, CH_3	1.86, s	1, 2, 3	12.6, CH_3	1.84, s	1, 2, 3
18	50.8, CH	4.13, m		48.1, CH	4.40, m	
19	64.4, CH_2	3.71, dd (11.8, 4.2) 3.86, dd (11.4, 3.8)		63.3, CH_2	4.14, dd (11.4, 6.0) 4.28 (11.2, 6.4), dd	
20	73.3, CH_2	3.60, dd (9.6, 3.6) 3.63, dd (10.0, 3.6)		71.1, CH_2	3.53, dd (9.8, 3.4)	
21	59.3, CH_3	3.38, s	20	59.2, CH_3	3.37, s	20
22				171.3, C		
					3.46, dd (9.6, 4.8)	
23				20.8, CH_3	2.07, s	22
NH		6.41, m			6.11, d (7.6)	

[a]HMBC data optimized for 8 Hz are from proton(s) stated to the indicated carbon.

II. 2. 2. b. Configuration of serinolamides C and D

The configuration of the double bond of **82** and **83** was determined based on the characteristic chemical shifts of the methyl group at C-17 (δ_C 12.6 ppm). As the chemical shifts of α carbons are dependent on the geometrical isomerism of the double bond, the one of the methyl group at C-17 (δ_C 12.6 ppm) indicated an *E*-geometry. Indeed, in *cis* alkenes, the α carbons are shielded from their positions in the alkane, where in *trans* alkenes, they are deshielded.[86]

The absolute configuration was determined by Marfey's analysis.[82] The retention time of the hydrolysates of both fatty acid amides matched with that of the synthetic (*S*)-*O*-methylserinol

(Figure II. 20), leading to the assignment of C-18 in **82** as the *S*-configuration, and *R*-configuration for **83** by following the CIP rules in light of the *O*-acetylated serinol.

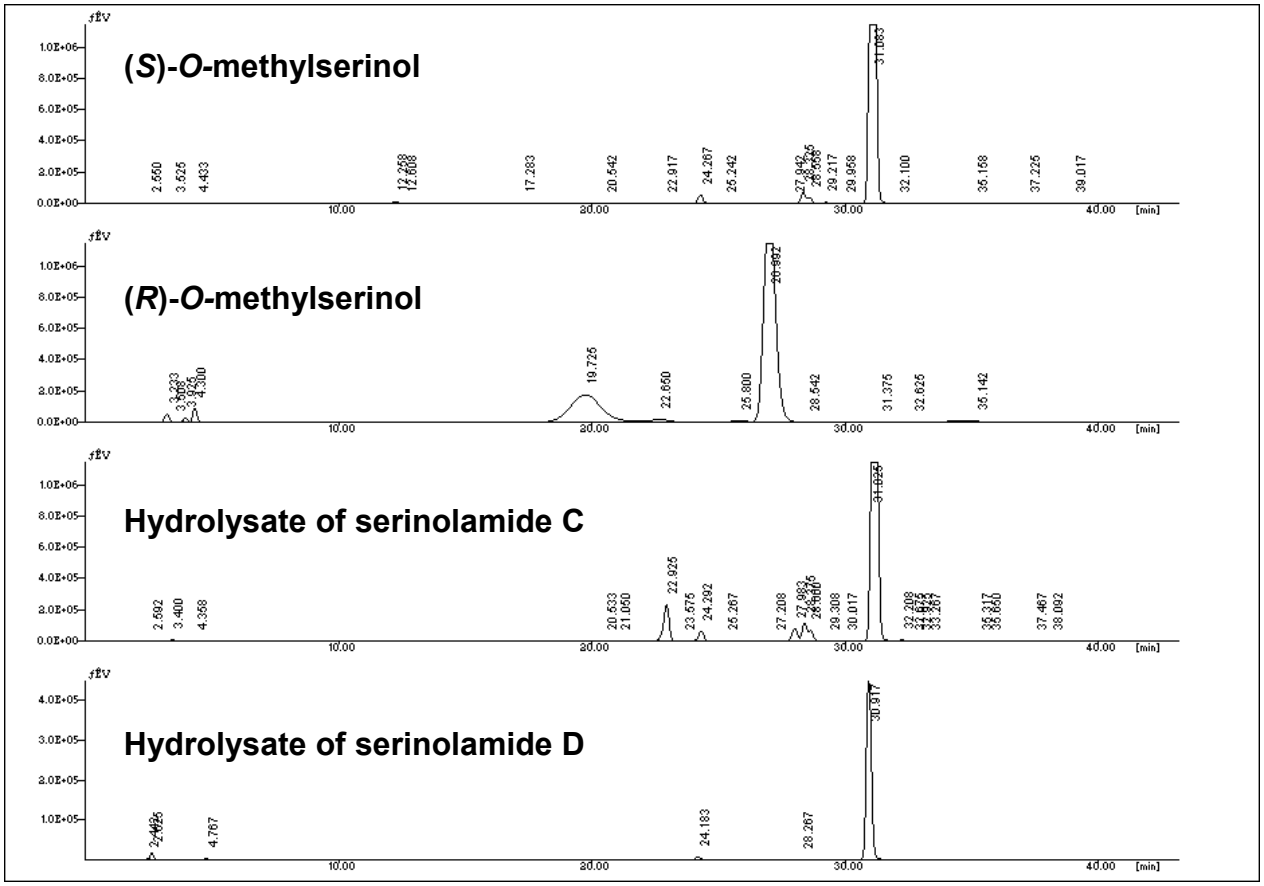

Figure II. 20: HPLC chromatograms of Marfey's derivatives of both synthetic *O*-methylserinol and both hydrolysates of **82** and **83**.

II. 2. 2. c. UV and IR data

The UV spectra (Figure II. 21) of both **82** and **83** showed low absorbance, with a λ_{max} of 219 nm (log ε 3.42) and 215 nm (log ε 4.46), respectively. This low absorbance observed for **82** and **83** is due to the weak unsaturated amide chromophore (λ_{max} of amido chromophore is 214 nm in H_2O).[87]

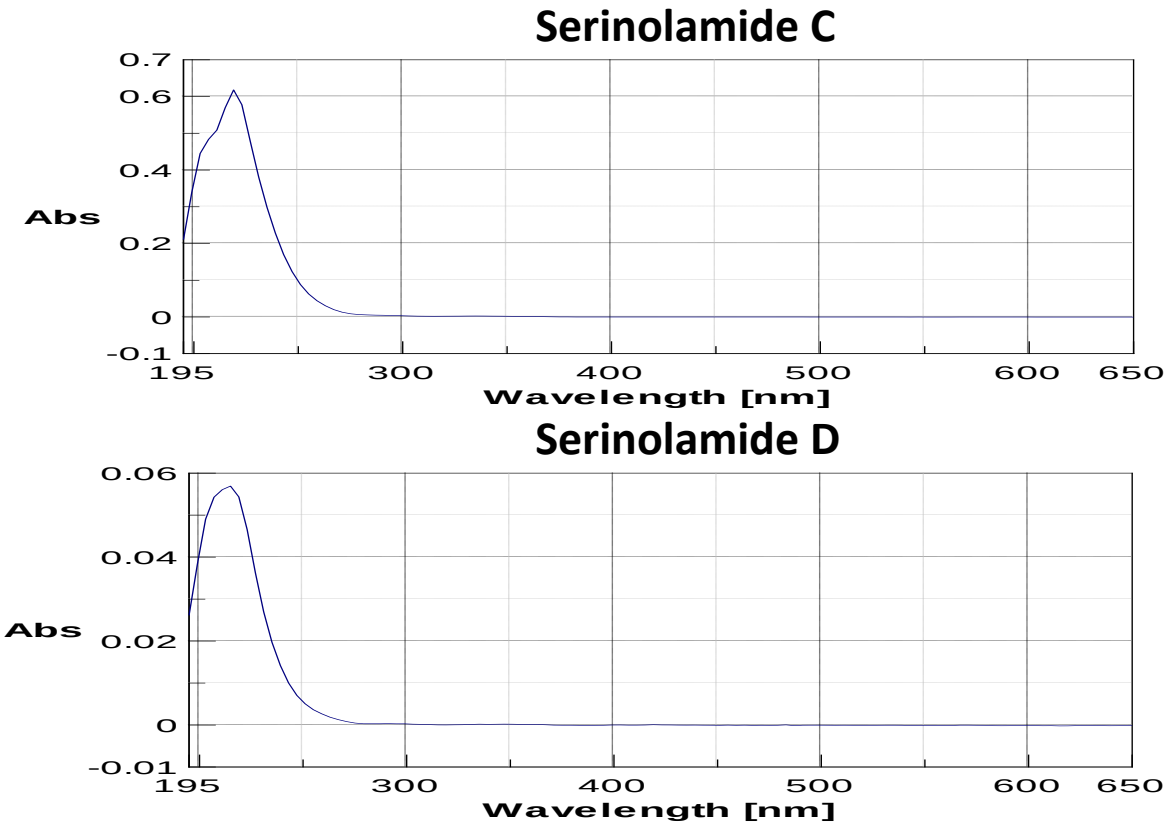

Figure II. 21: UV spectra of **82** and **83**.

The IR spectrum of **82** (Figure II. 22) shows characteristic signals such as hydroxy (3305 cm^{-1}), amide (1610 and 1552 cm^{-1}) and olefins (799 cm^{-1}). The IR spectrum of **83** (Figure II. 23) shows the same signals, except for the hydroxy group replaced by an ester (1741 cm^{-1}).

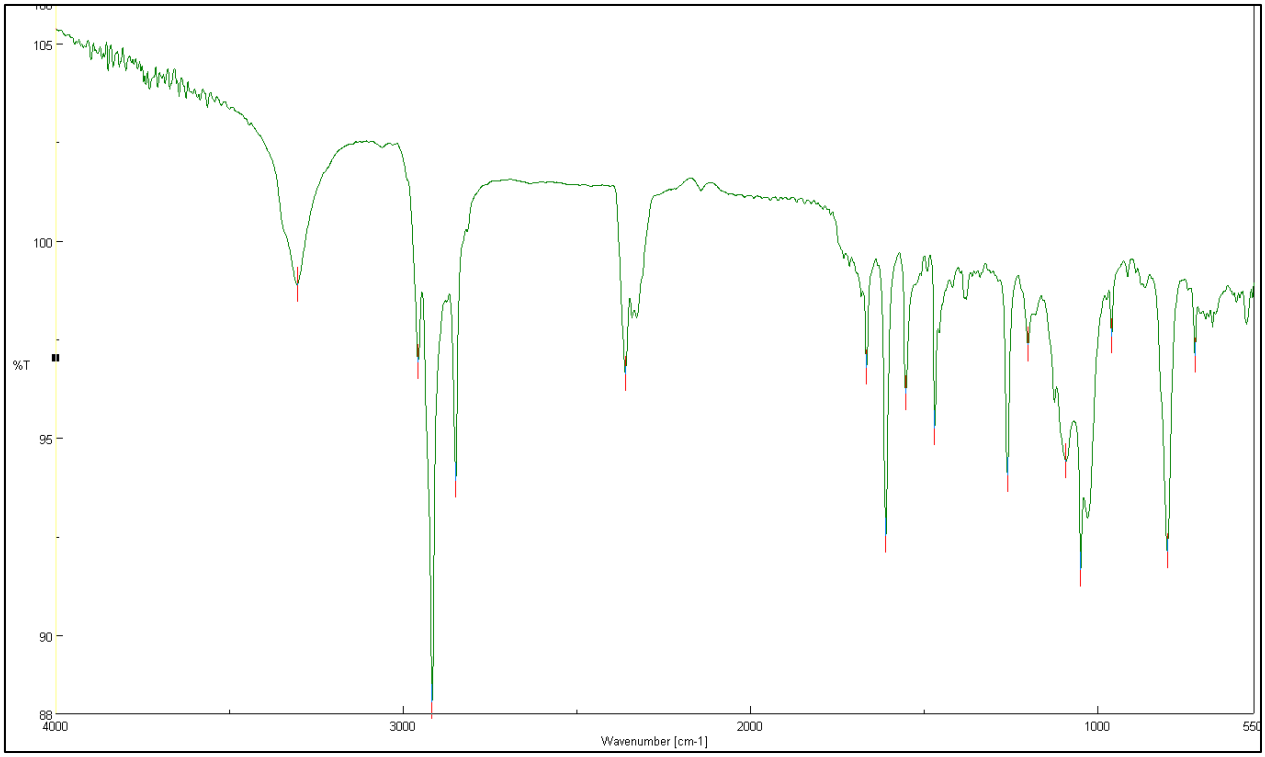

Figure II. 22: IR spectrum of **82**.

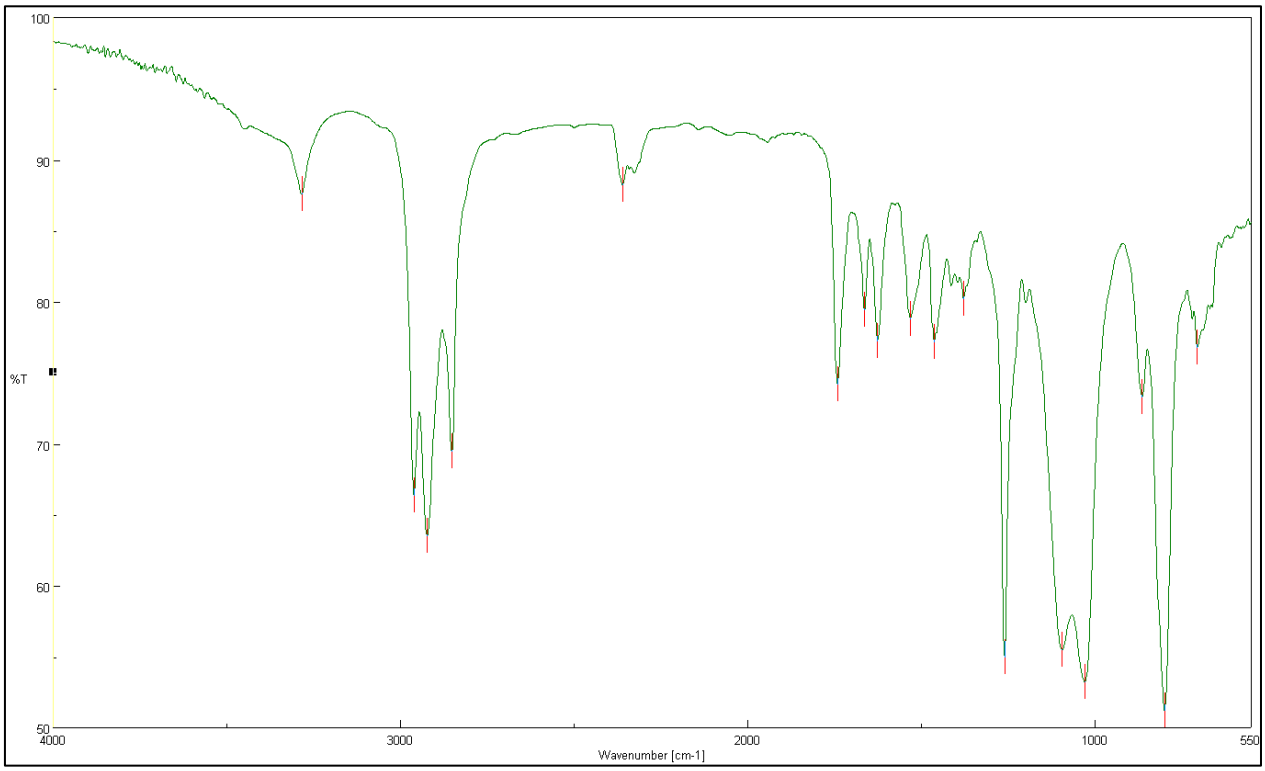

Figure II. 23: IR spectrum of **83**.

II. 3. Antifouling activity of serinolamides C and D

II. 3. 1. Materials and Methods

Same procedure as in Chapter 1 (section I. 4. 1.) was used to study the antifouling activity of both fatty acid amides, except that an extra experiment was added: the recovery test. Recovery test consists on collecting the non-settled living larvae after 120 hours of exposure and putting them in fresh marine water without compound. This test aims at observing if larvae are able to settle or not after 24, 48, 72, 96 hours or 7 days. In the first case, it means that the activity of the compound is reversible. On the other hand, if the larvae still can't settle after exposure, the activity of the compound is considered as irreversible so integrity of the larvae is affected.

II. 3. 2. Results

Serinolamides C (**82**) and D (**83**) were subjected to an antifouling assay using *Amphibalanus amphitrite* larvae. After an exposure time of 48 h, they inhibited the settlement of the larvae at concentrations below 1 µg/mL (EC_{50} values of 0.88 ± 0.16 and 0.04 ± 0.03 µg/mL, respectively, Figure II. 24). However, after an exposure time of 120 h at similar concentrations, barnacle larvae were able to settle. Although the two fatty acid amides slowed the settlement process considerably, they were unable to inhibit it completely. Recovery test for **83** showed that after 7 days, almost all the exposed larvae settled regardless of the tested concentration (Figure II. 25). Compound **83**, the most active fatty acid amide, has a reversible activity, which is important for an antifoulant in an ecologically friendly point of view. If the integrity of barnacle larvae is permanently affected, they won't never be able to settle so they will eventually die as cyprid don't feed and get their energy from their lipids stocked in oil droplets form that will finally be exhausted. If **83** is used in an antifouling paint, barnacle larvae won't attach to the surface and will try to find a non-protected surface.

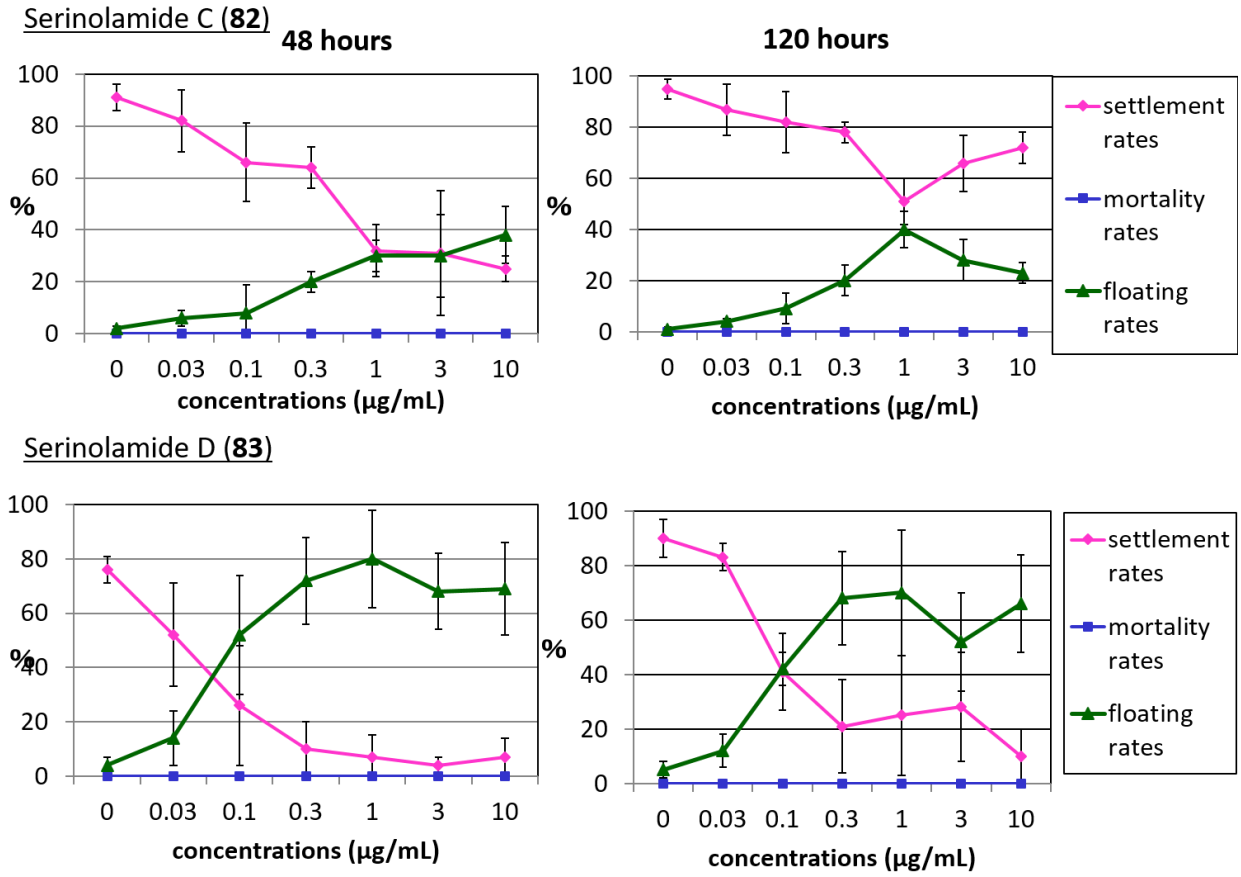

Figure II. 24: Antifouling activity of **82** and **83** on barnacle larvae after 48 and 120 hours of exposure. Error bars correspond to standard deviation (SD), n = 3.

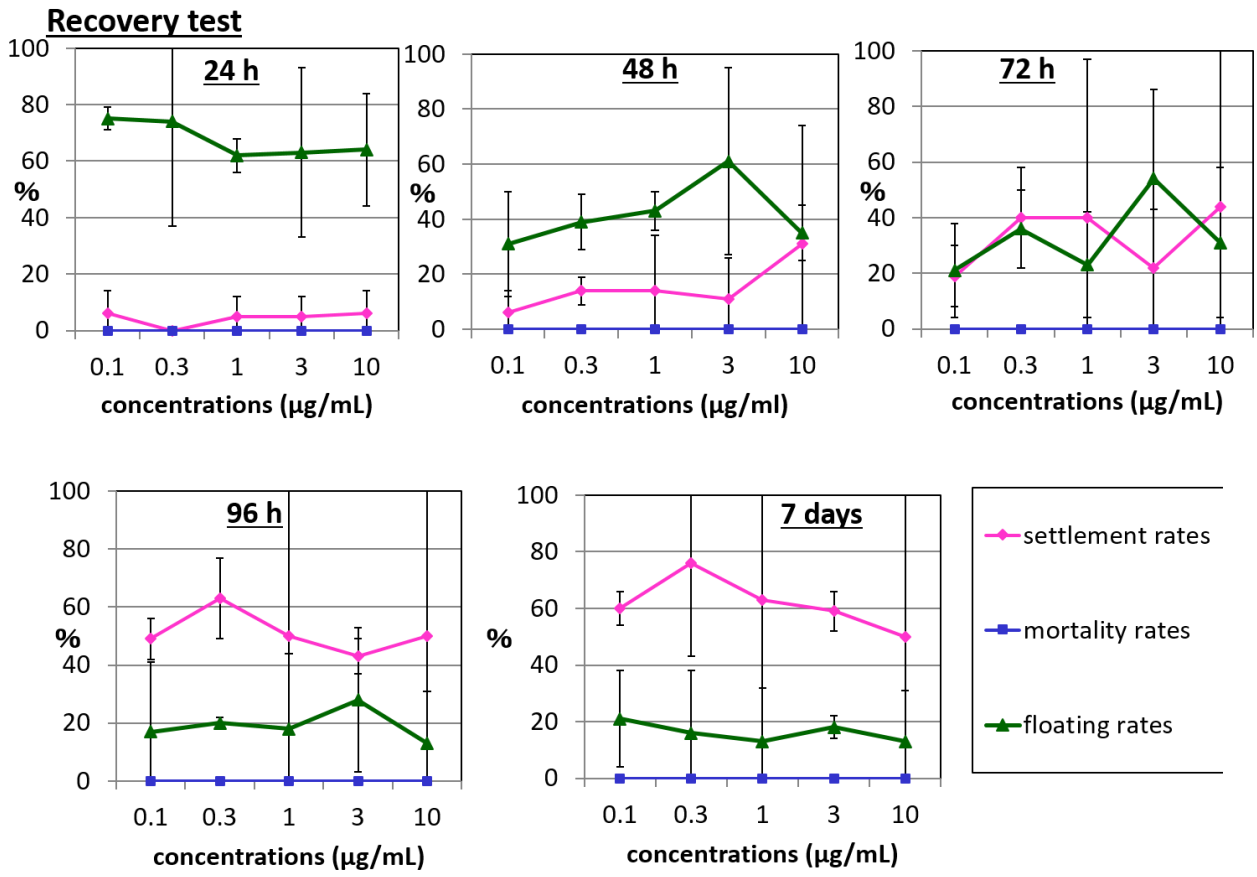

Figure II. 25: Recovery test after treatment with **83**. Error bars correspond to standard deviation (SD), n = 2.

II. 4. Discussion

The two new serinolamides C (**82**) and D (**83**) were isolated from a Red Sea *Okeania* sp. cyanobacterium, enlarging the number of serinolamides and, in general, the number of acyl amides isolated from cyanobacteria. It was interesting to see that, unlike serinolamides A (**89**) and B (**90**) which possess a serinol unit with a *R* configuration, **82** and **83** show a *S* configuration in their amide part. The position of the double bond was also different: for **89** and **90**, it was formed by C-4 and C-5, while for **82** and **83**, it was between C-2 and C-3. Semiplenamides A-E (**91**-**95**), isolated from *Lyngbya semiplena* collected in Papua New Guinea, also have this double bond at this position with a methyl attached to C-2.[88] As for **94** which is the acetylated form of **93**, **83** is the acetylated form of **82**.

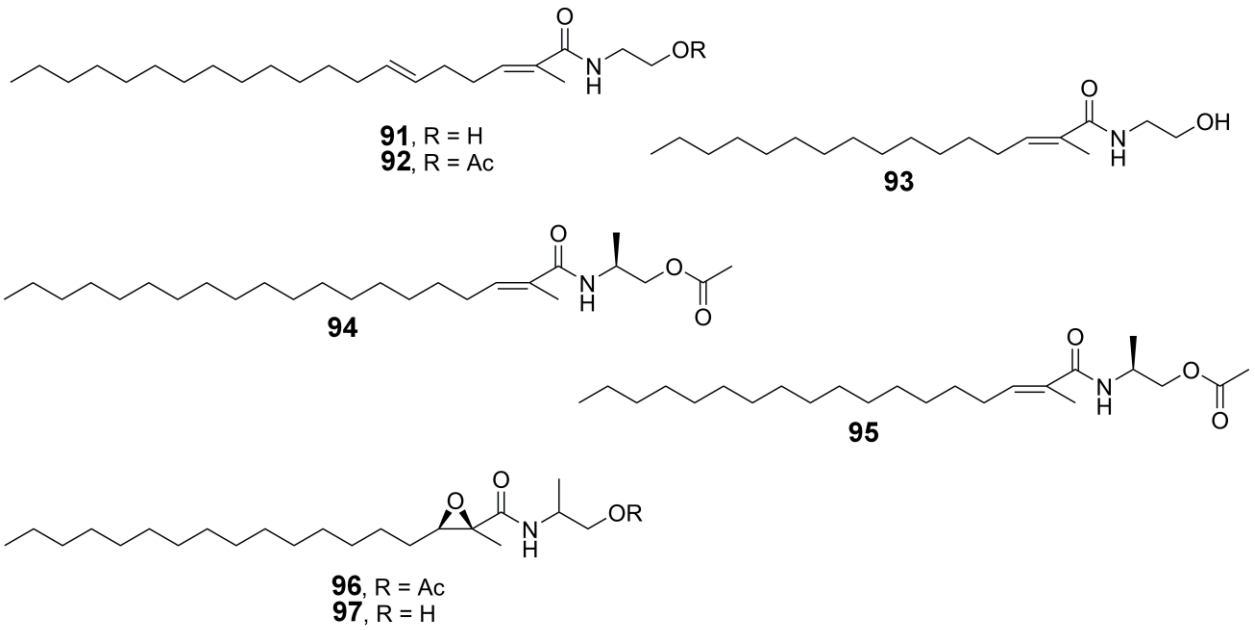

Compounds **89**-**92** and semiplenamides F (**96**) and G (**97**), together with grenadamide (**98**), mooreamide A (**99**) and columbamides A (**100**) and B (**101**), are cyanobacterial fatty acid amides acting on the cannabinoid receptors and though can be used to treat pain, cancer and diabetes.[84,85,88-94] Due to their similar structures, **82** and **83** could be cannabinomimetic fatty acid amides. Other compounds containing a fatty acyl chain and an amide unit have been isolated from cyanobacteria, mainly from species genetically close to *Okeania* sp., such as *Lyngbya*, *Moorea* and *Symploca* species. Lots of them were reported as cytotoxic, such as somocystinamide A (**102**)[95], guamamide (**103**)[96], jamaicamides A-C (**104-106**)[97], hermitamides A (**107**) and B (**108**)[98], isomalyngamide A (**109**) and some of its analogs[99] and pitiamides A (**110**) and B (**111**)[100]. In this study, **82** and **83** were tested on MCF7 breast cancer cells but, because they precipitated out of the medium, their activities could not be assessed.

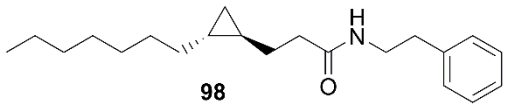

98

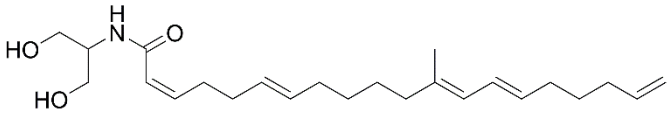

99

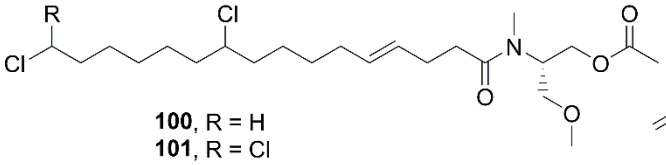

100, R = H
101, R = Cl

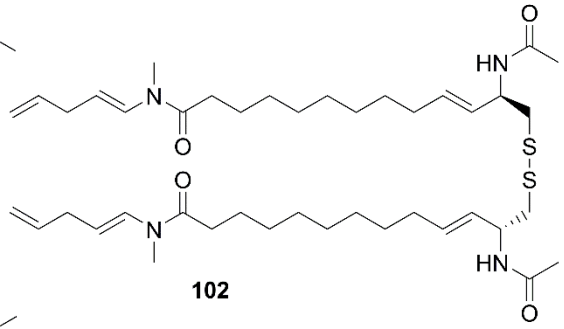

102

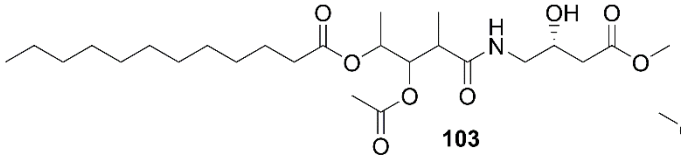

103

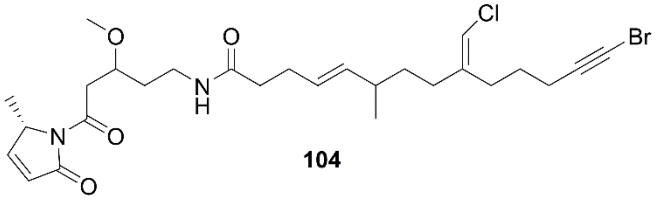

104

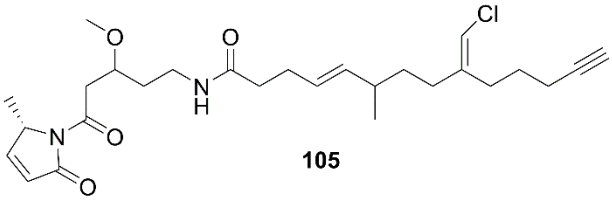

105

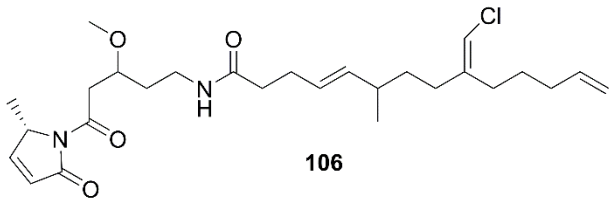

106

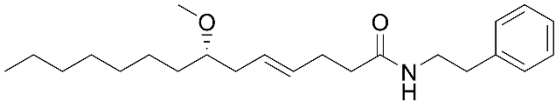

107

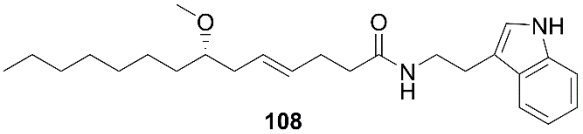

108

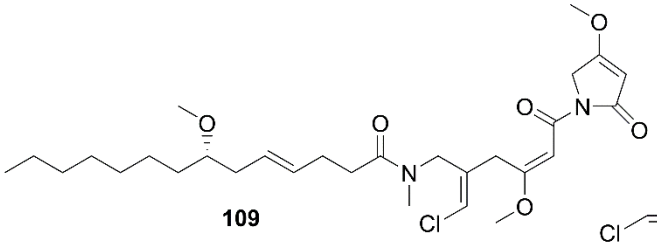

109

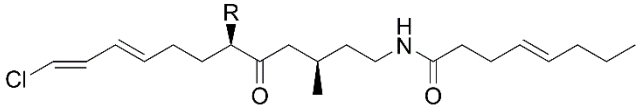

110, R = CH
111, R = H

Compounds **82** and **83** were tested on barnacle larvae and showed good antisettlement activity after 48-hour exposure by making the larvae floating. The acetylated fatty acid amide **83**

seemed more potent that its analog (EC_{50} of 0.04 and 0.88 µg/mL, respectively), showing that the acetyl group is important for the activity. However, as time passed, barnacle larvae were able to settle. When not disturbed by any molecule, larvae can freely swim in the water and attach anywhere, at the bottom of the well, on the wall under the water or on the wall at the surface of the water. Nevertheless, when floating, they can only attach to the wall at the surface of the water. That is probably why they took more time to settle when treated with serinolamides, because they have less possibilities. These fatty acid amides can slow down the settlement. Also, knowing the amphiphilic nature of fatty acid amides, they can be considered as slip agents or dispersants. Slip agents or dispersants reduce the coefficient of friction, making difficult for organisms to attach. The fatty acyl chain of fatty acids amides has high affinity to plastic such as polystyrene (which is the component of the 24-well culture plate used in the antifouling assay). For this reason, the hydrocarbon chain is embedded in polymer and the amide unit is facing air, forming a first layer of slip agent. Other molecules of fatty acid amides then form a second layer, with their amide groups facing the ones of the first layer because similar functional groups have affinity to each other. As a result, the two-layer coating, with the fatty acyl chains facing air, has hydrophobic properties which decrease the friction coefficient or, in other words, increase the slipperiness of the surface.[101] Because of this, barnacle larvae cannot attach to it. They probably only attached at the interface between water and air, where the coating is weaker (because only on the wall submerged). Because of these features, fatty acid amides such as oleamide (**112**) and erucamide (**113**), the most frequently used slip agents in industrial applications, are used in antifouling paints.[102] As a result, **82** and **83**, despite inhibiting barnacle larvae settlement only for few days, can be considered as potent antifoulants. In the described *in vitro* assay, no perturbation occurs but, in field assays, larvae could probably be removed easily from the water/air interface because of weak interaction with the surface.

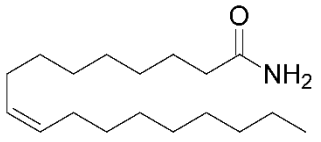

112

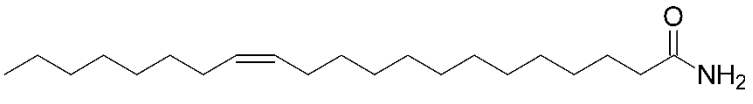

113

- Chapter III -

Isolation of Lyngbyabellins and the Known Antifouling Compound Dolastatin 16 from *Okeania* sp.

Together with **82** and **83** whose isolation was described in the previous chapter, *Okeania* sp. extract gave two new lyngbyabellins, O (**114**) and P (**115**), the known lyngbyabellins F (**116**), G (**117**) and H (**118**), 27-deoxylyngbyabellin A (**119**) and the known antifouling compound dolastatin 16 (**60**). This chapter aims at describing their isolation, the structure elucidation of the two new lyngbyabellins **114** and **115**, their bioactivities and an observed structure/activity relationship.

III. 1 Isolation of Lyngbyabellins F, G, H, O and P, 27-deoxylyngbyabellin A and Dolastatin 16

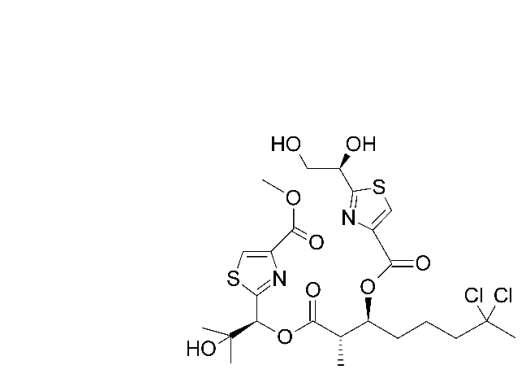

114

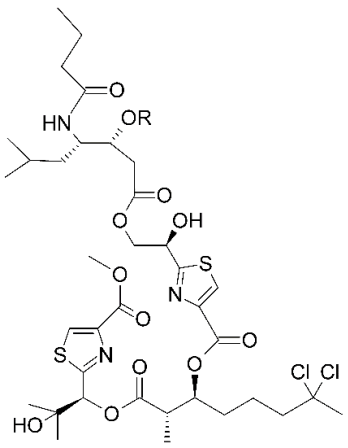

115, R = H
116, R = Ac

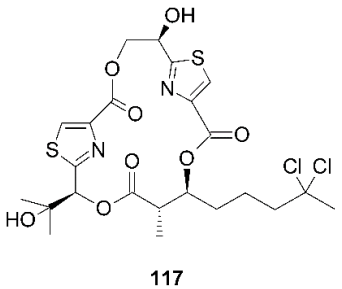

117

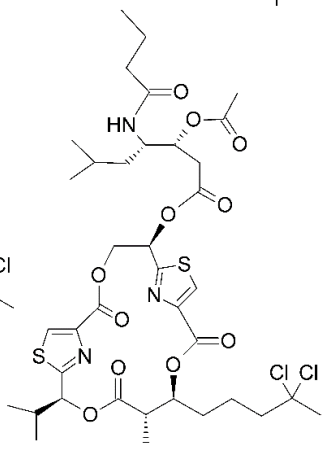

118

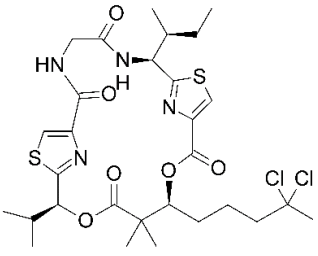

119

III. 1. 1. Materials and Methods

III. 1. 1. a. General Experimental Procedures

Same general experimental procedures as for **82** and **83** in Chapter II were employed.

III. 1. 1. b. Biological Material

The same biological material as in Chapter II was used.

III. 1. 1. c. Extraction and Isolation

Compounds **114**, **115** and **117**, together with **60**, were isolated from the same extract containing **82** and **83** described in Chapter II. Figure III.1 shows the isolation scheme used to obtain these three lyngbyabellins and **60**. The fraction eluted with 100% EtOAc (140 mg) was fractionated by RP-HPLC (Cosmosil Cholester 10 x 250 mm, 5 µm, 3 mL/min, UV detection at 210 nm, gradient 0–30 min, 40%–80% MeCN containing 0.05% (*v/v*) TFA) to yield fraction A (t_R 14.1 min, 3.4 mg), fraction B (t_R 16.4 min, 6.7 mg), fraction C (t_R 20.4 min, 4.4 mg), fraction D (t_R 22.3-24.9 min, 3.7 mg). Fraction A was further purified by RP-HPLC (Cosmosil Cholester 4.6 × 250 mm, 5 µm, 1 mL/min, UV detection at 210 nm, gradient 0–40 min, 40%–70% MeCN containing 0.05% (*v/v*) TFA) to yield **114** (t_R 9.6 min, 0.8 mg). Fraction B was further purified by RP-HPLC (Cosmosil Cholester 10 x 250 mm, 5 µm, 3 mL/min, UV detection at 210 nm, gradient 0–40 min, 40%–70% MeCN) to yield to the known compound **117** (t_R 20.7 min, 3.3 mg). Fraction C was further purified by RP-HPLC (Cosmosil Cholester 10 x 250 mm, 5 µm, 3 mL/min, UV detection at 210 nm, gradient 0–40 min, 40%–70% MeCN) to yield **115** (t_R 27.5 min, 1.9 mg). Fraction D was further purified by RP-HPLC (Cosmosil Cholester 4.6 × 250 mm, 5 µm, 1 mL/min, gradient 0–40 min, 60%–80% MeCN containing 0.05 % (*v/v*) TFA) to yield a subfraction (Fraction D', t_R 10.4 min, 7 mg), which was further purified by RP-HPLC (Cosmosil Cholester 4.6 × 250 mm, 5 µm, 1 mL/min, UV detection at 254 nm, gradient 0–40 min, 50%–70% MeCN) to give the known compound **60** (t_R 22.5 min, 1.5 mg).

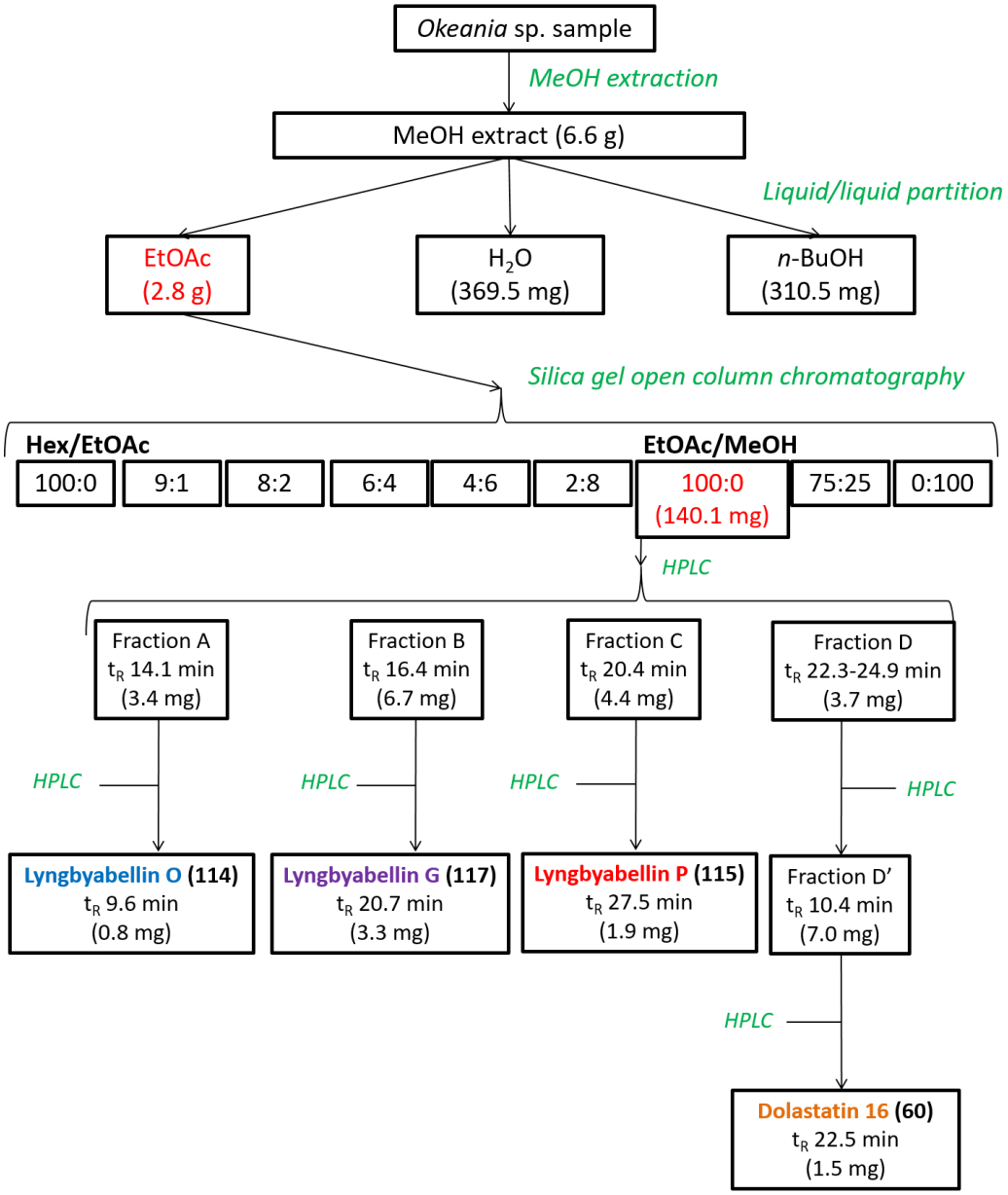

Figure III. 1: Isolation scheme for **114**, **115**, **117**, and **60** from homogenized *Okeania* sp. extract.

Compounds **116** and **118**, and **119** were obtained from another *Okeania* sp. extract. The only difference with the previous extract is the absence of homogenization before the MeOH extraction. Figure III. 2 explains the procedure. After the liquid/liquid partition and the silica gel open column chromatography on the EtOAc fraction (456.3 mg), the 4:6 (*v*/*v*) hexane/EtOAc fraction (31.8 mg) was fractionated by RP-HPLC (Cosmosil Cholester 10 x 250 mm, 5 µm, 3 mL/min, UV detection at 210 nm, gradient 0–60 min, 50%–70% MeCN) to yield fraction E (t_R 36.5 min, 1.2 mg), fraction F (t_R 39.0 min, 1.6 mg) and fraction G (t_R 46.1-46.5 min, 3.0 mg).

Fraction G was further purified by RP-HPLC (Cosmosil Cholester 10 x 250 mm, 5 µm, 3 mL/min, UV detection at 210 nm, gradient 0–60 min: 50–70% MeCN) to give **119** (t_R 36.3 min, 1.6 mg) and **118** (t_R 38.9 min, 1.1 mg). The 75:25 (*v*/*v*) EtOAc/MeOH fraction (103.8 mg) was also subjected to RP-HPLC separation (Cosmosil Cholester 10 x 250 mm, 5 µm, 3 mL/min, UV detection at 210 nm, gradient 0–30 min, 40%–80% MeCN) to yield fraction H (t_R 13.8 min, 3.4 mg), fraction I (t_R 16.4 min, 6.7 mg) and fraction J (t_R 23.2 min, 4.4 mg). Further purification of fraction H (Cosmosil Cholester 10 x 250 mm, 5 µm, 3 mL/min, UV detection at 210 nm, gradient 0–50 min, 30%–50% MeCN) gave extra amount of **114** (t_R 36.3 min, 1.6 mg), while fraction I (Cosmosil Cholester 10 x 250 mm, 5 µm, 3 mL/min, UV detection at 210 nm, gradient 0–30 min, 40%–50% MeCN) gave extra amount of **117** (t_R 28.9 min, 1.1 mg) and fraction J gave **116** (t_R 20.7 min, 1.1 mg).

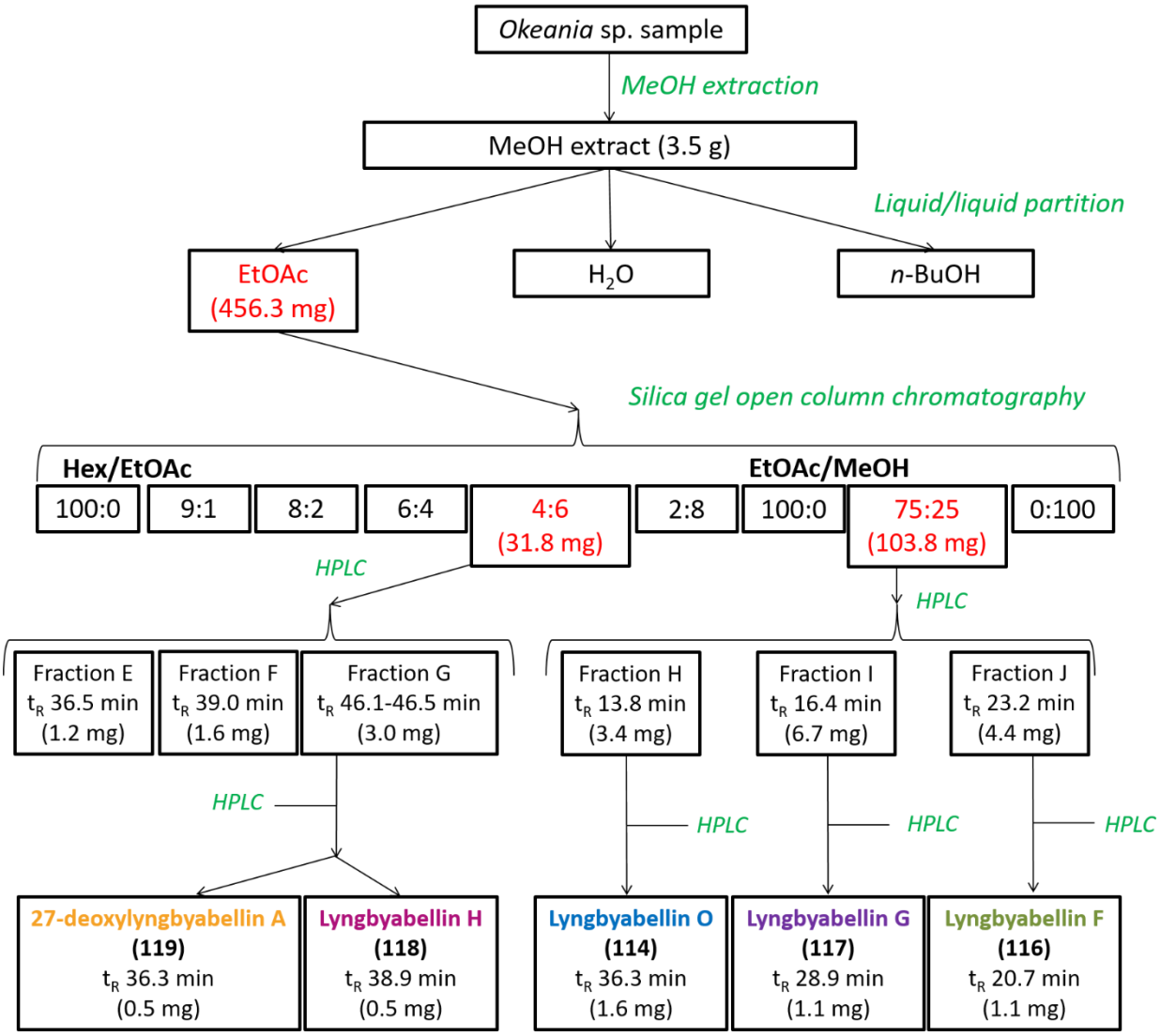

Figure III. 2: Isolation scheme for **114, 116-119** from non-homogenized *Okeania* sp. extract.

III. 1. 2. Results

After NP column chromatography on EtOAc fraction of *Okeania* sp., as explained in Chapter II, the 100% EtOAc subfraction was partitioned by RP HPLC to give the new **114** and **115**, and the known **60** and **117**. From another *Okeania* sp. MeOH extract, same liquid/liquid partition and NP column chromatography were performed. The 4:6 (v/v) mixture of hexane/EtOAc led to **118** and **119**, while the 75:25 (v/v) mixture of EtOAc/MeOH gave extra **114**, **116** and **117**.

III. 2. Characterization of lyngbyabellins O and P, and confirmation of the identities of lyngbyabellins F, G and H, 27-deoxylyngbyabellin A and dolastatin 16

III. 2. 1. Materials & Methods

III. 2. 1. a. Experimental Procedures

A JEOL 400 MHz spectrometer was used to record the ^{1}H NMR spectra of **116**, **118**, **119** and **60** and the ^{1}H and ^{13}C NMR spectra for **117**. The 1D and 2D spectra for **114** and **115** were recorded on a JEOL 600 MHz spectrometer. The ^{13}C NMR spectra for **118** and **119** were recorded on a Bruker 500 MHz spectrometer. All the NMR spectra were recorded in $CDCl_3$ (Cambridge Isotope Laboratories, Inc.) using the residual solvent peak ($CHCl_3$) as an internal reference (δ_H 7.27 and δ_C 77.00 ppm). UV spectra were recorded on JASCO multiwavelength UV detector MD-1510.

III. 2. 1. b. Chiral analyses of degradation products of lyngbyabellin O

The absolute configurations of **114** at C-14 and C-20 were determined by chiral-phase chromatography techniques. A small portion of **114** (0.6 mg) was dissolved in MeOH (2 mL) and ozonolyzed at – 78 °C for 25 min. The solvent was removed under a stream of Ar and the sample was hydrolyzed with 2 N NaOH at 90 °C for 7 h.[103] To determine the relative configuration at C-14, the hydrolysate was analyzed by chiral-phase ESI-LC-MS (column Astec Chirobiotic TAG 2.1 x 250 mm; 0.2 mL/min; ESI negative low mode; 1:1 0.1% aqueous formic acid / 1% NH_4OAc in MeOH; column oven: 20 °C) and the retention time was compared to the commercially available L- and D-glyceric acids (3.5 and 3.8 min, respectively). The hydrolysate was then methylated to

produce α,β-dihydroxyisovaleric (Dhiv) methyl ester. After derivatization by (*R*)-MTPA, the product from **114** and the standard synthetized Dhiv methyl esters were subjected to HPLC analysis and retention times compared.

III. 2. 1. c. Synthesis of (*R*)- and (*S*)-α, β-dihydroxyisovaleric acid methyl esters

The standards *R*- and *S*-Dhiv methyl esters were synthesized by Sharpless asymmetric dihydroxylation of methyl 3,3-dimethylacrylate (**120**) using AD-mix-α and AD-mix-β, respectively (Figure III. 3).[104] In a 25-mL round flask, 1,4 mg of AD-mix-α or β (containing 7.8 mg of ligand) was dissolved in 10 mL of *t*-BuOH/H_2O (1:1) and the mixture was stirred at room temperature until two clear phases appeared, the lower aqueous phase being bright yellow. Methanesulfonamide (95 mg) was added and the reaction mixture was cooled down to 0 °C until precipitation of some salts. Methyl 3,3-dimethylacrylate (0.11 g, 1 mmol) was added. The reaction mixture was stirred at 0 °C for 24 hours. The reaction was quenched by addition of solid sodium sulfite (1.5 g) and warm to room temperature for 30 minutes before addition of 10 mL EtOAc. Solvent partition was performed and the aqueous layer was washed three times with EtOAc. The combined organic layers were washed with 2 N KOH (1.12 g/mL) in a separation funnel and dried over anhydrous magnesium sulfate, filtrated and concentrated Purification by flash chromatography (silica gel, 1:1 Hex/EtOAc) lead to 7.58 mg of *R*-Dhiv methyl ester (**121**) with the AD-mix-α, and 7.41 mg of *S*-Dhiv methyl ester (**122**) with the AD-mix-β.

Table III. 1: Amount of each component of the synthesis of (*R*)- and (*S*)-α, β-dihydroxyisovaleric acids (**121-122**).

	Calculated (g)	**Mmol**	**MW (g/mol)**	**Equivalent**
120	0.11	1	114.143	1
AD-mix-α or β	1.4 (but 0.0078 of ligand)	0.01 (for ligand)	778.998	0.01
Methanesulfonamide	0.95	1	95.116	1
1:1 *t*-BuOH/H_2O	10 mL			0.2 (based on *t*-BuOH)

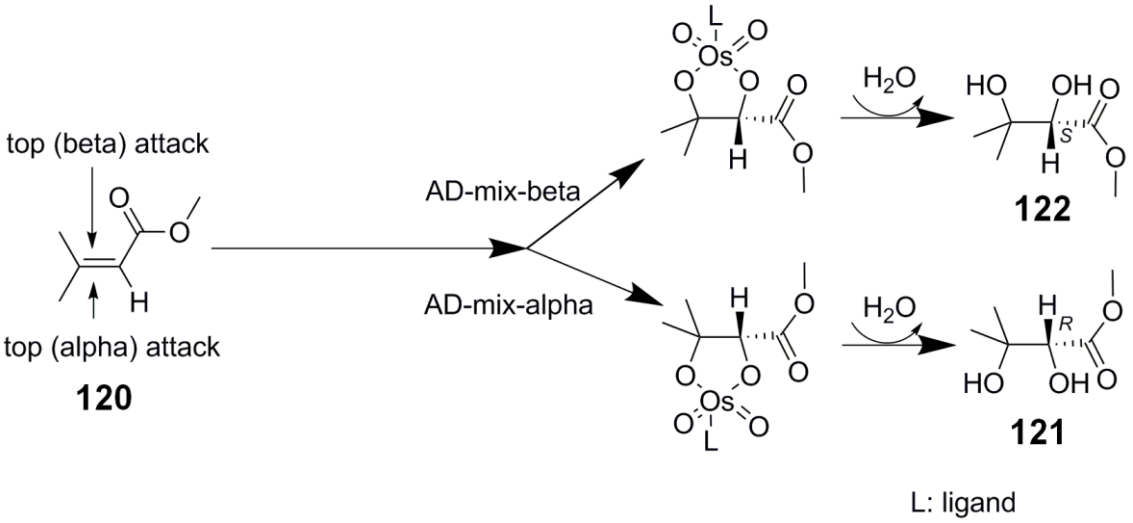

Figure III. 3: Mechanism of the synthesis of **121** and **122**.

III. 2. 1. d. Chiral analysis of Dhiv

As **121** and **122** were not separable by chiral HPLC, derivatization by MTPA was performed. The product obtained from base hydrolysis after ozonolysis of **114** and the standards **105** and **106** were derivatized using (*R*)-MTPA. The samples were dissolved in CH_2Cl_2, mixed with (*R*)-MTPA (50 µL of a solution of 50 µg/mL of MeCN) and heated for 1 h at 70 °C. The reaction was quenched by addition of EtOH (100 µL) and heating for 15 min at 70 °C.[105] After evaporation of the solvent, the samples were dissolved in MeOH and subjected to HPLC analysis (column Cosmosil 5C18-MS-II 4.6 x 250 mm, 5 µm, 1 mL/min, UV detection 254 nm, gradient 0–30 min, 20%–30% MeOH). The retention time of the MTPA derivative from the hydrolysate of **114** matched the one of the **122** standard (16.5 min, instead of 14.6 min for the **121** standard).

III. 2. 1. e. Mild methanolysis of lyngbyabellin G to give lyngbyabellin O

A portion of **117** (0.4 mg) was dissolved in MeOH (100 µL) and 0.1 M HCl in MeOH was added (900 µL). The mixture was heated at 85 °C for 45 min. The reaction was quenched by evaporation of the solvent. The product was then dissolved in MeOH for ESI-LC-MS analysis. The results showed that **117** was converted into **114**.

III. 2. 1. f. Deacetylation of lyngbyabellin F to give lyngbyabellin P

Compound **116** (1 µmol) was dissolved in MeOH (100 µL) and 0.1 M $NaOCH_3$ in MeOH was added (1 µL). After 15 min at room temperature, the reaction was quenched by evaporation of the solvent. The product was then dissolved in EtOH for ESI-LC-MS analysis. The results showed that **116** was converted into **115**. Compound **114** was also observed, probably due to methanolysis.

III. 2. 2. Results

III. 2. 2. a. Planar Structure of Lyngbyabellins O and P

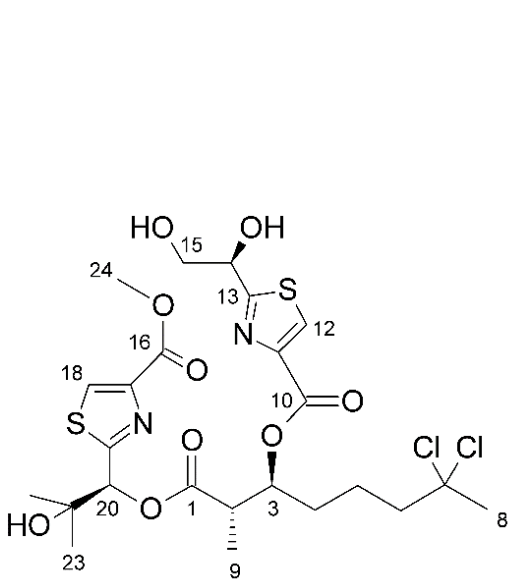

114

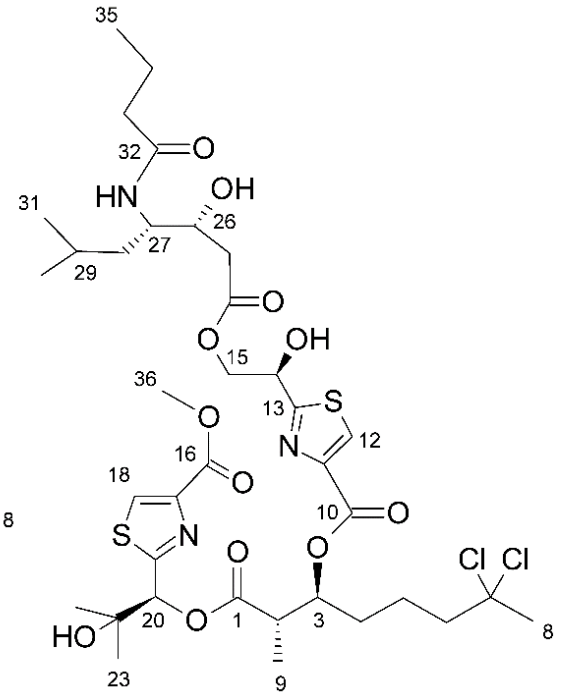

115

NMR and MS data analyses were used to determine the planar structures of **114** and **115**. ESI-TOF-MS analysis revealed that the molecular formulae of **114** and **115** were $C_{24}H_{32}Cl_2N_2O_4S_2$ and $C_{36}H_{52}Cl_2N_3O_{12}S_2$ with nine and 11 degrees of unsaturation, respectively. Both compounds contained two chlorine atoms, as exemplified by the 9:6:1 isotope peaks observed in the mass

spectra of **114** and **115** with *m/z* values of 627/629/631 and 854/856/858, respectively. The NMR data for **114** and **115** are summarized in Table III. 2.

The ^{1}H NMR spectrum of **114** (Figure III. 4 and Table III. 2) showed two deshielded signals (δ_H 8.17 and 8.24), whereas the ^{13}C NMR spectrum (Figure III. 5) contained signals consistent with eight sp^2 carbons (C-10 to C-13 and C-16 to C-19). Taken together, these data suggested the presence of two 2-alkylthiazole-4-carboxylates, which are typical of lyngbyabellins and dolabellin.[103] HMBC analysis (Figure III. 8) also confirmed the presence of two thiazole rings with correlations from H-12 to C-11 and C-13 and H-18 to C-17 and C-19. The remaining sp^2 carbon (C-1 δ_C 171.0) was assigned to the carbonyl group of a saturated ester. Between them, the two thiazole rings and the three carbonyl groups accounted for the nine degrees of unsaturation in **114**.

The ^{1}H NMR spectrum of **114** also showed a series of shielded, coupled resonance signals indicative of an aliphatic chain. A singlet corresponding to a methyl group at δ_H 2.12 was also detected, which showed a correlation to a methylene at δ_C 49.1 (C-6) and a dichlorinated carbon at δ_C 90.1 (C-7) by HMBC analysis, indicating an unusual *gem*-dichloro group. This group has been reported previously for lyngbyabellins A–K and M–N, as well as dolabellin and the hectochlorins.[103] HMBC and COSY analysis (Figure III. 6 and 8) indicated that this *gem*-dichloro group was attached to the aliphatic chain, with the C-9 methyl group attached to the C-2 methine.

Furthermore, HMBC analysis revealed correlations between H-20 and C-1, as well as correlations with C-19 of one of the thiazole ring systems and two methyl groups (C-22 and C-23), both of which were attached to an oxygenated non-protonated carbon (C-21) (forming fragment D) (Figure III. 9) COSY and HMBC data also revealed two partial structures: –CH(OH)CH$_2$OH (fragment A) and a methoxy attached to a carbonyl group (fragment E).

Unfortunately, no correlations connecting fragments A–E were observed. However, based on ^{1}H and ^{13}C NMR data similar to lyngbyabellins and detailed consideration of the many different combinations, the proposed structure was recognized as the best fit for the available data. The chemical shift of C-3 (δ_C 75.2) showed that this carbon should be attached to an oxygen atom. This proves that fragments C and D are attached. If C-17 of fragment D was attached to fragment A, it would be more deshielded, but attached to fragment E, its chemical shift corresponds to the one observed in the spectrum (Table III. 2). As the chemical shift of C-11 is almost identical to that of C-17, we can consider that it is also attached to a carboxyl, therefore to fragment C. The remaining fragment A is attached to fragment B at C-13.

Table III. 2. NMR spectroscopic data (^{1}H 600 MHz, ^{13}C 150 MHz, $CDCl_3$) for Lyngbyabellins O (**114**) and P (**115**)

	lyngbyabellin O (**114**)				lyngbyabellin P (**115**)			
position	δ_C, type	δ_H (*J* in Hz)	COSY	HMBC[a]	δ_C, type	δ_H (*J* in Hz)	COSY	HMBC[a]
1	171.0, C	-			171.0, C	-		
2	43.8, CH	3.00, dq (4.2, 6.6)	3, 9	1, 9	43.7, CH	3.03, dq (4.8, 7.2)	9	1
3	75.2, CH	5.43, dt (4.8, 12.0)	2, 4		75.0, CH	5.43, dt (7.8, 4.2)	4	
4	31.6, CH_2	1.81, m	3, 5	5	31.4, CH_2	1.82, m	3	
5	21.6, CH_2	1.81, m	4, 6		21.6, CH_2	1.79, m	6	
6	49.1, CH_2	2.18, 2.25, m	5	5	49.1, CH_2	2.18, 2.26, m	5	
7	90.1, C	-			90.1, C	-		
8	37.4, CH_3	2.12, s		6, 7	37.4, CH_3	2.12, s		6, 7
9	13.8, CH_3	1.28, d (6.6)		1, 2, 3	13.6, CH_3	1.29, d (6.6)		1, 3
10	166.4, C	-			160.9, C	-		
11	146.2, C	-			146.4, C	-		
12	129.0, CH	8.24, s		11, 13	129.0, CH	8.22, s		11, 13
13	179.7, C	-			173.0, C	-		
14	71.7, CH	5.09, br	15		70.0, CH	5.29, dd (3.6, 7.8)	15	
15	66.0, CH_2	4.02, brd (16.8)	14		67.8, CH_2	4.55, dd (11.4, 3.6) 4.59, dd (11.4, 7.8)	14	24
16	161.8, C	-			161.7, C	-		
17	146.1, C	-			146.2, C	-		
18	128.7, CH	8.17, s	20	17, 19	128.5, CH	8.17, s		17, 19
19	167.0, C	-			167.4, C	-		
20	78.3, CH	6.16, s	18	1, 19	78.4, CH	6.13, s		1, 19, 22, 23
21	72.2, C	-			72.0, C	-		
22	25.3, CH_3	1.18, s	23	20, 23	26.6, CH_3	1.38, s		20, 21, 23
23	26.9, CH_3	1.41, s	22	20, 21, 22	25.4, CH_3	1.19, s		20, 21, 11
24	52.6, CH_3	3.95, s		16	171.9, C	-		
25					37.5, CH_2	2.56, d (5.4)	26	24, 26, 27
26					71.8, CH	3.90, ddd (6.0, 6.0, 6.0)	25	
27					51.6, CH	4.07, m	27-NH, 28	
27-NH						5.52, d (8.4)	27	
28					39.0, CH_2	1.34, 1.50, m	27	
29					25.0, CH	1.63, m	30, 31	
30					23.5, CH_3	0.95, d (6.0)	29	28, 29, 31
31					21.5, CH_3	0.90, d (6.0)	29	28, 29, 30
32					174.3, C	-		
33					38.6, CH_2	2.20, m	34	32
34					19.2, CH_2	1.67, m	33, 35	32
35					13.7, CH_3	0.97, t (7.8)	34	34
36					52.5, CH_3	3.95, s		16

[a]HMBC optimized for 8 Hz are from proton(s) stated to the indicated carbon.

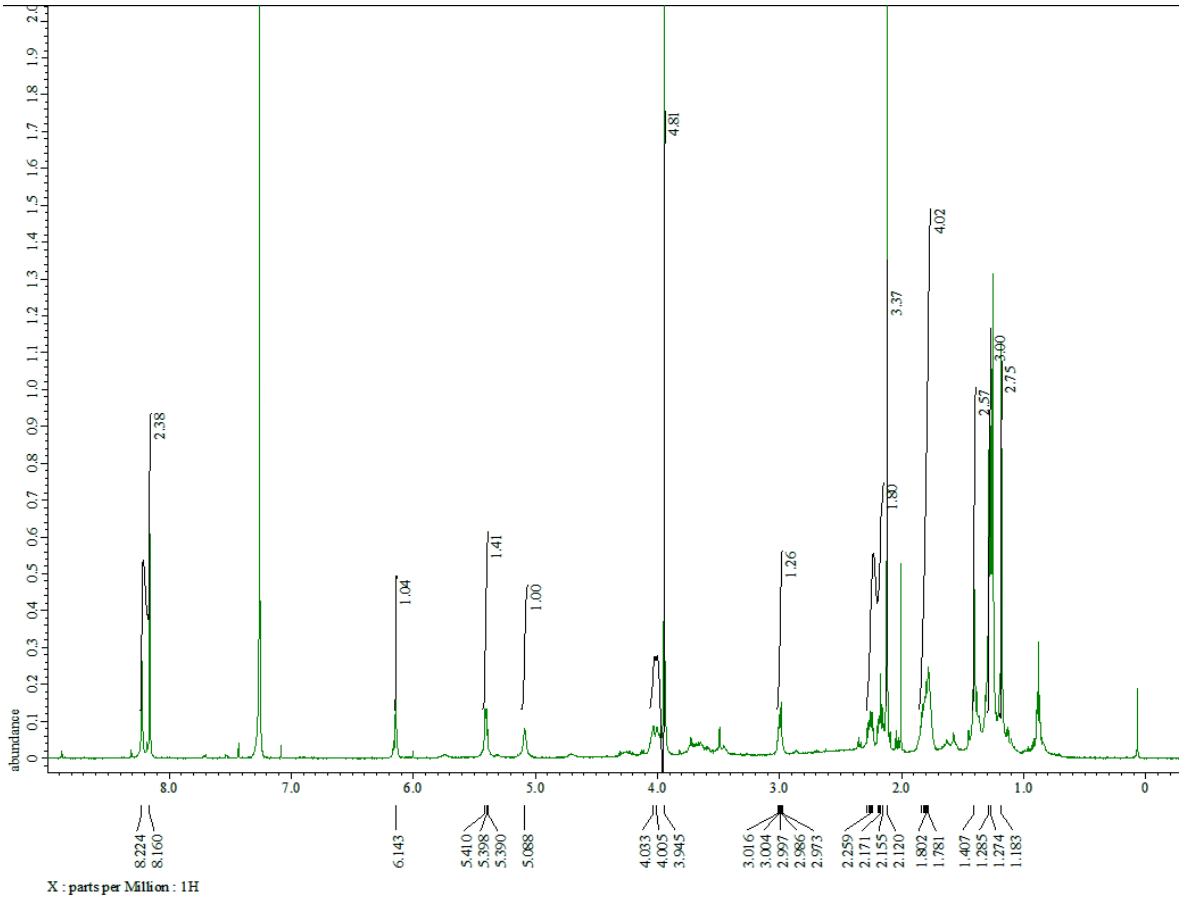

Figure III. 4: ^{1}H NMR spectrum of **114** (600 MHz, $CDCl_3$).

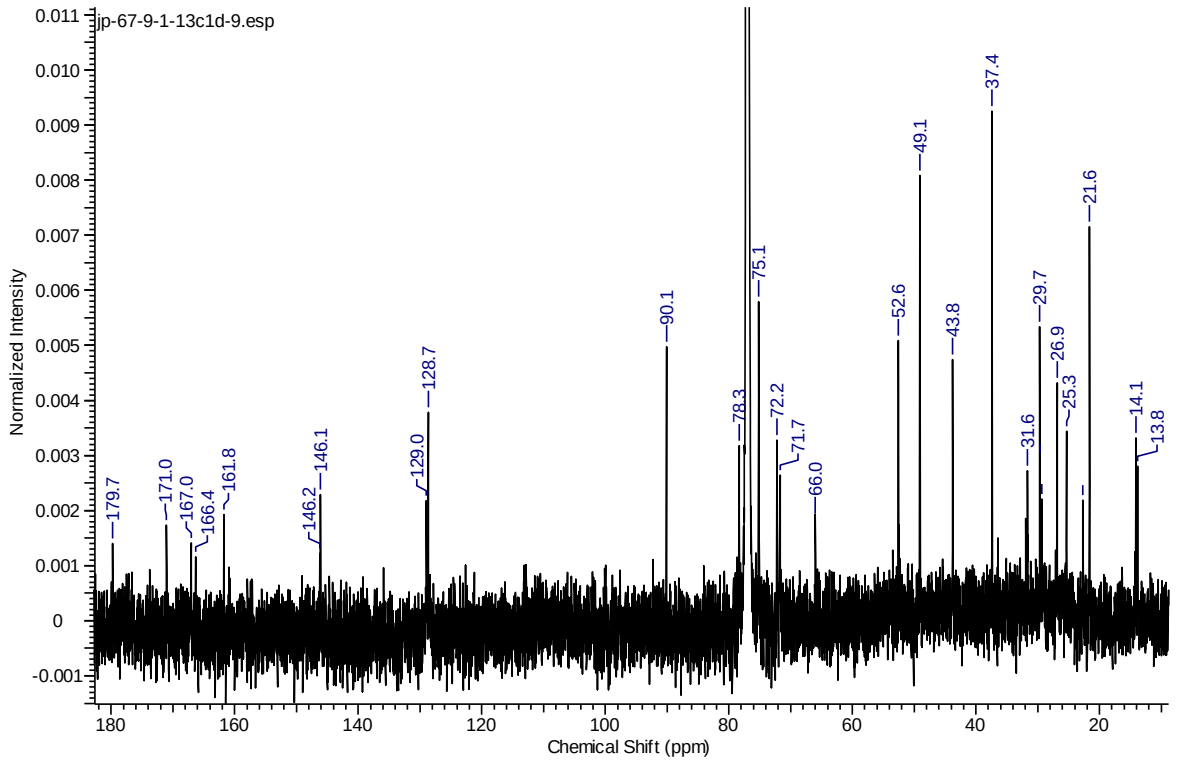

Figure III. 5: ^{13}C NMR spectrum of **114** (150 MHz, $CDCl_3$).

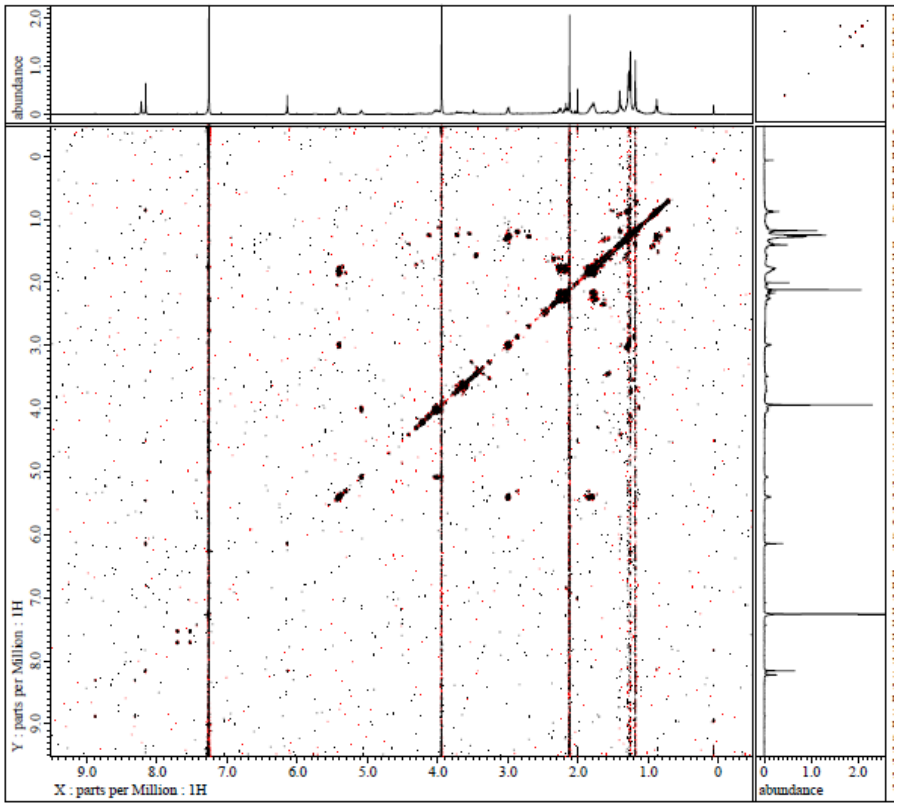

Figure III. 6: COSY spectrum of **114** (600 MHz, $CDCl_3$).

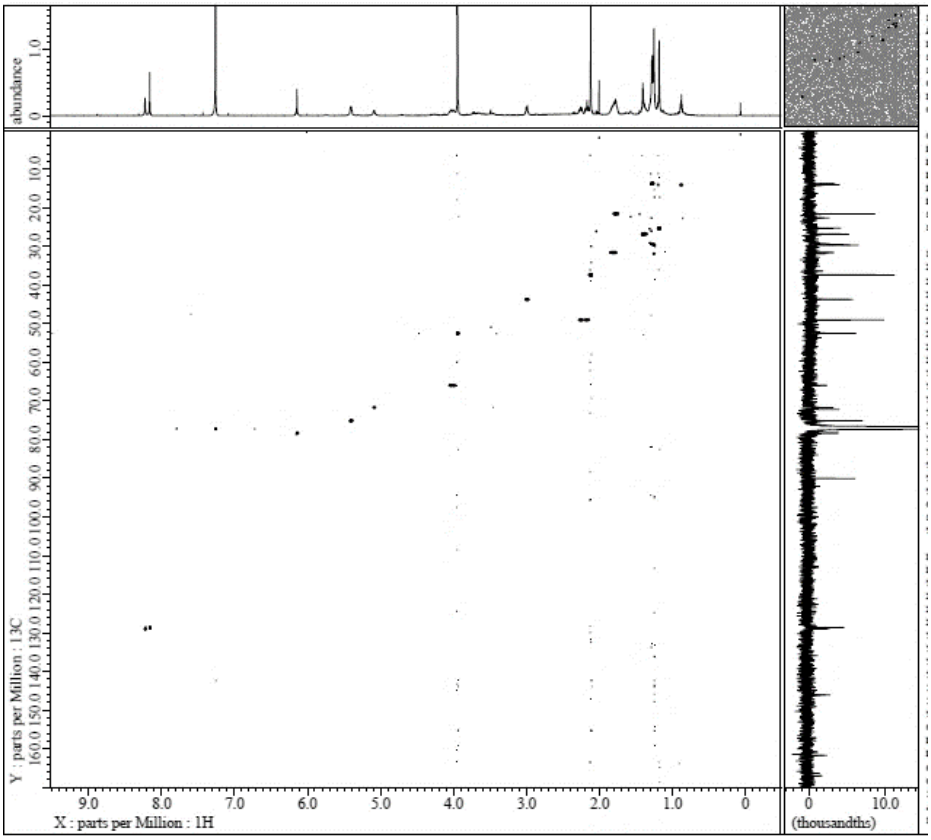

Figure III. 7: HSQC spectrum of **114** (600 MHz, $CDCl_3$).

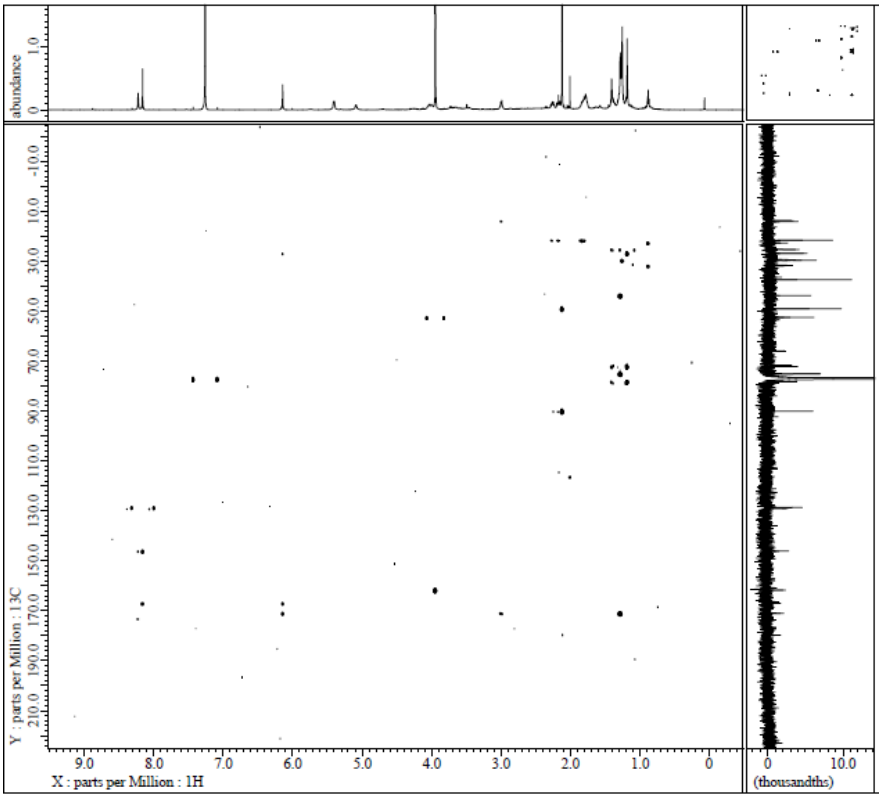

Figure III. 8: HMBC spectrum of **114** (600 MHz, $CDCl_3$).

Similar observations were recorded for **115**, except for the presence of an extra component corresponding to $C_{12}H_{22}NO_3$, which was determined to be attached to C-15 *via* an ester linkage based on an HMBC correlation from H-15 to C-24 (fragment A') (Figure III. 9). HMBC analysis also showed that C-24 was attached to a methylene moiety (C-25), which was linked to an oxygenated methine (δ_C 71.8). A correlation was also observed between H-25 and a methine group at C-27 (δ_C 51.6) by HMBC analysis, whereas ROESY analysis revealed a correlation (Figure III. 15) to a methylene (C-28). A signal corresponding to an amide proton at δ_H 5.52 (27-NH) showed a COSY correlation to H-27 (Figure 1), which was expanded into a modified leucine unit (C-24 to C-31) based on 2D NMR correlations, in a similar manner to lyngbyabellins E and E, **116**, **117**.[103] The 27-NH signal also showed a ROESY correlation to H-33 of an aliphatic chain (C-33 to C35), which was bonded to a carbonyl (C-32). Once again, no correlations were observed linking C-13 to C-14 (fragments A' and B'), C-10 to C-11(fragments B' and C'), C-3 to C-10 (fragments C' and D') or C-17 to C-16 (fragments D' and E'). The linkages between the different fragments were therefore established using a similar logic to that applied to **114**.

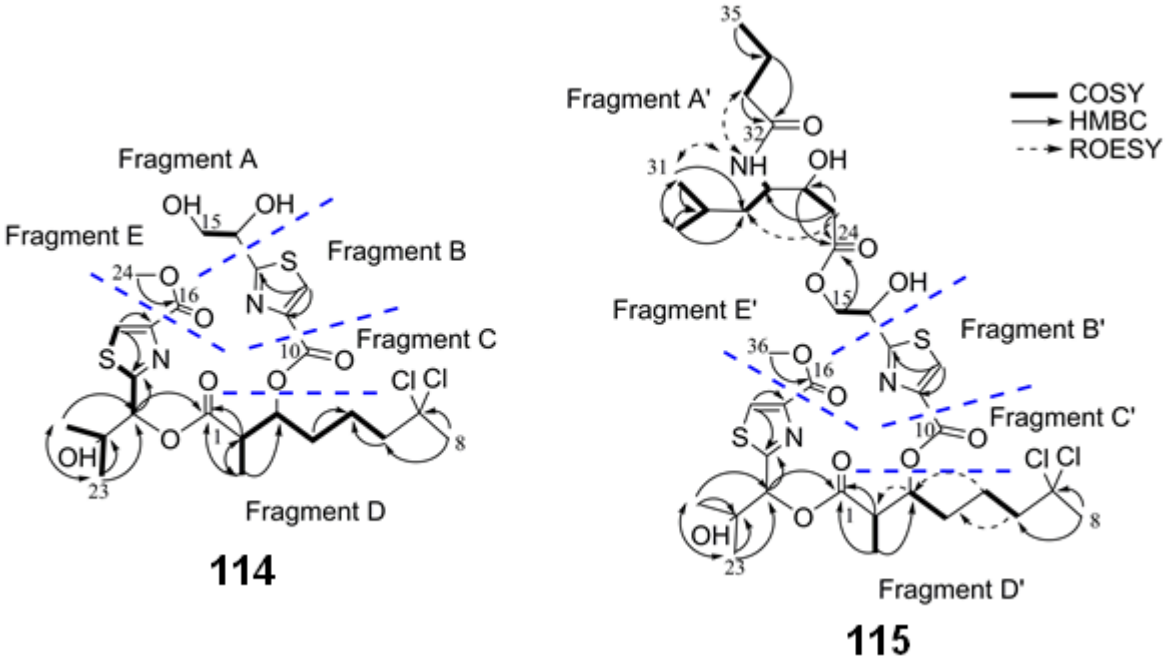

Figure III. 9: 2D NMR correlations for the partial structures of **114** (fragments A–E) and **115** (fragments A'–E').

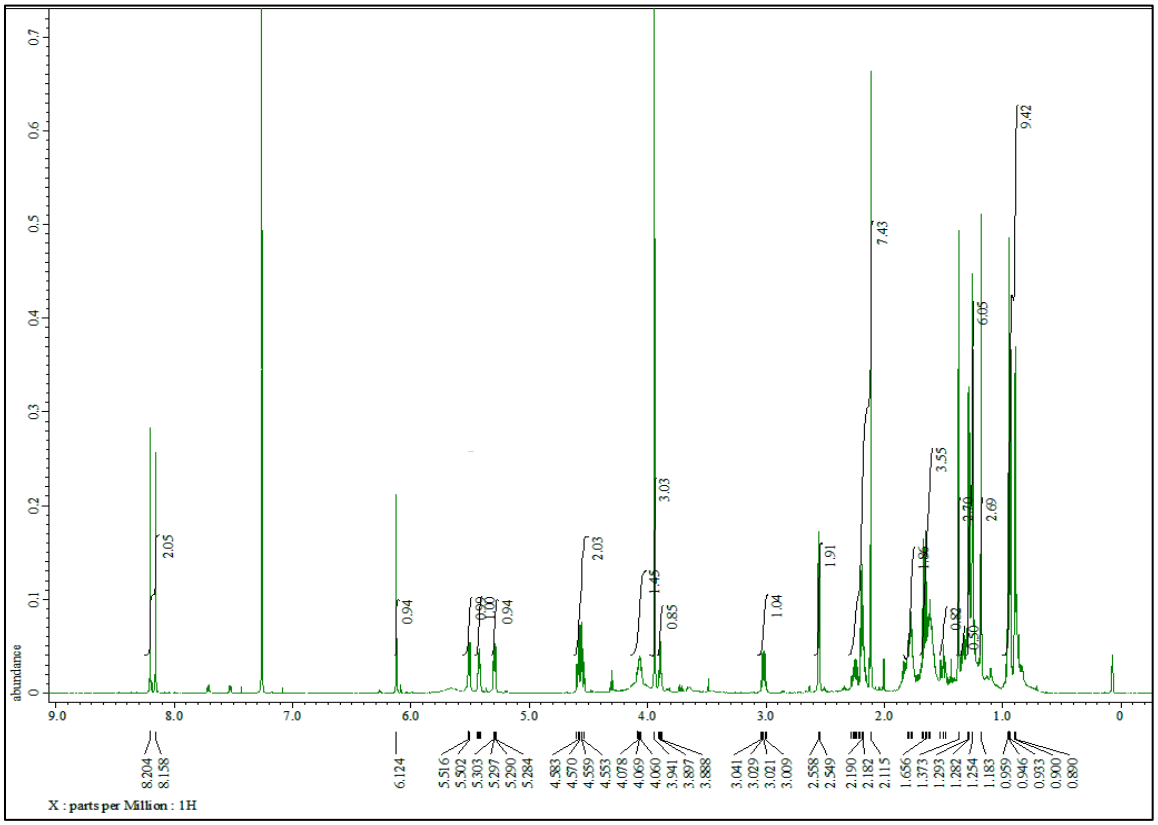

Figure III. 10: ^{1}H NMR spectrum of **115** (600 MHz, $CDCl_3$).

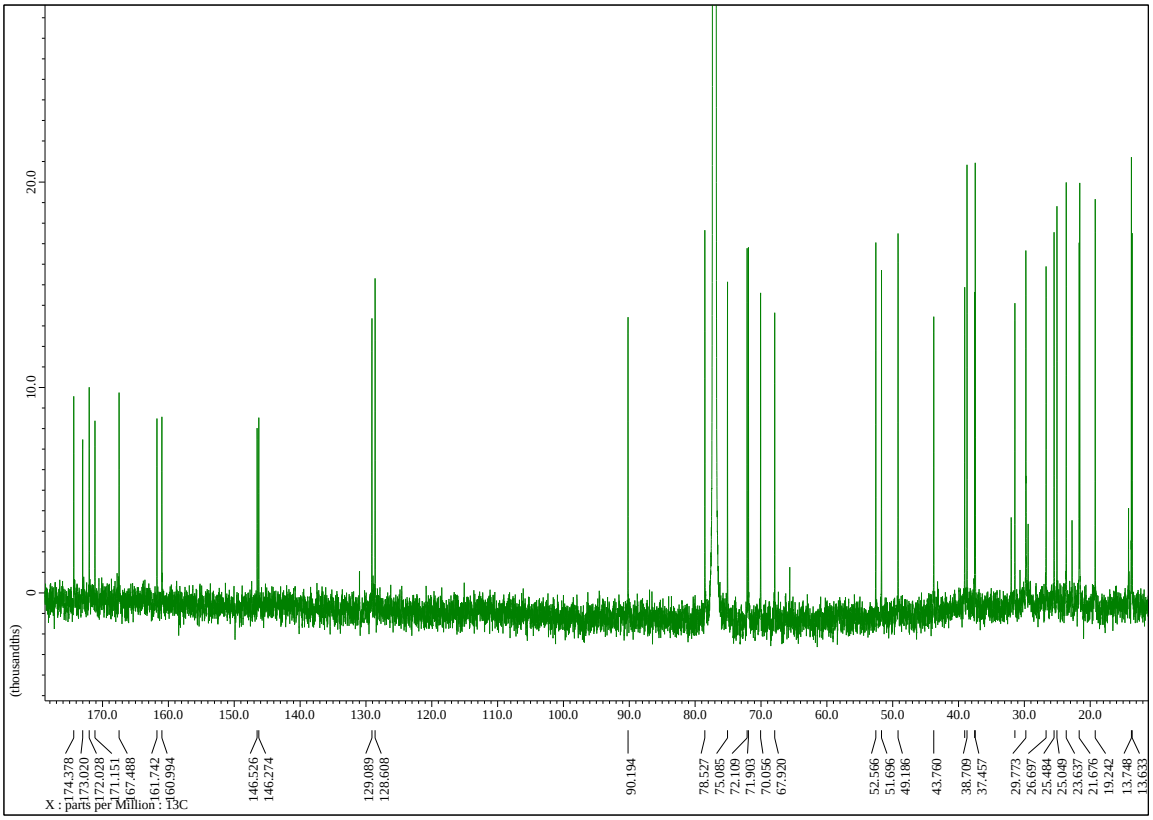

Figure III. 11: ^{13}C NMR spectrum of **115** (150 MHz, $CDCl_3$).

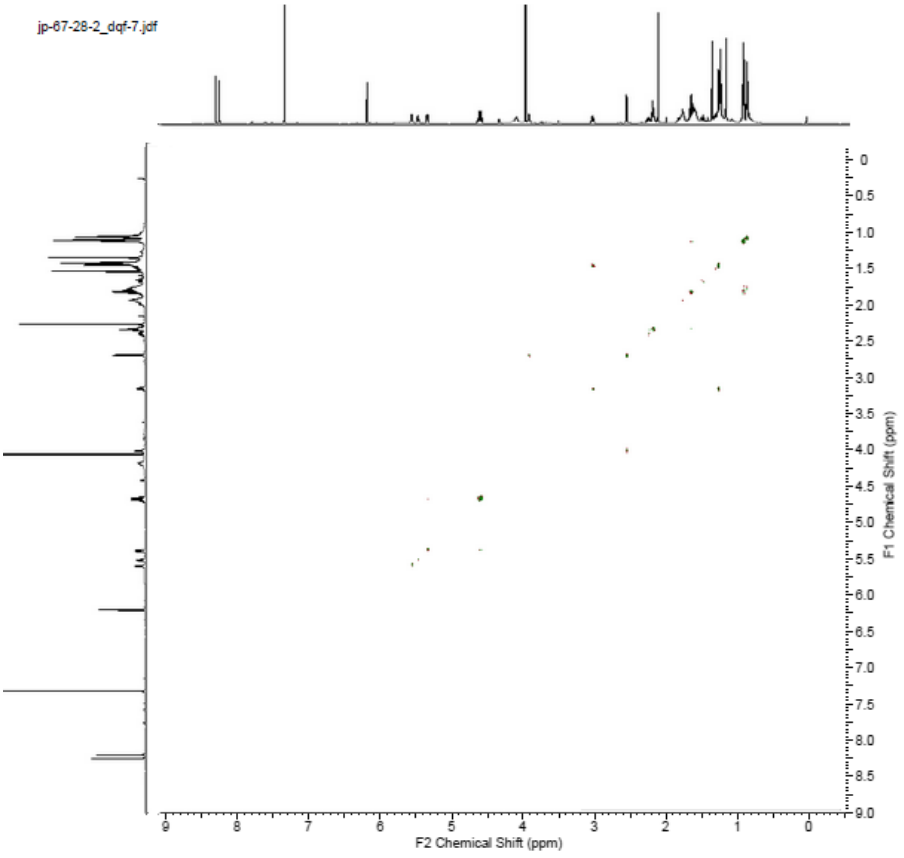

Figure III. 12: COSY spectrum of **115** (600 MHz, $CDCl_3$).

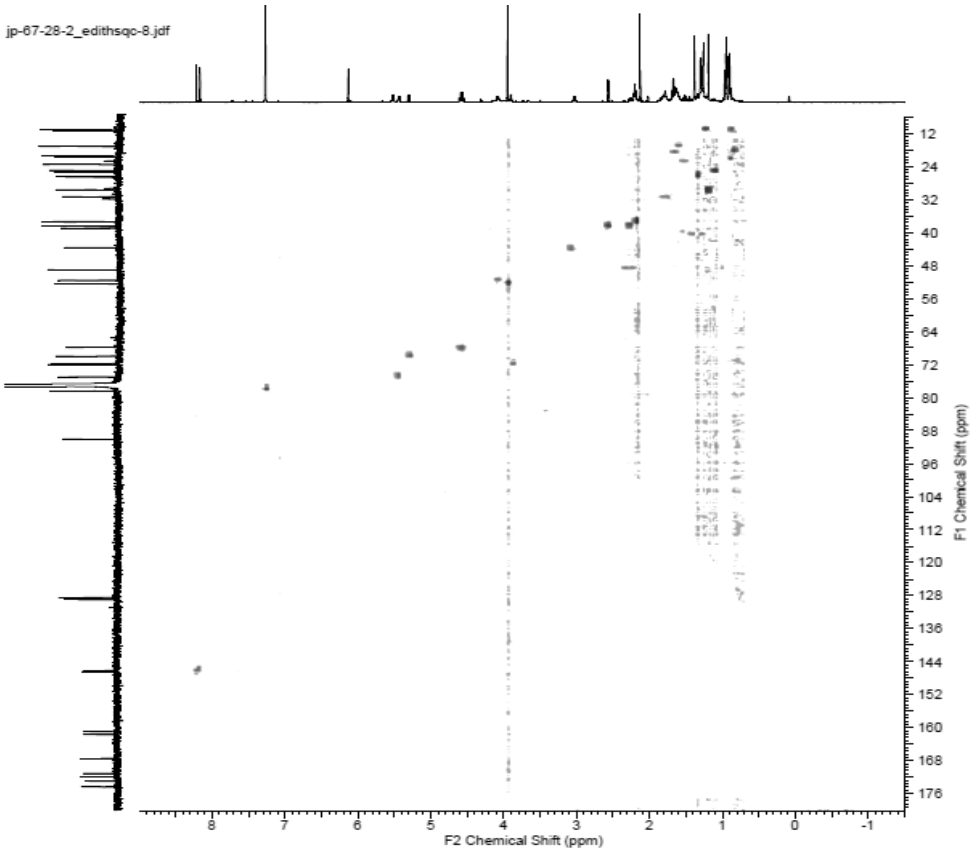

Figure III. 13: HSQC spectrum of **115** (600 MHz, $CDCl_3$).

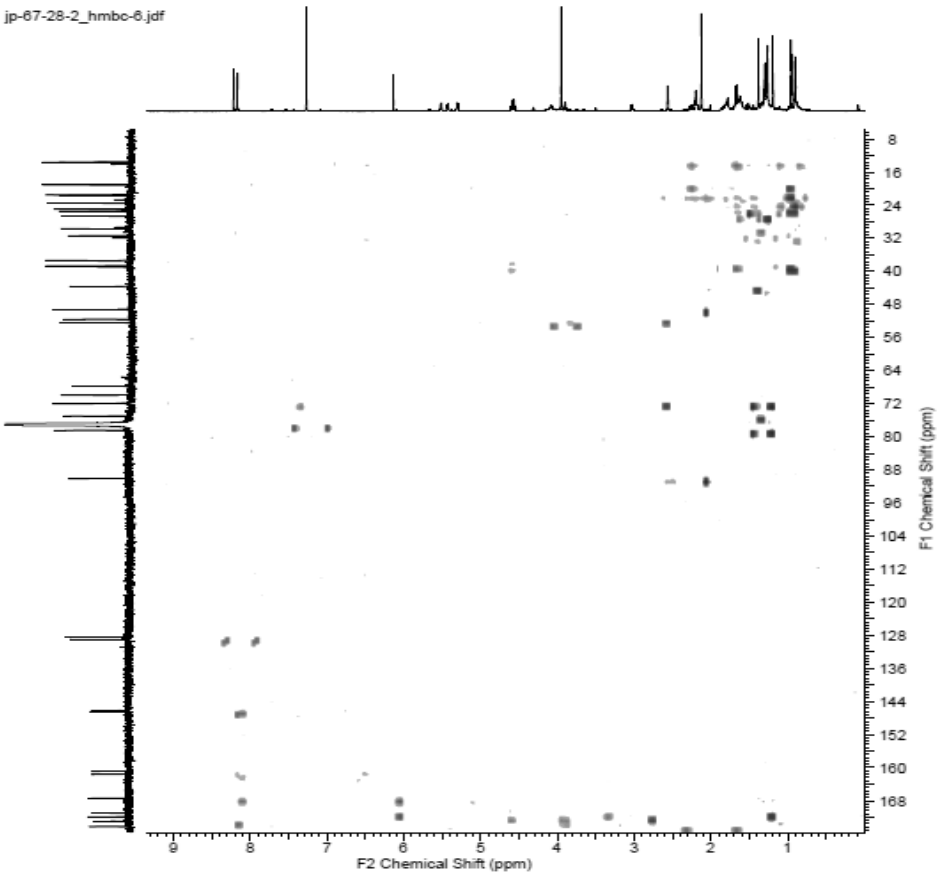

Figure III. 14: HMBC spectrum of **115** (600 MHz, $CDCl_3$).

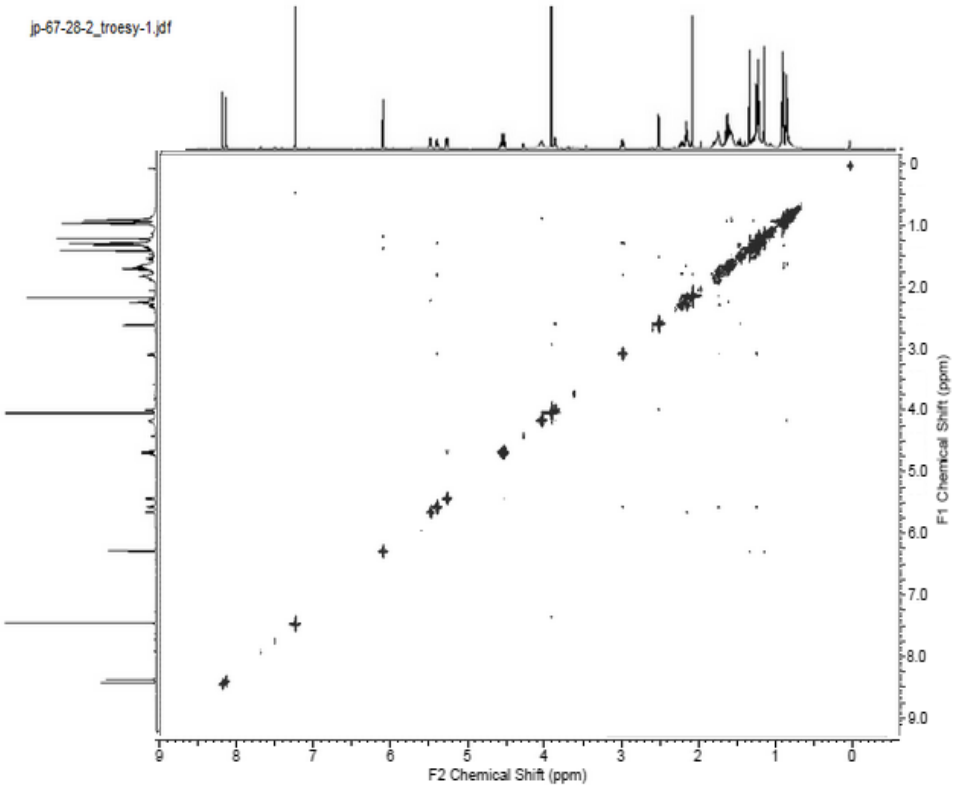

Figure III. 15: ROESY spectrum of **115** (600 MHz, $CDCl_3$).

The planar structure of **114** resembled that of **117**, which was also isolated from this *Okeania* sp. extract. The key difference between these two molecules is the open structure between C-15 and the ester attached to the second thiazole ring system. Likewise, the planar structure of **115** bears a striking resemblance to that of **116**, isolated from the same fraction, with the only major difference being an OH group at C-26 instead of an acetate group. Given that **114** and **115** were both found in the same fraction as **116** and **117** and share similar structural features, it is highly likely that they also have the same configuration.

III. 2. 2. b. Configuration of Lyngbyabellins O and P

Identical ^{1}H and ^{13}C NMR data for **117** compared to literature (the largest difference in ^{13}C chemical shifts is 0.028 ppm), together with similar specific rotation ($[\alpha]_D^{26}$ – 28.6 for the isolated compound and – 26 reported for lyngbyabellin G), proved that the isolated compound is the known lyngbyabellin G. Figure III. 16 shows the strategy used to determine the configuration of **114**. LCMS analysis (Figure III. 17) showed that mild methanolysis converted **117** into **114** so **114** has the same absolute configuration as **117**.

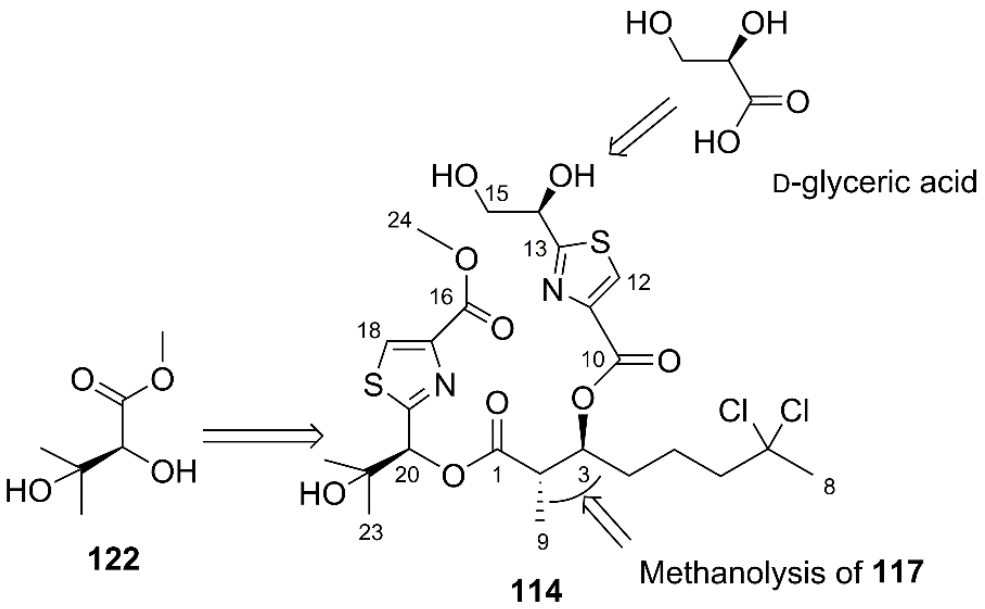

Figure 16: Strategy for the determination of the configuration of **114**.

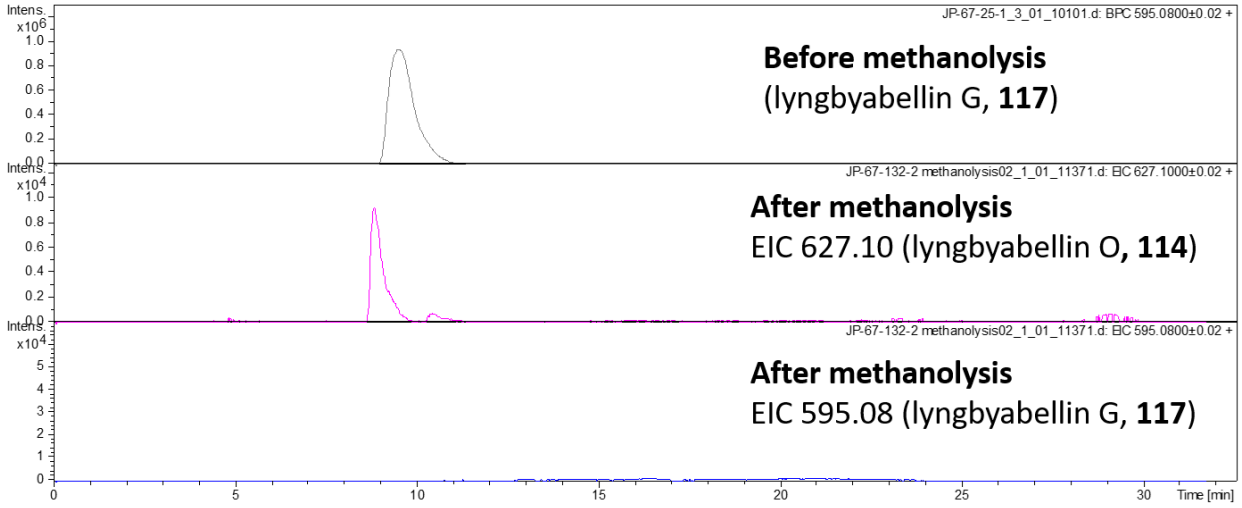

Figure III. 17: LCMS analysis of the result of methanolysis of **117**. Top: Extracted Ion Chromatogram (EIC) at 627.1 (**114**). Bottom: EIC at 595.08 (**117**). This shows that **117** was converted into **114**.

Chiral-phase chromatography experiments supported this information (Figure III. 18). After ozonolysis and subsequent base hydrolysis, the obtained α,β-dihydroxyisovaleric acid (Dhiv) residue was methylated (CH_2N_2). MTPA derivatization with (*R*)-MTPA was conducted on both synthetic **121** and **122** and the ozonolyzed/hydrolyzed/methylated natural product **114**. Chiral-phase HPLC with comparison of the retention times of the diastereomeric synthesized **121** and

122 (14.6 and 16.5 min, respectively) established the absolute configuration of the α,β-dihydroxyisovaleric acid methyl ester (16.6 min) of **114** as the *S* configuration at C-20.

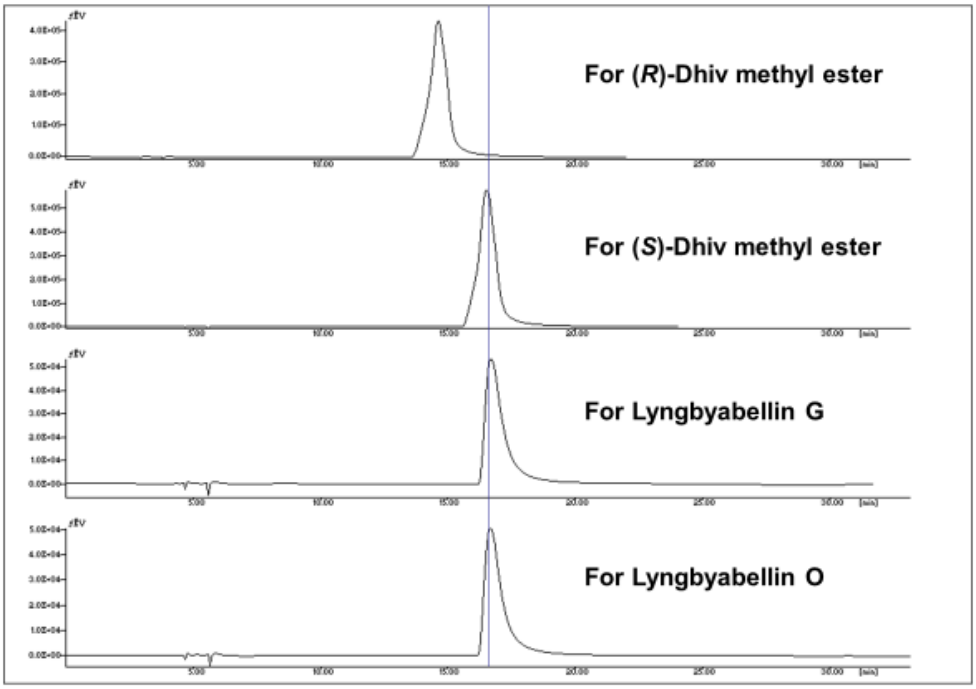

Figure III. 18: HPLC analysis of the **121** and **122** derivatives (standards and those obtained from **114** and **117**).

The ozonolyzed/hydrolyzed natural product **114** was confirmed to contain D-glyceric acid (3.8 min) by comparison of the retention times by ESI-LC-MS using a chiral-phase column of the commercially available L- and D-glyceric acids (3.5 and 3.8 min, respectively), giving an *R* configuration at C-14. Identical to **117**, **114** has a 2*S*, 3*S* configuration (Figure III. 19).

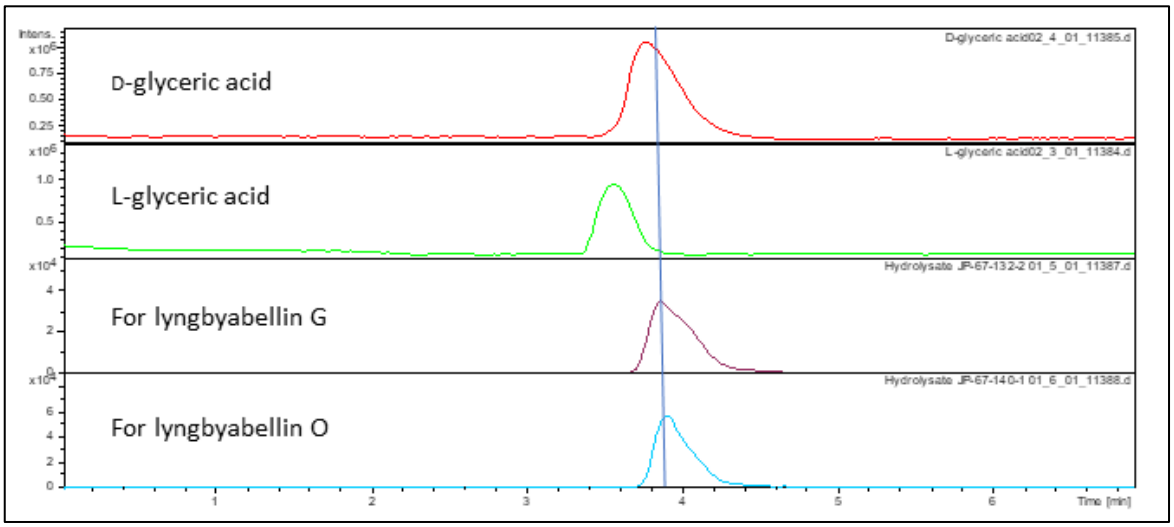

Figure III. 19: LCMS analysis of the glyceric residue obtained from **114** and **117**, and comparison with the commercially available standards.

Chemical shifts and the specific rotation of **116** ($[\alpha]_D^{26}$ – 7.8 for the isolated compound and – 6.5 reported for lyngbyabellin F; the largest difference in ^{13}C chemical shifts is 0.015 ppm, see section III. 2. 2. d) were similar to those reported for lyngbyabellin F. ESI-TOF-MS analysis showed that deacetylation ($NaOCH_3$) at C-26 of **116** led to the conversion into **115** (Figure III. 20). Degradation of **115** and **116** observed by ESI-TOF-MS analysis showed that both were converted into **114**, showing that these three compounds indeed share the same configuration. As a result, **115** has a 2*S*, 3*S*, 14*R*, 20*S*, 26*R* and 27*S* configuration.

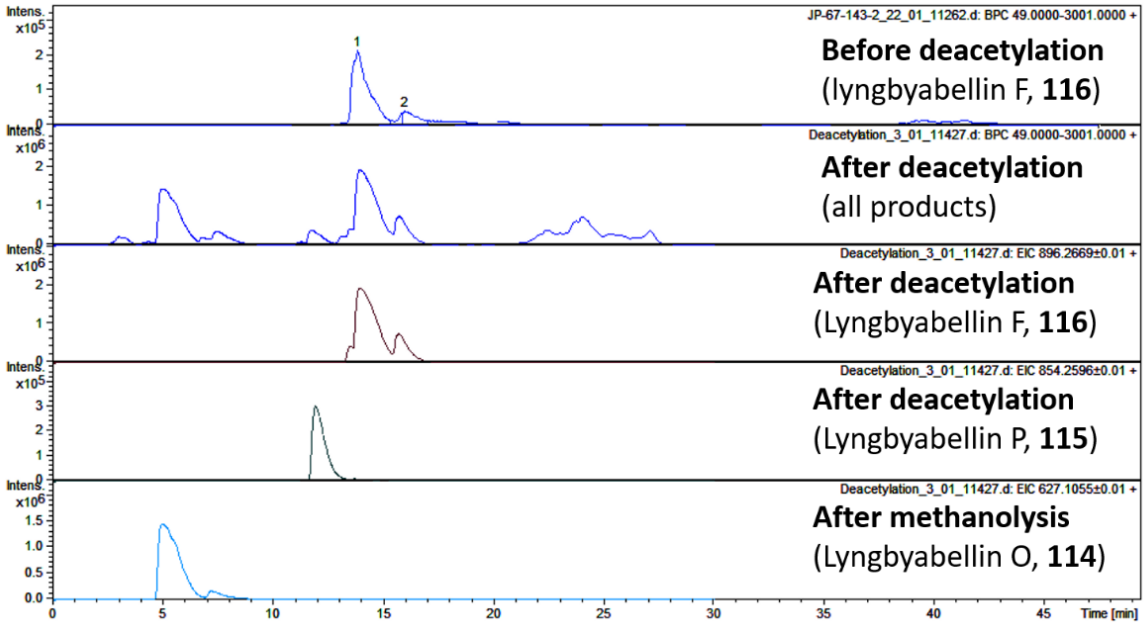

Figure III. 20: LCMS analysis of the deacetylation product of **116**. Top: base peak chromatogram. Second: EIC at 896.3 (**116**). Third: EIC at 854.3 (**115**). Bottom: EIC at 627.1 (**114**).

As observed for lyngbyabellin E that converted to **117**,[103] one ester linkage of **115** is apparently prone to methanolysis and a regioselective ester cleavage occurred at C-14, giving **114** which can be considered as an artifact of **115** and also **116**. Conversion of **117** into **114** is also possible by regioselective ester cleavage at C-16. This kind of conversion was observed for lyngbyabellin C which was converted into homohydroxydolabellin.[106]

III. 2. 2. c. UV data of lyngbyabellin O

The UV spectrum of **114** gave a λ_{max} of 243 nm (log ε 4.01) in MeOH (Figure III. 21).

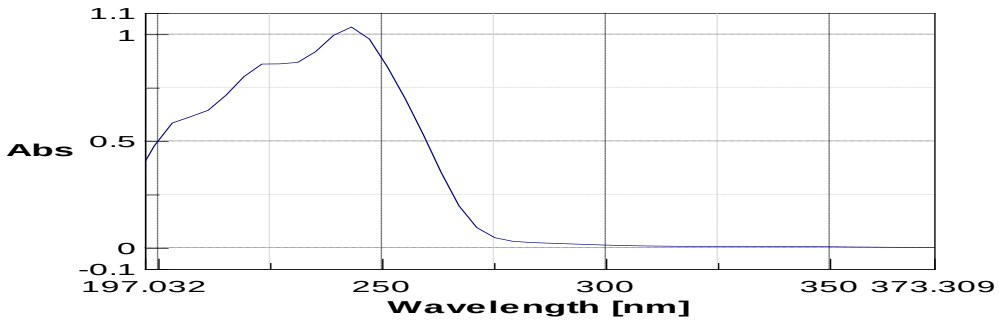

Figure III. 21: UV spectrum of **114**.

III. 2. 2. d. Confirmation of the identities of lyngbyabellins G, F and H, 27-deoxylyngbyabellin A and dolastatin 16

To verify the identities of the other isolated compounds which are believed to be known compounds, their 1D NMR spectra were recorded (Figures III. 22-29). For the lyngbyabellins, the differences of carbon chemical shifts between the isolated compounds from *Okeania* sp. and the reported values were calculated. All the differences were below 0.05, proving that the isolated lyngbyabellins in this Chapter III were the known lyngbyabellins F, G, H and 27-deoxylyngbyabellin A.[107] For **60**, its 1D ^{1}H NMR spectrum was like the reported one and its retention time and mass spectrum matched the ones of the standard that our laboratory has.

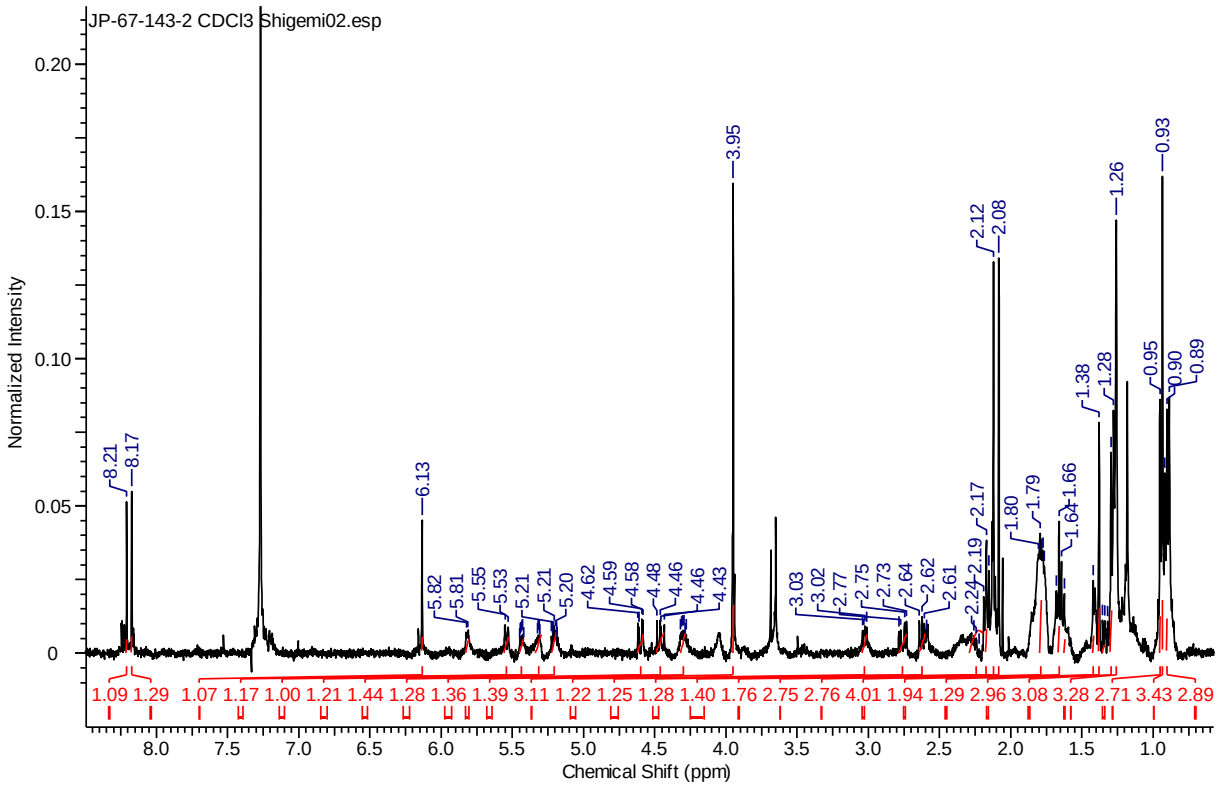

Figure III. 22: ^{1}H NMR spectrum of **116** (400 MHz, $CDCl_3$).

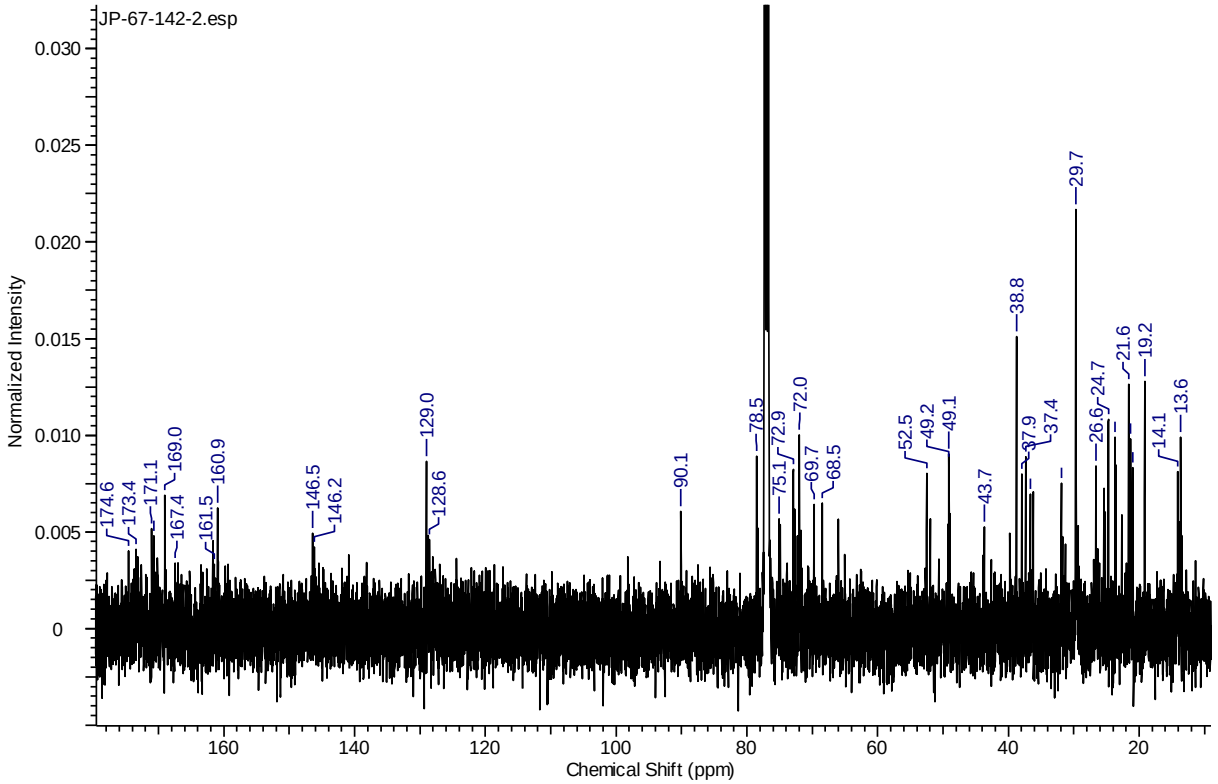

Figure III. 23: ^{13}C NMR spectrum of **116** (125 MHz, $CDCl_3$).

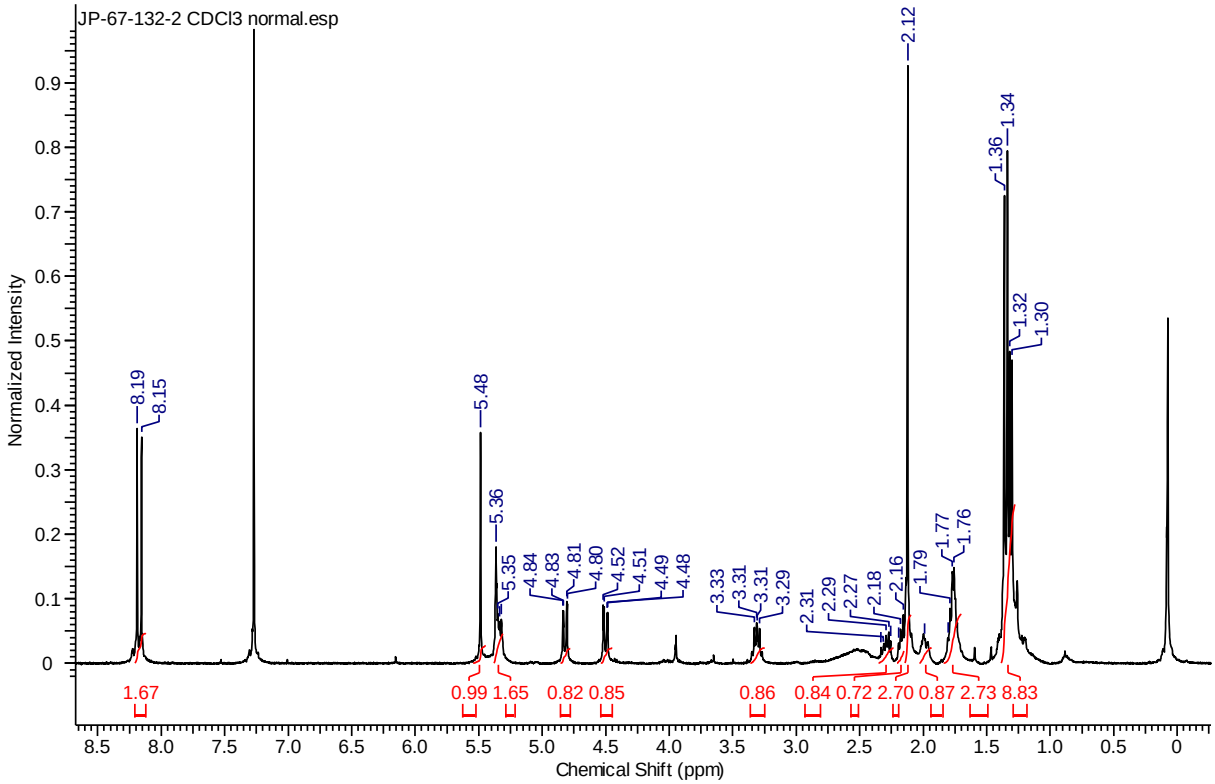

Figure III. 24: ^{1}H NMR spectrum of **117** (400 MHz, $CDCl_3$).

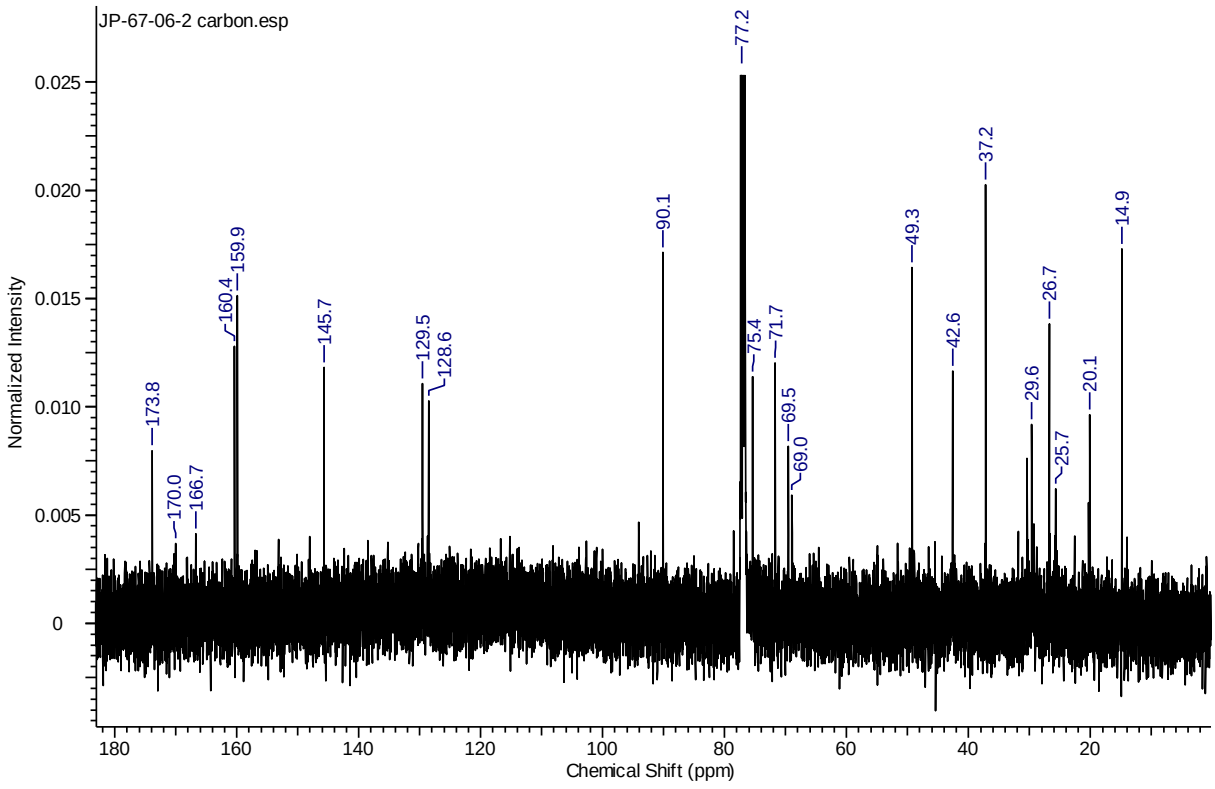

Figure III. 25: ^{13}C NMR spectrum of **117** (100 MHz, $CDCl_3$).

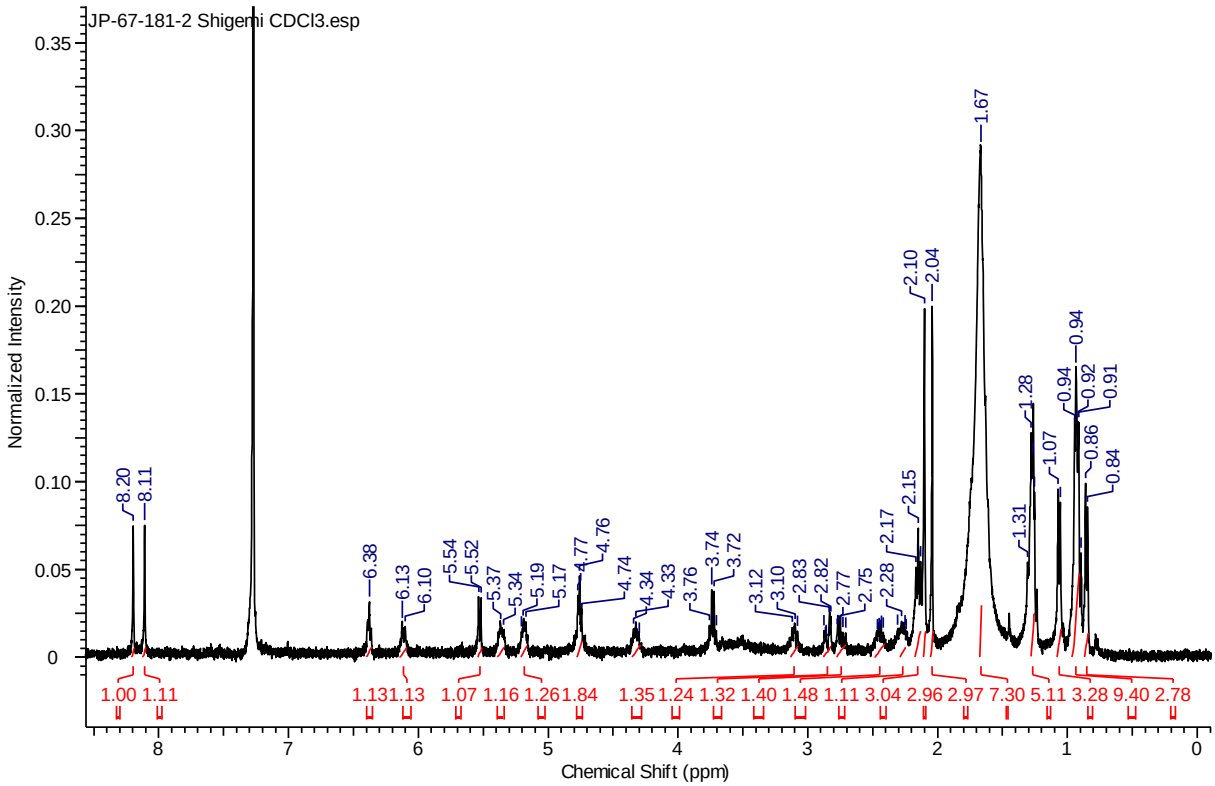

Figure III. 26: ^{1}H NMR spectrum of **118** (400 MHz, $CDCl_3$).

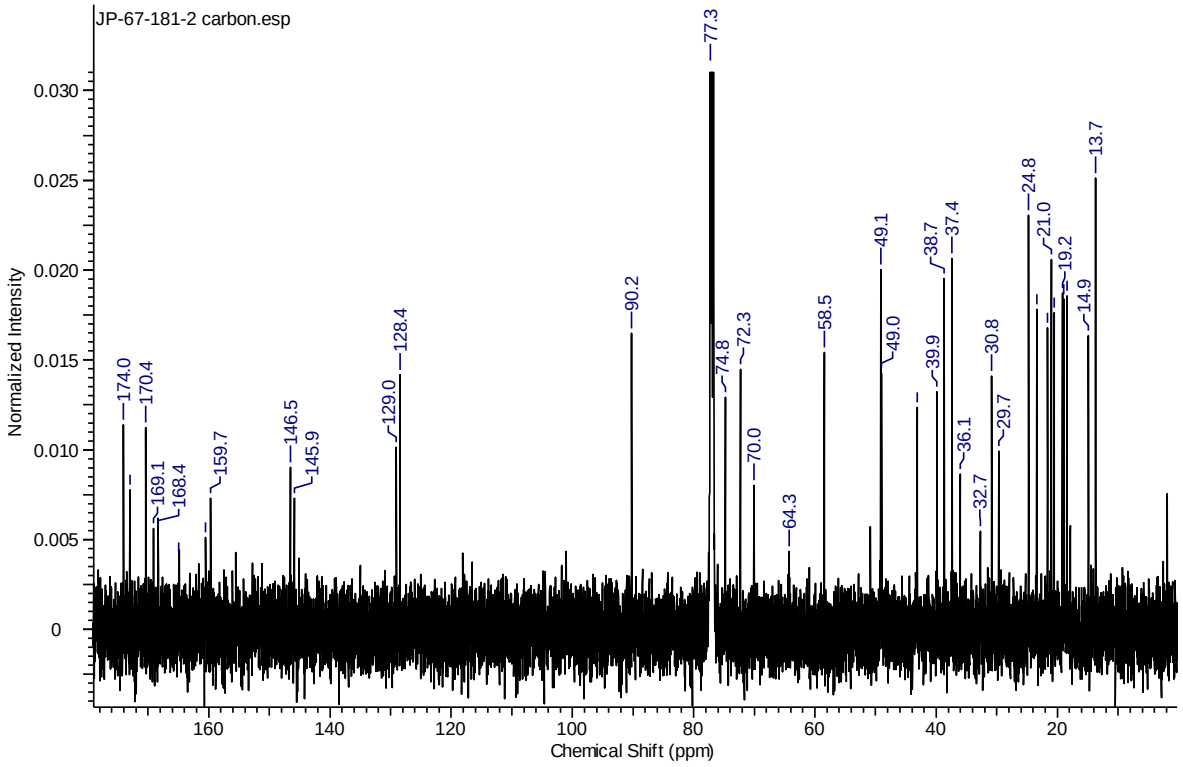

Figure III. 27: ^{13}C NMR spectrum of **118** (125 MHz, $CDCl_3$).

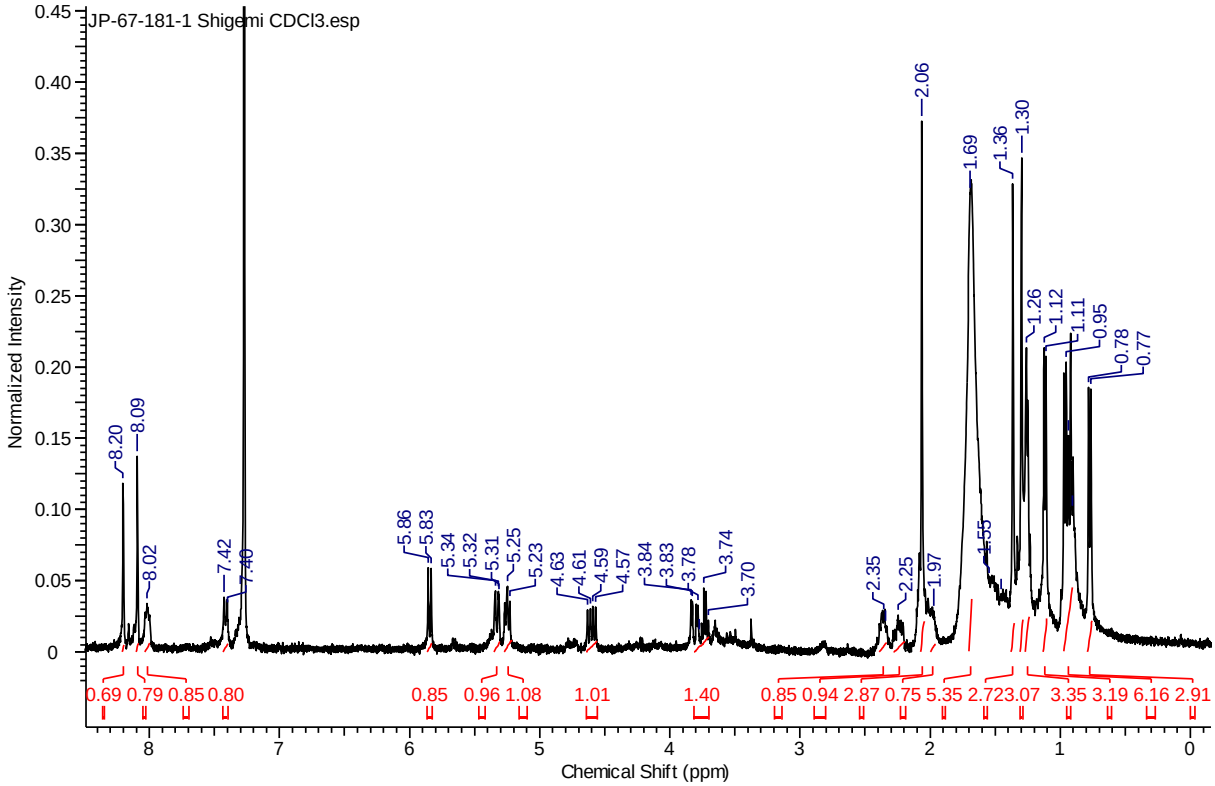

Figure III. 28: ^{1}H NMR spectrum of **119** (400 MHz, $CDCl_3$).

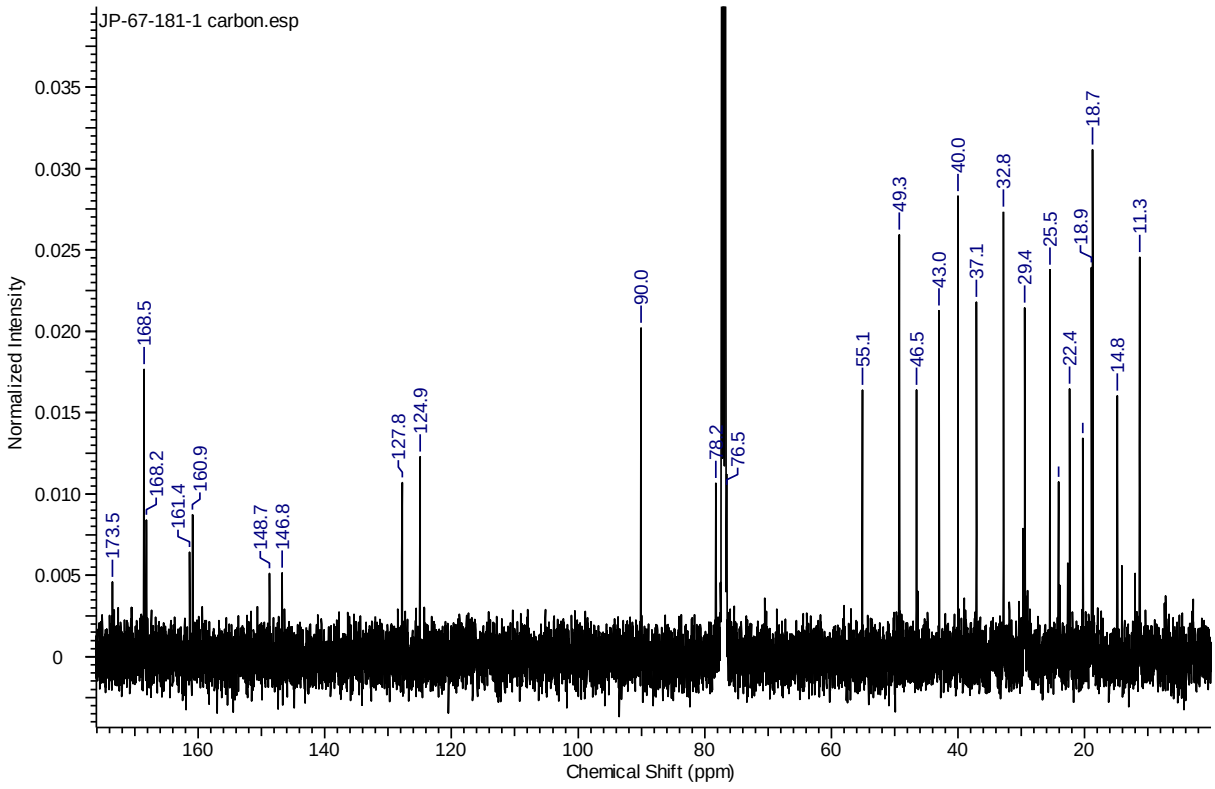

Figure III. 29: ^{13}C NMR spectrum of **119** (125 MHz, $CDCl_3$).

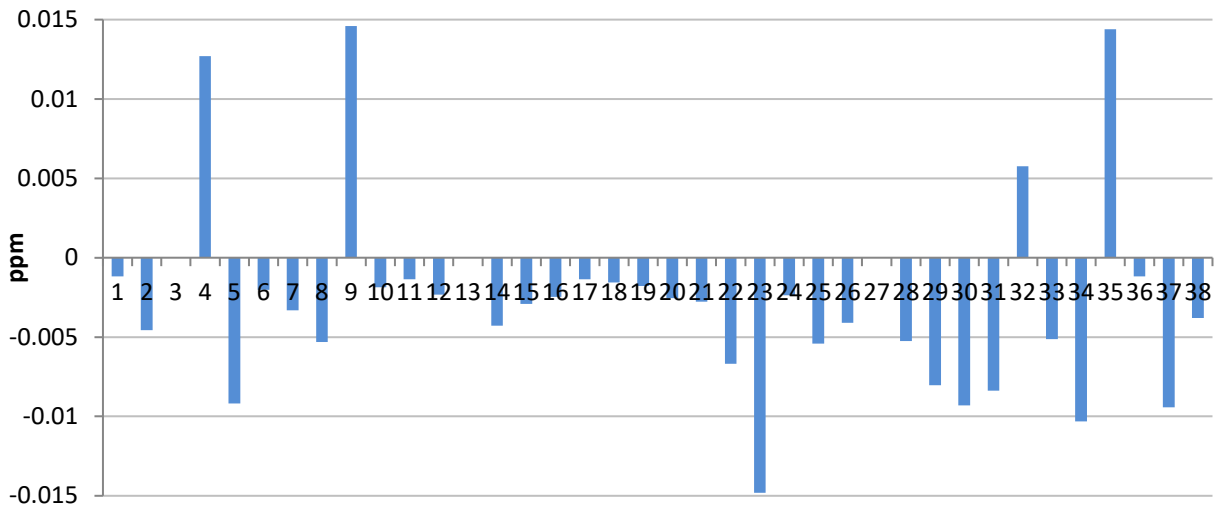

Figure III. 30: Difference of carbon shifts between **116** and the reported ones for lyngbyabellin F.

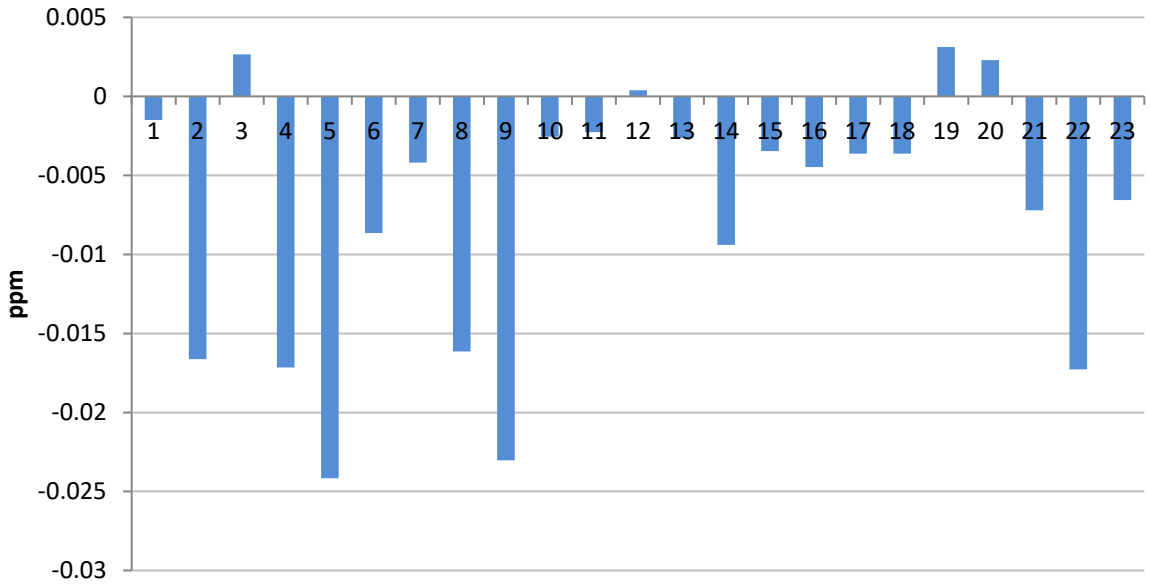

Figure III. 31: Difference of carbon shifts between **117** and the reported ones for lyngbyabellin G.

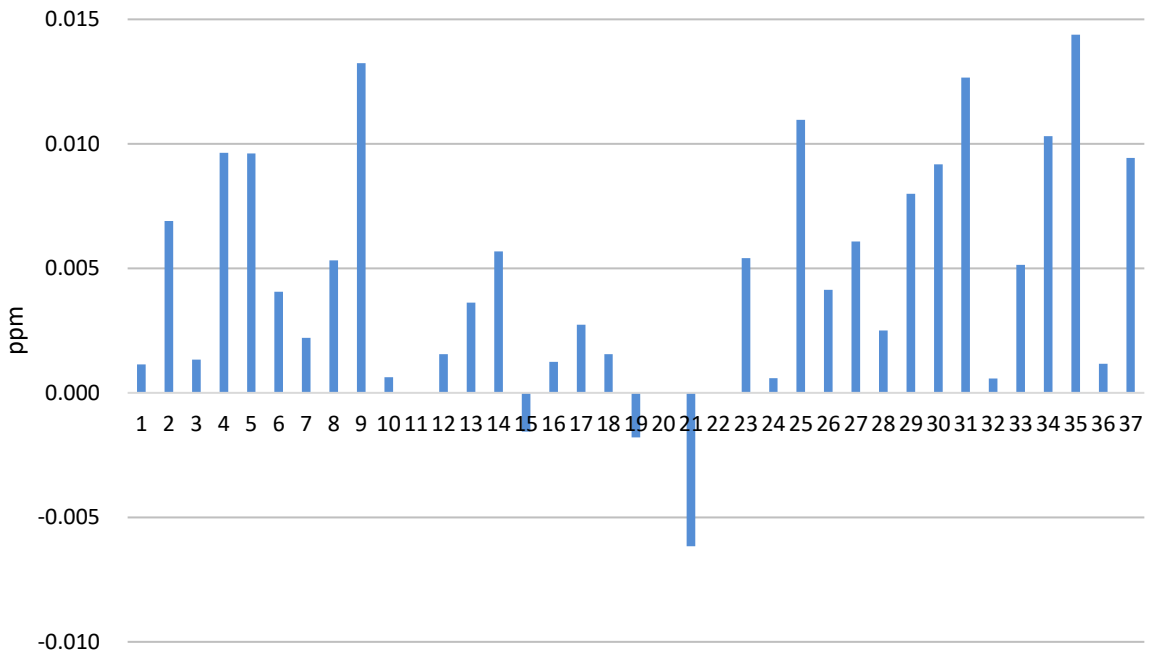

Figure III. 32: Difference of carbon shifts between **118** and the reported ones for lyngbyabellin H.

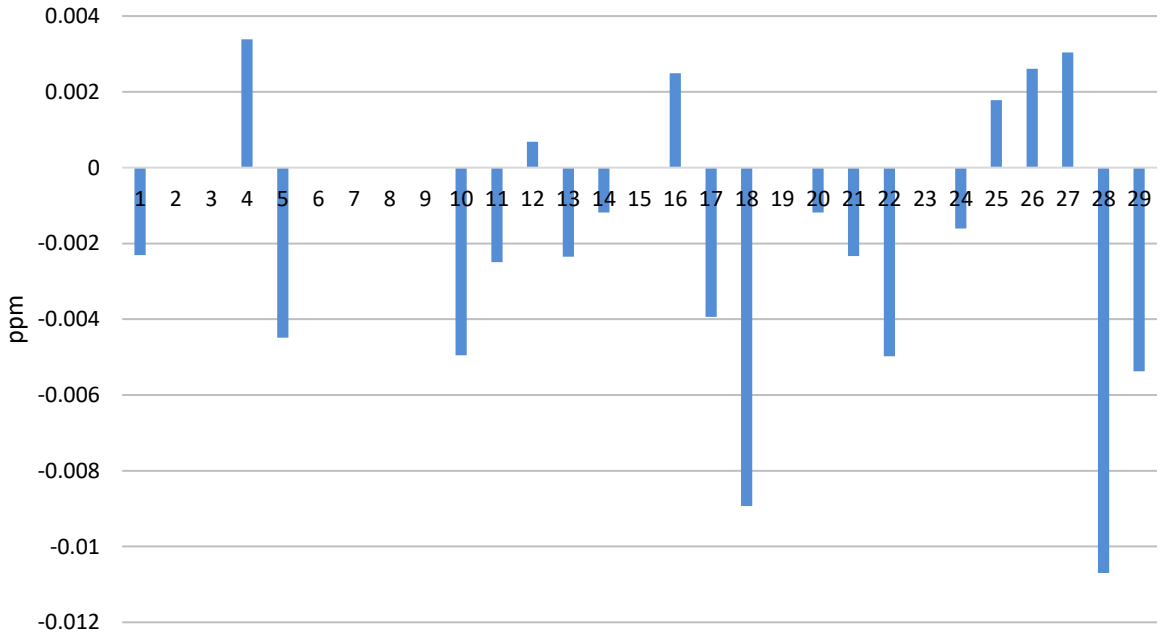

Figure III. 33: Difference of carbon shifts between **119** and the reported ones for 27-deoxylyngbyabellin A.

It is noteworthy to point out that the technique reported by Preciado and William to determine the configuration of statine unit in **116** at C-26 and C-27 succeeded.[108] Indeed, 1D NOE and examination of the α-methylene signals (H-25a and b) revealed an *R* and *S* configuration at C-26 and C-27, respectively. The downfield α-methylene signal (H-25a) showed a large coupling to

H-26 (7.8 Hz), and the upfield signal (H-25b) showed a smaller coupling to H-27 (6.0 Hz), giving a *R* configuration at C-26 (Figure III. 34).

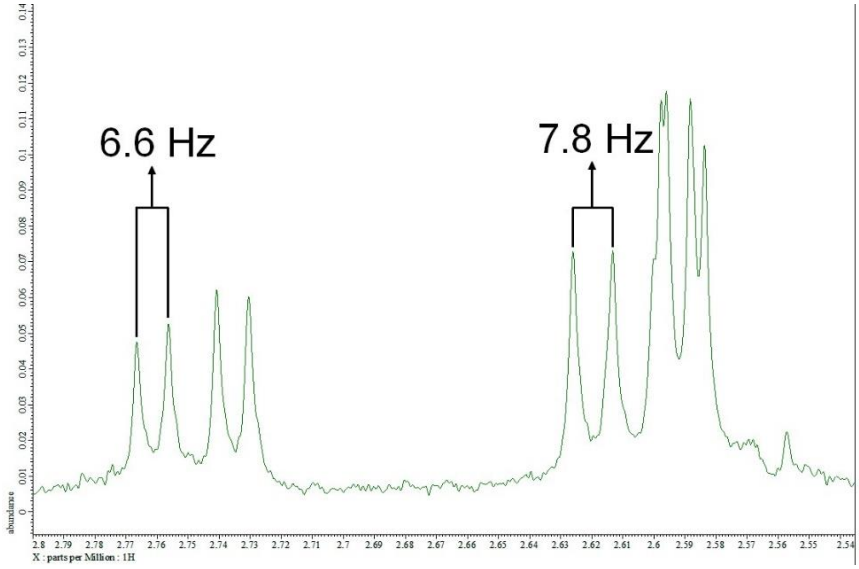

Figure III. 34: Coupling constants of the α-methylene signals H-25a and b of **116**.

NOE experiments gave the same observations as for **117**.[103] Low power irradiation at δ 4.12 (H-27) led to NOE enhancement of the resonances for H-26 and H_2-25, and irradiation at δ 5.60 (NH-27) to NOE enhancement of the resonances for H-26, H-27 and H-33 (Figure III. 35). However, the same technique could not be applied to **115** as the two α-methylene signals (H-25a and b) had the same chemical shifts (δ 2.56). This is probably due to the OH of **115** attached to C-26 which has less effect than the *O*-acetyl of **116**.

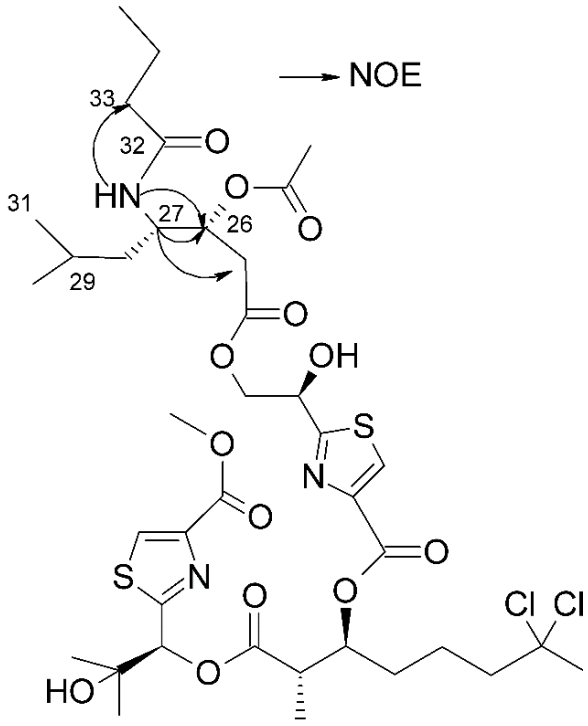

Figure III. 35: NOE correlations for **116** for the statine residue.

III. 3. Bioactivities

III. 3. 1. Materials and Methods

III. 3. 1. a. Cytotoxicity

The cytotoxicity of the compounds was determined by using a standard MTT assay based on the method reported by Mosmann[109]. Compounds were dissolved into RPMI-1640 medium (Wako) containing 10% of filtered ethanol so that the final concentration of ethanol does not exceed 1%. Concisely, MCF-7 breast cancer cells (Culture Collections, Public Health England) were maintained in RPMI-1640 medium with 10% FBS (Bio West). Cancer cells were seeded into 96-well plates (flat-bottom, polystyrene, Iwaki assay plates) at a density of 1.0 x 10^4 cells per well (90 µL). After 24 h at 37 °C with 5% CO_2, the cells were treated with different concentrations of the test compounds (10 µL) and incubated for 72 h under the same conditions. The medium was then removed and replaced with a 0.5 µg/mL MTT solution in RPMI-1640 medium with 10% FBS. The cells were then incubated again for 3 h under the same condition and in the dark. The MTT solution was then removed and the formed formazan crystals were dissolved in DMSO. After 15

minutes of incubation at 37 °C, the optical density was measured at 570 nm using a Thermo Labsystems Multiskan JX plate reader. Cisplatin (Sigma-Aldrich) was used as positive control, and 1% filtered ethanol was used as negative control. Three of four wells were used for each concentration.

III. 3. 1. b. Antifouling assay

Same procedure as in Chapter 1 (section I. 4. 1.) was used to study the antifouling activity of **114**, **115**, **117-119** and **60**.

III. 3. 2. Results

III. 3. 2. a. Cytotoxicity

The cytotoxicities of the isolated compounds were evaluated on MCF7 breast cancer cells (Figure III. 36). The IC_{50} values of lyngbyabellins **117**, **114** and **115** toward the MCF7 cells were 120 ± 2.1, > 160 and 9 ± 0.9 µM, respectively (n = 3). The IC_{50} values of **118** and **119** were 0.07 ± 0.03 and 0.31 ± 0.05 µM, respectively. These differences in the cytotoxicity could most likely be attributed to the differences in their structures. Cyclic lyngbyabellin with side chain (**118**) is the most active while an acyclic form or a lack of side chain decreases the cytotoxicity.[103]

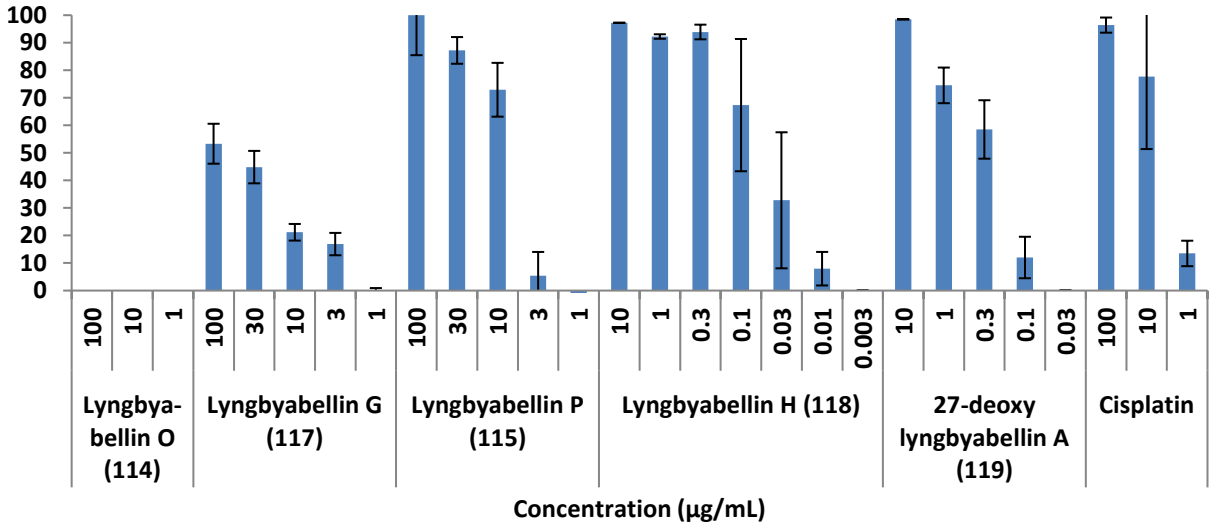

Figure III. 36: Inhibition of MCF7 cells growth by **114**, **115, 117-119** (cisplatin was used as control). (Error bars are for standard deviation, n = 3).

The results of a previous study showed that **60**, isolated from the sea hare *Dolabella auricularia*, inhibited the growth of several human cancer cell lines (IC_{50} 0.0012–0.00096 µg/mL).[45] Surprisingly, a total synthesis of this cyclodepsipeptide revealed that synthetic **60** did not exhibit any discernible cytotoxicity.[110] The authors attributed this lack of activity to a change in the conformation of the synthetic compound or the presence of a chemically undetected (yet extremely active) compound in the sample isolated from the natural source. A new synthesis of **60** confirmed its inactivity.[111] In this study, it was confirmed that **60** is non-cytotoxic but potently active toward barnacle larvae, as shown in the next section.

III. 3. 2. b. Antifouling activity

Compound **117** showed low activity (EC_{50} 4.41 ± 0.09 µg/mL), while **114** and **115** exhibited potent activity, with EC_{50} values of 0.24 ± 0.06 and 0.62 ± 0.10 µg/mL, respectively (Figure III. 37) after 48 hours of exposure. Compound **118** was inactive at 10 µg/mL. These results suggest that the larvae are more sensitive to the acyclic structure of **114** than the cyclic structure of **117**, and that the presence of a side chain decreases the activity (**114** and **117** being more active than **115** and **118**, respectively). Compound **119** was the most potent among the tested lyngbyabellins (Figure III. 38. EC_{50} 0.09 ± 0.01 µg/mL) but its activity is due to high toxicity (almost all the larvae were dead when exposed to 1 µg/mL of **119**, LC_{50} 1.1 ± 0.2 µg/mL). For all compounds, the activity remained after 120 hours of exposure. The compounds could inhibit the settlement and not only slowing it down like it was the case for serinolamides C and D in Chapter 2.

Compound **60**, which is well known as a powerful antifoulant,[44] exhibited high inhibition activity (EC_{50} 0.08 µg/mL) (Figure III. 39), and its activity remained intact even after 120 h. The observed antifouling activity of the *Okeania* sp. extract was therefore mainly attributed to **114** and **115** and **60** because the 100% EtOAc fraction from which they were isolated was the most active of all the fractions tested.

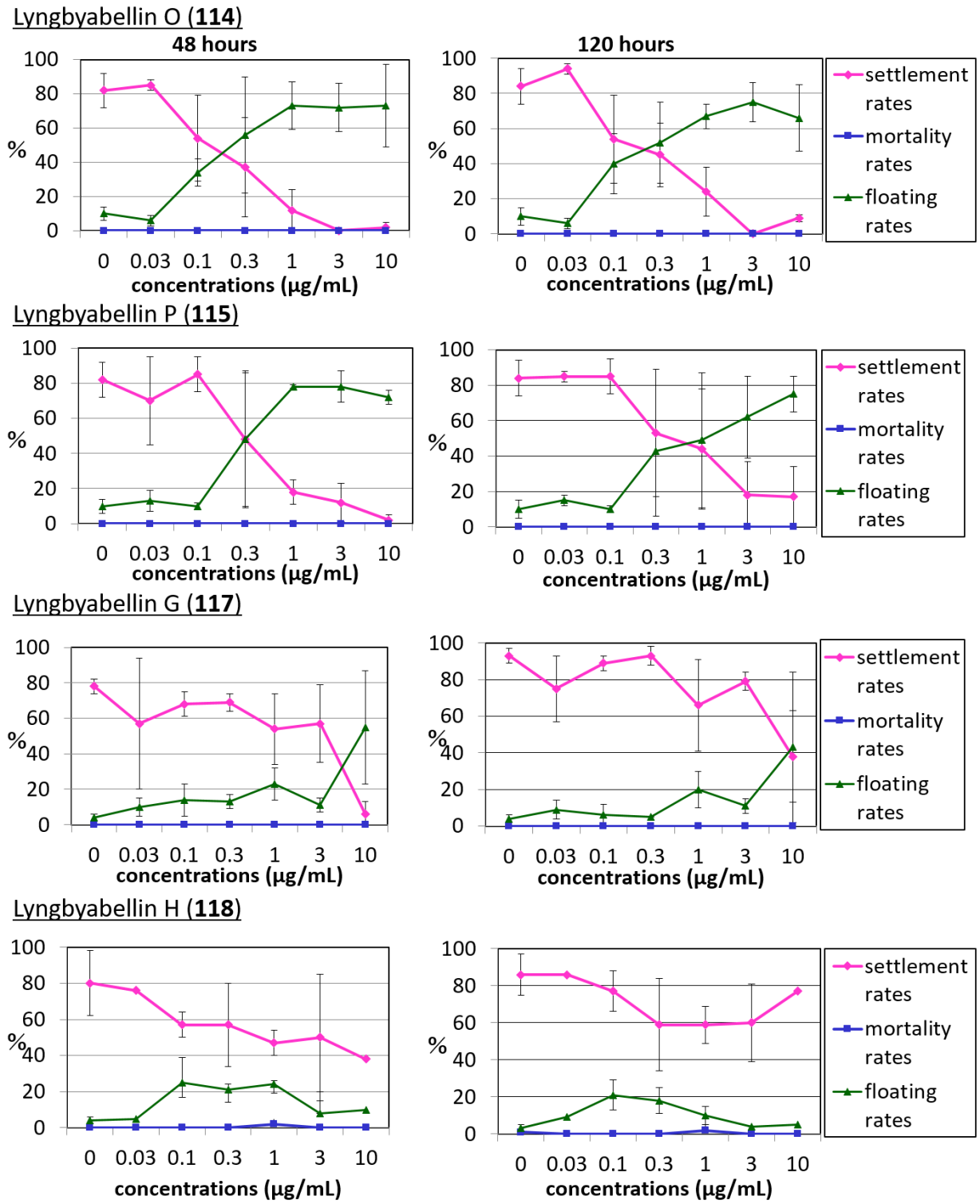

Figure III. 37: Antifouling activity of **114**, **115**, **117** and **118** on barnacle larvae after 48 and 120 hour-exposure. Error bars are for standard deviation. For **114**, **115** and **117**, n = 3. For **118**, n = 2 (except 0.03 and 10 µg/mL, n = 1).

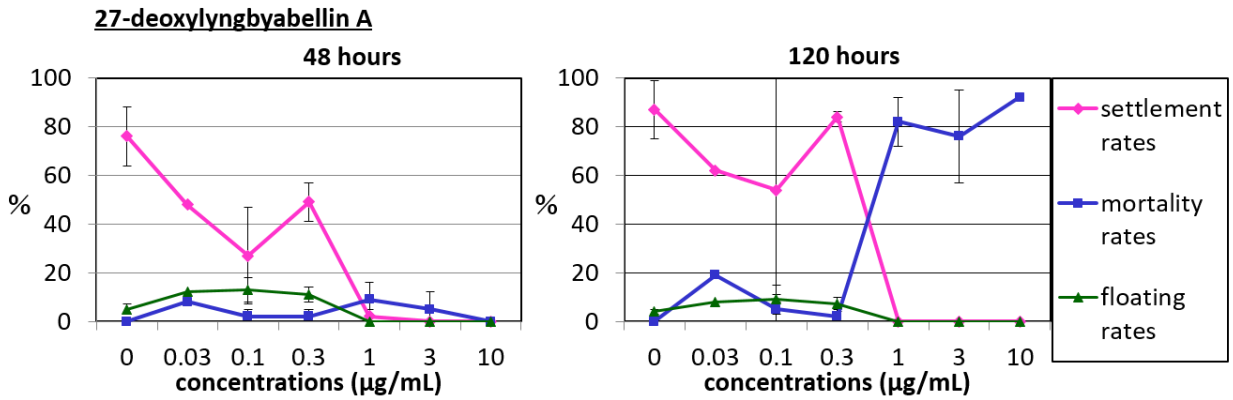

Figure III. 38: Antifouling activity of **119** on barnacle after 48 and 120 hour-exposure Error bars are for standard deviation (SD, n = 2, except for 0.03 and 10 µg/mL, n = 1).

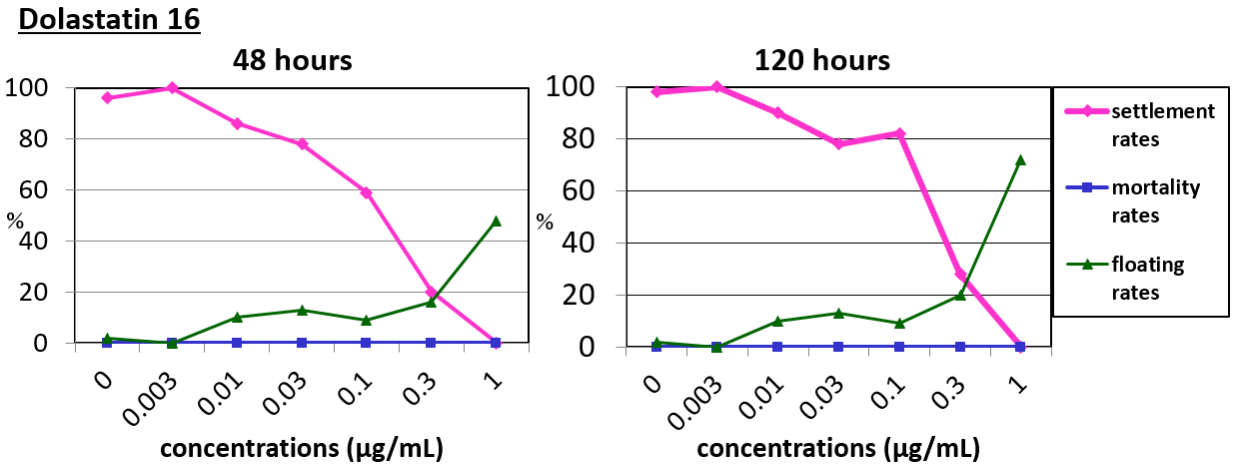

Figure III. 39: Antifouling activity of **60** on barnacle after 48 and 120 hour-exposure (n = 1).

III. 4. Discussion

An *Okeania* sp. extract, collected from the Red Sea, led to the isolation of two new lyngbyabellins: O (**114**) and P (**115**), known compounds from the same familly: lyngbyabellins F (**116**), G (**117**) and H (**118**) and 27-deoxylyngbyabellin A (**119**), and the known potent antifoulant dolastatin 16 (**60**).

Compound **60** was first isolated from the sea hare *Dolabella auricularia*[45] in 1997 and then from the cyanobacterium *Moorea producens* (previously *Lyngbya majuscula*) in 2002. This, together with isolation of other dolastatins from cyanobacteria, demonstrates that this family of compounds are originaly produced by cyanobacteria. Sea hare braze the microalgae and keep the

dolastatins inside them, probably for their own chemical defenses as several dolastatins display cytotoxicity.[112] This was believed to be the case for **60** which was first reported as highly inhibiting the growth of several human cancer cell lines (IC_{50} 0.0012–0.00096 μg/mL). However, a study of its synthetic form turned out to be inactive. This was attributed to a change in the conformation of the synthetic compound or the presence of a chemically undetected (yet extremely active) compound in the sample isolated from the natural source. Another synthesis of this cyclodepsipeptide by Casalme *et al.*[111] showed the same trend. Is there a possible degradation of the synthetic version of **60** during the assays or the first paper reporting the cytotoxicity of the natural compound got wrong results? To answer to this question, re-isolation and re-testing of the natural **60** was needed. The present study confirmed that the natural **60**, here isolated from the cyanobacterium *Okeania* sp., closely genetically related to *Moorea majuscula*, is non-cytotoxic, like the synthetic one, meanwhile keeping its potent antifouling activity previously reported for both natural[98] and synthetic one[111].

Two new lyngbyabellins **114** and **115**, were isolated together with the known **116-119**. As shown on Figure III. 40, lyngbyabellins **114-117** are related compounds. A structure/activity relationship was observed in both cytotoxicity and antifouling assays. As previously reported, side chain increases the inhibition of cells growth (**115** and **118** being more active than **114** and **117**) while the cyclic structure is prefered (**117** and **118** being more active than **114** and **115**). The side chain in **115** and **118** could play an important role in their superior cytotoxicity (IC_{50} 9 μM and 0.07 μM, respectively) over **114** and **117**; forming additional interactions with a common target, providing a different mode of action or simply improving its permeability. Compound **117** appeared less active on MCF7 cells that on H460 and Neuro-2a cells (2.2 and 4.8 μM, respectively).[103] Its mechanism of action in MCF7 cells is probably different than in H460 and Neuro-2a cells, or MCF7 cells are less sensitive to **117**. Concerning the antifouling activity, **114** was the most active, followed by **115**, **117** and then **118**. The flexibility of the acyclic structure may facilitate interactions with a common target, but addition of a side chain decreases them, as observed with **115**.

Table III. 3 lists all the lyngbyabellins, dolabellin (**128**) and two hectochlorins (**137** and **139**) and their reported cytotoxicity on different cell lines. Figures III. 40-42 show their structures for comparison. Beside cyclic compounds being more active than acyclic and the side chain increasing the cytotoxicity, another structure/activity relationship is observable. 27-deoxylyngbyabellin A (**119**), lyngbyabellins A (**134**) and N (**129**) are the most active compounds

with IC_{50} as low as 7.3, 21 or 4.8 nM! Interestingly, their upper part contains more nitrogen forming extra lactams and ressembles some dolastatins.

Table III. 3: Cytotoxicity (IC_{50} in µM) of lyngbyabellins, dolabellin and two hectochlorins on several cells lines.

Compounds	IC_{50}	Cells
Lyngbyabellin A (**134**)	0.047	HT29[113]
	0.022	HeLa[113]
	0.021	KB[114]
27-deoxylyngbyabellin A (**119**)	0.345	LoVo[114]
	0.012	HT29[113]
	0.0073	HeLa[113]
	0.31	MCF7
Lyngbyabellin B (**135**)	1.1	HT29[113]
	0.71	HeLa[113]
	0.1	CA46[115]
	1.0	PtK2[115]
Lyngbyabellin C (**130**)	2.1	KB[106]
	5.3	LoVo[106]
Lyngbyabellin D (**133**)	0.1	KB[116]
Lyngbyabellin E (**123**)	0.4	H460[103]
	1.2	Neuro-2a[103]
Lyngbyabellin F (**116**)	1.0	H460[103]
	1.8	Neuro-2a[103]
Lyngbyabellin G (**117**)	2.2	H460[103]
	4.8	Neuro-2a[103]
	120	MCF7[119]

Compounds	IC_{50}	Cells
Lyngbyabellin H (**118**)	0.2	H460[103]
	1.4	Neuro-2a[103]
	0.07	MCF7
Lyngbyabellin I (**127**)	1.0	H460[103]
	0.7	Neuro-2a[103]
Lyngbyabellin J (**131**)	0.054	HT29[103]
	0.041	HeLa[103]
Lyngbyabellin K (**126**)	Inactive	H460[117]
Lyngbyabellin L (**124**)	Inactive	H460[117]
Lyngbyabellin M (**136**)	Inactive	H460[117]
Lyngbyabellin N (**129**)	0.0048-1.8	H460[117]
	0.0409	HCT116[117]
Lyngbyabellin O (**114**)	Inactive	MCF7[119]
Lyngbyabellin P (**115**)	9	MCF7[119]
Dolabellin (**128**)	3.72	HeLa[118]
Hectochlorin (**137**)	0.02	CA46[115]
	0.3	PtK2[115]
	0.86	KB[120]
	1.2	NCI-H187[120]
Hectochlorin B (**136**)	0.31	KB[118]
	0.32	NCI-H187[120]

The isolation of two new lyngbyabellins from *Okeania* sp. increases the number of members of this chemical family formed by lyngbyabellins but also **128** and **137**-**141**. Indeed, all these compounds possess two thiazole rings and an unusual *gem*-dichloro group; except lyngbyabellin L (**124**) and 7-epilyngbyabellin L (**125**) which bear only one (Figure III. 40).

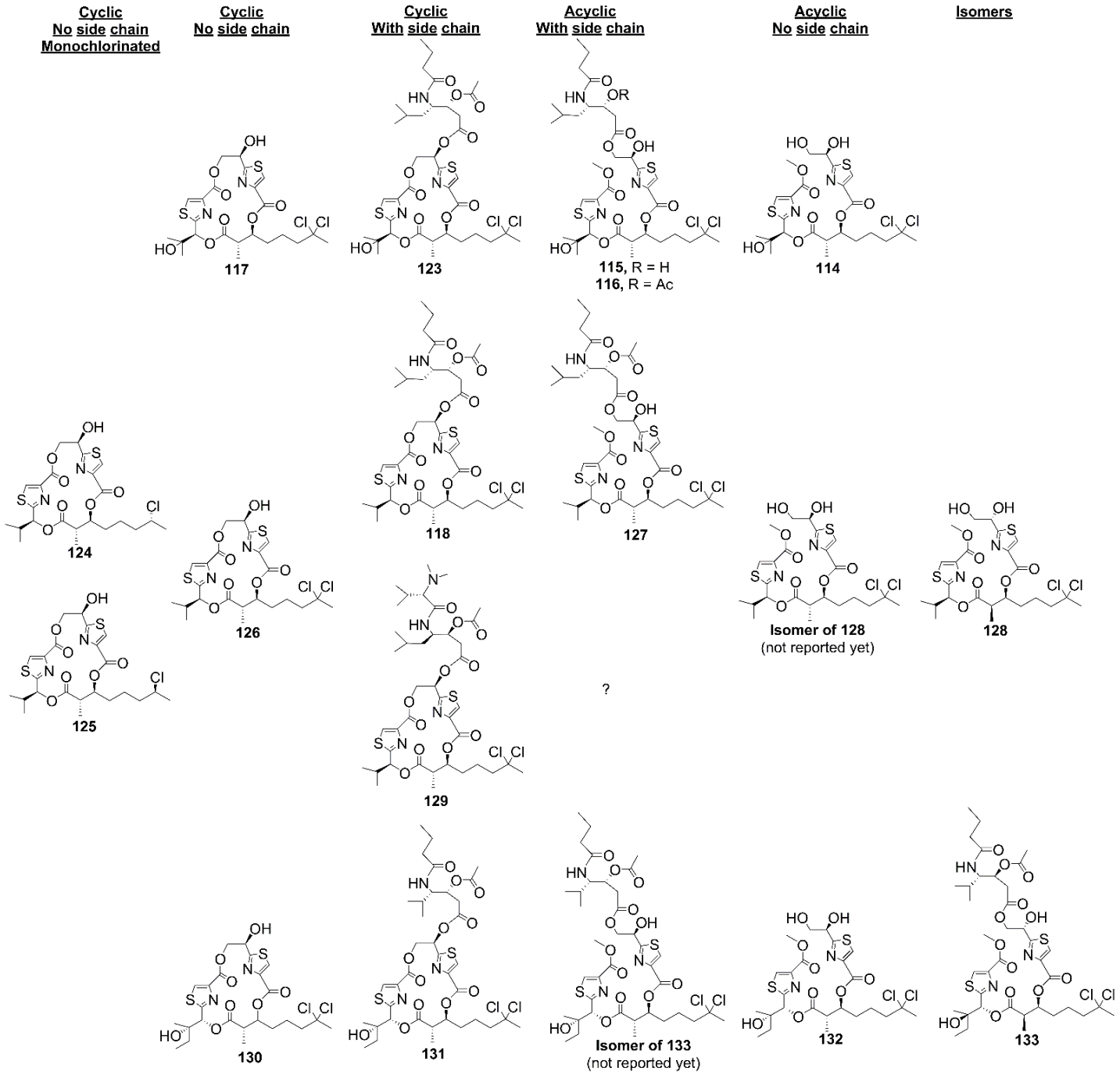

Figure III. 40: Relation between lyngbyabellins and dolabellins.

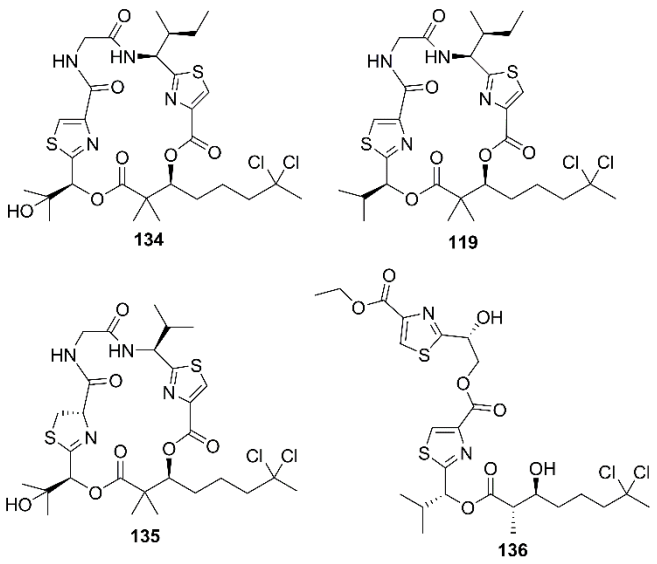

Figure III. 41: Structures of lyngbyabellins A (**134**), B (**135**) and M (**136**), and 27-deoxylyngbyabellin A (**119**).

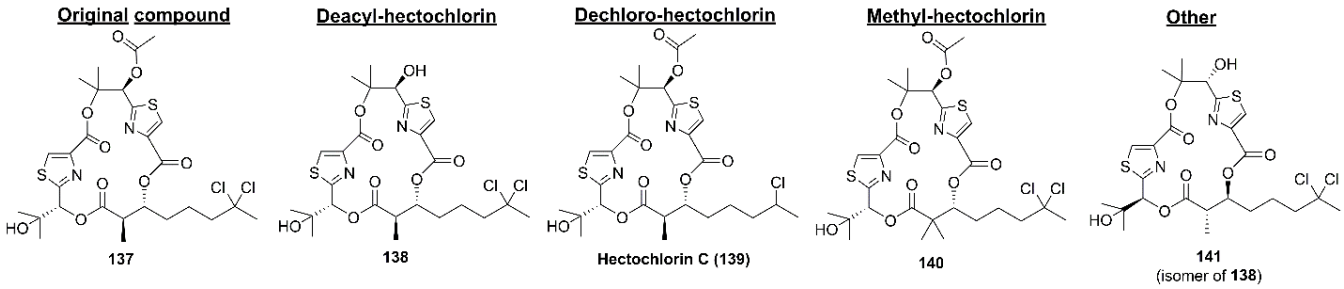

Figure III. 42: Structures of hectochlorins.

In this Chapter III, we saw that **117** (cyclic form without side chain) and **116** (acyclic form with a side chain), can be converted into **114** by a regioselective ester cleavage occurred at C-16 and C-14, respectively. This kind of conversion was previously reported for **123** converted into **117**, and **130** converted into **132**, suggesting that the acyclic compounds are likely artifacts. However, Williams *et al.*[116] hypothesized that both cyclic and acyclic analogues can be produced by the cyanobacteria as an evolutionary advantage by delaying the development of detoxification mechanisms by predators. Indeed, the production of diverse forms of toxins and antifeedants can lead to rapid bloom production in areas where there are lots of herbivores like on tropical coral reefs.[121] Figure III. 40 shows the relation between each kind of lyngbyabellins: cyclic and acyclic, both with or without side chain. As seen on this figure and previously reported, **128** is likely an artifact from a lyngbyabellin which was not reported yet. This hypothetic lyngbyabellin should have a 2*R* and 14*S* configuration, like only **133** possesses. 2*R* configuration is also found in

hectochlorins (except **140** which has two methyl groups attached to C-2) (Figure III. 42). 14*S* configuration is also found in **141**, an isomer of **138** and isolated from the Thai sea hare *Bursatella leachii* (but probably produced by a cyanobacterium).[120] This information suggests that other lyngbyabellin analogues with such features could exist. Indeed, as lyngbyabellins and hectochlorins are very related compounds, slight changes in their biosynthetic pathways could lead to new analogues. Figure III. 43 shows the almost identical 50 kb hybrid NRPS/PKS biosynthetic pathway of **134** and **137** which both exhibit antifungal and cytotoxic activities.[122]

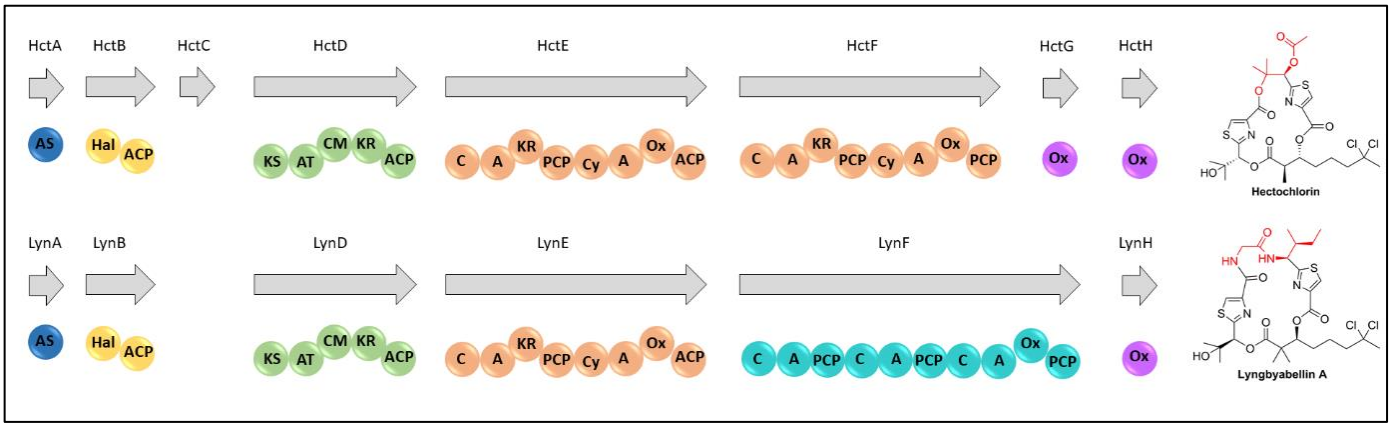

Figure III. 43: Biosynthetic pathway of hectochlorin (**137**) and lyngbyabellin A (**134**).

The HctA or LynA initial acyl-ACP synthethase activates hexanoic acid which undergoes chlorination by HctB/LynB to form the unusual *gem*-dichloro group at the penultimate carbon atom. Based on a study, HctB (and so LynB) is very specific to metabolize at the C-5 position and apparently transfers either a metal-bound hydroxy or chloro species at C-5 and, in a second reaction, it removes the remaining proton of C-5 to replaced it by a second chlorine.[123] Because of this, we can suppose that **124** and **125**, which bear only one chlorine, can be artifact due to a failure of the enzyme to replace the remaining proton at C-5 by a chlorine. After halogenation, a single acetate extension occurs, along with a *C*-methylation event catalyzed by HctD/LynD. For **134**, a double *C*-methylation takes place whereas a single methylation is observed in **137**. This double methylation from a single *C*-methyl transferase domain was not elucidated yet, as why this double methylation occurs in **134**, **135** and **140** and not in the other lyngbyabellins which undergo a single methylation like **137**. It was hypothesized that **140** could be biosynthetic shunt products[120], meaning that **134** and **135** could be too. After this methylation, the NRPS module HctE/LynE incorporates the α-hydroxic acid 2,3-dihydroxyisovaleric acid. Then a cysteine residue is added and it becomes heterocyclized and oxidized to form a thiazole ring. No function was identified for

HctC and no LynC was found. After HctE/LynE, the two biosynthetic pathways differ. For **137**, the bimodular HctF gene, which highly resembles of HctE, codes for an NRPS module which incorporates a second α-keto acid. This acid is then reduced to 2,3-dihydroxyisovaleric acid, and a second cysteine residue which, like the first one, becomes cyclized and oxidized to give the second thiazole ring of the molecule. In the case of **134**, LynF is a trimodular NRPS which incorporates glycine, isoleucine and cysteine, the latter being cyclized to a thiazole. After macrocyclization, both pathways release their products. No gene was found in this cluster to explain the addition of the acetate group at C-14 for **137**. This acetate group is probably added during a post-assembly modification from a protein encoded by a gene belonging to another cluster. This suggests that other clusters could be responsible of post-assembly modification at C-14, leading to the attachment of side chains as observed in lyngbyabellins.[122] As observed by Choi *et al.*, the side chain of **129** with *N*,*N*-dimethylvaline terminus resembles that of the dolastatin 10 (**142**).[117]

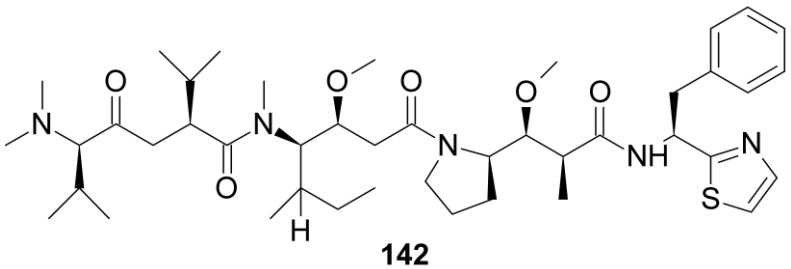

142

As for **115**, **116**, **118**, **123**, **127** and **133**, their side chain contains a statin unit which was first described in pepstatin (**143**)[124], an actinobacterial aspartic protease inhibitor, and then in grassystatins (**144-146**)[125], cyanobacterial compounds from *Symploca* sp. These similar features could suggest that the complex lyngbyabellins with a side chain represent hybridization and co-joining products of several natural product structures classes such as lyngbyabellins, dolastatins, grassystatins and more. These hypotheses could go further with reported hectochlorins as precursors of more complex molecules with same characteristic are lyngbyabellins. Cyanobacteria are rich sources of compounds and these findings show that they are still promising objects of research.

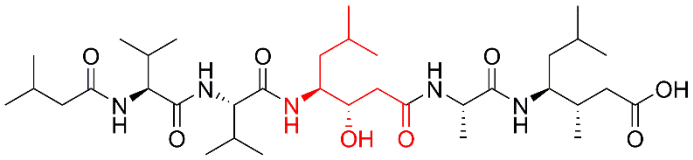

143

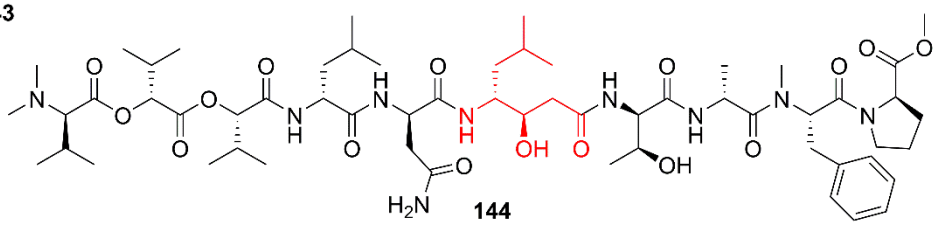

144

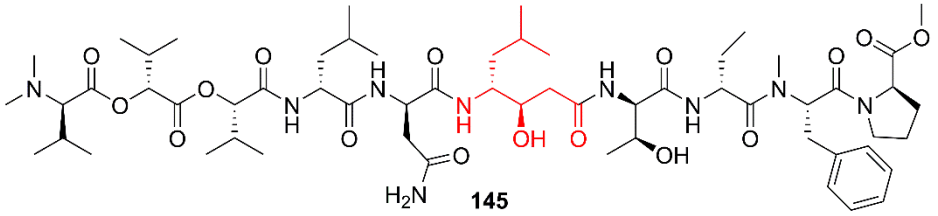

145

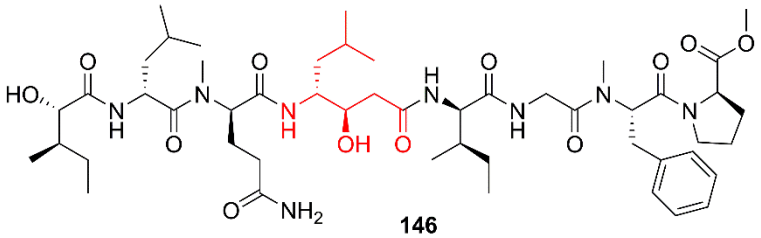

146

- GENERAL DISCUSSION -

In this study, extracts from two organisms, the sponge *Hyrtios* sp. and the cyanobacterium *Okeania* sp., isolated from the Red Sea, near Jeddah (Saudi Arabia), led to several antifouling compounds. Three previous papers studied the antifouling activity of crude extracts from Red Sea marine organisms, and only one paper reported active pure natural antifoulants from such organisms.[36,126-128] The results of this present study increase the number of evidences showing that Red Sea organisms are interesting sources of antifoulants. Antifouling compounds from the Red Sea are a quite new topic as the first paper about such activity was published in 2014.[36] However, lots of compounds with other bioactivity have been isolated from this unique environment. Recently, a team from Egypt reviewed about 435 compounds from 138 references.[129] Many of these compounds were cytotoxic, antiproliferative, antiviral, antibacterial and with anti-inflammatory activity. A *Hyrtios* sp. sponge has been reported to produce two sesquiterpene γ-methoxybutenolide, hyrtiosenolides A (**147**) and B (**148**).[130] Another one, *Hyrtios erecta*, led for instance to the isolation of seven cytotoxic compounds: salmahyrtisols A (**149**), B (**150**) and C (**151**), two scalarane-type sesquiterpenes (**152-153**), hyrtiosal (**154**) and scalarolide (**155**) and hyrtiomanzamine (**156**).[131,132] The sponge *Theonella swinhoei* affords two gross macrolides swinholide I (**157**) and hurghadolide A (**158**), which showed very potent cytotoxicity against human colon adenocarcinoma (IC_{50} 5.6 and 365 nM, respectively) by disrupting actin microfilaments like lyngbyabellins also do, and were also active against *Candida albicans*.[133] Cyanobacteria were also collected in the Red Sea, such as *Leptolyngbya* sp. which produces, among lots of compounds such as some dolastatins, grassypeptolides D (**159**) and E (**160**) which possess two thiazoline rings.[134]

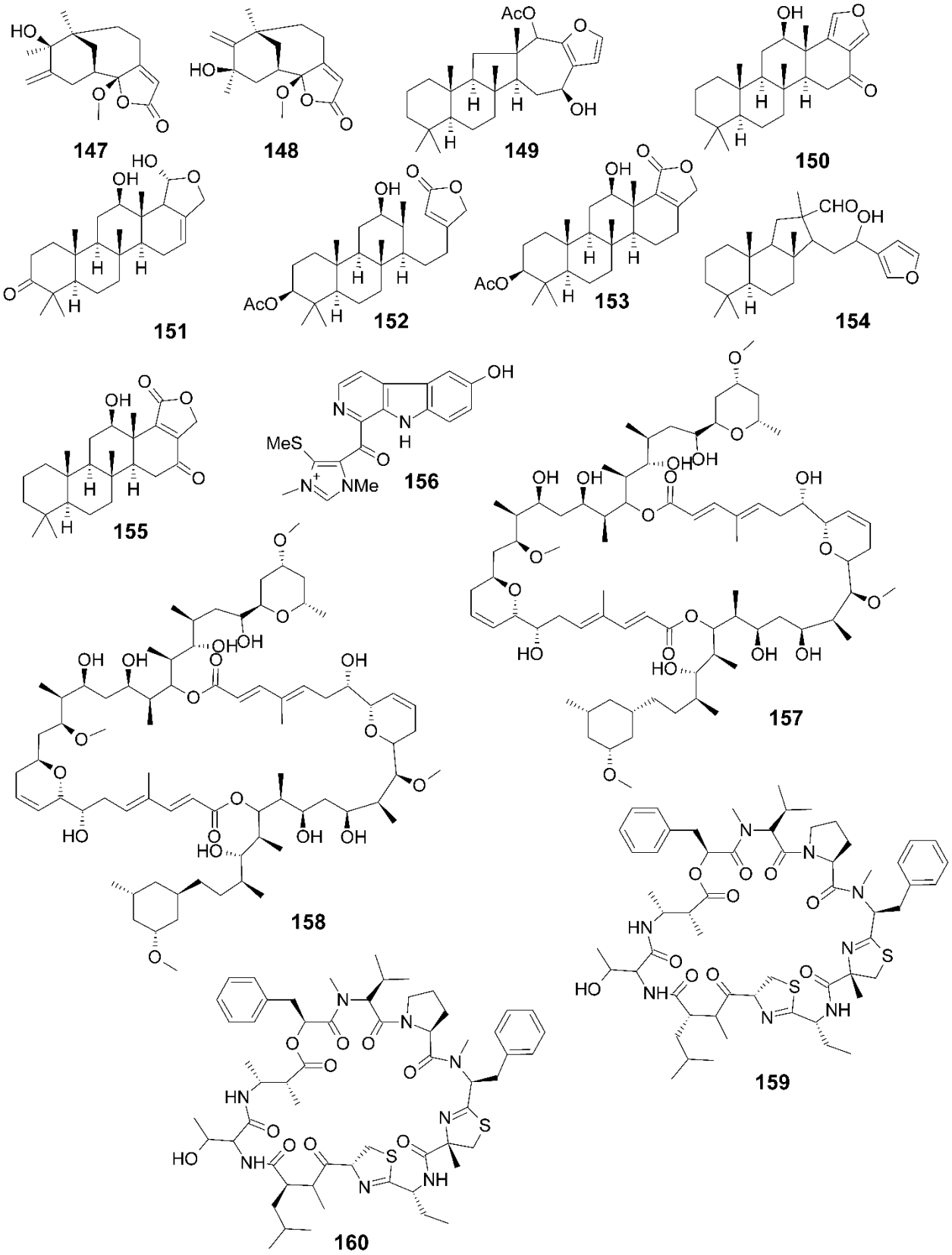

Three known compounds were isolated from *Hyrtios* sp. However, it is the first time that methyl-(*Z*)-octadec-11-enoate (**73**) was isolated from a natural source. Methyl-(5*Z*,9*Z*)-

hexacosa-5,9-dienoate (**72**), which can also be named methyl 5,9-hexacosadienoate, was apparently isolated from the sponge *Chondrosia* sp. A very close isomer, differing by only the position of the double bonds, Δ6,10, was isolated from a Red Sea sponge *Mycale euplectellioides*.[135] However, the assignment of the position of the double bonds is quite doubtful. Indeed, the paper reported an allylic proton (H-9) with a δ_H between 1.25-1.35 ppm. Moreover, wrong integrations were made for the protons, showing only one olefinic proton at about 5.4 ppm and two allylic protons at about 2.0 ppm whereas both signals seem to have the same integration. The paper also reported two carbons at 24.8 (C-4) and 25.0 ppm (C-3) but only the one at 25.0 is visible on the 1D ^{13}C NMR spectrum. By removing this C-4, and thanks to the COSY correlations between H-2 and H-3, a Δ5,9 compound is obtained: **72**. Their observations of the fragment ion peaks also confirm this hypothesis: a peak at *m/z* 141 was seen. This is a very specific ion for fatty acid methyl esters with a 5,9-double bond structure.[136] As a result, **72** was previously isolated from a Red Sea sponge but with a wrong reported structure.

The three compounds isolated from *Hyrtios* sp. showed anti-settlement activity on barnacle larvae, especially the two FAMEs **72** and **73** with potent EC_{50} (0.15 and 0.16 µM). Study of their mode of action would be interesting, especially if they display antioxidant activity like some FAMEs previously reported.[73] They could be incorporated into a paint and deter mussels and barnacles from settling as these organisms use oxidative chemistries to attach and metamorphose. However, we can wonder if these compounds are natural of artifacts as sponges as known prolific producers of fatty acids, not methyl ester derivatives.

Okeania sp. proved to be a prolific producer of interesting compounds. The two new fatty acid amides serinolamides C (**82**) and D (**83**) and two new lyngbyabellins, O (**114**) and P (**115**), were isolated and characterized, together with known compounds: lyngbyabellins F-H

(**116-118**), 27-deoxylyngbyabellin A (**119**) and dolastatin 16 (**60**). This study confirmed the structure/activity relationship reported by Han *et al.* stating that cyclic lyngbyabellins with a side chain were the most cytotoxic, followed by the acyclic forms with a side chain, the cyclic forms without side chain and the acyclic forms without side chain.[103] However, a new structure/activity relationship was observed in term of anti-settlement activity toward barnacle larvae: the most active form was the acyclic lyngbyabellin without side chain (**114**), followed by the acyclic form with side chain (**99**), the cyclic form without side chain (**117**) and the cyclic form with side chain (**118**). The side chain decreases the anti-settlement activity, probably by decreasing interactions with a target or its entry into the larvae. Acyclic compounds are probably more flexible, facilitating interactions and/or their entry into the larvae.

Finding known lyngbyabellins **116-119** and **60** in *Okeania* sp. extract shows that this genus is close to the genera *Lyngbya* and *Moorea*. Indeed, the genus *Okeania* was delineated from the genus *Lyngbya* in a phylogenetical study.[137] This same study informs that *Okeania* and *Lyngbya* cyanobacteria possess close hybrid NRPS/PKS biosynthetical pathways. It is thus not surprising to find lyngbyabellins in *Okeania* sp. In Chapter III, hypothesis was made about new lyngbyabellins and hectoclorins that are to be discovered. Post-assembly modifications can be made after the release of compounds from these hybrid NRPS/PKS biosynthetical pathways. Lyngbyabellin N (**129**) is a good example as a mix between a lyngbyabellin and a dolastatin. As *Okeania* sp. possesses the machinery to produce **60**, it could also produce hybrid lyngbyabellins in certain conditions. As a recently delineated genus, *Okeania* still have a lot to reveal. Up to now, only few compounds were reported from this genus, such as the antimalarial janadolide (**161**),[138] the Okinawan cytotoxic odoamide (**162**),[139] the chymotrypsin inhibitor urumamide (**163**),[140] the cytotoxic kurahyne B (**164**) isolated from an Okinawan strain,[141] the Panamanian medusamide A (**165**),[142] another antimalarial compound bastimolide A (**166**),[143]

the lethal toxin polycavernoside D (**167**),[144] whose previous analogues were isolated from the edible red alga *Polycavernosa tsudai* (or *Gracilaria edulis*) but found to be from cyanobacterial origin, the sterol *O*-acyltransferase inhibitors biseokeaniamides A, B and C (**168-170**)[145] and the three kohamamides A, B and C (**171-173**).[146]

While being very ancient and simple organisms, cyanobacteria still have a lot to reveal, about their biochemistry but also their genetics, and large-scale culture or valorization of blooming cyanobacteria could lead to the production of very potent bioactive compounds which could be used in various industrial fields (pharmaceutical, antifouling etc.).

Finally, this study increased the number of antifouling compounds from Red Sea organisms. Other extracts from these organisms proved to be potent and are waiting to be studied. Research in this field with such organisms is just starting and seems to be promising. Of course, antifoulants can be isolated from organisms inhabiting other places. Such compounds are not only findable in this sea. However, the Red Sea is a quite unique ecosystem. Indeed, it is partially isolated from the open ocean and, because of its location, surrounded by deserts, evaporation occurs, making this sea the warmest and most saline in the world. Moreover, there is a large maritime traffic there since the creation of the Suez Canal in 1869. This canal offers ships a shorter journey between the North Atlantic and the northern Indian Oceans by avoiding the South Atlantic and the southern Indian Oceans. As a consequence of this large maritime traffic, alien species could be introduced in the Red Sea. Because of these special conditions, Red Sea organisms probably produce unique compounds, including antifoulants, to adapt and live within the unique flora and fauna and high density of organisms the Red Sea offers. Therefore, the Red Sea is not the only reservoir of antifouling compounds but is probably one of the most legitimate area to search of such compounds.

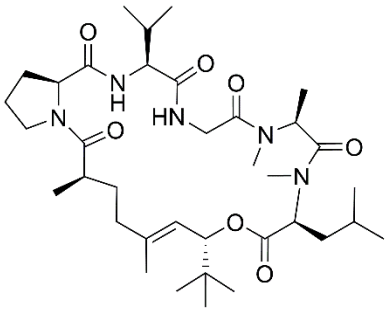

161

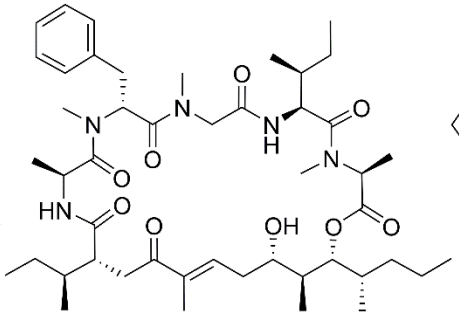

162

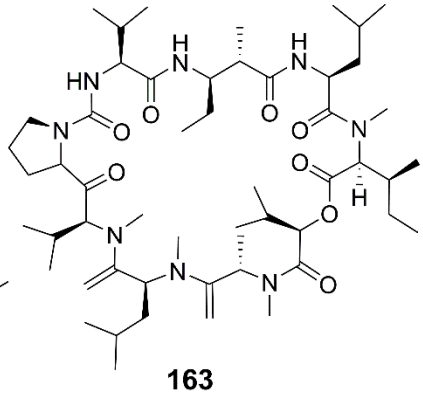

163

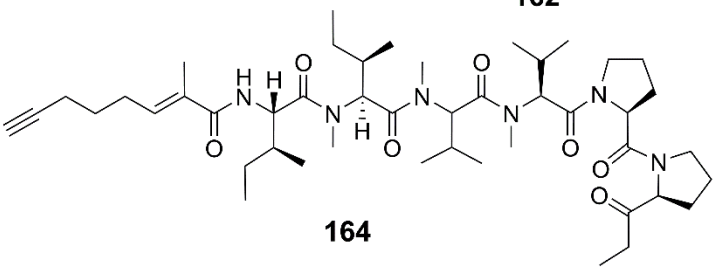

164

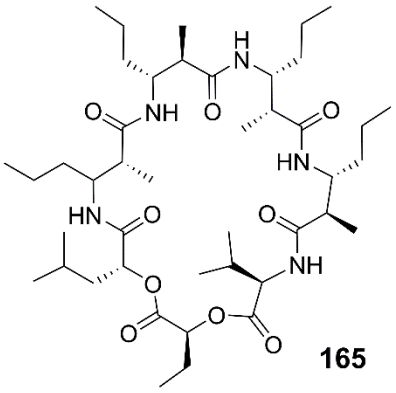

165

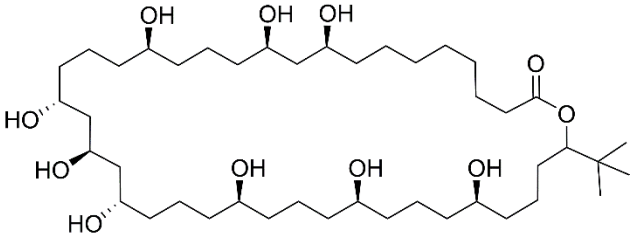

166

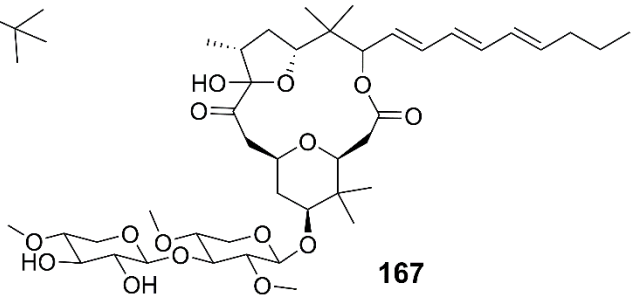

167

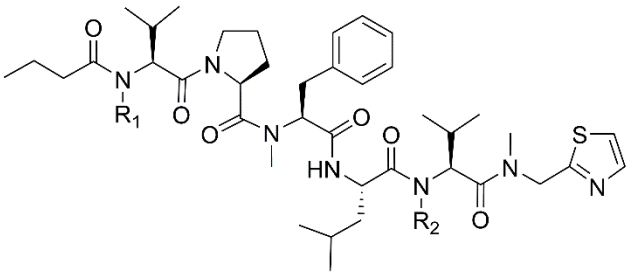

168: R_1 = Me R_2 = Me
169: R_1 = Me R_2 = H
170: R_1 = H R_2 = Me

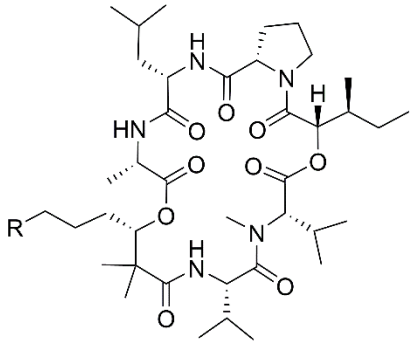

171: R =
172: R =
173: R =

REFERENCES

1. Lüttge U (1985). Epiphyten: Evolution und Ökophysiologie. *Naturwissenschaften 72*:557-566.
2. Wahl M (1989). Marine epibiosis. I. Fouling and antifouling: some basic aspects. *Mar. Ecol. Prog. Ser. 58*:175-189.
3. Railkin A. I. (2003). Marine biofouling: colonization processes and defenses. *CRC Press.* Page 28.
4. Schultz M. P., Bendick J. A., Holm E. R., Hertel W.M. (2011). Economic impact of biofouling on a naval surface ship. *Biofouling 27*: 87-98.
5. Davidson I. C., Brown C. W., Sytsma M. D., Ruiz G. M. The role of containerships as transfer mechanisms of marine biofouling species. *Biofouling 25*: 645-655.
6. Yebra D. M., Kiil S., Dam-Johansen K. (2004). Antifouling technology – past, present and future steps towards efficient and environmentally friendly antifouling coatings. *Prog. Org. Coat. 50*: 75-104.
7. Alzieu C. (2000). Environmental impact of TBT: the French experience. *Sci. Total Environ. 258*: 90-102.
8. Anderson C. D. (1998) TBT and TBT-free Antifouling againts efficiency and track record. IBC UK Conferences Limited; IBC: London, U.K.
9. Broberg Kristensen J. B., Meyer K. L., Søgaard Laursen S., Shipovskov S., Bensebacher F., Poulsen C. H. (2008). Antifouling enzymes and the biochemistry of marine settlement. *Biotechnol. Adv. 26*: 471-481.
10. Cao S., Wang J., Chen H., Chen D. (2011). Progress of marine biofouling and antifouling technologies. *Chin. Sci. Bull. 56*: 598-612.

11. Magin C. M., Cooper S. P., Brennan A. B. (2010). Non-toxic antifouling strategies. *Mater. Today 13*: 36-44.
12. Scardino A. J., Guenther J., de Nys R. (2008). Attachment point theory revisited: the fouling response to a microtextured matrix. *Biofouling 24*: 45-53.
13. Rajagopal S., Van der Velde G., Van der Gaag M., Jenner H.A. (2003). How effective is intermittent chlorination to control adult mussel fouling in cooling water systems? *Water Res. 37*: 329-338.
14. Kiil S., Weinell C. E., Pedersen M. S., Dam-Johansen K. (2001). Analysis of self-Polishing antifouling paints using rotary experiments and mathematical modeling. *Ind. Eng. Chem. Res. 40*: 3906-3920.
15. Yee L. H., Holmström C., Fuary E. T., Lewin N. C., Kjelleberg S. J., Steinberg P. D. (2007) Inhibition of fouling by marine bacteria immobilised in κ-carrageenan beads. *Biofouling 23:* 287-294
16. Lewin N. C. (2012). Ph.D thesis: Toward a "living paint": The development of a marine antifouling paint incorporating bacteria.
17. Bhakuni D. S., Rawat D. S. (2005). Bioactive marine natural products. Springer. ISBN 978-1-14020-3484-8
18. Montaser R., Luesch H. (2011). Marine natural products: a new wave of drugs? *Future Med. Chem. 3*: 1475-1489.
19. Fusetani N. (2004). Biofouling and antifouling. *Nat. Prod. Rep. 21*: 94-104.
20. Fusetani N. (2011). Antifouling marine natural products. *Nat. Prod. Rep. 28*: 400-410.
21. Qian P. Y., Li Z., Xu Y., Li Y., Fusetani N. (2015). Mini-review: marine natural products and their synthetic analogs as antifouling compounds: 2009-2014. *Biofouling 31*: 101-122.

22. Chen L., Qian P.Y. (2017). Review on molecular mechanisms of antifouling compounds: an update since 2012. *Mar. Drugs 15*: 264-283.
23. Lai D., Liu D., Deng Z., van Ofwegen L., Proksch P., Lin W. (2012). Antifouling Eunicellin-Type Diterpenoids from the Gorgonian *Astrogorgia* sp. *J. Nat. Prod. 75*: 1595-1602.
24. Li X.Y., We H.X., Xu Y., Shao C.L., Qian P.Y. (2013). Antifouling activity of secondary metabolites isolated from Chinese marine organisms. *Mar. Biotechnol. 15*: 552-558.
25. Sun J-F., Han Z., Zhou X-F. Yang B., Lin X., Liu J., Peng Y., Yang X-W., Liu Y. (2012). Antifouling briarane type diterpenoids from South China Sea gorgonians *Dichotella gemmacea*. *Tetrahedon 69*: 871-880.
26. Keifer P. A., Rinehard K. L. (1986). Renillafoulins, Antifouling diterpenes from the sea pansy *Renilla reniformis* (Octocorallia). *J. Org. Chem. 51*: 4450-4454.
27. Gerhart D. J., Rittschof D., Mayo S. W. (1988). Chemical ecology and the search for marine antifoulants. Studies of a predator-prey Symbiosis. *J. Chem. Ecol. 14*: 1905-1917.
28. Webster N. S., Taylor M. W. (2012). Marine sponges and their microbial symbionts: love and other relationships. *Envion. Microbiol. 14*: 335:346.
29. Hedner E., Sjögren M., Hodzic R., Andersson R., Göransson U., Jonsson P. R., Bohlin L. (2008). Antifouling activity of a dibrominated cyclopeptide from the marine sponge *Geodia barretti*. *J. Nat. Prod. 71*: 330-333.
30. Hirota H., Tomono Y., Fusetani N. (1996). Terpenoids with antifouling activity against barnacle larvae from the marine sponge *Acanthella cavernosa*. *Tetrahedron 52*: 2359-2368.
31. Okino T., Yoshimura E., Hirota H., Fusetani N. (1995). Antifouling kalihinenes from the marine sponge *Acanthella cavernosa*. *Tetrahedron Lett. 36*: 8637-8640.

32. Hirota H., Okino T., Yoshimura E., Fusetani N. (1998). Five new antifouling sesquiterpenes from two marine sponges of the genus *Axinyssa* and the nudibranch *Phyllidia pustulosa*. *Tetrahedon 54*: 13971-13980.

33. Tsoukatou M., Maréchal JP., Hellio C., Novaković I., Tufegdzic S., Sladié D., Gašić M.J., Clare A.S., Vagias C., Roussis V. (2007). Evaluation of the activity of the sponge metabolites avarol and avarone and their synthetic derivatives against fouling micro- and macroorganisms. *Molecules 12*:1022-1034.

34. Sjögren M., Dahlström M., Hedner E., Honsson P.R., Vik A., Gundersen LL., Bohlin L. (2008). Antifouling activity of the sponge metabolite agelasine D and synthesised analogs on *Balanus improvisus*. *Biofouling 24*:251-258.

35. Hanssen K.O., Cervin G., Trepos R., Petitbois J., Haug T., Hansen E., Andersen J.H., Pavia H., Hellio C., Svenson J. (2014). The bromotyrosine derivative ianthelline isolated from the Arctic marine sponge *Stryphnus fortis* inhibits marine micro-and macrobiofouling. *Mar. Biotechnol. 16*:684-694.

36. Al-Lihaibi S. S., Abdel-Lateff A., Alarif W. M., Nogata Y., Ayyad S-E. N., Okino T. (2015). Potent antifouling metabolites from Red Sea organisms. *Asian J. Chem. 27*: 2252-2256.

37. Umezawa T., Oguri Y., Matsuura H., Yamazaki S., Suzuki M., Yoshimura E., Furuta T., Nogata Y., Serisawa Y., Matsuyama-Serisawa K., Abe T., Matsuda F., Suzuki M., Okino T. (2014). Omaezallene from red alga *Laurencia* sp.: Structure Elucidation, Total Synthesis, and Antifouling Activity. *Angew. Chem. 53*:3909-3912.

38. Ryu G., Yoon O. S. (2003). Studies on marine natural antifoulant laurinterol. *Korean J. Env. Biol. 29*:1-8.

39. Oguri Y., Watanabe M., Ishikawa T., Kamada T., Vairappan C. S., Matsuura H., Kaneko K., Ishii T., Suzuki M., Yoshimura E., Nogata Y., Okino T. (2017). New marine antifouling compounds from the red alga *Laurencia* sp. *Mar. Drugs 15*: 267-276.

40. Shao C-L., Xu R-F., Wang C-Y., Qian P-Y., Wang K-L., Wei M-Y. (2015). Potent antifouling marine dihydroquinolin-2(IH)-one-containing alkaloids from the gorgonian coral-derived fungus *Scopulariopsis* sp. *Mar. Biotechnol. 17*: 408-415.

41. Sun Y-L., Zhang X-Y., Nong X-H., Xu X-Y., Qi S-H. (2016). New antifouling macrodiolides from the deep-sea-derived fungus *Trichobotrys effuse* DFFSCS021. *Tetrahedron Lett. 57*: 366-370.

42. Xing Q., Gan L-S., Mou X-F., Wang W., Wang C-Y., Wei M-Y., Shao C-L. (2016). Isolation, resolution and biological evaluation of pestalachlorides E and F containing both point and axial chirality. *RSC Adv. 6*: 22653-22658.

43. Dahms H-U., Ying X., Pfeiffer C. (2006). Antifouling potential of cyanobacteria: a mini-review. *Biofouling 22*: 317-327

44. Tan L. T., Goh B. P. L., Tripathi A., Teo, S. L. M. (2010). Natural antifoulants from the marine cyanobacterium *Lyngbya majuscula*. *Biofouling 26*, 685-695.

45. Pettit G. R., Xu J-P., Hogan F., Williams M. D., Doubek D. L., Schmidt J. M, Cerny R. L., Boyd M. R. (1997). Isolation and structure of the human cancer cell growth inhibitory cyclodepsipeptide dolastatin 16. *J. Nat. Prod. 60*, 752-754.

46. Zhang Y-F., Zhang H., He L., Liu C., Xu Y., Qian P-Y. (2012). Butenolide Inhibits Marine Fouling by Altering the Primary Metabolism of Three Target Organisms. *ACS Chem. Biol. 7*: 1049-1058.

47. Cho J. Y. (2012). Glycoclycerolipids isolated from marine derived *Streptomyces coelescens* PK206-15. *Biosci. Biotechnol. Biochem. 76*: 1746-1751.

48. Nishikawa K., Nakahara H., Shirokura Y., Nogata Y., Yoshimura E., Umezawa T., Okino T., Matsuda F. (2011) Total synthesis of 10-isocyano-4-cadinene and its stereoisomers and evaluations of antifouling activities. *J. Org. Chem. 76*: 6558-6573.

49. Cahill P.L., Kuhajek J.M. (2014). Polygodial: a contact active antifouling biocide. *Biofouling 30*: 1035-1043.

50. Moodie L. W. K., Trepos R., Cervin G., Larsen L., Larsen D. S., Pavia H., Hellio C., Cahill P., Svsenson J. (2017). Probing the structure–activity relationship of the natural antifouling agent polygodial against both micro- and macrofoulers by semisynthetic modification. *J. Nat. Prod. 80*: 515-525.

51. Pérez M., Garcia M., Stupak M., Blustein G. (2015). Disminución del contenido de cobre en pinturas “antifouling” de matriz soluble, uso del eugenol como aditivo. *Bol. Invest. Mari. Cost. 44*: 81-290.

52. Skattebøl L., Nilsen N. O., Stenstrøm Y., Andreassen P., Willemsen P. (2006). The antifouling activity of some juvenoids on three species of acorn barnacle, *Banalus*. *Pest Manag. Sci. 62*: 610-616.

53. Almeida J. R. and Vasconcelos V. (2015). Natural antifouling compounds: effectiveness in preventing invertebrate settlement and adhesion. *Biotechnol. Adv. 33*: 343-357.

54. Darwin Correspondence Project, “Letter no. 1489,” accessed on 25 October 2017, http://www.darwinproject.ac.uk/DCP-LETT-1489.

55. Carballeira N. M., Reyes E. D., Shalabi F. (1993). Identification of novel iso/anteiso nonacosadienoic acids from the phospholipids of the sponges *Chondrosia remiformis* and *Myrmekioderma styx*. *J. Nat. Prod.56*: 1850-1855.

56. Yamamoto K., Shibahara A., Nakayama T., Kajimoto G. (1991). Determination of double-bond positions in methylene-interrupted dienoic fatty acids by GC-MS as their dimethyl disulfide adducts. *Chem. Phys. Lipids 60*: 39-50.

57. Vincenti M., Guglielmetti G., Cassani G., Tonini C. (1987). Determination of double bond position in diunsaturated compounds by mass spectrometry of dimethyl disulfide derivatives. *Anal. Chem. 59*: 694-699.

58. N. H. Meyer and Zangger K. (2014). Enhancing the resolution of multi-dimensional heteronuclear NMR spectra of intrinsically disordered proteins by homonuclear broadband decoupling. *Chem. Commun. 50*:1488-1490.

59. Castañar L and Parella T. (2015). Broadband ^{1}H homodecoupled NMR experiments: recent developments, methods and applications. *Magn. Reson. Chem. 53*: 399-426.

60. John Wiley & Sons (1976). *Topics of Carbon-13 Spectroscopy vol. 2*: 81-87.

61. D. H. Williams and I. Fleming (1980). *Spectroscopic Methods in Organic Chemistry, 3rd ed.*, McGraw-Hill, UK.

62. Kitano Y., Ito T, Suzuki T., Nogata Y., Shinshima K., Yoshimura E., Chiba K., Tada M., Sakaguchi I (2002). Synthesis and antifouling activity of 3-isocyanotheonellin and its analogues. *J. Chem. Soc., Perkin Trans.1*: 2251-2255.

63. Rittschof D., Maki J., Mitchell R., Costlow J. D. (1986). Ion and neuropharmacological studies of barnacle settlement. *Netherlands J. Sea Res. 20*: 269-275.

64. Kon-ya K., Endo M. (1995). Catechlolamines as settlement inducers of barnacle larvae. *J. Mar. Biotechnol 2*: 79-81.

65. Yamamoto H., Shimizu K., Tachibana A., Fusetani N. (1999). Roles of dopamine and serotonin in larval attachment of the barnacle. *J. Exp. Zoolog. 284*: 746-758.

66. Beiras R. and Widdows J. (1995). Effect of the neurotransmitters dopamine, serotonin and norepinephrine on the ciliary activity of mussel (*Mytilus edulis*) larvae. *Mar. Biol. 122*: 597-603.

67. Wu H-H., Tian L., Chen G., Xu N., Wang Y-N., Sun S., Pei Y-H. (2009). Six compounds from marine fungus Y26-02. *J. Asian Nat. Prod. Res. 11*: 748-751.

68. Rod'kina S. A. (2005). Fatty acids and other lipids of marine sponges. *Russ. J. Mar. Biol. 31*: 549-560.

69. Kornprobst J-M. and Barnathan G. (2010). Demospongic acids revisited. *Mar. Drugs 8*: 2569-2577.

70. http://lipidhome.co.uk/ms/methesters/me-arch/me_to2db/M0591.htm (accessed on October 27, 2017).

71. Mena P. L., Pilet O., Djerassi C. (1984). Phospholipid studies of marine organisms. 7. Stereospecific synthesis of (5*Z*,9*Z*)-, (5*Z*,9*E*)-, (5*E*,9*Z*)-, and (5*E*,9*E*)-5,9-hexacosadienoic Acid. *J. Org. Chem. 49*: 3260-3264.

72. Chandrasekaran M., Kannathasan K., Venkatesalu V. (2008). Antimicrobial activity of fatty acid methyl esters of some members of *Chenopodiaceae* . *Z. Naturforsch 63*: 331-336.

73. Mea P., Araújo S. G., Morais M. I., Sá N. P., Lima C. M., Rosa C. A., Sigueira E. P., Johann S., Lima L. (2017). Antifungal and antioxidant activity of fatty acid methyl esters from vegetable oils. *An Acad. Bras. Cienc. 89*: 1671-1681.

74. Gao M., Su R., Wang K., Li X., Lu W. (2013). Natural antifouling compounds produced by a novel fungus *Aureobasidium pullulans* HN isolated from marine biofilm. *Mar. Pollut. Bull. 77*: 171-176.

75. Bazes A., Silkina A., Douzenel P., Faÿ F., Kervarec N., Morin D., Berge J-P., Bourgougnon N. (2009). Investigation of the antifouling constituents from the brown alga *Sargassum muticum* (Yendo) Fensholt. *J. Appl. Phycol. 21*: 395-403.

76. Bhattarai H. D., Ganti V. S., Paudel B., Lee Y. K., Lee H. K., Hong Y. K., Shin H. W. (2007). Isolation of antifouling compounds from the marine bacterium, *Shewanella oneidensis* SCH0402. *World. J. Microb. Biot. 23*: 243-249.

77. Xu Y., Li H., Li. X., Xiao X., Qian P-Y. (2009). Inhibitory effects of a branched-chain fatty acid on larval settlement of the polychaete *Hydroides elegans*. *Mar. Biotechnol. 11*: 495-504.

78. Abdel-Lateff A., Elkhayat E. S., Fouad M. A., Okino T. (2009). Aureobasidin, new antifouling metabolite from marine-derived fungus *Aureobasidium* sp. *Nat. Prod. Comm. 4*: 389-394.

79. Del Grosso C. A., McCarthy T. W., Clark C. L., Cloud J. L., Wilker J. J. (2016). Managing redox chemistry to deter marine biological adhesion. *Chem. Mater. 28*: 6791-6796.

80. Essock-Burns T., Gohad N. V., Orihuela B., Mount A. S., Spillman C. M., Wahl K. J., Rittschof D. (2016). Barnacle biology before, during and after settlement and metamorphosis: a study of the interface. *J. Exp. Biol. 220*: 194-207.

81. Winnikoff J. R., Glukhov E., Dorrestein P. C., Gerwick W.H. (2014). Quantitative molecular networking to profile marine cyanobacterial metabolomes. *J. Antibiot. 67*: 105-112.

82. Gao Y-R., Guo S-H., Zhang Z-X., Mao S., Zhang Y-L., Wang Y-Q. (2013). Concise synthesis of (+)-serinolamide A. *Tetrahedron Lett. 54*: 6511-6513.

83. Engene N., Rottacker E. C., Kaštovský J., Byrum T., Choi H., Ellisman M. H., Komárek J., Gerwick W. H. (2012). *Moorea producens* gen. nov., sp. nov. and *Moorea bouillonii* comb. nov., tropical marine cyanobacteria rich in bioactive secondary metabolites. *Int. J. Syst. Evol. Microbiol. 62*: 1171-1178.
84. Gutiérrez M., Pereira A. R., Debonsi H. M., Ligresti A., Di Marzo V., Gerwick W. H. (2011). A cannabinomimetic lipid from a marine cyanobacterium. *J. Nat. Prod., 74*: 2313-2317.
85. Montaser R., Paul V. J., Luesch H. (2012). Marine cyanobacterial fatty acid amides acting on cannabinoid receptors. *ChemBioChem 13*: 2676-2681.
86. Dorman D. E., Jautelat M., Roberts J. D. (1971). Carbon-13 nuclear magnetic resonance spectroscopy. Quantitative correlations of the carbon chemical shifts of acyclic alkenes *J. Org. Chem. 36*: 2757-2766.
87. Sharma B.K. (1972). Instrumental methods of chemical analysis. Krishna Prakashan Media. ISBN 81-8283-019-2.
88. Han B., McPhail K. L., Ligresti A., Di Marzo V., Gerwick W. H. (2003). Semiplenamides A−G, Fatty acid amides from a Papua New Guinea collection of the marine cyanobacterium *Lyngbya semiplena*. *J. Nat. Prod. 66*: 1364-1368.
89. Sitachitta N., Gerwick W. H. (1998). Grenadadiene and grenadamide, cyclopropyl-containing fatty acid metabolites from the marine cyanobacterium *Lyngbya majuscula*. *J. Nat. Prod. 61*: 681-684.
90. Mevers E., Matainaho T., Allara M., Di Marzo V. Gerwick W. H. (2014). Mooreamide A: a cannabinomimetic lipid from the marine cyanobacterium *Moorea bouillonii*. *Lipids 49*: 1127-1132.

91. Kleigrewe K., Almaliti J., Tian I. Y., Kinnel R. B., Korobeynikov A., Monroe E. A., Duggan B. M., Di Marzo V., Sherman D. H., Dorrestein P. C., Gerwick L., Gerwick W. H. (2015). Combining mass spectrometric metabolic profiling with genomic analysis: A powerful approach for discovering natural products from cyanobacteria. *J. Nat. Prod. 78*: 1671-1682.
92. Walker J.M., Hohmann A.G. (2005). Cannabinoid mechanisms of pain suppression. In: Pertwee RG (ed) Cannabinoids. Springer, Berlin Heidelberg.
93. Guzmán M. (2003). Cannabinoids: potential anticancer agents. *Nat. Rev. Cancer 3*: 745-755.
94. Ramos J.A., Gómez M., de Miguel R. (2005). Effects on development. In: Pertwee RG (ed) Cannabinoids Springer, Berlin Heidelberg.
95. Nogle L. M. and Gerwick W. H. (2002). Somocystinamide A, a novel cytotoxic disulfide dimer from a Fijian marine cyanobacterial mixed assemblage. *Org. Lett. 4*: 1095-1098.
96. Williams P. G., Yoshida W. Y., Moore R. E., Paul V. J. (2004). Micromide and guamamide: Cytotoxic alkaloids from a species of the marine cyanobacterium *Symploca*. *J. Nat. Prod. 67*: 49-53.
97. Edwards D. J., Marquez B. L., Nogle L. M., McPhail K., Goeger D. E., Roberts M.A., Gerwick W. H. (2004). Structure and biosynthesis of the jamaicamides, new mixed polyketide-peptide neurotoxins from the marine cyanobacterium *Lyngbya majuscula*. *Chem. & Biol. 11*: 817-833.
98. Tan L. T., Okino T., Gerwick W. H. (2000). Hermitamides A and B, toxic malyngamide-type natural products from the marine cyanobacterium *Lyngbya majuscula*. *J. Nat. Prod. 63*: 952-955.
99. Chang T. T., More S. V., Lu I-H, Hsu J-C, Chen T-J, Jen Y. C., Lu C-K, Li W-S. (2011) Isomalyngamide A, A-1 and their analogs suppress cancer cell migration in vitro. *Eur. J. Med. Chem. 46*: 3810-3819.

100. Cai W., Matthews J. H., Paul V. J., Luesch H. (2016). Pitiamides A and B, multifunctional fatty acid amides from marine cyanobacteria. *Planta Med. 82*: 897-902.

101. Wypych G. Handbook of antiblocking, release, and slip additives. ChemTec. Publishing. Page 53.

102. Getachew P., Getachew M., Joo J., Choi Y. S., Hwang D. S., Hong Y-K. (2016). The slip agents oleamide and erucamide reduce biofouling by marine benthic organisms (diatoms, biofilms and abalones). *Toxicol. Environ. Health Sci. 8*: 341-348.

103. Han B., McPhail K. L., Gross H., Goeger D. E., Mooberry S. L., Gerwick W. H. (2005). Isolation and structure of five lyngbyabellin derivatives from a Papua New Guinea collection of the marine cyanobacterium *Lyngbya majuscula*. *Tetrahedron 61*: 11723-11729.

104. Sharpless K. B., Amberg W., Bennami Y. L., Crispino G. A., Hartung J. Jeong K-S., Kwong H-L., Morikawa K., Wang Z-M, Xu D., Zhang X-L. (1992). The osmium-catalyzed asymmetric dihydroxylation: a new ligand class and a process improvement. *J. Org. Chem. 57*: 2768-2771.

105. Paul B. D., Jemionek J., Lesser D., Jacobs A. (2004). Enantiomeric separation and quantitation of (+/-)-amphetamine, (+/-)-methamphetamine, (+/-)-MDA, (+/-)-MDMA, and (+/-)-MDEA in urine specimens by GC-EI-MS after derivatization with (R)-(-)- or (S)-(+)-alpha-methoxy-alpha-(trifluoromethy)phenylacetyl chloride (MTPA). *J. Anal. Toxicol. 28*: 449-455.

106. Luesch H., Yoshida W. Y., Moore R. E., Paul V. J. (2002). Structurally diverse new alkaloids from Palauan collections of the apratoxin-producing marine cyanobacterium *Lyngbya* sp. *Tetrahedron 58*: 7959-7966.

107. Chûjö R., Hatada K., Kitamaru R., Kitayama T., Sato H., Tanaka Y. (1987). NMR measurement of identical polymer samples by round Robin method I. Reliability of chemical shift and signal intensity measurements. *Polym. J. 19*: 413-424.

108. Preciado A. and Williams P. G. (2008). A simple microscale method for determining the relative stereochemistry of statine units. *J. Org. Chem. 73*: 9228-9234.

109. Mosmann T. (1983). Rapid colorimetric assay for cellular growth and survival: application to proliferation and cytotoxicity assays. *J. Immunol. Methods 65*: 55-63.

110. Pettit G. R., Smith T. H., Arce P. M., Flahive E. J., Anderson C. R., Chapuis J-C., Xu J-P., Groy T. L., Belcher P. E., Macdonald C. B. (2015). Antineoplastic agents. 599. Total synthesis of dolastatin 16. *J. Nat. Prod. 78*: 476-485.

111. Casalme L. O., Yamauchi A., Sato A., Petitbois J. G., Nogata Y., Yoshimura E., Okino T., Umezawa T., Matsuda F. (2017). Total synthesis and biological activity of dolastatin 16. *Org. Biomol. Chem. 15*: 1140-1150.

112. Poncet J. (1999). The dolastatins, a family of promising antineoplastic agents. *Curr. Pharm. Des. 5*: 139-162.

113. Matthew S., Salvador L. A., Schupp P. J., Paul V. J., Luesch V. J. (2010). Cytotoxic Halogenated Macrolides and Modified Peptides from the Apratoxin-Producing Marine Cyanobacterium Lyngbya bouillonii from Guam. *J. Nat. Prod. 73*: 1544-1552.

114. Luesch H., Yoshida W. Y., Moore R. E., Paul V. J., Mooberry S. L. (2000). Isolation, structure determination, and biological activity of lyngbyabellin A from the marine cyanobacterium *Lyngbya majuscula*. *J. Nat. Prod. 63*: 611-615.

115. Marquez B. L., Watts K. S., Yokochi A., Roberts M. A., Verdier-Pinard P., Jimenez J. I., Hamel E., Scheuer P. J., Gerwick W. H. (2002). Structure and absolute stereochemistry of hectochlorin, a potent stimulator of actin assembly. *J. Nat. Prod. 65*: 866-871.

116. Williams P. G., Luesch H., Yoshida W. Y., Moore R. E., Paul V. J. (2003). Continuing studies on the cyanobacterium *Lyngbya* sp.: isolation and structure determination of 15-norlyngbyapeptin A and lyngbyabellin D. *J. Nat. Prod. 66*: 595-598.

117. Choi H., Mevers E., Byrun T., Valeriote F. A., Gerwick W. H. (2012). Lyngbyabellins K–N from two Palmyra atoll collections of the marine cyanobacterium *Moorea bouillonii*. *Eur. J. Org. Chem. 27*: 5141-5120.

118. Sone H., Kondo T., Kiryu M., Ishiwata H., Okika M., Yamada K. (1995). Dolabellin, a cytotoxic bisthiazole metabolite from the sea hare *Dolabella auricularia*: structural determination and synthesis. *J. Org. Chem. 60*: 4774-4781.

119. Petitbois J. G., Casalme L. O., Lopez J. A. V., Alarif W. M., Abdel-Lateff A., Al-Lihaibi S. S., Yoshimura E., Nogata Y., Umezawa T., Matsuda F., Okino T. (2017). Serinolamides and lyngbyabellins from an *Okeania* sp. cyanobacterium collected from the Red Sea. *J. Nat. Prod. 80*: 2708-2715.

120. Boudreau P. D., Monroe E. A., Mehrotra S., Desfor S., Korobeynikov A., Sherman D. H., Murray T. F., Gerwick L., Dorrestein P. C., Gerwick W. H. (2015). Expanding the Described Metabolome of the Marine Cyanobacterium Moorea producens JHB through Orthogonal Natural Products Workflows. *PloS One 10*. E0133297.

121. Paul V. J., Arthur K. E., Ritson-Williams R., Ross C., Sharp K. (2007). Chemical defenses: from compounds to communities. *Biol. Bull. 213*: 226-251.

122. Kleigrewe K., Gerwick L., Sherman D. H., Gerwick W. H. (2016). Unique marine derived cyanobacterial biosynthetic genes for chemical diversity. *Nat. Prod. Rep. 33*: 348-364.

123. Ramaswamy A. V., Sorrels C. M., Gerwick W. H. (2007). Cloning and biochemical characterization of the hectochlorin biosynthetic gene cluster from the marine cyanobacterium *Lyngbya majuscula*. *J. Nat. Prod. 70*: 1977-1986.

124. Umezawa H., Aoyagi T., Morishima H., Matsuzaki M., Hamada M., Takeuchi T. (1970). Pepstatin, a new pepsin inhibitor produced by actinomycetes. *J. Antibiot. 23*: 259-262.

125. Kwan J. C., Eksioglu E. A., Liu C., Paul V. J., Luesch H. (2009). Grassystatins A-C from marine cyanobacteria, potent cathepsin E inhibitors that reduce antigen presentation. *J. Med. Chem. 52*: 5732-5747.

126. Soliman Y. A., Mohamed A. S., NaserGomaa M. (2014). Antifouling activity of crude extracts isolated from two Red Sea puffer fishes. *Egyp. J. Aquat.Res. 40*: 1-7.

127. Al-Sofyani A., Marimuthu N., Wilson J. J., Pugazhendi A., Dhavamani J. (2016). Antifouling effect of bioactive compounds from selected marine organisms in the Obhur Creek Red Sea. *J. Ocean Univ. China 15*: 465-470.

128. Soliman Y. A. A., Brahim A. M., Moustafa A. H., Hamed M. A. F. (2017). Antifouling evaluation of extracts from Red Sea soft corals against primary biofilm and biofouling. *Asian Pac. J. Trop. Biomed. 5*: 601-611..

129. Abou El-Ezz R., Ibrahim A., Habib E., wahba A., Kamel H., Afifi M., Hassanean H., Ahmed S. (2017). Review of natural products from marine organisms in the Red Sea. *IJPSR 8*: 940-974.

130. Youssef D. T. A., Singab A. N. B., Van Soest R. W. M., Fusetani N. (2004). Hyrtiosenolides A and B, two new sesquiterpene γ-methoxybutenolides and a new sterol from a Red Sea sponge *Hyrtios* species. *J. Nat. Prod. 67*: 1736-1739.

131. Youssef D. T. A., Yamaki R. K., Kelly M. Scheuer P. J. (2002). Salmahyrtisol A, a novel cytotoxic sesterterpene from the Red Sea sponge *Hyrtios erecta*. *J. Nat. Prod. 65*: 2-6.

132. Bourguet-Kondracki M. L., Martin M. T., Guyot M. (1996). A new β-carboline alkaloid isolated from the marine sponge *Hurtios erecta*. *Tetrahedron Lett. 37*: 3457-3460.

133. Youssef D. T. A. and Mooberry S. L. (2006). Hurghadolide A and swinholide I, potent actin-microfilaments disrupters from the Red Sea sponge *Theonella swinhoei*. *J. Nat. Prod. 69*: 154-157.

134. Thornburg C. C., Thimmaiah M., Shaala L. A., Hau A. M., Malmo J. M., Ishmael J. E., Youssef D. T. A., McPhail K. L. (2011). Cyclic dipsipeptides, grassypeptolides D and E and ibuepidemethoxylyngbyastatin 3, from a Red Sea *Leptolyngbya* cyanobacterium. *J. Nat. Prod. 74*: 1677-1685.

135. Mohamed G. A., Abd-Elrazek A. E. E., Hassanean H. A., Alahdal A. M., Almohammadi A., Youssef D. T. A. (2014). New fatty acids from the Red Sea sponge *Mycale euplectellioides*. *Nat.Prod. Res. 28*: 1082-1090.

136. Dobson G., Christie W. W. (2002). Mass spectrometry of fatty acid derivatives. *Eur. J. Lipid. Sci. Technol. 104*: 36-43.

137. Engene N., Paul V. J., Byrum T., Gerwick W. H., Thor A., Ellisman M. H. (2013). Five chemically rich species of tropical marine cyanobacteria of the genus *Okeania* GEN. NOV. (*Oscillariales, Cyanoprokaryota*). *J. Phycol. 49*: 1095-1106.

138. Ogawa H., Iwasaki A., Sumimoto S., Kanamori Y., Ohno O., Iwatsuki M., Ishiyama A., Hokari R., Otoguro K., Omura S., Suenaga K. (2016). Janadolide, a cyclic polyketide-peptide hybrid possessing a *tert*—butyl group from an *Okeania* sp. marine cyanobacterium. *J. Nat. Prod. 79*: 1862-1866.

139. Sueyoshi K., Kaneda M., Sumimoto S., Oishi S., Fujii N., Suenaga K., Teruya T. (2016). Odoamide, a cytotoxic cyclodepsipeptide from the marine cyanobacterium *Okeania* sp. *Tetrahedron 72*: 5472-5478.

140. Kanamori Y., Iwasaki A., Sumimoto S., Suenaga K. (2016). Urumamide, a novel chymotrypsin inhibitor with a β-amino acid from a marine cyanobacterium *Okeania* sp. *Tetrahedron Lett. 57*: 4213-4216.

141. Okamoto S., Iwasaki A., Ohno O., Suenaga K. (2015). Isolation and structure of kurahyne B and total synthesis of the kurahynes. *J. Nat. Prod. 78*: 2719-2725.

142. Fenner A. M., Engene N., Spadafora C., Gerwick W. H., Balunas M. J. (2016). Medusamide A, a Panamanian cyanobacterial depsipeptide with multiple β-amino acids. *Org. Lett. 18*: 352-355.

143. Shao C-L., Linington R. G., Balunas M. J., Centeno A., Boudreau P., Zhang C., Engene N., Spadafora C., Mutka T. S., Kyle D. E., Gerwick L., Wang C-Y., Gerwick W. H. (2015). Bastimolide A, a potent antimalarial polyhydroxy macrolide from the marine cyanobacterium *Okeania hirsuta*. *J. Org. Chem. 80*: 7849-7855.

144. Navarro G., Cummings S., Lee J., Moss N., Glukhov E., Valeriote F. A., Gerwick L., Gerwick W. H. (2015). Isolation of polycavernoside D from a marine cyanobacterium. *Environ. Sci. Technol. Lett. 2*: 166-170.

145. Iwasaki A., Tadenuma T., Sumimoto S., Ohshiro T. Ozaki K., Kobayashi K., Teruya T., Tomoda H., Suenaga K. (2017). Beseokeaniamides A, B and C, sterol *O*-aceyltransferase inhibitors from an *Okeania* sp. marine cyanobacterium. *J. Nat. Prod. 80*: 1161-1166.

146. Iwasaki A., Shiota I., Sumimoto S., Matsubara T., Sato T., Suenaga K. (2017). Kohamamides A, B, and C, cyclic depsipeptides from an *Okeania* sp. marine cyanobacterium. *J. Nat. Prod. 80*: 1948-1952.

- ACKNOWLEDGEMENTS -

Firstly, I would like to express my sincere gratitude to Dr. C. Hellio for giving me the contacts which allowed me to join and conduct my research in the Hokkaido University. I also thank my supervisor, Prof. T. Okino, for accepting me in his laboratory, for all his help, his valuable guidance and everything I learnt from him. I could not have imagined having a better advisor and mentor for my Ph.D study. A special gratitude also goes to Dr. Julius Lopez, my Senpai, who was the first student I met in the laboratory and who also gave me lots of advices in my research but also in my life in Sapporo.

I am grateful to Prof. T. Umezawa, Prof. F. Matsuda and Dr. L. Casalme of the Faculty of Environmental Earth Science, Hokkaido University, Japan, for their help and useful advices for the synthesis conducted in this research. I learnt a lot from them as it was the first time for me to conduct chemical synthesis.

My sincere thanks to Dr. Y. Nogata from CRIEPI and Ms. E. Yoshimura for conducting all the antifouling assays presented in this study and for teaching me the procedure when I went to their laboratory. This research would not have been possible without your collaboration.

I would like to thank Dr. M. Morikawa and Dr. M. Kurasaki of the Faculty of Environmental Earth Science, Hokkaido University, Japan, for allowing us to use their genetics and cell culture facilities, respectively, and Dr. Y. Kumaki of the High-Resolution, NMR laboratory, Dr. Y. Fukushi and Dr. Y. Takata of the GC-MS and NMR laboratory, Hokkaido University, Japan, for conducting the NMR and GC-MS analyses described in this study.

With a special mention to Dr. W. Alarif, Dr. A. Abdel-Lateff and Prof. S. Al-Lihaibi from King Abdulaziz University, Saudi Arabia, for providing me with the extracts.

Of course, I do not forget all Okino lab members who encouraged me a lot, helped me and with who I spent good times. I also thank all my friends in Sapporo or elsewhere in Japan for all the good times we spent during these four last years.

Finally, I thank my mother and my sister who were a great support during these four years far from them, and also my best friend Emeline who visited me in Summer 2016. It was so nice to take vacations with her, especially in Akan-ko!

I also deeply thank the Hokkaido University for the scholarship it provided me. It was a great help for my life in Sapporo.

Thanks for all your encouragement!

- APPENDIX -

Antifouling activity of cyanobacterial extracts from the Red Sea

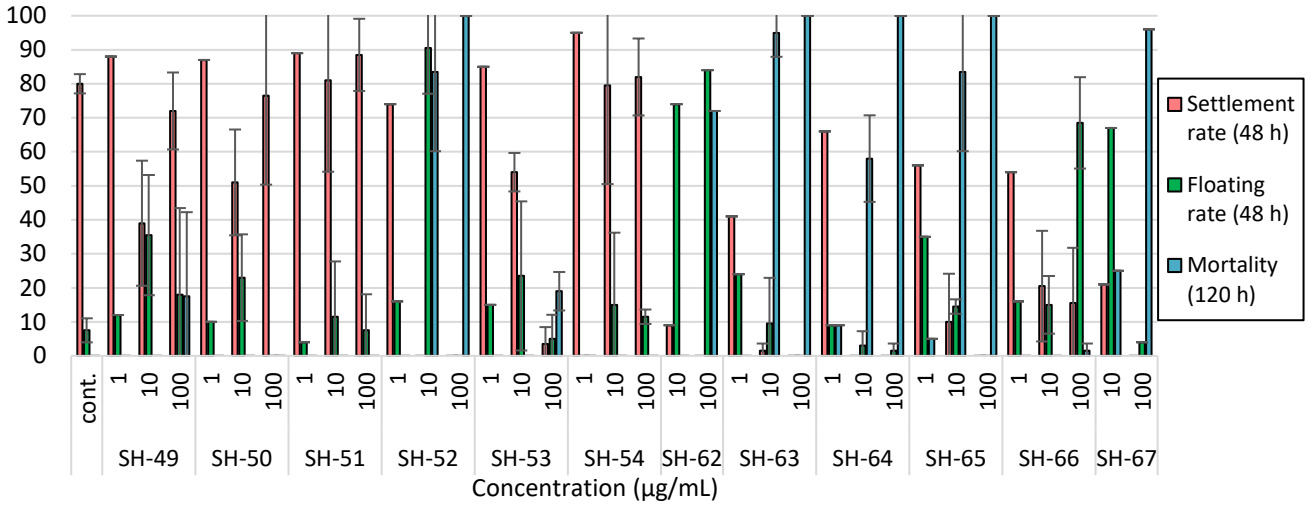

Figure S1: Antifouling activity of Saudi Arabia cyanobacterial extracts tested on barnacle larvae after 48 and 120 hours of exposure.

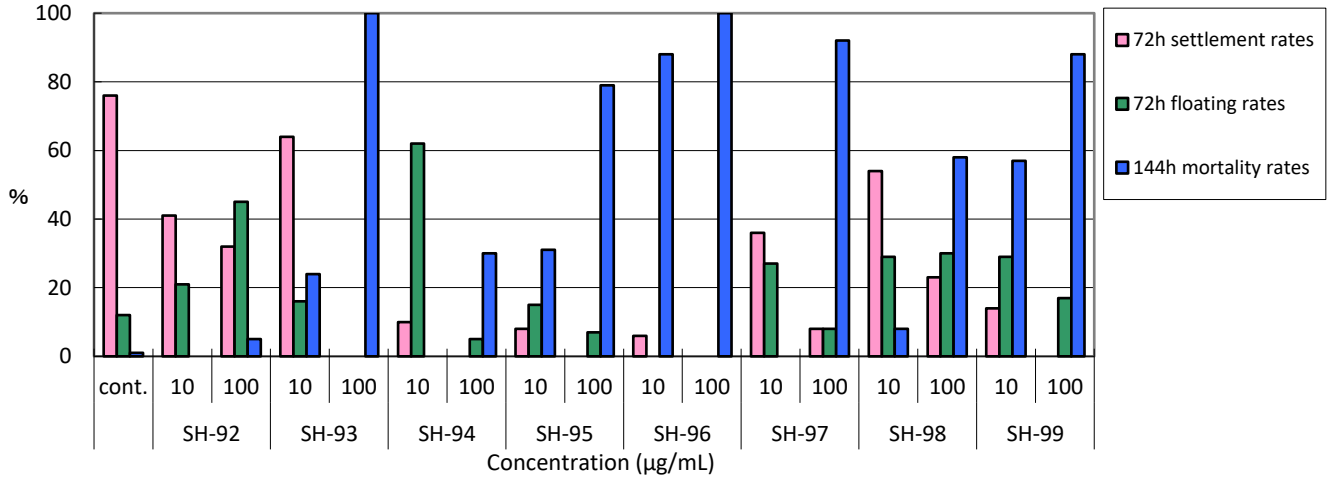

Figure S2: Antifouling activity of other Saudi Arabia cyanobacterial extracts tested on barnacle larvae after 72 and 144 hours of exposure.

Table S3: Identity of the cyanobacterial extracts tested on barnacle larvae.

Code	Identity
SH-49	*Moorea producens* S1301, EtOAc fraction
SH-50	*Moorea producens* S1301, BuOH fraction
SH-51	*Moorea producens* S1301, H_2O fraction
SH-52	*Symploca* sp. S1302, EtOAc fraction
SH-53	*Symploca* sp. S1302, BuOH fraction
SH-54	*Symploca* sp. S1302, H_2O fraction
SH-62	Blue-green algae Depth 15.6 m #1 (June 2014)
SH-63	Blue-green algae Depth 15.6 m #2 (June 2014)
SH-64	Blue-green algae Depth 15.6 m #3 (June 2014)
SH-65	Blue-green algae Depth 15.6 m #4 (June 2014)
SH-66	Blue-green algae Depth 15.6 m #5 (June 2014)
SH-67	Blue-green algae Depth 15.6 m #6 (June 2014)
SH-92	Blue-green algae #1 (Oct 2014)
SH-93	Blue-green algae #2 (Oct 2014)
SH-94	Blue-green algae #3 (Oct 2014)
SH-95	Blue-green algae #4 (Oct 2014)
SH-96	Blue-green algae #5 (Oct 2014)
SH-97	Blue-green algae #6 (Oct 2014)
SH-98	Blue-green algae #7 (Oct 2014)
SH-99	Blue-green algae #8 (Oct 2014)

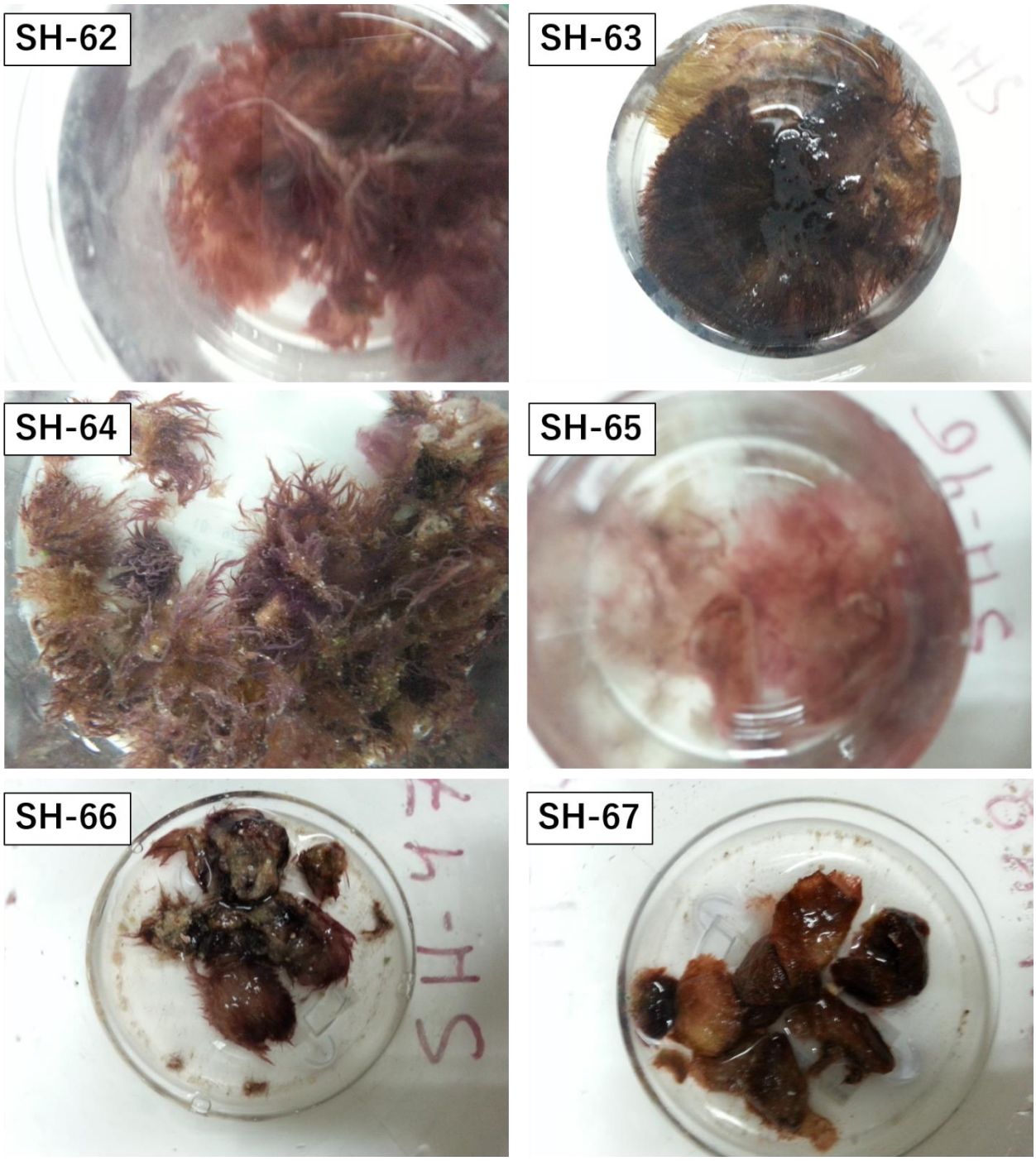

Figure S4: Pictures of the cyanobacterial samples SH-62 to SH-67.

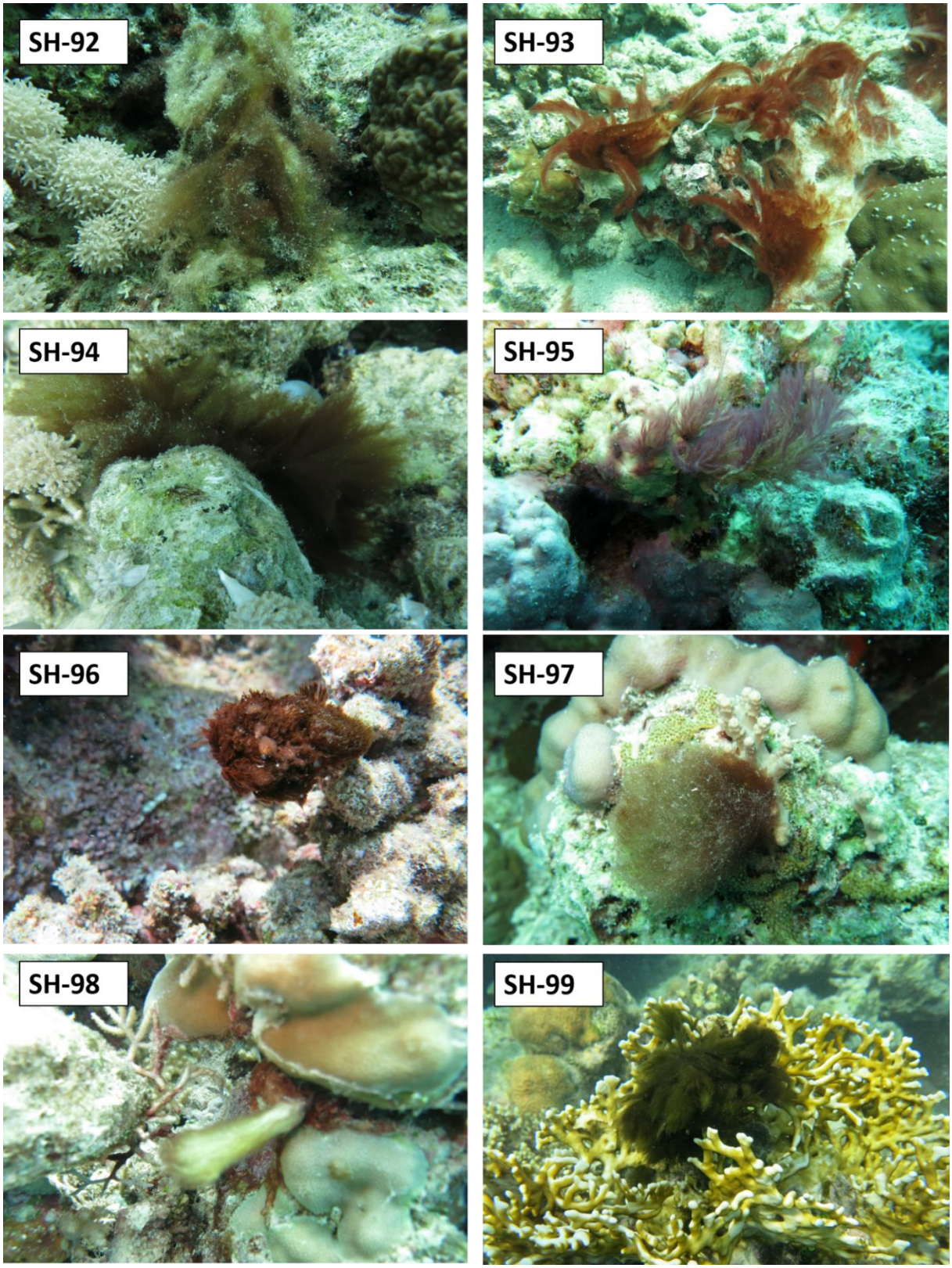

Figure S5: Underwater pictures of the cyanobacterial samples SH-92 to SH-99.

Phthalates from the sponge *Hyrtios* sp.

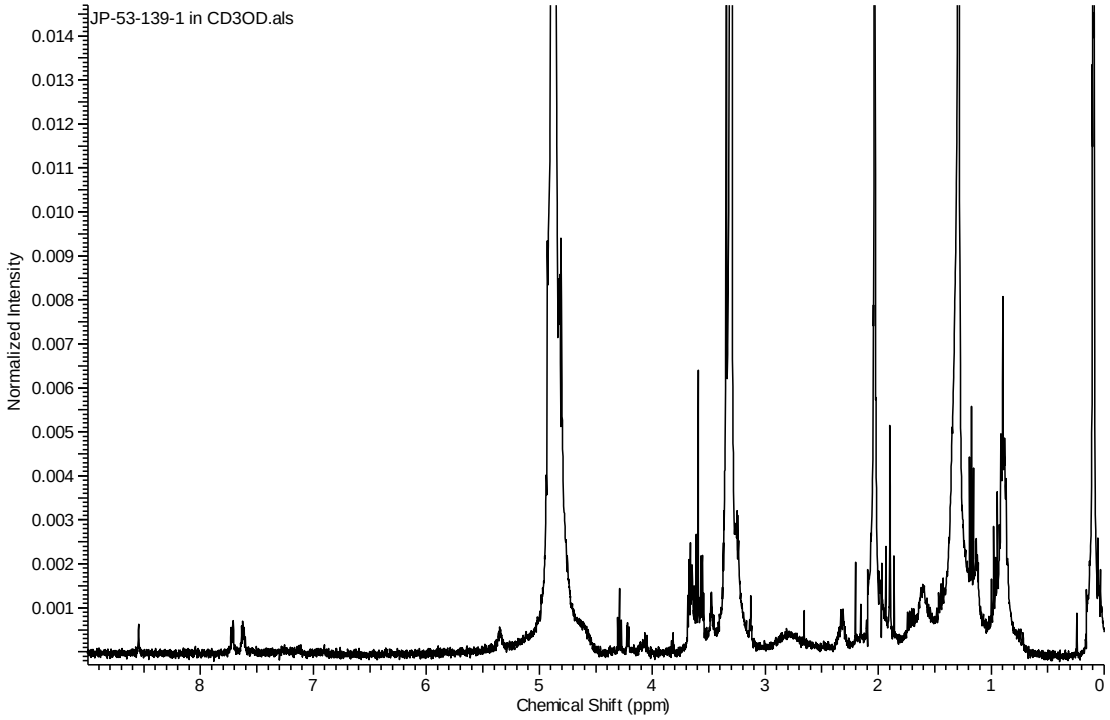

Figure S6: ^{1}H NMR spectrum of phthalate # 1 (400 MHz, CD_3OD).

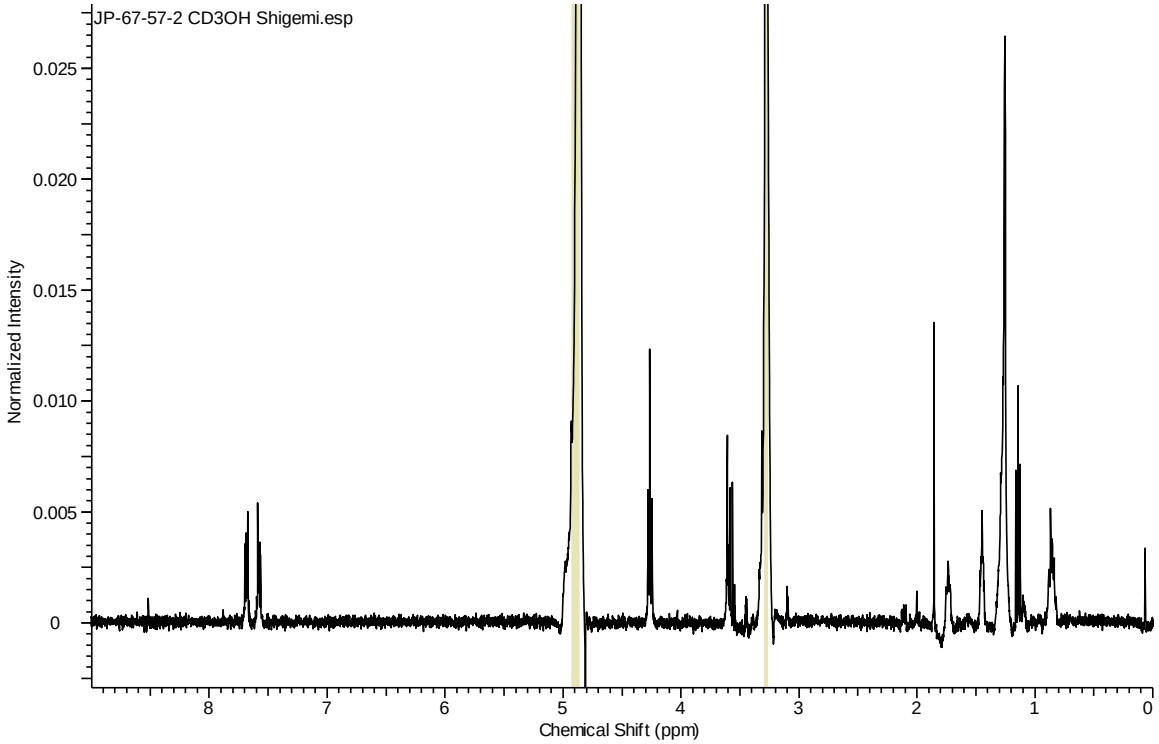

Figure S7: ^{1}H NMR spectrum of phthalate # 2 (400 MHz, CD_3OD).

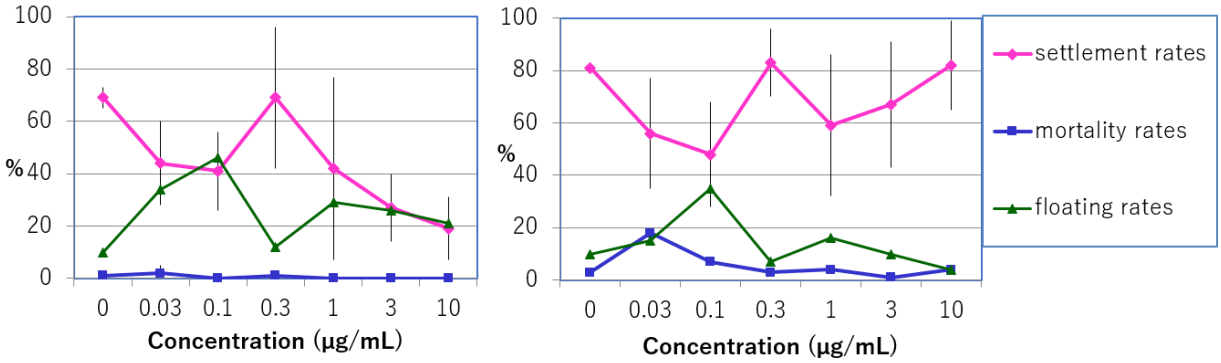

Figure S8: Antifouling results of phthalate # 1 on barnacle larvae (settlement and floating rates after 48 hours, mortality after 120 hours exposure).